Generation of novel pristinamycin I derivatives by mutasynthesis

Dissertation

der Mathematisch-Naturwissenschaftlichen Fakultät

der Eberhard Karls Universität Tübingen

zur Erlangung des Grades eines

Doktors der Naturwissenschaften

(Dr. rer. nat.)

vorgelegt von

M.Sc. Oliver Hennrich

aus Reutlingen

Tübingen

2025

Gedruckt mit Genehmigung der Mathematisch-Naturwissenschaftlichen Fakultät der Eberhard Karls Universität Tübingen.

Tag der mündlichen Qualifikation:	09.07.2025
Dekan:	Prof. Dr. Thilo Stehle
1. Berichterstatter:	Prof. Dr. Wolfgang Wohlleben
2. Berichterstatterin:	Prof. Dr. Heike Brötz-Oesterhelt

Erklärung

Ich, Oliver Hennrich, erkläre hiermit, dass ich diese Arbeit selbstständig und nur mit den angegebenen Hilfsmitteln verfasst habe. Ferner sind alle Stellen, welche im Wortlaut oder dem Sinn nach den Werken anderer Autoren entnommen sind, durch Angabe der Quellen gekennzeichnet. Eine detaillierte Beschreibung meiner eigenen Leistungen in gemeinsamen Publikationen ist im Anhang beigefügt.

Oliver Hennrich

_____

Tübingen, den_____

Contents

1. Summary

Procurement of new antibiotics is the main way of fighting the threat to human health posed by the increasing prevalence of antibiotic resistances amongst pathogenic microorganisms. One way to obtain new antibiotics is to modify the chemical structure of proven compounds to, for example, improve their overall effectiveness as antibiotics or to circumvent specific resistance mechanisms against them. One such approach, termed mutasynthesis, combines selective precursor feeding with genetic modification of an original producer strain to introduce desired features into complex compounds. Since the genetic modifications target genes involved in the supply of specific precursors, mutasynthesis can only be employed by understanding the genetic background of the respective synthesis pathways. This work is focused on the streptogramin antibiotic pristinamycin, which is a combination of two synergistically active protein synthesis inhibitors, used as an antibiotic of last resort, primarily against methicillin- and vancomycin resistant pathogens. However, resistances against pristinamycin are endangering its use against those organisms. First, our knowledge about the diversity of streptogramin gene clusters, in general, was expanded. To this end, the streptogramin biosynthetic gene clusters from multiple producers were compared. This comparison included clusters described and characterized in literature, recently discovered yet unexplored clusters, as well as one cluster from *Streptomyces kurssanovii,* which was identified as a streptogramin producer in this work. Clusters, which code for the synthesis of the same compounds, were found to be highly similar in most regions, showing that the structure of previously reported clusters is conserved in other producers. Second, pristinamycin I, the streptogramin B component of pristinamycin, was modified by mutasynthesis. Two new halogenated and bioactive derivatives of pristinamycin I were generated and purified in this study. The structures of the new derivatives were elucidated by NMR, and their overall antimicrobial potency, as well as their effect on streptogramin resistant organisms, were shown to be comparable to that of natural pristinamycin I.

2. Zusammenfassung

Die Findung neuer Antibiotika ist die wichtigste Strategie, um die Bedrohung für die menschliche Gesundheit durch die zunehmende Verbreitung von Antibiotikaresistenzen unter pathogenen Mikroorganismen zu bekämpfen. Ein Ansatz hierfür stellt die Veränderung der chemischen Struktur bewährter Verbindungen dar, um beispielsweise ihre generelle Wirksamkeit als Antibiotika zu verbessern oder bestimmte Resistenzmechanismen gegen sie zu umgehen. Ein solcher Ansatz, die so genannte Mutasynthese, kombiniert die selektive Zufütterung von Antibiotika-Vorstufen mit der genetischen Veränderung eines ursprünglichen Produzentenstamms. Gewünschte Eigenschaften können so in komplexe Verbindungen eingebracht werden. Da die gentechnischen Veränderungen auf Gene abzielen, welche an der Synthese spezifischer Vorstufen beteiligt sind, kann die Mutasynthese nur angewandt werden, wenn der genetische Hintergrund der jeweiligen Synthesewege verstanden ist. Im Mittelpunkt dieser Arbeit steht das Streptogramin-Antibiotikum Pristinamycin, eine Kombination aus zwei synergistisch wirkenden Proteinbiosynthese-Inhibitoren, welches als Notfallantibiotikum gegen Methicillin- und Vancomycin-resistente Krankheitserreger eingesetzt wird. Resistenzen gegen Pristinamycin gefährden jedoch den Einsatz gegen diese Erreger. Als ersten Schritt erweitert diese Arbeit den Forschungsstand über die Diversität von Streptogramin-Biosynthese Gencluster im Allgemeinen. Zu diesem Zweck wurden die Streptogramin-Biosynthese-Gencluster mehrerer Produzenten miteinander verglichen. Dieser Vergleich umfasste aus der Literatur bekannte und charakterisierte Cluster, kürzlich entdeckte aber noch unerforschte Cluster sowie ein Cluster aus Streptomyces kurssanovii, eine Art, welche in dieser Arbeit als Streptogramin-Produzent identifiziert wurde. Der Vergleich zeigt, dass Cluster welche für die Synthese derselben Verbindungen kodieren, in großen Teilen sehr ähnlich sind. Dies verdeutlicht, dass die Struktur der zuvor beschriebenen Cluster auch in anderen Produzenten konserviert ist. Zudem wurde Pristinamycin I, die Streptogramin-B-Komponente von Pristinamycin, durch Mutasynthese modifiziert. In dieser Arbeit wurden zwei neue halogenierte und bioaktive Derivate von Pristinamycin I hergestellt und aufgereinigt. Die Strukturen der neuen Derivate wurden mittels NMR aufgeklärt und ihre allgemeine antimikrobielle Wirksamkeit sowie ihre Wirkung auf Streptogramin-resistente Organismen erwiesen sich als vergleichbar mit der von natürlichem Pristinamycin I.

3. Introduction

3.1. Antibiotics

Antibiotics are substances which kill microorganisms or inhibit their growth. They are secondary metabolism products of mostly bacteria, fungi, and plants, with some notable synthetic exceptions, such as sulfonamides or quinolones. Regardless of their origin, substances defined as antibiotics are of low molecular weight (between 150 and 5000 Da) and active at concentrations of less than 1 mg/ml (Lancini and Parenti, 1982) Classification of antibiotics can be based on multiple criteria, like mode of action (e.g. protein synthesis inhibitors, cell wall synthesis inhibitors) or chemical structure (e.g. peptide antibiotics, polyketide antibiotics; Gräfe, 1992).

Antibiotics are of great importance in modern medicine. Before they became readily available during the 1940s, bacterial infectious diseases like cholera, typhus, syphilis, and tuberculosis were one of the leading causes of death (Mohr, 2016). Effective treatment of infectious diseases, as well as new medical procedures like organ transplants and open-heart surgery, have been made possible by the use of antibiotics and extended the average human life span by approximately 23 years (Hutchings et al., 2019). Bacterial resistance to antibiotics has, however, been observed soon after their widespread use. For example, 50% of *Staphylococcus aureus* isolates were resistant to penicillin only seven years after the first use of the drug (Scheffler et al., 2012). Antimicrobial resistance (AMR) is the product of a multifactorial complex process involving the increasing effectiveness of resistance genes and their proliferation in bacterial populations via horizontal gene transfer (Prescott, 2014). The main facilitator of AMR is the widespread use of antibiotics, which leads to selection for resistant strains (Prescott, 2014).

The spread of antibiotic resistance amongst pathogens leads to complications in the treatment of the associated infections, which results in a growing number of deaths caused by bacterial infections. Almost five million deaths associated with AMR have been estimated for the year 2019 (Murray et al., 2022). Studies predict that by 2050 infections with antibiotic resistant microorganisms will cause the death of an estimated 10 million people per year unless drastic action is taken (O´Neil et al., 2016). The issue of AMR is exacerbated by the decreasing number of new antibiotics which find their

way into the market (Hutchings et al., 2019). AMR is one of the biggest threats to public health of the 21st century and it is obvious that novel antibiotics are needed to treat infections caused by antibiotic resistant pathogens (Murray et al., 2022; Scheffler et al., 2010). Most classes of antibiotics in clinical use today have been discovered during the so called 'Golden Age' of antibiotics, heralded by the discovery of penicillin in 1928 by Alexander Fleming and ranging from the 1940s to the 1960s (Baltz et al., 2016). The main strategy to obtain new antibiotics with clinical applications during this golden age was the systematic screening of, mainly soil dwelling, bacteria in bioassays for the production of antimicrobial compounds. This approach was pioneered by Selman Waksman and his colleagues and led, amongst others, to the discovery of streptomycin (Waksman, 1944), the first antibiotic used to treat tuberculosis. The main focus was being placed on the phylum *Actinomycetota* (formerly *Actionobacteria*), which includes the producers of about two thirds of all known antibiotics in clinical use today (Hutchings et al., 2019; Barka et al., 2016).

3.2. The genus *Streptomyces* as potent producers of antibiotics

Streptomycetes (members of the genus *Streptomyces*) are Gram-positive, predominantly soil dwelling organisms of the phylum *Actinomycetota* (Barka et al., 2016; Oren and Garrity, 2021). The morphology of streptomycetes is highly diverse based on their state of differentiation. Growth of streptomycetes usually starts with a germinating spore. After germination, the spore grows into a fungus-like, branching filament, called substrate mycelium. During the growth, which occurs at the tip of the hyphae, septa are introduced in regular intervals. The resulting compartments contain multiple copies of the chromosome. The chromosomes of streptomycetes are large, mostly linear and have a high GC-content of about 74% (Wright and Bibb, 1992). Nutritional limitation and other causes of stress induce the formation of the hydrophobic aerial mycelium. In contrast to the substrate mycelium, the aerial mycelium grows up and out of the substrate. Numerous spore septa are introduced (up to 100 per hyphae) as the aerial mycelium matures, allowing for the differentiation and separations of spores which completes the streptomycetes life cycle (Wright and Bibb, 1992; Chater, 1993).

Streptomycetes are of particular importance as potent producers of biologically active compounds, which include many antibiotics. The phylum of *Actinomycetota* is regarded as the most prolific group of antibiotic producers. Of the substantial number of antibiotics produced by members of this phylum, about 80% originate from the genus *Streptomyces* alone (Barka et al., 2016). Antibiotics produced by streptomycetes include representatives of different compound classes, such as tetracyclines, streptogramins aminoglycosides, glycopeptides and more (Barka et al., 2016). Models have suggested that the total number of antibiotics produced by streptomycetes might be as high as 100.000, most of which have not been identified yet (Watve et al., 2001). Antibiotics are secreted into the environment most likely to give the producing organisms an advantage against competitors. Antibiotic biosynthesis is genetically encoded by the producer organism and the respective genes, which include those required for precursor supply, assembly, resistance and regulation, are often organized in so-called biosynthetic gene clusters (BGC).

3.3. The bacterial ribosome as a drug target

The bacterial ribosome is a complex, macromolecular machinery responsible for protein biosynthesis (Voorhees and Ramakrishnan, 2013) and target for many clinically relevant antibacterial drugs (Poehlsgaard et al., 2005). The bacterial 70S ribosome consists of the small 30S and the large 50S ribosomal subunit, composed of ribosomal RNA and ribosomal proteins. Antibiotics targeting the bacterial ribosome can be grouped into the ones that target the 30S, and those that target the 50S subunit (Wilson, 2014). Most antibiotics that target the 30S subunit interfere either with the delivery of aminoacyl-tRNAs or the transfer of tRNAs within the ribosome during translocation. These antibiotics include, amongst others, the aminoglycosides and tetracyclines (Wilson, 2014). The antibiotics that target the 50S subunit primarily disrupt peptide bond formation or the elongation of nascent peptide chains. Representative substance classes are macrolides, lincosamides, pleuromutilins, phenicols, and streptogramins (Wilson, 2014).

3.4. Streptogramin antibiotics, mode of action, resistance, and application

Streptogramins are a group of clinically and industrially important antibiotics that target the bacterial ribosome and are primarily produced by the genus *Streptomyces*. Examples of streptogramins and their respective producers include pristinamycin

produced by *Streptomyces pristinaespiralis*, virginiamycin produced by *Streptomyces virginiae,* and viridogrisein/griseoviridin produced by *Streptomyces griseoviridis*.

Chemically, streptogramins are a mixture of two structurally unrelated compounds that are co-synthesized by their respective producers. They feature at least one streptogramin A (S_A) type and one streptogramin B (S_B) type compound that are naturally produced in a 2:1 to 1:1 S_A/S_B ratio (Cocito, 1979). Often, however, multiple congeners of the respective compounds are produced in variable proportions (Barriere et al., 1998). S_A antibiotics are polyunsaturated macrolactones synthesized by hybrid polyketide synthase (PKS) - nonribosomal peptide synthetase (NRPS) systems. S_B antibiotics are cyclic hexa- or heptadepsipeptides derived from NRPS biosynthetic pathways (Barriere et al., 1998; Johnston et al., 2002; Fig. 1).

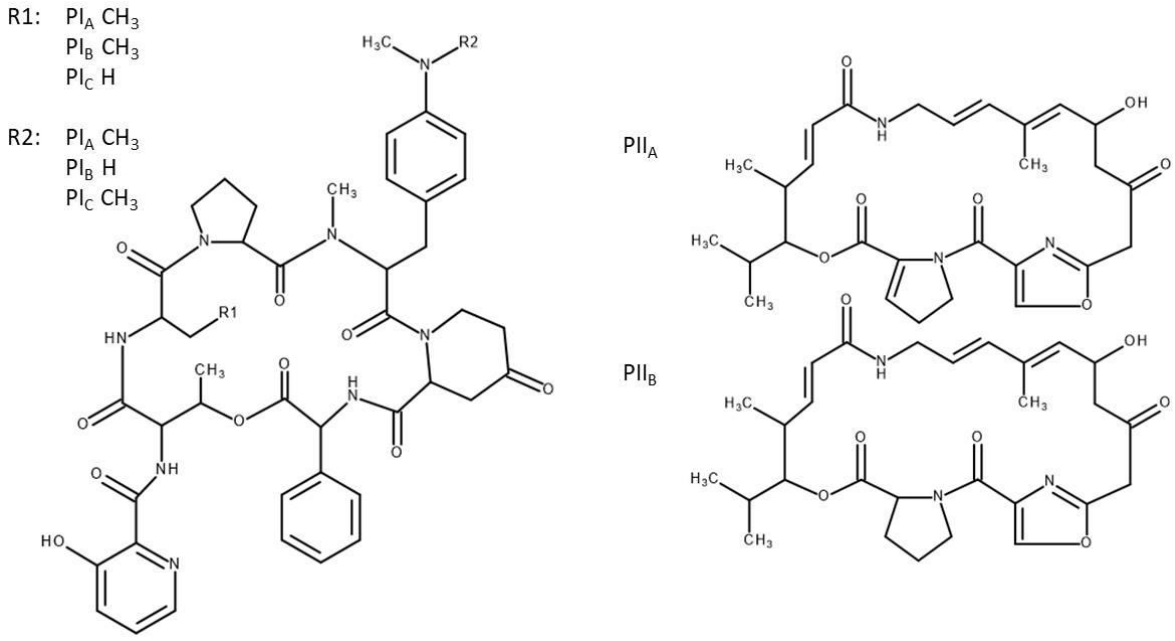

Figure 1: Structures of the S_B Pristinamycin I (left), the S_A Pristinamycin II (right) as well as their natural congeners.

Streptogramins inhibit the bacterial protein biosynthesis as a mode of action. Both streptogramin components bind to closely adjacent locations at the 50S subunit of the bacterial ribosome via hydrogen bonds and hydrophobic interactions with the 23S rRNA (Harms et al., 2004). S_A group antibiotics bind at the entrance of the ribosomal exit tunnel at the peptidyl transferase catalytic center (PTC). By overlapping the acceptor (A) and donor (P) substrate binding sites (Tu et al., 2005; Hansen et al.,

2003), they block the attachment of tRNAs to both locations (Vanuffel and Cocito, 1996), preventing the elongation of the nascent peptide chain. Additionally, the uracil residue 2585 (*E. coli* numbering) of the 23S rRNA is rotated by 180° upon S_A binding (Harms et al., 2004). This conformational change, which persists even after the removal of the compound, prevents U2585 from fulfilling its proposed role, which is the positioning of P-site substrates during peptide bond formation (Harms et al., 2004). The S_B group binding site is located inside the ribosomal exit tunnel, which is shared as a binding site with macrolides like erythromycin. This shared binding site leads to a competition between macrolides and S_B antibiotics for binding to the ribosome if both substances are present, as shown for erythromycin and virginiamycin S (Parfait et al., 1981). By occupying this space, S_B antibiotics cause a misalignment of the peptidyl-tRNA at the P-site which leads to a blockage of the elongation and premature release of the nascent peptide chain after the formation of a few peptide bonds (Chinal et al., 1987). Both streptogramin groups have a bacteriostatic effect, but display a synergistic activity when administered in combination, leading to a bactericidal effect (Cocito et al., 1997). Binding of S_A compounds to the ribosome causes the rotation of an adenine residue 2062 by about 90° (Harms et al., 2004). Thereby, the binding affinity of the S_B component to the ribosome in this conformation is increased (Cocito et al., 1997), leading to an approximately 100-fold decrease of the minimal inhibitory concentration (MIC) of the S_A/S_B combination, compared to that of the respective single compound (Vanuffel and Cocito, 1996).

Because of the unrelated chemical structure and separate binding sites of S_A and S_B groups, most resistance mechanisms against streptogramin antibiotics confer resistance to one or the other compound but not both. However, most Gram-negative bacteria (with the exception of some members from genera like *Neisseria*, *Haemophilus*, and *Legionella*) display an intrinsic resistance to both groups (Johnston et al., 2014; Mast et al., 2014). This observation is attributed to the rather large compound size and hydrophobicity of streptogramins, which prevent the compounds from passing through the outer membrane of Gram-negatives (Seoane et al., 2000). Furthermore, mutations of the 23S rRNA at residue A2062 have been shown to cause a combined S_A and S_B resistant phenotype in the Gram-positive *Streptococcus pneumoniae* (Depardieu et al., 2001).

Target modification by 23S rRNA methylation can cause resistance to streptogramins. Mono- or dimethylation of A2058 is the most prominent form of resistance against S_B antibiotics (Johnston et al., 2014). This modification is catalysed by methyl transferases, which are encoded by ubiquitous plasmid borne *erm* genes. These modifications confer resistance to not only S_B antibiotics, but also macrolide and lincosamide antibiotics, and thus was termed MLS_B resistance (Svetlov et al., 2021). For S_A antibiotics, resistance by target modification is achieved by methylation of the adenine residue 2503 by the methyl transferase Cfr encoded by the gene *cfr* (Long et al., 2006). Next to S_A antibiotics, Cfr also confers resistance against phenicols, lincosamides, oxazolidinones and pleuromutilins (the $PhLOPS_A$ group). The c*fr* gene has been found on plasmids but also on chromosomes (Reisser et al., 2020).

Furthermore, resistance to S_A or S_B can be achieved by inactivation of the respective compound. S_B antibiotics can be linearised by Vgb lyases through an elimination reaction at the ester bond between the threonine and phenylglycine residues, leading to an inactive compound (Mukhtar et al., 2001). The most prominent resistance mechanism against S_A antibiotics is their inactivation by acetylation of the compounds C_{14} alcohol by the family of Vat acetyltransferases, encoded by *vat* genes (Kehoe et al., 2003). The *vgb* and *vat* genes, coding for Vgb and Vat, respectively, are often plasmid borne and co-localized on the same plasmid in staphylococci (Canu et al., 2001).

Resistance against S_A and S_B can also be conferred by *vga* and *msr* genes, respectively. Both groups of genes code for a family of ATP-binding cassette (ABC) domain containing proteins. While these proteins show characteristics of ABC transporters and have therefore been proposed to be drug exporters, more recent investigations point towards a resistance mechanism by ribosome protection (Sharkey et al., 2016). *Vga* genes are also plasmid borne and frequently accompanied by *vat* and *vgb* genes in staphylococci (Reisser et al., 2020).

Streptogramins are active against Gram-positive pathogens, such as staphylococci, streptococci and most enterococci, as well as some Gram-negative pathogens, e.g. *Moraxella catarrhalis*, *Neisseria* spp., and *Legionella pneumophila* (Mast et al., 2014, Reisser et al., 2020). Their activity against methicillin- or vancomycin resistant

pathogens, including strains of *Staphylococcus aureus* and *Enterococcus faecium (*Reisser et al., 2020*),* is an important factor in the clinical context (Reisser et al., 2020). Two commercial streptogramin formulations have been approved for clinical use. These are Pyostacine® (Sanofi-Aventis, Gentilly, France), which consists of pristinamycin I and pristinamycin II, and Synercid® (Pfizer, New York, USA), which consists of the respective semi-synthetic derivatives quinopristin and dalfopristin. Pristinamycin, produced by *Streptomyces pristinaespiralis*, has been used as an orally administered antibiotic in France for over 50 years and is currently also used in Tunisia and Lithuania (Reisser et al., 2020). As a semisynthetic pristinamycin derivative with increased solubility properties, Synercid® is the only injectable streptogramin antibiotic in clinical use. The therapeutic use has been approved in the USA in 1999 and 2001 in Europe. However, its use in Europe has since been discontinued (Reisser et al., 2020). Disadvantages of Synercid® are, besides clinical limitations (an intravenous catheter is needed) and high costs (Reisser et al., 2020), serious side effects like arthralgia or myalgia (Delgado et al., 2000). Another semisynthetic pristinamycin derivative, NXL-103 (combination of linopristin and flopristin) underwent phase II clinical trials, which were concluded in 2010, but the substance was not introduced into the market since then (Reisser et al., 2020). The first discovered streptogramin, virginiamycin produced by *Streptomyces virginiae*, has been used as a feed additive in livestock for decades due to its properties as growth promoter and for disease prevention. While the use of virginiamycin for this purpose was forbidden in Europe by 1999, it is still used as a feed additive in countries like Canada, China, Japan, and the USA (Mast et al., 2014). Additionally, virginiamycin is used to prevent contamination of fermenters in the industrial production of ethanol (Bischoff et al., 2016).

3.5. Pristinamycin biosynthesis

The synthesis of streptogramins requires a large number of specialized enzymes for multiple functions. These include precursor supply, assembly, regulation, and self-resistance. The respective genes are organized in a large BGC. The *S. pristinaespiralis* pristinamycin ‘supercluster’ (Fig. 2), which is responsible for the synthesis of pristinamycin, spans 210 kb in size (Mast et al. 2011a).

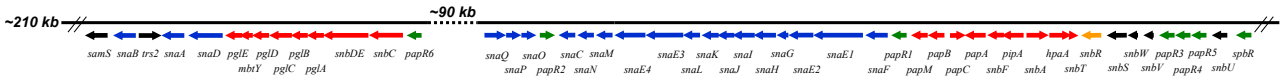

Figure 2: The pristinamycin supercluster of *Streptomyces pristinaespiralis* PR11. Genes are shown as arrows indicating the respective orientation. Colors indicate the function of encoded enzymes: red = PI synthesis, blue = PII synthesis, green = regulation, yellow = self-resistance, black = unknown (Mast et al., 2011a).

Most genes involved in the regulation of pristinamycin synthesis are located on the right border of the cluster. Here, one *Streptomyces* antibiotic regulator protein (SARP) type activator gene (*papR4*), two TetR type regulator genes (*papR3*, *papR5*) and one γ-butyrolactone receptor gene (*spbR*) are clustered together (Mast et al., 2011a). A putative cytochrome P450 monooxygenase encoded by *snbU* has been suggested to be involved in γ-butyrolactone-like synthesis (Handel et al., 2020). Further regulatory genes, including two SARP type activator genes (*papR1*, *papR2*) and one response regulator gene (*papR6*), are scattered throughout the cluster. One putative resistance gene is present in the cluster in the form of a member of the major facilitator superfamily (*snbR*; Mast et al., 2011a). An additional putative drug exporter, which confers resistance to both streptogramin types as well as rifampicin, is encoded by the gene *ptr* outside of the cluster borders (Bamas-Jacques et al., 1999; Blanc et al., 1995a).

Pristinamycin II (PII) is assembled by a hybrid PKS/NRPS, encoded by five genes (*snaE1-4, snaD*) as well as a group of six mono functional enzymes (encoded by *snaG, snaH, snaI, snaJ, snaK* and *snaL*). The products of three additional genes (*snaA, snaB* and *snaC*) are responsible for the conversion of the intermediate PII_B to the predominant PII congener PII_A (Fig. 1) by oxidation of the D-proline residue to dehydroproline (Blanc et al., 1995b). Most PII precursors are derived from the primary metabolism with the exception of the initial starter unit isobutyryl-CoA, which is likely to be synthesized from valine by the branched-chain α-keto acid decarboxylase SnaF and then installed by the hybrid PKS/NRPS SnaE1 (Mast et al., 2011a). The assembly of pristinamycin I (PI) is performed by a large NRPS, encoded by three genes (*snbA*, *snbC* and *snbDE*). SnbA activates the first amino acid (AA) 3-hydroxypicolinic acid,

followed by the incorporation of L-threonine and D-α-aminobutyric acid by SnbC. SnbDE catalyzes the subsequent incorporation of the L-proline, 4-N,N-dimethylamino-L-phenylalanine, 4-oxo-L-pipecolinic acid, and L-phenylglycine (L-Phg) residues followed by the cyclisation and release of PI. Furthermore, the production of PI requires the biosynthetic pathways for the four non-proteinogenic AA precursors 3-hydroxypicolinic acid (3-HPA), 4-oxo-L-pipecolinic acid (OPPA), 4-N,N-dimethylamino-L-phenylalanine (DMAPA) and L-phenylglycine (L-Phg). The biosynthesis of these precursors is known to involve the products of twelve genes (*hpaA*, *pipA*, *snbF*, *papA*, *papB*, *papC*, *papM,* and *pglA-E*). HpaA is required for the synthesis of 3-hydroxy picolinic acid (3-HPA) (Blanc et al., 1996). The involvement of three additional gene products (encoded by *snaC*, *snaO* and *snaQ*) in 3-HPA synthesis has been suggested based on their homology to respective genes from *Streptomyces* sp. NRRL12068, the producer of the 3-HPA containing benzoxazole antibiotic A33853, but has not been shown experimentally for pristinamycin biosynthesis (Yun et al., 2019). *pipA* and *snbF* code for OPPA synthesis enzymes and the *pap*-operon codes for the enzymes needed for DMAPA synthesis (Mast et al., 2011a; Blanc et al., 1997). L-Phg synthesis is encoded by the *pgl*-operon. The products of the five *pgl* genes catalyze the stepwise synthesis of L-Phg starting with phenylpyruvate, which is derived from the shikimate pathway (Mast et al., 2011b; Osipenkov et al., 2018; Wohlleben et al., 2012). The *pgl* operon of *S. pristinaespiralis* is the first known natural synthesis pathway for L-Phg (Mast et al., 2011b).

3.6. The non-proteinogenic amino acid phenylglycine

Phenylglycines (Phgs) represent a rare family of non-proteinogenic AA and are components of a diverse group of bioactive secondary metabolites (e.g. PI, vancomycin, ramoplanin; Al Toma et al., 2015). Phgs feature a unique structural property in the direct attachment of the phenyl group to the α-carbon. When Phgs are part of a fixed peptide backbone, the flexibility of their phenyl group is restricted compared to that of other aromatic AA (Al Toma et al., 2015). While the effects of this property on Phg containing compounds is not clear, it might be important for bioactivity (Al Toma et al., 2015). For example, the reduced flexibility of the phenyl group in Phg is suggested to allow the compounds they are part of to maintain stable conformations,

which are essential for interaction with their respective targets, at a lower entropic cost (Walker and Clardy, 2021). A recent study from Walker and Clardy on a machine learning bioinformatics approach to predict bioactivities from BGCs found that BGCs containing Phg encoding genes are explicitly associated with the production of compounds that display antibacterial activity (Walker and Clardy, 2021). Phg and derivatives thereof are of commercial interest since they are used as starting blocks for the synthesis of semisynthetic antibiotics, e.g. D-Phg is used for the synthesis of β-lactam antibiotics, such as penicillins and cephalosporins, while D-4-hydroxyphenylglycine (Hpg) is used as a building block for the synthesis of polyoxins (Al Toma et al., 2015). However, since Phg are prone to racemisation, employing them as constituents in chemical synthesis approaches is challenging (Al Toma et al., 2015). The conventional chemical methods used for deprotection of AA and/or macrocyclisation of peptides often cause racemisation of the Phg residue, which complicates the synthesis of the desired compound (Al Toma, et al. 2015; Elsawy et al., 2011).

3.7. Mutasynthesis

While natural compounds constitute the majority of known antibiotics, artificial modifications to these molecules are often attempted to improve their bioactivity, pharmacokinetic properties or to address antibiotic resistance (Majhi et al., 2020). Many clinically important antibiotics are derivatives of natural compounds, modified to make them more potent (Majhi et al., 2020; Lewis, 2020; Kennedy, 2008). The modification of natural products can be achieved by different methods. Total chemical synthesis, for example, relies exclusively on chemical transformations without using any natural producer (Prusov, 2013). While this approach provides highly controlled conditions, many natural compounds cannot be synthesized due to their complex chemical structures. Furthermore, substance yields are often very low when many reaction steps are required (Sun et al., 2015). Semi-synthesis utilizes intermediates or fully formed natural products as starting points for further modification (Weist et al., 2004) and has provided many relevant drugs (e.g. clindamycin, rifamycin SV synercid, amoxicillin, cefacitrile, retapamulin; Majhi et al., 2020; Hutchings et al., 2019). Precursor-directed biosynthesis is an approach that does not rely on chemical

synthesis, but instead exploits the substrate promiscuity of the biosynthetic machinery of the natural producer (Sun et al., 2015). The basic principle is to provide altered precursor molecules to the organism and rely on the biosynthetic machinery to implement it into the original compound (Kennedy, 2008). This allows for the modification of complex natural compounds. Not all supplied precursors are, however, efficiently incorporated. Furthermore, the alternative precursor will have to compete with the usually preferred natural precursor for incorporation, decreasing the yield of the desired compound. Finally, both, the modified as well as the original compound, are produced in this process. The generated substances may have similar chemical and physical properties, which can make downstream purification challenging (Kennedy, 2008). Some of these problems can be overcome by a refined version of precursor directed biosynthesis, named mutasynthesis. This method was introduced by Kenneth L. Rinehart in 1977 (Rinehart, 1977). The mutasynthesis approach utilizes mutants of natural product producers that are blocked in the synthesis of a target precursor by either gene deletion or silencing. This allows for precursor feeding experiments in strains that do not produce the original precursor anymore and in consequence cannot synthesize the respective natural product (Fig. 3). Instead, feeding of precursor derivatives to the respective mutant strain enables the production of the desired antibiotic derivative in a natural product-free background. Likewise, precursor derivatives do not have to compete with the original precursor, increasing the likelihood of incorporation and overall yield. While the first mutasynthesis experiments were conducted with mutants generated by random mutagenesis, knowledge of the natural compound biosynthetic pathways allows for targeted manipulation of producer strains by genetic engineering methods for mutant construction (Kennedy, 2008). Mutasynthesis has been successfully applied for the derivatization of various different compound classes, such as polyketides (Weissman, 2007; Eichner et al., 2012; Toscano et al., 1983), nonribosomal peptides (Hojati et al., 2002; Weist et al., 2004), aminoglycosides (Delzer et al., 1984), alkaloids (Winand et al., 2021) aminocoumarins (Galm et al., 2004) and more. The lincosamide antibiotic lincomycin for example was modified by mutasynthesis. The gene *lmbX,* which is necessary for the synthesis of the lincomycin precursor 4-propyl-L-proline, was deleted in the natural lincomycin producer *Streptomyces lincolnensis* ATCC 25466. Two derivatives of 4-propyl-L-proline (4-butyl-L-proline and 4-pentyl-L-proline) were

then fed to the mutant. The mutasynthesis approach yielded two new lincomycin derivatives, of which one (4-pentyl-4-depropyllincomycin) showed increased activities against low-level lincosamin resistant staphylococci compared to the original compound (Ulanova et al., 2010). Mutasynthesis was also used in studies involving *S. gandocaensis* DHS334, the producer of the peptide antibiotics cahuitamycin A-C. Here, the deletion of the gene *cahI* (Δ*cahI*), necessary for the synthesis of the cahuitamycin A and B starter unit salicylate, led to the abolishment of cahuitamycin A and B synthesis. Cahuitamycin C, which incorporates 6-methylsalicylate as its starter unit was produced exclusively in Δ*cahI*. Feeding of the blocked mutant with seven salicylate derivatives led to the isolation of two new cahuitamycin derivatives (cahuitamycin D and E), which showed an increased potency in inhibiting biofilm formation of *Acinetobacter baumannii* compared to cahuitamycin A-C (Park et. al, 2016).

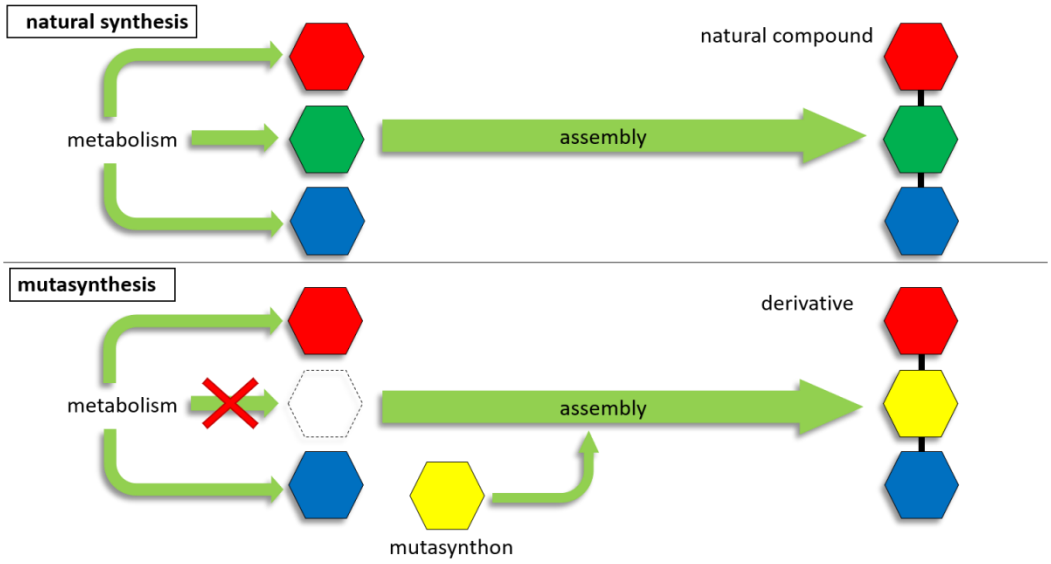

Figure 3: Schematic presentation of the mutasynthesis principle. Colored hexagons represent the different antibiotic building blocks. The mutasynthon is shown as yellow hexagon. The biosynthesis products are indicated by connected black lines (Publication 1, mod.).

4. Research Goals

The goal of this thesis is to improve our understanding of the diversity of streptogramin BGCs. For this purpose, the pristinamycin BGC of *Streptomyces pristinaespiralis*, which codes for the production of PI and its synergistic S_A partner compound PII, is compared to BGCs of other streptogramin producers. This analysis shall include already known streptogramin BGCs, as well as a BGCs from newly identified streptogramin producers. The concrete understanding of the genetic basis of streptogramin biosynthesis is a prerequisite for genetic manipulation of the streptogramin producer organism, which will be employed to reach the second goal of this thesis. Here, new derivatives of the S_B antibiotic PI will be generated by mutasynthesis. New PI derivatives will be isolated and purified to evaluate their bioactivity against PI susceptible and resistant organisms.

5. Results

5.1. Identification of new streptogramin producers and characterization of the corresponding biosynthetic gene clusters

Streptogramins are a unique class of antibiotic mixtures. The corresponding BGCs code for the biosynthetic pathways of two chemically unrelated compounds and their respective precursors. So far, three streptogramin BGCs have been characterized. These include the pristinamycin BGC from *Streptomyces pristinaespiralis* (Mast et al., 2011a), the virginiamycin BGC from *Streptomyces virginiae* (Pulsawat 2007), and the griseoviridin (GV) /viridogrisein (VG) BGC from *Streptomyces griseoviridis* (Xie et al., 2012). More producers of streptogramin antibiotics are known (Ahmed and Donaldson, 2007), however the respective BGCs have not been characterized. To understand the genetic background of how different streptogramin producers accomplish the production of the respective compounds, various streptogramin BGCs should be compared. Additional new streptogramin producing strains and their corresponding BGCs were identified before: A bioactivity screening with mode of action studies that included 500 strains from the Actinomycetes strain collection of the University of Tübingen led to the identification of two previously unknown streptogramin producers *Streptomyces* sp. Tü 2975 and Tü 3180 (Wex et al., 2021). One further streptogramin producer, *Streptomyces* sp. SW4 was identified following bioactivity screenings of actinomycetes strains from the biodiversity hotspot Indonesia (Aziz et al., 2018). Additionally, new streptogramin producers shall be identified and their BGCs compared to the known BGCs they most closely resemble. In the current study, all so far known and recently identified streptogramin BGCs are compared with each other to unveil genetic similarity as well as differences, which can ultimately help to assign compound characteristics to specific coding genes and may set a basis for studying evolutionary development of streptogramin BGCs.

5.1.1. Identification of novel streptogramin producers and their respective streptogramin BGCs

Tü 2975 and Tü 3180 are confirmed producers of pristinamycin and griseoviridin/viridogrisein, respectively (Wex et al., 2021). To investigate the

respective BGCs, genomic DNA from both strains was first extracted and the PacBio RS II platform was employed to sequence the respective genomes for Publication 3. The assembled genome sequences were subsequently analysed with antiSMASH 4.0 for the identification of BGCs. The predicted BGCs (20 for Tü 2975, 27 for Tü 3180) were manually reviewed, revealing potential BGCs coding for the synthesis of the respective produced streptogramins. For Tü 2975, region 2 was found to contain a cluster, which showed >60% similarity to a known pristinamycin BGC, while the genome of Tü 3801 contained a cluster that showed >70% similarity to a known griseoviridin/viridogrisein BGC located on region 25 (Publication 3). To find additional new streptogramin producers, genome sequenced strains of the DSMZ strain collection were screened *in silico*. By specifically searching amongst DSMZ strains, prospective producers can easily be accessed and tested for streptogramin production. All known streptogramin BGCs contain the so called *pgl* operon, coding for the enzymes that enable the synthesis of the non-proteinogenic amino acid Phg. *pglA* is the first gene of this operon, encoding a Phg dehydrogenase. This enzyme and correspondingly the coding gene is unique for L-Phg and thus hints at streptogramin biosynthesis. Accordingly, the occurrence of *pglA* within a given genome sequence should be an indication for streptogramin producers. Therefore, the PglA amino acid (AA) sequence was chosen to search for respective homologs in genome sequenced DSMZ strains. A BLAST search using the translated AA sequence of the *pglA* gene from *S. pristinaespiralis* PR11 revealed a putative protein of the enoyl-CoA hydratase/isomerase family (WP_189473706) with 96% identity in the strain *Streptomyces kurssanovii* DSM 40162. Analysis with antiSMASH 4.0 predicted 23 BGCs, of which one (region 1 (NZ_BMTN01000016) closely matched the pristinamycin BGC of *S. pristinaespiralis* PR11. *S. kurssanovii* was cultivated as liquid culture in three different media (R5, HT7T, and NL800) and crude extraction of the whole cultures were performed with ethyl acetate. Bioactivity assays against *B. subtilis* ATCC 6633 (Pelzer et al., 1999) confirmed the production of an antibacterial compound by *S. kurssanovii* after fermentation for 72 h in NL800 at 28°C. Bioactive crude extracts were analysed via HPLC-MS and pristinamycin I/II were identified based on their respective *m/z* signals (525.3+1 for PII and 866.5+1 for PI; Fig. 4), confirming *S. kurssanovii* as a new pristinamycin producer.

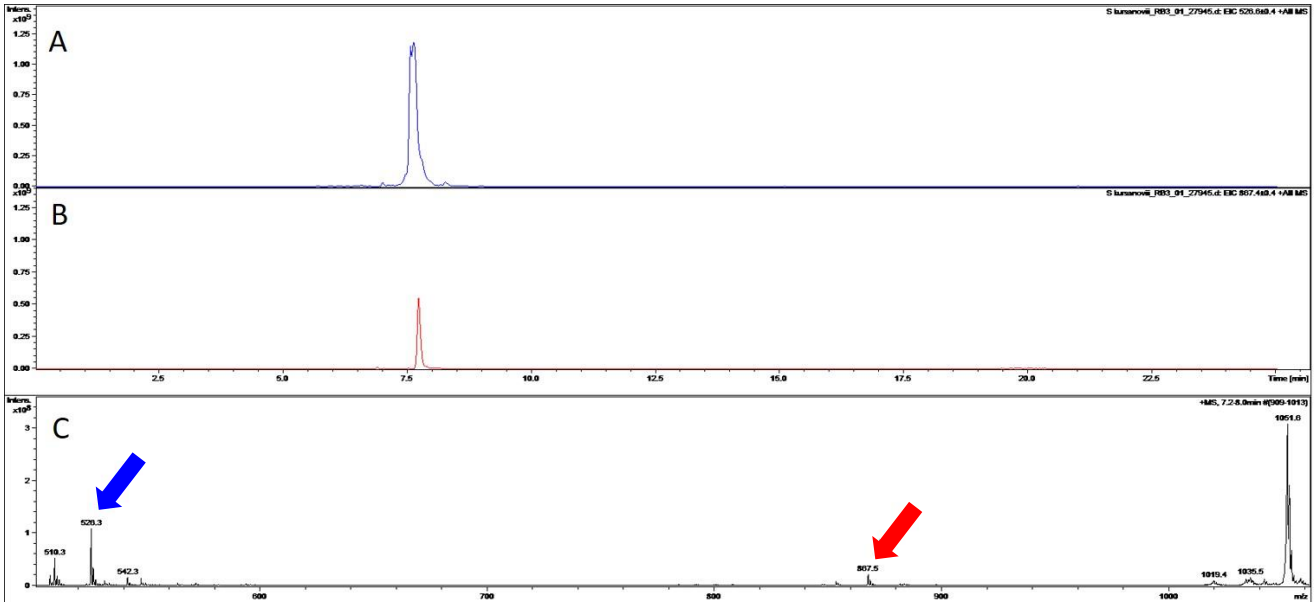

Figure. 4: HPLC-MS analysis of *S. kurssanovii* fermentation broth crude extract. **A** and **B** are the positive mode extracted ion chromatogram for PII and PI, respectively. **C** is the corresponding mass spectrum from 7.2 to 8 min. The *m/z* signals for PII (526.3) and PI (867.5) are marked with a blue and red arrow, respectively.

5.1.2. Comparison of different streptogramin BGC types

The three known streptogramin BGCs (*prs*, *sgv* and *vir*) and the four newly described ones were grouped into cluster "types" based on the compounds produced. The *prs* type resembles the pristinamycin BGC originally described for *S. pristinaespiralis*, which enables the host to produce PI and PII (Fig. 5). The *prs* type was in this study also identified in the new streptogramin producer strains SW4, Tü 2975, and *S. kurssanovii* and the respective clusters were designated prs^{SW4}, prs^{2975} and prs^{kurs}. The *sgv* BGC type was originally described for *S. griseoviridis* and enables the host to produce VG and GV (Fig. 5). A *sgv* type BGC was identified to be present in Tü 3180 and was designated sgv^{3180}. The last type, and the only one without multiple representatives, is the *vir* type from *S. virginiae*, which is responsible for the production of virginiamycin S (VS) and M (VM) (Fig. 5).

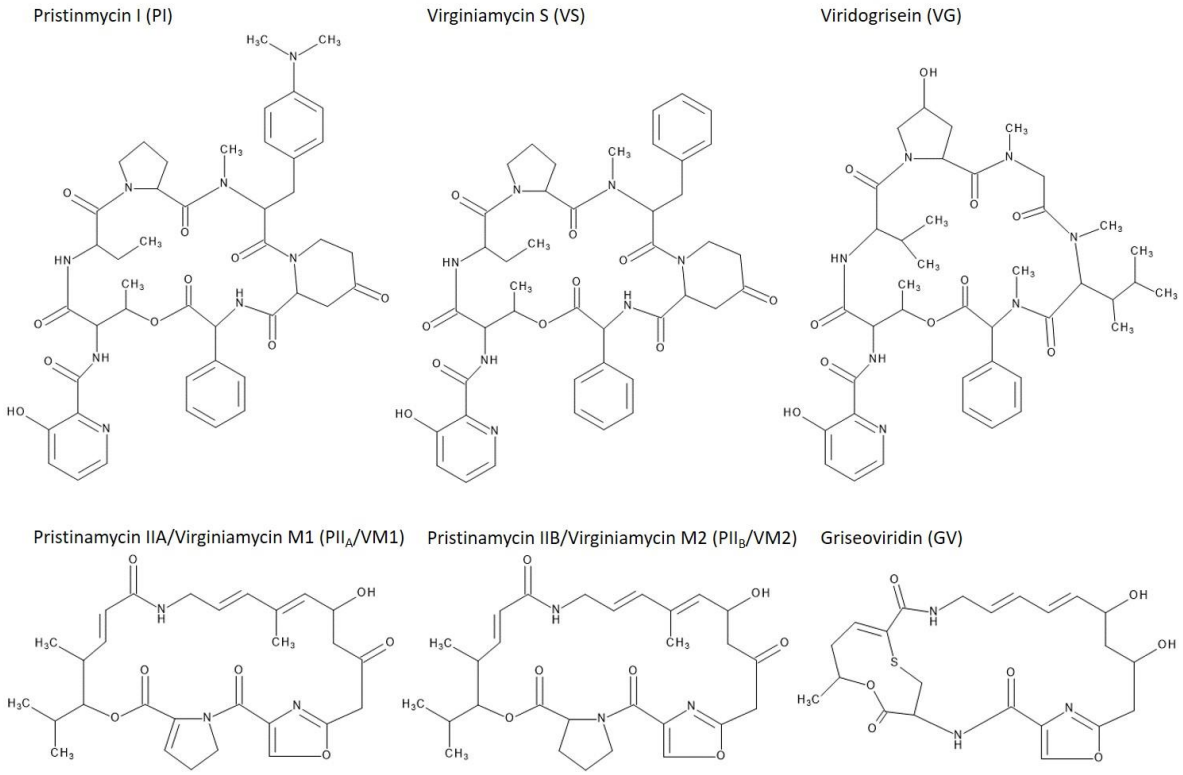

Figure 5: Structures of the molecules that make up pristinamycin (PI/PII), virginiamycin (VS/VM) and viridogrisein (VG)/griseoviridin (GV). PII and VM are identical in structure and two natural congeners, PII_A/VM1 and PII_B/VM2, are shown.

The three known BGC types are compared concerning their overall organisation (Fig. 6). Additionally, the newly discovered streptogramin BGCs from SW4, Tü 2975, and *S. kurssanovii* are compared with the original *prs* cluster from *S. pristinaespiralis*. The streptogramin BGC discovered in Tü 3180 is compared with the original *sgv* cluster from *S. griseoviridis*. Genes of the new streptogramin BGCs are referred to by their NCBI locus IDs.

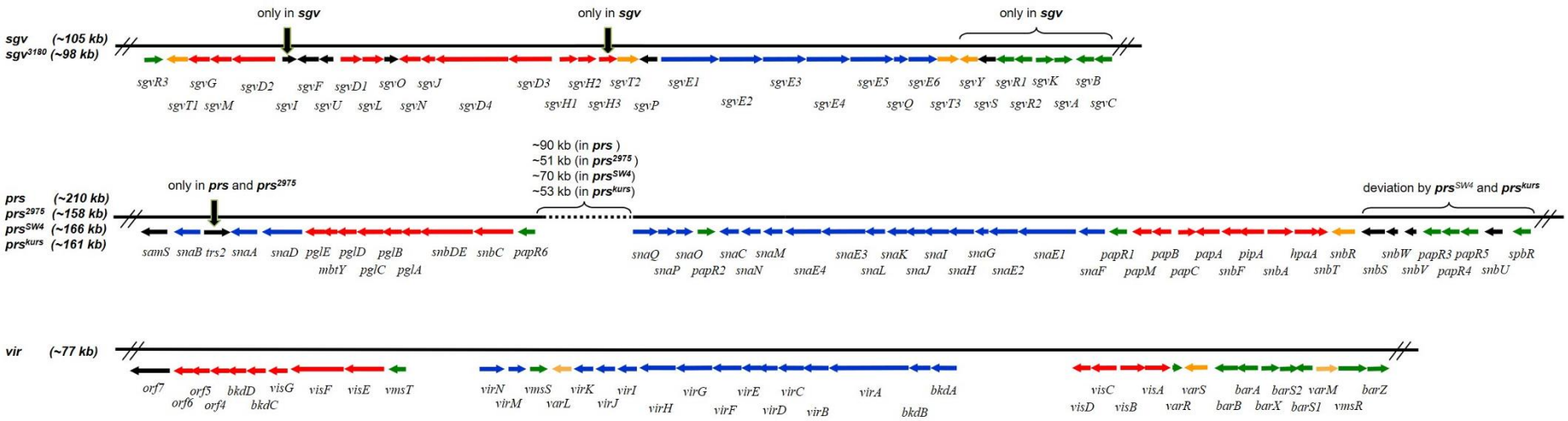

Figure 6: Overview over the organization of three streptogramin BGC types *sgv*, *prs,* and *vir*, including the respective sizes. Genes are coloured according to the function of the encoded proteins: red = PI synthesis, blue = PII synthesis, green = regulation, yellow = self-resistance, black = unknown. The dotted line in the *prs* type marks large intergenic regions of unknown function with their respective sizes being displayed above. Further areas of variation are marked with arrows for single ORFs and curved brackets for groups of ORFs. (Mast et al., 2011a; modified)

To get an overview of the enzymes encoded in the streptogramin clusters, a comprehensive comparison table has been compiled (Tab. 1). All genes found in any of the three cluster types and their confirmed or proposed function were listed.

Table 1: Genes of the different streptogramin gene clusters and the confirmed/proposed function of the encoded enzymes (+ = homolog present; - = no homolog present). Colour code of the biosynthetic role: red = S_B synthesis, blue = S_A synthesis, green = regulation, yellow = self-resistance, black = unknown.

ORF *(following the naming in S. pristinaespiralis, if not marked otherwise, asterisk = experimental evidence for function of product)*	**Biosynthetic role**	**Function**	***Gene (or analogous gene) present in the given streptogramin clusters***						
			prs	***prs^{SW4}***	***prs^{2975}***	***prs^{kurs}***	***vir***	***sgv***	***sgv^{3180}***
samS	S_B assembly	S-adenosylmethionine synthetase	+	+	+	+	-	-	-
*snaB**	S_A tailoring	PIIA synthase subunit B	+	+	+	+	-	-	-
*trs2**	-	S200/IS605 family transposase	+	-	+	-	-	-	-
*snaA**	S_A tailoring	PIIA synthase subunit A	+	+	+	+	-	-	-
*snaD**	S_A assembly	PII peptide synthetase	+	+	+	+	*orf7*	*sgvE5, sgvE6*	+
*pglE**	S_B precursor synthesis	Hydroxyphenylglycine aminotransferase	+	+	+	+	*orf6*	-	-
*mbtY**	(S_B assembly)	MbtH-like protein	+	+	+	+	*orf5*	*sgvJ*	+
*pglD**	S_B precursor synthesis	Thioesterase type II	+	+	+	+	*orf4*	*sgvH3*	-
*pglC**	S_B precursor synthesis	Pyruvate dehydrogenase E1 component β-subunit	+	+	+	+	*bkdD*	*sgvH2*	+
*pglB**	S_B precursor synthesis	Pyruvate dehydrogenase E1 component α-subunit	+	+	+	+	*bkdC*	*sgvH1*	+
*pglA**	S_B precursor synthesis	Hydroxyacyl-dehydrogenase	+	+	+	+	*visG*	*sgvN*	+
snbDE	S_B assembly	PI synthetase 3 and 4	+	+	+	+	*visF*	*sgvD4*	+
snbC	S_B assembly	PI synthetase 2	+	+	+	+	*visE*	*sgvD2*	+
*papR6**	regulation	Response regulator	+	+	+	+	*vmsT*	-	-
*snaQ**	S_B precursor synthesis	Flavin-dependent oxidoreductase	+	+	+	+	*virN*	*sgvF*	+
*snaP**	S_A tailoring/assembly	Thioesterase	+	+	+	+	*virJ*	*sgvI*	-

*snaO**	S_B precursor synthesis	Sarcosine oxidase	+	+	+	+	*virM*	*sgvS*	+
*papR2**	regulation	SARP-type regulator	+	+	+	+	*vmsS*	*sgvR3*	+
snaC	S_A tailoring	NADH:FMN oxidoreductase	+	+	+	+	-	-	-
*snaN**	(S_A assembly)	4'-phosphopantetheinyl transferase	+	+	+	+	*virK*	-	-
*snaM**	S_A assembly	Acyltransferase	+	+	+	+	*virI*	*sgvQ*	+
*snaE4**	S_A assembly	Hybrid NRPS/PKS (PKSIV)	+	+	+	+	*virH*	*sgvE4*	+
*snaE3**	S_A assembly	Hybrid NRPS/PKS (III), PKS (PKSII)	+	+	+	+	*virG, virF*	*sgvE3*	+
*snaL**	?	Unknown	+	-	-	+	-	-	-
*snaK**	S_A assembly	Enoyl-CoA hydratase	+	+	+	+	*virE*	-	-
*snaJ**	S_A assembly	Enoyl-CoA hydratase	+	+	+	+	*virD*	-	-
*snaI**	S_A assembly	HMG-CoA synthase-like protein	+	+	+	+	*virC*	-	-
*snaH**	S_A assembly	β-ketoacyl-ACP synthase	+	+	+	+	*virB*	-	-
*snaG**	S_A assembly	Acyl carrier protein (ACP)	+	+	+	+	-	-	-
*snaE2**	S_A assembly	Hybrid PKS/NRPS (PKSI)	+	+	+	+	*virA*	*sgvE2*	+
*snaE1**	S_A assembly	Hybrid PKS/NRPS (PKSI)	+	+	+	+	*bkdB, virA*	*sgvE1*	+
*snaF**	S_A precursor synthesis	Branched-chain α-keto acid decarboxylase76/84	+	+	+	+	*bkdA*	-	-
*papR1**	regulation	SARP-type regulator	+	+	+	+	-	-	-
papM	S_B precursor synthesis	N-Methylase	+	+	+	+	-	-	-
papB	S_B precursor synthesis	Mutase	+	+	+	+	-	-	-
papC	S_B precursor synthesis	Dehydrogenase	+	+	+	+	-	-	-
papA	S_B precursor synthesis	p-aminobenzoate synthase	+	+	+	+	-	-	-
snbF	S_B precursor synthesis	Cytochrome P450 monooxygenase	+	+	+	+	*visD*	-	-
pipA	S_B precursor synthesis	Lysine cyclodeaminase	+	+	+	+	*visC*	-	-
snbA	S_B assembly	PI synthetase 1	+	+	+	+	*visB*	*sgvD1*	+
hpaA	S_B precursor synthesis	L-lysine 2-aminotransferase	+	+	+	+	*visA*	*sgvL*	+
*snbT**	?	4-oxalocrotonate tautomerase	+	+	+	+	-	*sgvO*	+
snbR	resistance	Protein of the Major Facilitator Superfamily	+	+	+	+	*varS*	*sgvT1*	+
*snbS**	?	Methylmalonyl-CoA decarboxylase α-SU	+	+	+	+	-	-	-
*snbW**	?	Hypothetical protein SghaA1_39280	+	+	+	+	-	-	-

*snbV**	?	Hypothetical protein pSLA2-L_p058	+	-	-	+	-	-	-
*papR3**	regulation	TetR-type regulator	+	-	-	+	*barB*	-	-
*papR4**	regulation	SARP-type regulator	+	-	-	+	-	*sgvR2*	-
*papR5**	regulation	TetR-type regulator	+	+	-	+	-	*sgvR1*	-
*snbU**	?	Cytochrome P450 monooxygenase	+	+	+	+	-	*sgvP*	+
*spbR**	regulation	Autoregulator receptor protein	+	+	+	+	*barA*	*sgvB*	-
SgvU (sgv)	?	hypothetical protein	-	-	-	-	-	+	+
sgvD3 (sgv)	S_B precursor synthesis/assembly	NRPS, for generation and addition of 4-hydroxy-D-proline	-	-	-	-	-	+	+
sgvG (sgv)	S_B precursor synthesis	branched-chain amino acid aminotransferase	-	-	-	-	-	+	+
sgvM (sgv)	S_B precursor synthesis	SAM-dependent methyltransferase, for N,beta-dimethyl-L-leucine production	-	-	-	-	-	+	+
sgvA (sgv)	regulation	AfsA-like, GBL biosynthesis	-	-	-	-	*barX*	+	-
sgvK (sgv)	regulation	ketoreductase, GBL biosynthesis	-	-	-	-	*barS1*	+	-
sgvC (sgv)	regulation	phosphatase, GBL biosynthesis	-	-	-	-	-	+	-
barS2 (vir)	regulation	dehydratase, GBL biosynthesis	-	-	-	-	+	-	-
vmsR (vir)	regulation	TetR family transcriptional regulator	-	-	-	-	+	-	-
varR (vir)	regulation	TetR family transcriptional regulator	-	-	-	-	+	-	-
sgvT2 (sgv)	resistance	ABC transporter protein	-	-	-	-	*varL*	+	+
sgvT3 (sgv)	resistance	EmrB/QacA subfamily drug resistance transporter	-	-	-	-	-	+	+
sgvY (sgv)	resistance	streptogramin B lyase	-	-	-	-	-	+	-

To investigate the relationship between the carriers of the various streptogramin BGCs, the type strain genome server (TYGS; Meier-Kolthoff and Göker, 2019) platform was used to construct a phylogenomic tree which was then visualized by the Iroki webservice (Moore et al., 2020; Fig. 7). Whole genome sequences were used for the generation of the tree.

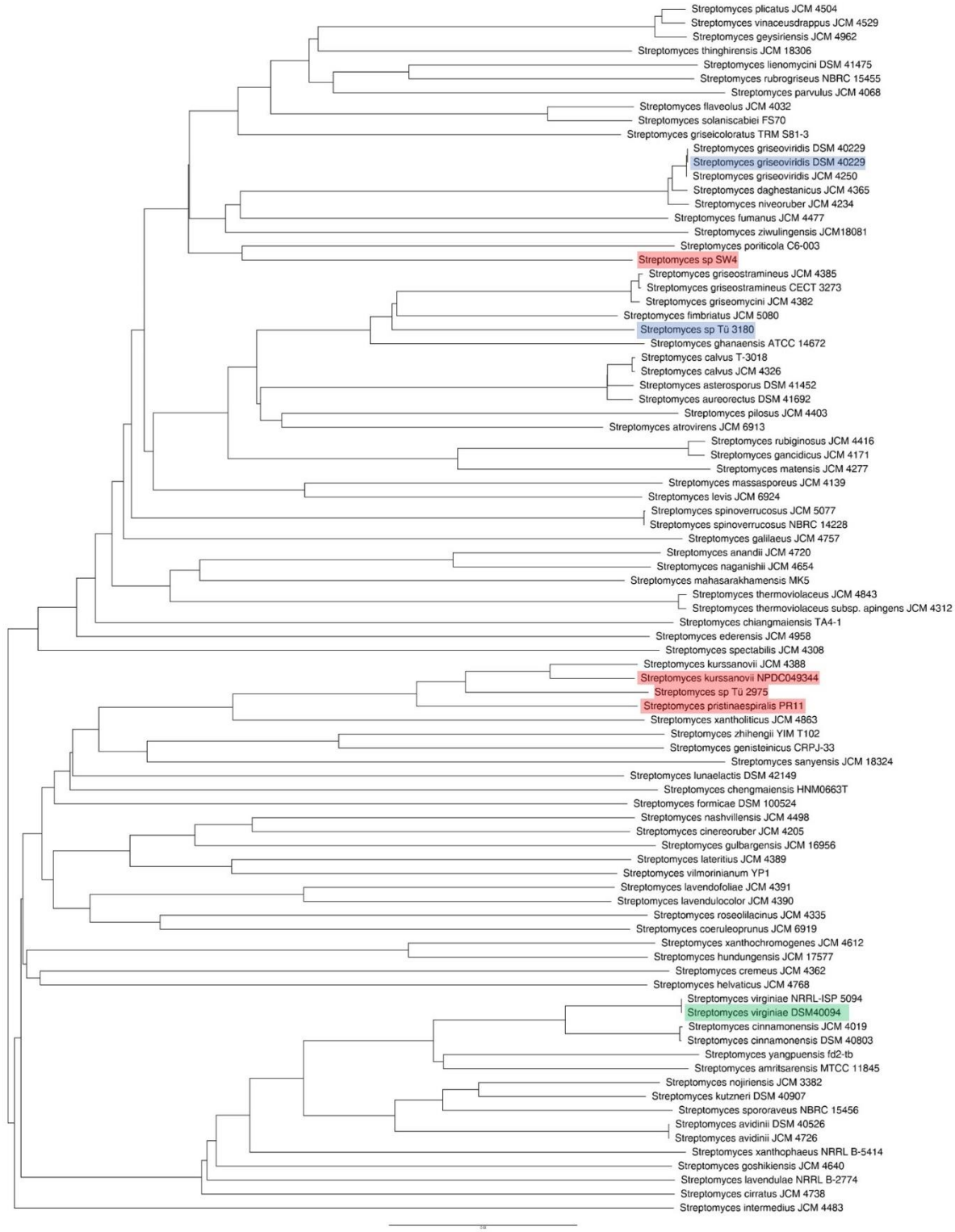

Figure 7: Phylogenomic relationship of the streptogramin BGC carriers investigated in this thesis on a whole genome level. Queried organisms are marked with a coloured background. blue: carriers of a *sgv* type BGC; red: carriers of a *prs* type BGC; green: carrier of the *vir* type BGC.

5.1.3. The *prs* type BGC

The *prs* type clusters are the largest clusters overall (*prs*: 210 kb, prs^{SW4}: 166 kb, prs^{kurs}: 161 kb, prs^{2974}: 158 kb; Fig. 6). The large size has multiple reasons. First, regions of varying, but substantial size (51-90 kb) and unknown function are located in all *prs* type clusters in addition to the genes associated with pristinamycin production. The *prs* type is also the most thoroughly researched in this comparison (Mast et al., 2011a; Mast et al., 2015). As all genes involved in the synthesis of PI and PII are known for the *prs* type, its defined borders are likely to contain the whole cluster, while the *sgv* and *vir* types might miss some genes. The genes coding for PI and PII synthesis are not strictly separated from each other in the *prs* type, giving the clusters a mosaic appearance.

The nucleotide sequences of the three *prs* type representatives were compared to *prs* of *S. pristinaespiralis* PR11 using Clone Manager 9. The following percent identities were obtained: 90% for prs^{2975}, 89% for prs^{kurs} and 69% for prs^{SW4}. This comparison excludes the large intergenic regions (IGRs; Fig. 6) of unknown function, which will be discussed separately below (5.1.4). Additionally, eight genes (upstream of *snbR*) at the right cluster border are excluded from the comparison, as a continuous sequence for this area is not available for prs^{kurs}. The three new representatives of the *prs* type therefore show a high overall nucleotide sequence identity with *prs* from *S. pristinaespiralis*. The carriers of prs^{2975} and prs^{kurs}, *Streptomyces* sp. Tü2957 and *S. kurssanovii*, respectively, also show a close relationship to *Streptomyces pristinaespiralis* PR11 on a whole genome level (Fig. 7). *Streptomyces* sp. SW4, carrier of prs^{SW4}, is however less closely related to the other *prs* type carriers. The cluster comparison revealed that homologs of all genes necessary for precursor supply and pristinamycin assembly can be found in all *prs* type BGCs of the newly identified producer strains and are organised in the same way as in *prs* (Tab. 1). Most regulatory genes are also found in the same organisation in all *prs* type BGCs. An exception is prs^{SW4}, which deviates from *prs* in the “regulatory island” region at the right cluster border. In *prs,* this region includes the regulatory genes *papR3*, *papR4*, *papR5,* and *spbR*, as well as some genes of unknown function (*snbS, snbW, snbV, snbU*). In prs^{SW4}, a putative TetR-type regulator, which shows 56% AA identity with PapR5, is encoded by a gene (SW4_3_00271) located between the homologs of *snbR* (SW4_3_00270) and *snbS (*SW4_3_00272*)*. Homologs of *snbV*, *papR3*, *papR4,* and

papR5 are missing in *prs*^{SW4} but an additional gene (SW4_3_00277) coding for a putative TetR-like regulator with 67% AA identity to SpbR is located directly upstream (further towards the right border) of the respective *snbU* homolog (SW4_3_00276). In *S. kurssanovii*, the regulatory island on the right cluster border seems to be missing at first glance. However, homologs to most genes of the regulatory island (with the exception of *snbS*) can be found in a different region of the assembly. This region is contig 9 (NZ_BMTN01000009.1; Fig. 8), while the rest of the cluster is located on contig 16 (NZ_BMTN01000016.1). Since the homologs share high nucleotide sequence identity (92% on average) to those found in *prs* and are organized in the exact same order, an error in the genome assembly seems to be the most likely reason for the apparently missing regulatory island in *prs*^{kurs}. *prs* and *prs*^{2975} both also feature a transposase coding gene (*trs2* in *prs* and 2975_1_00119 in *prs*^{2975}) between the genes *snaA* and *snaB* in *prs* and their homologs 2975_1_00118 and 2975_1_00120 in *prs*^{2975}. *prs*^{kurs} carries a transposase gene (IE119_RS27120) between the genes IE119_RS27125 and IE119_RS27115, which are homologs of *snaE1* and *snaF* from *prs*, respectively.

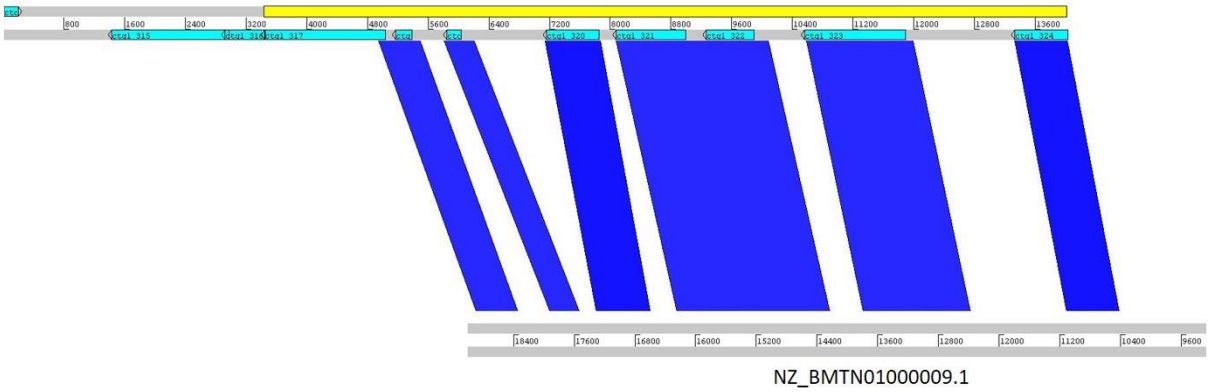

Figure 8: Nucleotide sequence similarity between the right cluster border of *prs* from *S. pristinaespiralis* PR11 (top, the sequence corresponding to the missing right border on *S. kurssanovi* contig 16 is marked in yellow), and contig 9 of the *S. kurssanovii* genome assembly (bottom). Blue indicates stretches of sequence similarity.

5.1.4. The *prs* type intergenic region

All *prs* type BGCs contain an additional subcluster of so far unknown function. A role in the synthesis of PI or PII is unlikely, since all pristinamycin encoding genes have been identified and are accounted for outside this IGR (Mast et al., 2011a). Despite

their overall high similarity, the four *prs* type clusters show variations in large parts of the IGR. In *S. pristinaespiralis* PR11, the IGR includes 87 ORFs of which 32 have been described as forming a potential type II polyketide BGC and were labelled as *cpp* (cryptic *pristinaespiralis* polyketide) cluster (Mast et al., 2011a). No biosynthesis product of the *cpp* cluster has been identified so far and the function of the remaining 55 ORFs in *prs* have not been investigated.

To compare the IGRs of the four *prs* type clusters, their nucleotide sequences were aligned using prfectBLAST (version 2.0) and visualised with Artemis (version 18.2; Fig. 9). All stretches shown have a BLAST bit-score of at least 350. This was the threshold chosen to avoid cluttering by very short stretches, without losing substantial amounts of information. The prs^{2975} and prs^{kurs} IGRs have an overall nucleotide sequence identity of 89%. For the purpose of clarity, both IGRs are therefore represented as one in Fig. 9.

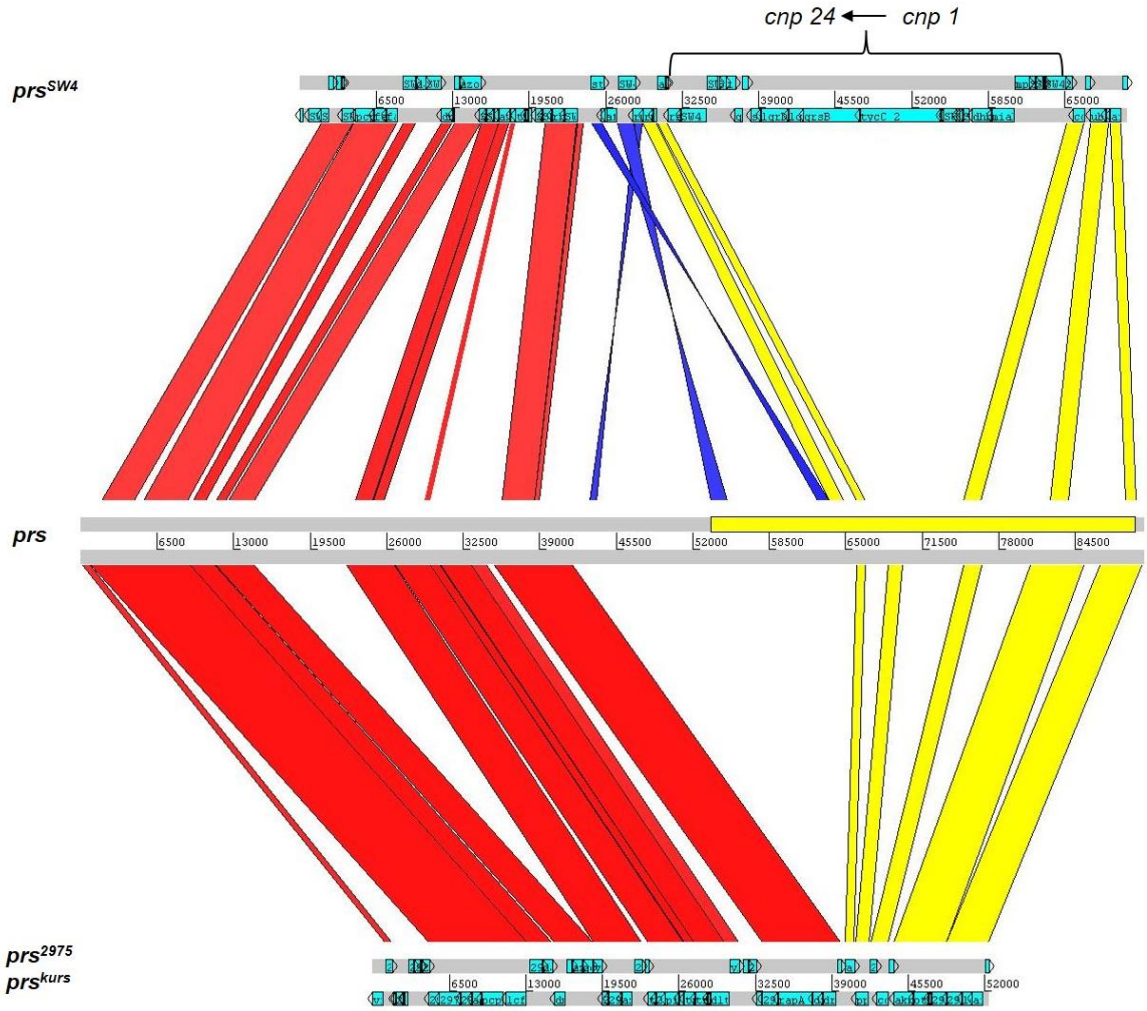

Figure 9: Sequence similarity between the intergenic regions in the pristinamycin clusters of SW4 (*prs*^{SW4}), *S. pristinaespiralis* PR11 (*prs*), and Tü 2975/*S. kurssanovii* DSM 40162 (*prs*^{2975}/*prs*^{kurs}). The proposed *cpp* cluster of *prs* and the respective sequence similarities are marked in yellow. Blue indicates inverted stretches of similarities and red marks similarities in regions of unknown function.

High sequence similarity was observed in the “left” part of all IGRs, which is the sequence region upstream of the pristinamycin specific regulator gene *papR6*. The *prs*^{2975}/*prs*^{kurs} IGRs share homology with that of *prs* on almost their entire lengths (Fig. 9). They do however lack multiple stretches that are present in the *prs* IGR. Specifically, large parts of the *cpp* cluster are missing. Like with *prs*^{2975}/*prs*^{kurs}, the IGR of *prs*^{SW4} shows sequence similarities to the *prs* IGR over the length of the whole region. While parts of the *cpp* cluster are also missing in the IGR of *prs*^{SW4}, it does

feature more “unique” areas. The most prominent differences to the *prs* IGR are found in the “middle” and “right” part of the IGR subcluster. Here, the *prs*^{SW4} IGR includes 24 ORFs that are neither found in *prs*, nor in *prs*^{2975}/*prs*^{kurs}. These ORFs were designated *cnp 1-24* (cryptic non-ribosomal peptide, Fig. 9, Tab. 2) since seven of the *prs*^{SW4} IGR ORFs (*cnp5, 7, 13, 14, 15, 16, 17*) code for enzymes related to non-ribosomal peptide (NRP) synthesis.

Table 2: ORFs unique to the IGR of *prs*^{SW4}. ORFs with predicted function related to NRP synthesis are highlighted in green.

ORF	antiSMASH locus ID	proposed function (based on annotation by NCBI)
cnp1	SW4_3_00204	hypothetical protein
cnp2	SW4_3_00203	hypothetical protein
cnp3	SW4_3_00202	hypothetical protein
cnp4	SW4_3_00201	hypothetical protein
cnp5	SW4_3_00200	Enduracididine beta-hydroxylase
cnp6	SW4_3_00199	tRNA-2-methylthio-N(6)-dimethylallyladenosine synthase
cnp7	SW4_3_00198	Dimodular nonribosomal peptide synthase
cnp8	SW4_3_00197	hypothetical protein
cnp9	SW4_3_00196	hypothetical protein
cnp10	SW4_3_00195	hypothetical protein
cnp11	SW4_3_00194	hypothetical protein
cnp12	SW4_3_00193	hypothetical protein
cnp13	SW4_3_00192	Tyrocidine synthase 3
cnp14	SW4_3_00191	Gramicidin S synthase 2
cnp15	SW4_3_00190	Linear gramicidin synthase subunit D
cnp16	SW4_3_00189	Linear gramicidin synthase subunit D
cnp17	SW4_3_00188	Surfactin synthase subunit 2
cnp18	SW4_3_00187	hypothetical protein
cnp19	SW4_3_00186	Na(+)/H(+)-K(+) antiporter GerN
cnp20	SW4_3_00185	L-isoleucine-4-hydroxylase
cnp21	SW4_3_00184	hypothetical protein
cnp22	SW4_3_00183	Ferredoxin-NADP reductase
cnp23	SW4_3_00182	hypothetical protein
cnp24	SW4_3_00181	Small ribosomal subunit biogenesis GTPase RsgA

In addition, a region within the IGR of *prs*^{SW4} does in part align invertedly to *prs* (Fig. 9). In the IGR of *prs*^{SW4}, this region contains five ORFs (SW4_3_00176, SW4_3_00175, SW4_3_00174, SW4_3_00173 and SW4_3_00172) which are present on *prs* (Tab. 3). The respective ORFs in *prs*, (H3L99_RS01180 outside the *cpp* cluster; *cpp32, cpp28,* and *cpp25* inside the *cpp* cluster) are not located as close

together as those in *prs*^{SW4}, but retain the same order (if the sequence is inverted; Tab. 3). These findings indicate that a recombination event might have taken place in this region of the original IGR.

Table 3: ORFs found in a region of the *prs*^{SW4} IGR that inversely aligns to the *prs* IGR (- = no sequence similarity).

locus ID in *prs*^{SW4}	ORF name/locus ID in *prs*	proposed function (based on annotation by NCBI)
SW4_3_00176	H3L99_RS01180	dTDP-4-dehydrorhamnose 3,5-epimerase family
SW4_3_00175	*cpp32*	NDP-hexose 2,3-dehydratase
SW4_3_00174	*cpp28*	oxidoreductase
SW4_3_00173	-	-
SW4_3_00172	*cpp25*	dTDP-glucose 4,6-dehydratase

5.1.5. The *vir* type BGC

The *vir* type is the smallest known streptogramin BGC (77 kb). It does not contain an IGR like the *prs* type. Most of the genes involved in VM/VS biosynthesis are homologs of those found for PI/PII synthesis in *prs* and are organized in the same manner (Fig. 6). There are however exceptions as follows. Even though VM1 is identic to PIIA and VM2 is identic to PIIB, no homologs to the *prs* genes *snaB* and *snaA*, which are essential for the conversion of PIIB to PIIA, are present in *vir*. How the conversion of VM2 to VM1 is realised, is unknown but the products of *virM* and *virN* are suggested to be responsible (Pulsawat et al., 2006). Unlike PI, VS does not include DMAPA but N-methyl-L-phenylalanine (Fig. 5). This explains why homologs of the genes that encode DMAPA synthesis (*papA*, *papC*, *papB*, *papM*) in the *prs* type are missing in *vir* (Tab. 1). Besides *varS*, a homolog to *snbR* from *prs*, *vir* contains two additional putative resistance genes (*varL* and *varM*). *varL* and *varM* both code for ABC transporters (Kitani et al., 2010). *vir* contains three TetR (*barB*, *varR and barZ)* type regulator genes in contrast to the two (*papR3*, *papR5*) found in *prs* and one response regulator gene (*vmsT*). However, only two SARP type regulator genes (*vmsS*, *vmsR*) are found in *vir,* compared to three in *prs (papR1, papR2,* and *papR4)*. *vir* also includes a γ-butyrolactone receptor gene (*barA*). Three genes (*barX*, *barS1* and *barS2*) are suggested in the synthesis of the corresponding γ-butyrolactone (Shikura et al., 2002; Lee et al., 2008 and 2010). *vir* also misses a number of genes which are found in *prs*, which do not have a known function (*snaG, snbT, snbS, snbW, snbV*).

5.1.6. The *sgv* type BGC

The *sgv* type is smaller than the *prs* type but larger than *vir* (*sgv*: 105 kb, *sgv*^{3180}: 89 kb). Similar to the *vir* type, the *sgv* type does not contain an IGR. GV and VG synthesis genes are strictly separated in *sgv* in contrast to the mosaic organisation of *prs* and *vir*. GV and VG structurally differ from PI and PII far more than VM and VS (Fig 6). This is reflected by the genes involved in precursor supply. Unlike PII and VM, GV incorporates acetyl-CoA, which is drawn from the primary metabolism, as its starter unit instead of isobutyryl-CoA. In agreement with this, *sgv* does not contain a homolog of the corresponding branched-chain α-keto acid decarboxylase *snaF*, which is needed for the synthesis of Isobutyryl-CoA. Where PI and VS incorporate DMAPA and N-methyl-phenylalanine, respectively, at position five and OPPA at position six, VS deviates by incorporating three AA in this segment of the backbone (sarcosine, N,β-dimethyl-leucine and L-alanine) instead. This explains why the *vir* type cluster lacks homologs of the synthesis genes for DMAPA or OPPA (*papM*, *papB*, *papC*, *papA*, *snbF*, *pipA*; Tab. 1). Unique non-proteinogenic precursors that have to be synthesised for VG assembly are N,β-dimethyl-leucine and 4-hydroxy-D-proline. In agreement with the need to synthesize N,β-dimethyl-leucine, two genes, *sgvG* and *sgvM*, coding for a branched-chain amino acid aminotransferase and a SAM-dependent methyltransferase respectively (Xie et al., 2012), are found as an operon in the *sgv* type. The biosynthetic pathway for the VG precursor 4-hydroxy-D-proline is not fully elucidated. 4-hydroxy-L-proline is thought to be synthesised first and epimerised to the D form by the first module of the corresponding NRPS (encoded by *sgvD3*) before incorporation into the peptide backbone (Xie et al., 2012). No gene that codes for the expected 4-hydroxylase needed for 4-hydroxy-L-proline synthesis can be found in the *sgv* type cluster. While L-phenylsarcosine is only found in VG, it most likely follows a similar synthesis pathway as L-Phg (Xie et al., 2012) and is methylated during or after incorporation. Homologs of the L-Phg synthesis associated genes *pglA-D* (*sgvN*, *sgvH1*, *sgvH2*, *sgvH3*) are found in accordance with this in *sgv*. A homolog of the aminotransferase gene *pglE* is however missing. Regulation involves two SARP type activator genes (*sgvR2, sgvR3*) and one TetR-type regulatory gene (*sgvR1*). Additionally, a γ-butyrolactone receptor gene (*sgvB*) and potential γ-butyrolactone synthesis genes (*sgvA*, *sgvK*, *sgvC*) are present. Four genes associated with self-

resistance are found throughout the *sgv* type cluster, coding for a member of the major facilitator superfamily (*sgvT1*), an ABC transporter protein (*sgvT2*), an EmrB/QacA subfamily drug resistance transporter (*sgvT3*), as well as a streptogramin B lyase (*sgvY*). The *sgv* type is the only known streptogramin cluster type to include a streptogramin B lyase gene. Streptogramin B lyases are proteins which are encoded by genes that are often found on plasmids that confer resistance against both, S_A and S_B antibiotics, to pathogens.

Comparison of the *sgv*^{3180} nucleotide sequence to that of *sgv* from *S. griseoviridis* using Clone Manager 9 revealed an overall sequence identity of 70%. This comparison excludes larger regions that are missing from *sgv*^{3180} (Fig. 6). On a whole genome level, *S. griseoviridis* and *Streptomyces* sp. Tü3180 do not share the same close relationship as most carriers of the *prs* type BGCs (Fig. 7). Most of the genes in *sgv,* which are suggested to be involved in precursor supply and VG/GV assembly, have homologs in *sgv*^{3180} (Tab. 1). The only one of these genes missing in *sgv*^{3180} is a homolog of *sgvH3,* which encodes the putative branched-chain α-keto acid dehydrogenase SgvH3. SgvH3 is suggested to be a homolog of PglD from *S. pristinaespiralis,* which is a thioesterase involved in the synthesis of L-Phg. It was shown by gene deletion experiments that SgvH3 is not essential for GV synthesis in *S. griseoviridis* and its definitive role is unknown (Xie et al., 2012). Furthermore, homologs of most of the genes which are proposed to be involved in regulation (*sgvR2*, *sgvR1*, *sgvB*, *sgvA*, *sgvK*, *sgvC*), the streptogramin B lyase gene *sgvJ* and the sarcosine oxidase coding gene *sgvS* are missing in *sgv*^{3180}. While the reason for this missing regulatory region in sgv^{3810} might be a genome assembly error, the respective genes could not be found elsewhere in the Tü 3810 genome sequence data. Overall, *sgv*^{3180} is highly similar in sequence and organization to *sgv* from *S. griseoviridis*, but does not contain the last ≈8,2 kbp of the *sgv* clusters right border (Fig. 6).

5.2. Production of new antibiotics by mutasynthesis

New antibacterial compounds can be obtained from the structural modification of known antibiotics. While synthetic chemistry provides many opportunities for the modification of antibiotics, an alternative approach involves the modification of antibiotic natural compounds by the targeted supplementation of the corresponding producer strain. Supplying an antibiotic producer with selected analogs of the natural

product precursors can lead to the incorporation of these analogs into the biosynthetic assembly line of the antibiotic and thus the subsequent generation of novel compounds.

Publication 2, describes the successful employment of this method, known as precursor directed biosynthesis, to generate new derivatives of the nucleoside antibiotic amicetin by fermentation of *Streptomyces sp*. SHP22-7. Three previously unknown natural derivatives were identified in addition. Since production of the natural derivatives was low, isolation and structural analysis of the natural amicetin derivatives necessitated the cultivation and extraction of 26 L SHP22-7 culture (Publication 2).

To increase both, the chances of installing a precursor analog into the final compound and the amount of derivative produced, mutasynthesis is a suitable method. The goal of Publication 1 was to generate new congeners of the streptogramin B type antibiotic pristinamycin I. The L-phenylglycine residue of PI is a suitable target for derivatization because of its uniqueness and its structural importance for many clinically relevant antibiotics, characterized by the presence of Phg or Phg-like residues (Fig. 10)

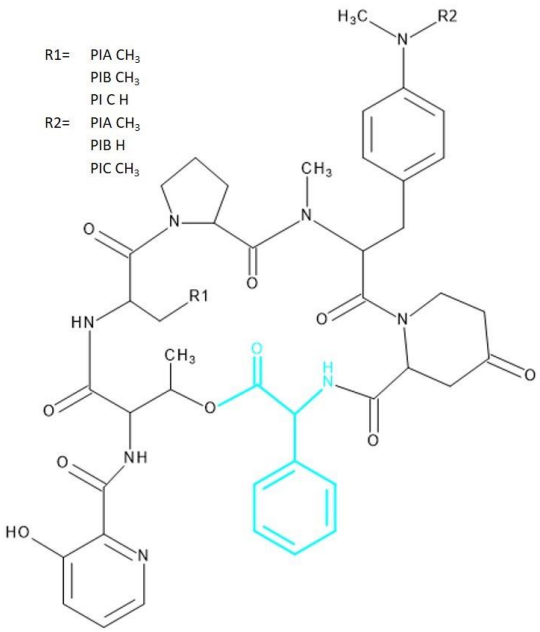

Figure 10: Structures of PI and its congeners PIA, PIB, and PIC. The L-Phg residue is highlighted in blue.

Preliminary modeling analysis using SeeSAR software was carried out by P. Klahn with the crystal structure of PI bound to the 70S ribosome of *Deinococcus radiodurans* (Harms et al., 2004), to estimate where exactly the Phg residue is positioned and what effect the derivatization might have (Fig. 11). Thereby it was found that the Phg residue resides in a binding pocket within the ribosome, whereby the para-carbon atom of L-Phg is distanced between 4.11 and 10.21 Å away from the ribosomal backbone, providing enough space for modification at the para-position, without causing sterical interference within the binding pocket. Additionally, L-Phg is expected to be involved in the binding of PI to its target at the bacterial 23S RNA of the bacterial ribosome. It is also located in a way that sterical clashes with its surroundings due to modifications at the aromatic sidechain are unlikely.

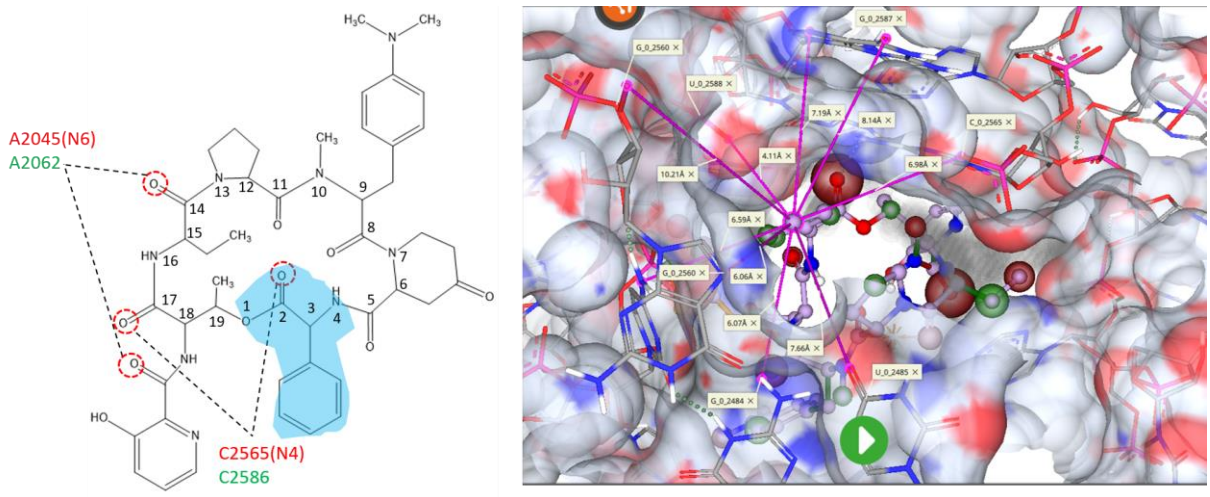

Figure 11: Left: Interactions of PI with 23S rRNA according to Harms et al. 2004. The hydrogen bonds towards 23S rRNA nucleotides are indicated as interrupted lines. Nucleotide numbering is according to the *E. coli* (in green) and *D. radiodurans* (in red) ribosomal crystal structure. Phg residue is highlighted in blue. Right: SeeSAR modeling data showing the distances (in Å) from the PI Phg residue to the 50 S ribosomal subunit of *D. radiodurans* (data provided by P. Klahn).

Finally, L-Phg is the last residue to be added to the PI backbone. Synthetic derivatives therefore do not have to be “dragged along” for most of the PI assembly. It was reasoned that this would increase the likelihood of L-Phg derivative incorporation as there are fewer reaction steps where deviations from the natural substrate L-Phg could interference with the actions of the NRPS machinery. All of the mentioned reasons led to the decision to modify PI by substitution of its L-Phg residue (Fig. 10). To this end,

derivatives of the non-proteinogenic amino acid precursor L-Phg were fed to a genetically modified strain of the natural producer *S. pristinaespiralis*.

5.2.1. Generation of a *S. pristinaespiralis* mutant suitable for mutasynthesis

To make use of the mutasynthesis principle, knowledge of the respective biosynthetic pathway is a prerequisite to inactivate the synthesis of the precursor that is supposed to be substituted. The biosynthetic pathway for L-Phg in *S. pristinaespiralis* is well characterized by the generation and complementation of deletion mutants for the involved genes (*pglA-D*; Mast et al., 2011b).

The results of Publication 4 provide further information about the effect of deleting genes belonging to the *pgl* operon. Here, a synthetic Phg synthesis pathway was constructed for heterologous expression. Amongst other strains, various mutants of *S. pristinaespiralis* were tested as hosts. While investigating the effect of a *pglE* deletion in *S. pristinaespiralis* as a host, the respective mutant *S. pristinaespiralis MpglE* has been shown to still produce a small amount of Phg (Publication 4). Deletion of *pglE* is therefore insufficient to abolish L-Phg synthesis and to create a suitable *S. pristinaespiralis* mutasynthesis mutant.

Additionally, the *pglA* mutant *S. pristinaespiralis MpglA* was available from previous work, which was confirmed as L-Phg deficient strain (Mast et al., 2011b). Therefore, *MpglA* was used as a basis for the construction of a *S. pristinaespiralis* mutant suitable for mutasynthesis of PI derivatives. To facilitate detection and purification of PI derivatives and to eliminate the antibiotic background activity caused by PII, the production of the S_A type was abolished. For this purpose, the hybrid PKS/NRPS enzyme encoding gene *snaE1*, which is essential for PII biosynthesis, was inactivated by homologous recombination. Homologous flanks of the coding region of *snaE1* were amplified from genomic DNA of *S. pristinaespiralis* PR11 by PCR. Both regions were cloned into the *E. coli* cloning vector pK18 and a thiostrepton resistance cassette was added in between for selection, which yielded the knockout construct pK18MsnaE1. pK18MsnaE1 was transferred to *S. pristinaespiralis MpglA* by PEG mediated protoplast transformation. The generation of the double mutant *S. pristinaespiralis* Δ*pglA*Δ*snaE1* was confirmed by PCR (Fig S26, supplementary information Publication 1).

5.2.2. Verification of the suitability of the *S. pristinaespiralis* Δ*pglA*Δ*snaE1* mutant for the mutasynthesis approach

The pristinamycin production of the *S. pristinaespiralis* Δ*pglA*Δ*snaE1* double mutant was analysed to assess its suitability for the mutasynthesis approach. *S. pristinaespiralis* PR11 was used as a control. The double mutant was cultivated with and without the addition of 100 µM L-Phg to the culture medium. Both strains were grown for 48 h in HT7T medium. Cultures were extracted with ethyl acetate and crude extracts were analysed by HPLC and used for bioactivity tests against *B. subtilis* ATCC 6633. Crude extracts of *S. pristinaespiralis* PR11 showed peaks with characteristic retention times (8.2 and 10.3 min) and UV-Vis spectra (data not shown) for PI and PII, respectively, in HPLC analysis and also exhibited bioactivity against *B. subtilis* (Fig. 12 A, B). Extracts of *S. pristinaespiralis* Δ*pglA*Δ*snaE1* neither showed peaks, characteristic for PI nor PII and did not exhibit inhibition against *B. subtilis* (Fig. 12 C, D). Extracts of the double mutant supplemented with L-Phg showed only a peak with a retention time of 8.3 min and a UV-Vis spectrum characteristic for PI, as well as exhibited bioactivity against *B. subtilis* (Fig. 12 E, F). These results confirmed that *S. pristinaespiralis* Δ*pglA*Δ*snaE1* is suitable to be used as mutasynthesis strain for PI derivatization.

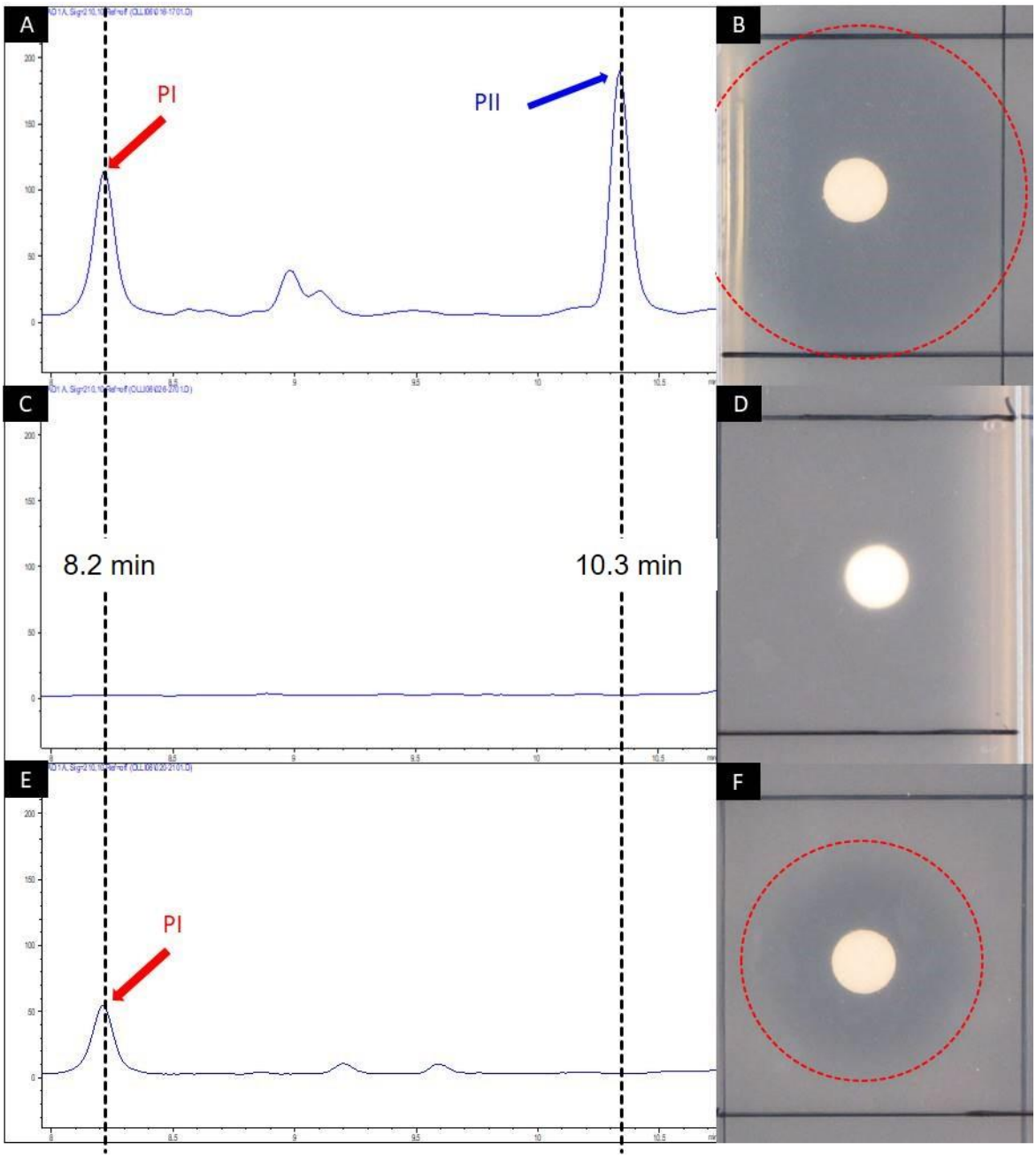

Figure 12: HPLC spectrum of crude extract samples from *S. pristinaespiralis* wild-type (A), *S. pristinaespiralis* Δ*pglA*Δ*snaE1* (C) and Δ*pglA*Δ*snaE1* supplemented with 100 µM L-Phg (E). Chromatogram shows peaks measured at 210 nm. PI- and PII-specific peaks were detected at retention time 8.2 and 10.3 min, and are indicated by red and blue arrows, respectively. Disc diffusion assays with the respective extract samples against *B. subtilis* (B, D, and F). Inhibition zones are marked with red circles (Publication 1, mod.).

5.2.3. Generation of new PI derivatives by mutasynthesis

Twelve mutasynthons were used in feeding experiments with *S. pristinaespiralis* Δ*pglA*Δ*snaE1* as described above (Tab. 4). Fermentation broths were extracted with

ethyl acetate and analysed via HPLC/MS. Supplementation with six mutasynthons (D-Phg, 2,5-dihydro-D-Phg, 4-fluoro-L-Phg, 2-fluoro-DL-Phg, 4-chloro-DL-Phg, 4-hydroxy-DL-Phg) led to the production of compounds that matched the mass of the corresponding PI derivative, which was calculated based on the mass of the natural PIA (866.4, PubChem 2.1) plus the mass of the respective additions to the L-Phg residue (Tab. 4). Three mutasynthesis samples, those of cultures supplemented with D-Phg, 4-fluoro-L-Phg, 4-chloro-DL-Phg, showed bioactivity against *B. subtilis* ATCC6633 (Tab. 4). PI production of *S. pristinaespiralis* Δ*pglA*Δ*snaE1* was however generally low and unstable, even when fed with the natural precursor L-Phg, when compared to *S. pristinaespiralis* PR11. The most stable production was observed after supplementation with 4-fluoro-L-Phg and 4-chloro-DL-Phg, which resulted in of the respective PI derivatives, named fluoro-PI and chloro-PI, respectively. Further work was therefore focused on isolation and structural characterization of fluoro-PI and chloro-P. As a control, unchanged PI (produced from *S. pristinaespiralis* Δ*pglA*Δ*snaE1* supplemented with L-Phg) was used and referred to as C-PI.

Table 4: List of tested mutasynthons with indication if PI derivatives with expected masses have been detected by HPLC/MS analysis and antibacterial activity observed in bioassays (n.t. = not tested). + = derivative/bioactivity observed; - = not observed.

Mutasynthon	**calculated mass of PI derivative**	**new PI-derivative/mass detected**	**bioactivity against *B. subtilis***
D-Phg	866.4	+	+
2,5-dihydro-D-Phg	868.4	+	n.t.
4-fluoro-L-Phg	884.4	+	+
2-fluoro-DL-Phg	884.4	+	n.t.
4-chloro-DL-Phg	900.4	+	+
2-chloro-DL-Phg	900.4	-	n.t.
4-bromo-DL-Phg	944.3	-	n.t.
4-amino-DL-Phg	881.4	-	n.t.
4-hydroxy-DL-Phg	882.4	+	n.t.
2,2-di-Phg	942.4	-	n.t.
3-(trifluoromethyl)-DL-Phg	934.4	-	n.t.
4-(trifluoromethyl)-L-Phg	934.4	-	n.t.

Preliminary structural confirmation of the halogenated PI derivatives was conducted by HPLC-MS/MS analysis. First, a sample containing C-PI was analysed to characterise the fragmentation pattern of PI. Three prominent and reoccurring mass signals (*m/z* 578.3, 663.3, 839.4) were identified and assigned to fragments of the PI parent ion, which all contained the L-Phg residue (Fig. S1 a, supplementary information publication 1). HPLC-MS/MS analysis of extracts from 4-fluoro-L-Phg and 4-chloro-DL-Phg supplemented *S. pristinaespiralis* Δ*pglA*Δ*snaE1* cultures showed a similar fragmentation pattern. The *m/z* signals were however shifted by the mass of the corresponding incorporated halogen atom, resulting in a mass shift of +18 and +34 in the extracts of 4-fluoro-L-Phg and 4-chloro-DL-Phg supplemented cultures, respectively (Fig. S1 b and c, supplementary information publication 1). The mass shift accounts for the loss of one hydrogen atom, which explains the shift by the mass of the respective halogen -1. These results suggested the successful incorporation of the respective mutasynthons into PI which resulted in the production of the novel pristinamycin derivatives fluoro-PI and chloro-PI.

Larger scale production and isolation of halogenated PI derivatives was carried out to verify the chemical structures of the PI derivatives by NMR. In total, 6 L and 12 L of

culture were extracted for fluoro-PI and chloro-PI isolation, respectively. Extracts were purified by flash-chromatography and preparative HPLC, resulting in pure fractions of both halogenated PI derivatives. Purification was carried out with the help of Karen Harms (research group Microbial Drugs, HZI Braunschweig). For fluoro-PI, two fractions, F2 (1,54 mg) and F2.1 (1,88 mg), were obtained, whereas one pure fraction, F3 (0,6 mg), was obtained for chloro-PI (Protocol S1 and S2, Fig. S2 and S3, supplementary information Publication 1). Fractions F2.1 and F3 were subjected to H-NMR-spectral analysis, which confirmed the expected structures of fluoro-PI and chloro-PI, respectively (Table 2 and 3, Publication 1). NMR analysis was performed by Dr. Frank Surup (research group Microbial Drugs, HZI Braunschweig).

5.2.4. Bioactivity profile of the halogenated PI derivatives generated by mutasynthesis

5.2.4.1. Quantitative bioactivity tests with pure halogenated PI derivatives

To determine the antibiotic potency of the halogenated PI derivatives, minimal inhibition concentration (MIC) assays against a panel of standard test organisms were conducted. However, since pure chloro-PI was not available in sufficient amounts, only fluoro-PI was analysed in MIC assays. For MIC assays, the pure fraction F2.1 was used, while pure PI (Sanofi Aventis) served as a control (Tab. 5). Both, fluoro-PI and PI, inhibited the growth of *B. subtilis* and *S. aureus* but did not inhibit Gram-negative or fungal test strains (Tab. 5). The observed MICs of PI were 2,1 µg/ml for *B. subtilis* and 16,7 µg/ml for *S. aureus.* Fluoro-PI MICs were 4,2 µg/mg for *B. subtilis* and 33,3 µg/mg for *S. aureus.* With the MICs for fluoro-PI being in a similar range as those of PI, it can be concluded that the fluorinated derivative is similar in potency as the natural pristinamycin compound. MIC assays were performed by Dr. Frank Surup.

Table 5: MIC assay of pristinamycin IA (PI) and fluoro-PI derivative against standard test organisms. Inhibited organisms are highlighted in bold. (n.i. = not identified).

		PI	fluoro-PI	
test organism	**DSM-Nr.**	**MIC µg/mL**	**MIC µg/mL**	**positive control**
Schizosaccharomyces pombe	70572	n.i.	n.i.	Nystatin
Pichia anomala	6766	n.i.	n.i.	Nystatin
Mucor hiemalis	2656	n.i.	n.i.	Nystatin
Candida albicans	1665	n.i.	n.i.	Nystatin
Rhodotorula glutinis	10134	n.i.	n.i.	Nystatin
Acinetobacter baumannii	30008	n.i.	n.i.	Ciprofloxacin
Escherichia coli	1116	n.i.	n.i.	Oxytetracyclin
Bacillus subtilis	**10**	**2,1**	**4,2**	Oxytetracyclin
Mycobacterium smegmatis	ATCC 700084	n.i.	n.i.	Kanamycin
Staphylococcus aureus	**346**	**16,7**	**33,3**	Oxytetracyclin
Pseudomonas aeruginosa	PA14	n.i.	n.i.	Gentamycin
Chromobacter violaceum	30191	n.i.	n.i.	Oxytetracyclin

To investigate cytotoxicity of fluoro-PI, fraction F2.1 was tested against the human cell lines KB3.1 and L929 in cytotoxicity assays (Tab. 6). No morphological change of cells was observed and only a low inhibition of proliferation was detected in cell line KB3.1. Therefore, fluoro-PI has no obvious cytotoxic effect. Cytotoxicity assays were performed by Dr. Frank Surup.

Table 6: Cytotoxicity assay of fluoro-PI derivative against human cell lines (* = no changed cells, no cytotoxic activity; ** = no changed cells, low inhibition in proliferation)

Compound name	KB3.1 cell line	Tox-Nr.	L929 cell line	Tox-Nr.
fluoro-PI (F2.1)	**	**3548**	*	**3549**

5.2.4.2. Bioactivity tests against clinical isolates

To discern whether the halogenated PI derivatives inhibited clinically relevant microorganisms, further bioactivity assays were performed against clinical pathogens, amongst them streptogramin resistant strains. As the amount of pure PI derivatives was limited, methanolic solutions of crude extracts and semi purified fractions thereof were used. “Semi purified” refers to fractions obtained by small scale semi preparative

HPLC runs to remove some of the residual background from the crude extracts in order to ensure that the observed bioactivity was caused by the respective PI derivative. Efforts were made to equalize the amount of PI derivatives used in these experiments by calculations based on HPLC chromatograms of the respective extracts and standard curves with pure PI. Bioassays were conducted as zone of inhibition tests.

Crude extracts were tested against organisms from the WHO priority list of pathogens. The test panel included Gram-negative (*Escherichia coli* DSM 1103, *Proteus vulgaris* DSM 2140, *Pseudomonas aeruginosa* DSM 1117) and Gram-positive bacteria (*Staphylococcus aureus* DSM 18827, *Enterococcus faecium* DSM 20477) bacteria, as well as fungi (*Candida albicans* DSM 1386, *Trichophyton rubrum* DSM 16111; Tab. S1, supplementary information publication 1). Filter discs were loaded with crude extracts of fluoro-PI, chloro-PI, C-PI, and pure PI to contain approximately 0,5 µg of the respective compound. All tested substances inhibited the growth of *E. faecium* DSM 20477 while only Synercid® inhibited *S. aureus* DSM 18827 (Fig. 13). None of the tested substances inhibited any of the remaining strains.

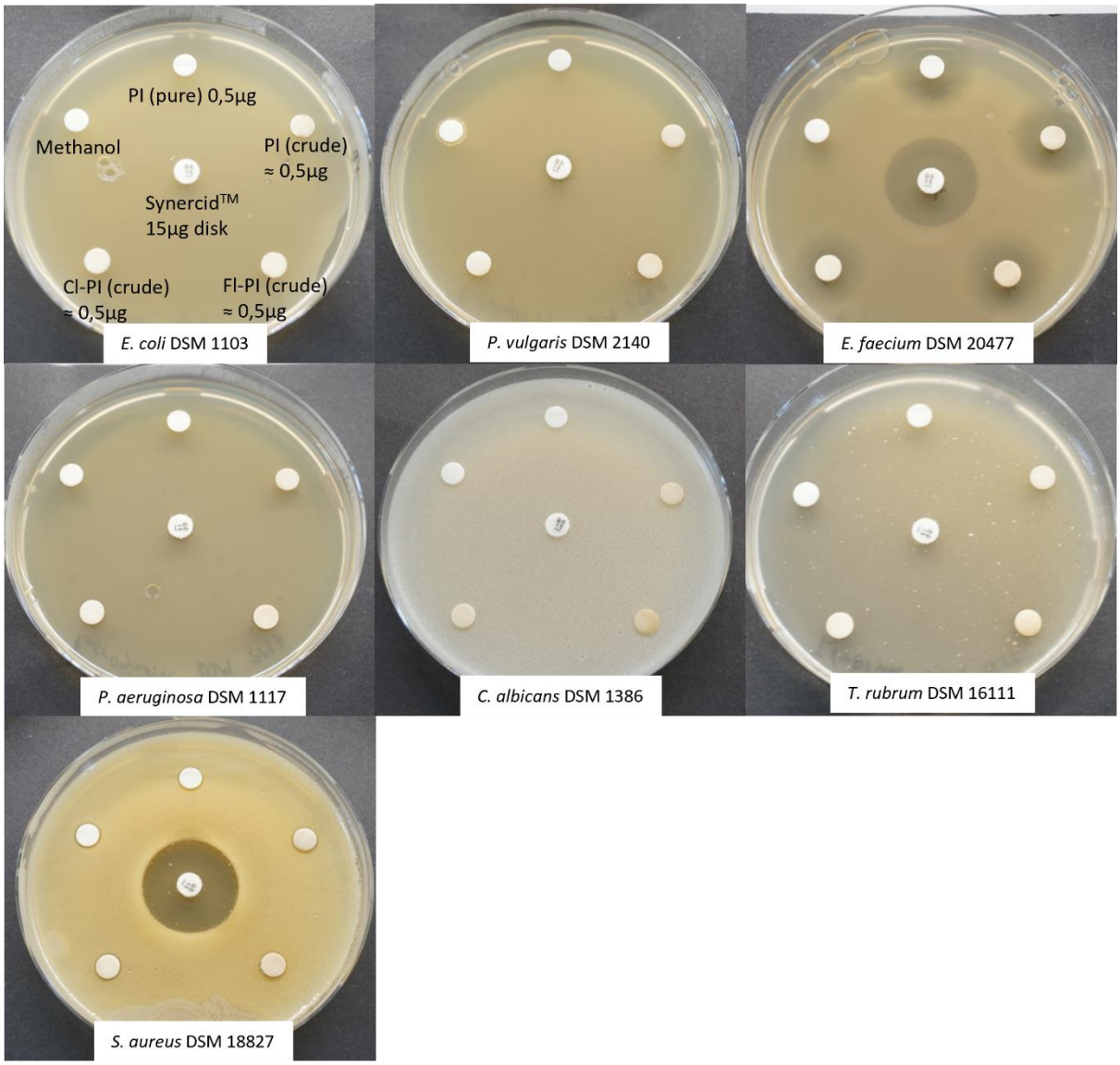

Figure 13: Results of the agar diffusion test of PI derivatives against clinically relevant pathogens. Synercid® filter discs were used as a positive, filter discs with methanol as negative control. The pattern of sample application follows that of the *E. coli* DSM 1103 example.

Semi purified fractions of PI derivatives were tested in combination with the corresponding S_A antibiotic PII to investigate their combined activity. Of the previous bioassay test panel, only the streptogramin sensitive *S. aureus* DSM 18827 and *E. faecium* DSM 20477 were tested in this experiment. To investigate if the new PI derivatives inhibit organisms which are specifically streptogramin resistant, two further clinical *S. aureus* isolates, CIP 111304 and CIP 108540, which both carry resistance genes against S_A and S_B antibiotics, were included (Tab. S1, Supplementary

Information publication 1). Filter discs were loaded with semi purified fractions of fluoro-PI, chloro-PI, C-PI and pure PI to contain approximately 5 µg of the respective compound. The test was conducted with and without the additional application of 5 µg pure PII to each disc. All tested semi pure fractions showed inhibition against the respective test organisms, similar to that of pure PI (Fig. 14). The same holds true for the combinations of semi pure fractions with pure PII, which showed similar inhibition as the control mixture of PI with PII. *S. aureus* CIP 111304 and CIP 108540 were not inhibited by the application of PI nor its derivatives alone (Fig. 14). This indicates that resistance mechanisms against streptogramins, here specifically against the S_B type PI, confers resistance to the halogenated PI derivatives as well. Both *S. aureus* test strains, CIP 111304 and CIP 108540, were however inhibited by combinations of PI or its derivatives in combination with pure PII.

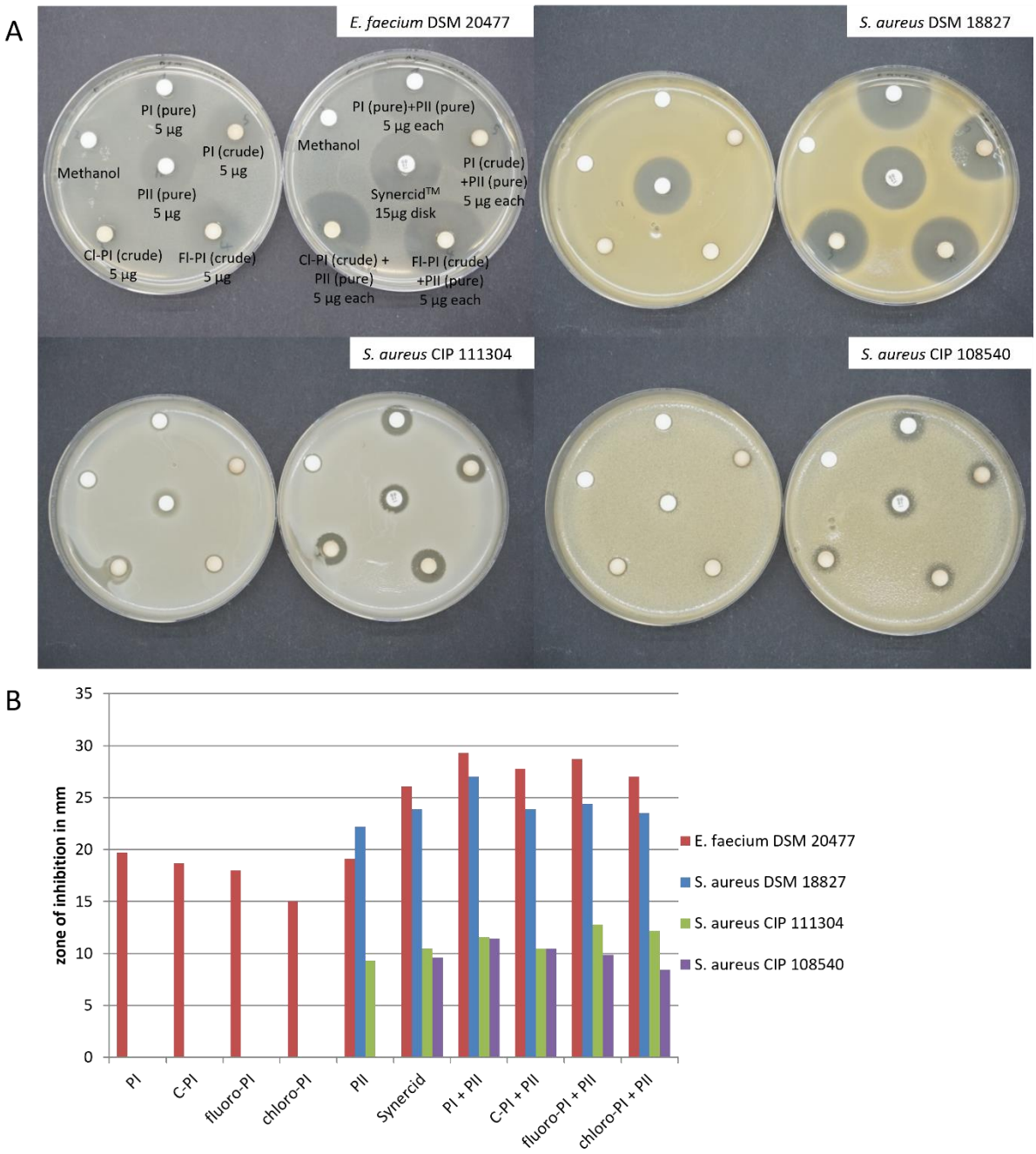

Figure 14: Results of the agar diffusion test of PI derivatives alone and in combination with PII against streptogramin susceptible clinical isolates. Semi purified samples of C-PI, fluoro-PI, chloro-PI were used as well as pure PI and PII. All S_B samples were applied with and without the addition of PII. Synercid® filter discs were used as a positive, filter discs with methanol as negative control. **A:** Inhibition zones caused by PI derivatives. The pattern of sample application follows that of the *E. faecium* DSM 20477 example. **B**: Diameter of inhibition zones caused by PI derivatives.

Altogether, the experiments concerning the bioactivity of fluoro-PI and chloro-PI showed that both new pristinamycin derivatives are antimicrobially active, with the

potency of these new derivatives being very similar to that of the natural PI. Fluoro-PI and chloro-PI are also active against the same organisms as PI. Finally, resistance mechanisms against streptogramin antibiotics protect test organisms against fluoro-PI and chloro-PI, as well as against PI.

6. Discussion

6.1. Identification of a new streptogramin producer and characterization of known streptogramin BGCs

In this work, available genome data of strains from the DSMZ strain collection were screened for the biosynthetic potential to synthesize L-Phg, using the phenylglycine dehydrogenase gene *pglA* from *S. pristinaespiralis* as a reference. Screening for genes involved in the synthesis of Phgs can lead to the identification of novel peptide antibiotics containing Phg residues which, as proposed in a previous study, are associated specifically with antibacterial activities (Walker and Clardy et al., 2021). In recent years genome mining has developed into a potent tool for the identification of novel natural compounds with bioactivity. Genes, which code for enzymes known to be involved in the synthesis of certain bioactivity-conferring features, can be used in screenings to identify compounds containing these features. Multiple approaches were reported, which led to the identification of either entirely new compounds or additional members of antibiotic families (Bauman et al., 2021). For example, searching the UniProt database against the diazeniumdiolate synthesis genes from *Paraburkholderia graminis* led to the discovery of new gramibactin A-like siderophores from multiple plant-associated bacteria (Hermenau et al., 2019). In another recent example screening for NRPS domains, which introduce the acyl-substituent into lipopeptide antibiotics, led to the discovery of the cryptic *cil* BGC in *Paenibacillus mucilaginosus* and ultimately to the chemical synthesis of the new lipopeptide cilagicin (Wang et al., 2022). In this thesis, *S. kurssanovii* was identified as a novel producer of the L-Phg-containing S_B antibiotic PI as well as the corresponding S_A antibiotic PII. Based on the results presented here, *pglA* is a suitable screening candidate to find further BGCs coding for the synthesis of Phg-containing, potentially bioactive, compounds.

The putative, previously unknown streptogramin BGCs of *S. kurssanovii* and three further unexplored streptogramin producers, *Streptomyces* sp. SW4, Tü2975 and Tü3108 were compared with already described streptogramin BGCs (Mast et al., 2011a; Pulsawat et al., 2007; Xie et al., 2012). As expected, the streptogramin BGCs of organisms that produce the same compounds are highly similar in organisation and

share almost all the genes involved in the synthesis of the respective compounds. Concerning the relationship between the types of streptogramin BGCs, differences in the overall organisation between the original pristinamycin (*prs*) and viridogrisein/griseoviridin (*sgv*) clusters that have been observed before (Mast et al., 2014) could be reaffirmed. There it was remarked that the *prs* and *vir* clusters show a mosaic or "intermingled" structure, in which genes associated with S_A and S_B synthesis are not separated from each other but are distributed over the entire cluster. In the *sgv* cluster however, a "highly modular and systematic" organisation was observed. These differences were confirmed here to be true for all the newly identified *prs* type clusters and the *sgv* clusters, respectively (Fig. 6). With regard to an evolutionary origin of streptogramin BGCs it could be expected that the genes for the synthesis of S_A and S_B were initially separated. Following this hypothesis, as proposed by Mast et al., the *sgv* type would be the more ancient streptogramin BGC amongst those compared here. Concerning the carriers of the streptogramin types, phylogenomic analysis using the TYGS webservice revealed that most streptogramin producers, which carry a *prs* type BGC show an overall close phylogenetic relation to each other (Fig. 7). This close relationship and the presence of transposase genes found in the respective *prs* clusters (*prs*, prs^{2975} and prs^{kurs}) hints at the acquisition of a *prs* type BGC by a common ancestor of *S. pristinaespiralis*, *S. kurssanovii,* and *Streptomyces* sp. Tü 2975 through horizontal gene transfer rather than their independent acquisition. Interestingly, *Streptomyces* sp. SW4 is an exception to this observation, as it appears to be more closely related to carriers of the *sgv* type (*S. griseoviridis* and *Streptomyces* sp. Tü 3180). And while SW4 indeed carries a *prs* type BGC (prs^{SW4}), it is the one with the lowest overall nucleotide sequence identity (69%) to the reference *prs* from *S. pristinaespiralis*. This means that prs^{SW4} and SW4 seem less closely related to the other *prs* types and their carriers, respectively. Therefore, since SW4 is more closely related to the carriers of the, proposedly, more ancient *sgv* type BGCs, it is possible that SW4 belongs to a lineage of original *prs* type carriers which might also be the origin of the streptogramin BGCs found in *S. pristinaespiralis*, *S. kurssanovii* and *Streptomyces* sp. Tü 2975.

The regulation of streptogramin production in *S. pristinaespiralis* is well studied and resembles a complex signalling network including γ-butyrolactone receptors, TetR-

type regulators and SARPs in which both, PI and PII biosynthesis, are co-regulated (Mast et al., 2015). Comparable co-regulation systems are known for the streptogramin production in *S. griseoviridis and S. virginiae* (Xie et al., 2012; Pulsawat et al., 2009). Just recently, two further new streptogramin producers (*Streptomyces* sp. DSM40973 and DSM41931) were shown to be affected by heterologous expression of the principal streptogramin synthesis activator gene *papR2* from *S. pristinaespiralis*. Intriguingly, *papR2* expression inhibited the production of streptogramins in these strains rather than promoting it (R. Makitrynskyy, personal communication 2024), indicating that the regulation of streptogramin synthesis is not universal amongst different producers. Since the streptogramin BGCs investigated here are highly similar to their respective reference BGC, it is likely that regulation is working much in the same way as in those reference BGCs. It would however still be an interesting next step to elucidate the regulatory networks of the new BGCs to confirm whether the synthesis of the respective S_A and S_B compounds are regulated in the same manner as is known for *prs*, *sgv* and *vir*.

The streptogramin BGC *prs* of *S. pristinaespiralis* contains a large IGR, which includes a putative BGC for which no metabolic product is known (Mast et al., 2011a). The presence of a transposase encoding gene hints at the acquisition of the whole IGR via horizontal gene transfer. In this study, similar IGRs were also found within the *prs* type BGCs of *S. kurssanovii*, *Streptomyces* sp. Tü 2975, and *Streptomyces* sp. SW4. Nucleotide sequence similarity between the different IGRs was found over large stretches. Only part of the proposed *cpp* subcluster, originally described for the IGR of *prs* (Mast et al., 2014), are found in the other IGRs. The fact that the *cpp* subcluster is not conserved within the *prs* type clusters indicates that there is no evolutionary advantage for the carriers to retain it. The high overall similarity between the IGRs makes it very likely that they have not been acquired separately by *S. pristinaespiralis*, SW4, TÜ 2975, and *S. kurssanovii*, but rather have evolved from a more ancient “original” carrier of the *prs* type BGC. However, a large section of the prs^{SW4} IGR that contains genes connected to NRP synthesis, here named as the *cnp* subcluster, was not found in any of the other *prs* type BGCs. Interestingly, BLAST database search revealed that a sequence which is highly similar to the *cnp* subcluster (coverage 66%, identity 77%) can be found on the large plasmid pNBC00162 of *Streptomyces* sp.

NBC00162. The *cnp* subcluster might therefore originate from the acquisition of a mobile element like pNBC00162 by horizontal gene transfer. In general, the IGRs of the *prs* type BGCs might be a hotspot for recombination events.

By characterizing new streptogramin BGCs, the findings presented here serve to showcase the highly conserved nature of streptogramin BGCs of the same type. At the same time, previously described differences between the *prs* and *sgv* type BGCs are confirmed.

6.2. New halogenated PI derivatives generated by mutasynthesis

Modification of the chemically complex S_B antibiotic PI was achieved by employing the mutasynthesis principle. Two new PI derivatives, fluoro-PI and chloro-PI, were generated. The influence of the introduced halogens on the bioactivity of PI was investigated. Fluoro-PI and chloro–PI were employed in a series of bioactivity assays against streptogramin sensitive and -resistant organisms. The bioactivity spectrum for both halogenated PI derivatives was shown to match that of natural PI described in the literature (Reissier et al., 2020). Moreover, the inhibitory effect of the halogenated PI derivatives in combination with pure PII also matched that of natural PI. The same observations were also made when testing the new derivatives against strains which carried genes that confer resistance to streptogramins. The results of these combinatory assays suggest that the natural synergy between PI and PII is not disturbed or enhanced in the case of the halogenated PI derivatives. However, a checkerboard assay (Berenbaum, 1978) would be necessary for confirmation. The antimicrobial potency of fluoro-PI as determined by MIC assays was slightly lower than that of the natural PI control and the MIC values given for PI in the literature (Cocito, 1979). The presence of halogenated residues in bioactive natural compounds often has a major influence on bioactivity (Neumann et al., 2008). For example, the glycopeptide antibiotics vancomycin and balhimycin both feature two chlorine substituents, which are of significant importance to bioactivity, since glycopeptides which lack them are far less potent (Cooper et al., 1999). Because of the influence halogenated residues can have on bioactivity, biosynthesis of halogenated natural products has been intensively studied over the last decades in an attempt to understand how halogenation occurs during synthesis and to prepare the way for the engineering of novel compounds (Neumann et al., 2008). For fluoro-PI and chloro–PI

such an influence could however not be observed. In summary, the results show that the newly generated halogenated PI derivatives have the same antibacterial spectrum (including resistant organisms), display an at least additive inhibition effect in combination with PII and are similar in potency to natural PI.

While mutasynthesis has been shown to be a viable method for the substitution of the L-Phg residue of PI, the used Δ*pglA*Δ*snaE1* mutant only produced low amounts of PI derivatives in an inconsistent manner. Since even the production of "natural" PI by feeding of L-Phg was low compared to the parental strain PR11 (Fig. 12), the low PI derivative production rate can likely be attributed to a loss of fitness in the mutant strain, rather than being limited by the incorporation of the L-Phg derivatives. Specifically, while the Δ*pglA*Δ*snaE1* mutant showed growth comparable to PR11 and accumulated comparable amounts of biomass in liquid culture, it was observed that the mutant did not sporulate on solid media. Life cycle dependent differentiation is an important factor for secondary metabolite production in streptomycetes (Chater, 1993), which might explain why the amount of PI produced by the Δ*pglA*Δ*snaE1* mutant was lower compared to the WT. So far it is unknown what exactly caused the mutant to display sporulation deficiency, since both genes targeted for deletion are situated in the streptogramin BGC. It has been shown before that the deletion of *snaE1* and *snaE2*, resulting in the abolishment of PII production, leads to a reduction of PI production in *S. pristinaespiralis* HCCB10218 by 20-40% (Meng et al., 2017). The same study proposed that PII might act as a coactivator or inducer of PI biosynthesis, which would explain why its absence might have a negative effect on the production of PI. It is worth testing if a single mutant *S. pristinaespiralis* Δ*pglA,* would be able to produce higher yields of PI derivatives. Other ways to increase production might be the manipulation of regulatory genes. Overall production of pristinamycin has been shown to be increased by 150% and 300% upon the deletion of the TetR-like repressor genes *papR3* and *papR5* respectively, while overexpression of the SARP-type activator genes *papR1* and *papR2* led to an increased production of 100% each (Mast et al., 2015).

In an optimized producer strain, additional PI derivatives could be generated by the same mutasynthesis approach. As predicted by *in silico* modelling with the crystal structure of PI bound to the ribosomal and as confirmed by the bioactivity studies with

halogenated PI derivatives generated here, the L-Phg residue presents a target for modification that does not interfere with the basic activity of PI, encouraging further modifications. The same modelling analysis also showed that e.g. iodination at the para-position of Phg could increase binding affinities and thus may lead to an improved binding of the modified PI substance (P. Klahn, personal communication 2023). Furthermore, an amino group at the L-Phg residue might be used for the attachment of suitable conjugates, such as siderophores, potentially allowing PI derivatives to penetrate into and kill Gram-negative bacteria which are largely intrinsically resistant to streptogramin antibiotics. Such siderophore conjugates have been shown to increase the effectiveness of a variety of antibiotics against Gram-negative bacteria (Negash et al., 2019). Iodo-PI and amino-PI could be generated in a mutasynthesis approach by feeding para-iodo-Phg and para-amino-Phg, respectively, to the *S. pristinaespiralis* Δ*pglA*Δ*snaE1* mutant, or a further optimized mutasynthesis strain as described above.

Beyond the substitution of the L-Phg residue to achieve the improvements mentioned above, modification of PI by mutasynthesis could also target the 3-hydroxypicolinic acid (Hpa) residue. Deletion of the Hpa synthesis gene *hpaA* should abolish Hpa synthesis, providing a suitable mutasynthesis strain. When PI is bound to the ribosome, the Hpa residue is in close proximity to the crucial nucleotide A2058. PI derivatives with Hpa substitutions might include compounds which can bind to ribosomes with ErmE mediated methylation (MLS_B resistance) of A2058 (P. Klahn, personal communication 2023). Hpa also coordinates a Mg^{2+} ion essential for the binding of the streptogramin B lyases which inactivate PI by linearization (Korczynska et al., 2007). Therefore, Hpa substitution might present an opportunity to effect two resistance mechanisms at once.

Resistance by linearization of the streptogramin type B molecule might however also be addressed by another modification. The target of the streptogramin B lyases is the ester which is formed between L-Thr and L-Phg during cyclisation of PI. This macrolactonization is performed by the NRPS SnbDE. The replacement of this ester with a more thermodynamically stable peptide bond has been proposed to be a way to overcome PI resistance (Mukhtar et al., 2005). Mahlert et al. showed that the thioesterase domain of SnbDE accepts substrates other than L-Thr (L-Ser was

accepted even better than the natural substrate) and can, at least *in vitro*, form a peptide bond instead of an ester (Mahlert et al., 2005). There, a cyclised PI derivative was synthesized in which L-Thr was successfully replaced with L-diamino propionic acid (DAP). However, no information regarding the effect of this substitution on bioactivity was reported. The only comparable work so far was the hybridisation of PI with tyrocidine (Mukhtar et al., 2005), resulting in a chimeric compound not susceptible to streptogramin B lyases and bioactive against multiple Gram-positive pathogens, but with an unknown mode of action. It might be possible to produce the compound synthesized by Mahlert et. al *in vivo* in *S. pristinaespiralis* to characterize its bioactivity and test its susceptibility to streptogramin B lyases. Since mutasynthesis cannot be used to replace the proteinogenic L-Thr, engineering of the NRPS SnbC (specifically the first A domain) would likely have to be performed to facilitate the incorporation of DAP into PI.

Altogether this work shows that that mutasynthesis is a powerful tool to derivatise chemically complex secondary metabolites such as PI.

7. References

Al Toma RS, Brieke C, Cryle MJ, and Sussmuth RD. Structural aspects of phenylglycines, their biosynthesis and occurrence in peptide natural products. *Nat Prod Rep*. 2015, 32, 1207-1235. 10.1039/c5np00025d.

Aziz S, Mast Y, Wohlleben W, and Gross H. Draft genome sequence of the pristinamycin-producing strain *Streptomyces* sp. SW4, isolated from soil in Nusa Kambangan, Indonesia. *Microbiology Resource Announcements*. 2018, 7, 10.1128/mra. 00912-00918.

Bamas-Jacques N, Lorenzon S, Lacroix P, De Swetschin C, and Crouzet J. Cluster organization of the genes of *Streptomyces pristinaespiralis* involved in pristinamycin biosynthesis and resistance elucidated by pulsed-field gel electrophoresis. *Journal of Applied Microbiology*. 1999, 87, 939-948. https://doi.org/10.1046/j.1365-2672.1999.00955.x.

Barka EA, Vatsa P, Sanchez L, Gaveau-Vaillant N, Jacquard C, Meier-Kolthoff JP, Klenk HP, Clement C, Ouhdouch Y, and van Wezel GP. Taxonomy, Physiology, and Natural Products of Actinobacteria. *Microbiol Mol Biol Rev*. 2016, 80, 1-43. 10.1128/MMBR.00019-15.

Barriere J, Berthaud N, Beyer D, Dutka-Malen S, Paris J, and Desnottes J. Recent developments in streptogramin research. *Current pharmaceutical design*. 1998, 4, 155.

Bauman KD, Butler KS, Moore BS, and Chekan JR. Genome mining methods to discover bioactive natural products. *Nat Prod Rep*. 2021, 38, 2100-2129. 10.1039/d1np00032b.

Berenbaum M. A method for testing for synergy with any number of agents. *Journal of Infectious Diseases*. 1978, 137, 122-130.

Bischoff KM, Zhang Y, and Rich JO. Fate of virginiamycin through the fuel ethanol production process. *World J Microbiol Biotechnol*. 2016, 32, 76. 10.1007/s11274-016-2026-3.

Blanc V, Salah-Bey K, Folcher M, and Thompson CJ. Molecular characterization and transcriptional analysis of a multidrug resistance gene cloned from the pristinamycin-producing organism, *Streptomyces pristinaespiralis*. *Mol Microbiol*. 1995a, 17, 989-999. 10.1111/j.1365-2958.1995.mmi_17050989.x.

Blanc V, Lagneaux D, Didier P, Gil P, Lacroix P, and Crouzet J. Cloning and analysis of structural genes from *Streptomyces pristinaespiralis* encoding enzymes involved in the conversion of pristinamycin IIB to pristinamycin IIA (PIIA): PIIA synthase and NADH:riboflavin 5'-phosphate oxidoreductase. *Journal of Bacteriology*. 1995b, 177, 5206-5214. 10.1128/jb.177.18.5206-5214.1995.

Blanc V, Gil P, Bamas-Jacques N, Lorenzon S, Zagorec M, Schleuniger J, Bisch D, Blanche F, Debussche L, Crouzet J, and Thibaut D. Identification and analysis of genes from *Streptomyces pristinaespiralis* encoding enzymes involved in the biosynthesis of the 4-dimethylamino-L-phenylalanine precursor of pristinamycin I. *Mol Microbiol*. 1997, 23, 191-202. 10.1046/j.1365-2958.1997.2031574.x.

Canu A, and Leclercq R. Overcoming bacterial resistance by dual target inhibition: the case of streptogramins. *Curr Drug Targets Infect Disord*. 2001, 1, 215-225. 10.2174/1568005014606152.

Chater KF. Genetics of differentiation in Streptomyces. *Annu Rev Microbiol*. 1993, 47, 685-713. 10.1146/annurev.mi.47.100193.003345.

Chinali G, Moureau P, and Cocito CG. The action of virginiamycin M on the acceptor, donor, and catalytic sites of peptidyltransferase. *J Biol Chem*. 1984, 259, 9563-9568.

Cocito C. Antibiotics of the virginiamycin family, inhibitors which contain synergistic components. *Microbiol Rev*. 1979, 43, 145-192. 10.1128/mr.43.2.145-192.1979.

Cocito C, Di Giambattista M, Nyssen E, and Vannuffel P. Inhibition of protein synthesis by streptogramins and related antibiotics. *J Antimicrob Chemother*. 1997, 39 Suppl A, 7-13. 10.1093/jac/39.suppl_1.7.

Cooper MA, and Williams DH. Binding of glycopeptide antibiotics to a model of a vancomycin-resistant bacterium. *Chemistry & biology*. 1999, 6, 891-899.

Darken MA, Berenson H, Shirk RJ, and Sjolander NO. Production of tetracycline by *Streptomyces aureofaciens* in synthetic media. *Appl Microbiol*. 1960, 8, 46-51. 10.1128/am.8.1.46-51.1960.

Delgado G, Jr., Neuhauser MM, Bearden DT, and Danziger LH. Quinupristin-dalfopristin: an overview. *Pharmacotherapy*. 2000, 20, 1469-1485. 10.1592/phco.20.19.1469.34858.

Delzer J, Fiedler H-P, Müller H, Zähner H, Rathmann R, Ernst K, and König WA. New nikkomycins by mutasynthesis and directed fermentation. *The Journal of Antibiotics*. 1984, 37, 80-82.

Depardieu F, and Courvalin P. Mutation in 23S rRNA responsible for resistance to 16-membered macrolides and streptogramins in *Streptococcus pneumoniae*. *Antimicrob Agents Chemother*. 2001, 45, 319-323. 10.1128/AAC.45.1.319-323.2001.

Eichner S, Knobloch T, Floss HG, Fohrer J, Harmrolfs K, Hermane J, Schulz A, Sasse F, Spiteller P, and Taft F. The interplay between mutasynthesis and semisynthesis: generation and evaluation of an ansamitocin library. *Angewandte Chemie-International Edition*. 2012, 51, 752.

Elsawy MA, Hewage C, and Walker B. Racemisation of N-Fmoc phenylglycine under mild microwave-SPPS and conventional stepwise SPPS conditions: attempts to develop strategies for overcoming this. *J Pept Sci*. 2012, 18, 302-311. 10.1002/psc.2398.

Fahim A, and William AD. Chemistry and Biology of the Streptogramin A Antibiotics. *Mini-Reviews in Organic Chemistry*. 2007, 4, 159-181. http://dx.doi.org/10.2174/157019307780599315.

Galm U, Dessoy MA, Schmidt J, Wessjohann LA, and Heide L. In vitro and in vivo production of new aminocoumarins by a combined biochemical, genetic, and synthetic approach. *Chem Biol*. 2004, 11, 173-183. 10.1016/j.chembiol.2004.01.012.

Giancarlo Lancini FP. Antibiotics - An Integrated View *Springer-Verlag*.1982. 10.1007/978-1-4612-5674-8.

Gräfe U. Biochemie der Antibiotika 1992 *Spektrum Akademischer Verlag*.

Handel F, Kulik A, Wex KW, Berscheid A, Saur Julian S, Winkler A, Wibberg D, Kalinowski J, Brötz-Oesterhelt H, and Mast Y. Ψ-Footprinting approach for the identification of protein synthesis inhibitor producers. *NAR Genomics and Bioinformatics*. 2022, 4. 10.1093/nargab/lqac055.

Hansen JL, Moore PB, and Steitz TA. Structures of five antibiotics bound at the peptidyl transferase center of the large ribosomal subunit. *J Mol Biol*. 2003, 330, 1061-1075. 10.1016/s0022-2836(03)00668-5.

Harms JM, Schlünzen F, Fucini P, Bartels H, and Yonath A. Alterations at the peptidyl transferase centre of the ribosome induced by the synergistic action of the streptogramins dalfopristin and quinupristin. *BMC Biology*. 2004, 2, 4. 10.1186/1741-7007-2-4.

Hermenau R, Ishida K, Gama S, Hoffmann B, Pfeifer-Leeg M, Plass W, Mohr JF, Wichard T, Saluz H-P, and Hertweck C. Gramibactin is a bacterial siderophore with a diazeniumdiolate ligand system. *Nature Chemical Biology*. 2018, 14, 841-843.

Hojati Z, Milne C, Harvey B, Gordon L, Borg M, Flett F, Wilkinson B, Sidebottom PJ, Rudd BA, and Hayes MA. Structure, biosynthetic origin, and engineered biosynthesis of calcium-dependent antibiotics from *Streptomyces coelicolor*. *Chemistry & biology*. 2002, 9, 1175-1187.

Hutchings MI, Truman AW, and Wilkinson B. Antibiotics: past, present and future. *Curr Opin Microbiol*. 2019, 51, 72-80. 10.1016/j.mib.2019.10.008.

Katz L, and Baltz RH. Natural product discovery: past, present, and future. *J Ind Microbiol Biotechnol*. 2016, 43, 155-176. 10.1007/s10295-015-1723-5.

Kehoe LE, Snidwongse J, Courvalin P, Rafferty JB, and Murray IA. Structural basis of Synercid (quinupristin-dalfopristin) resistance in Gram-positive bacterial pathogens. *J Biol Chem*. 2003, 278, 29963-29970. 10.1074/jbc.M303766200.

Kennedy J. Mutasynthesis, chemobiosynthesis, and back to semi-synthesis: combining synthetic chemistry and biosynthetic engineering for diversifying natural products. *Nat Prod Rep*. 2008, 25, 25-34. 10.1039/b707678a.

Kitani S, Yamauchi T, Fukushima E, Lee CK, Ningsih F, Kinoshita H, and Nihira T. Characterization of varM encoding type II ABC transporter in *Streptomyces virginiae*, a Virginiamycin M1 producer. *Actinomycetologica*. 2010, 24, 51-57.

Korczynska M, Mukhtar TA, Wright GD, and Berghuis AM. Structural basis for streptogramin B resistance in *Staphylococcus aureus* by virginiamycin B lyase. *Proceedings of the National Academy of Sciences*. 2007, 104, 10388-10393.

Lee YJ, Kitani S, Kinoshita H, and Nihira T. Identification by gene deletion analysis of barS2, a gene involved in the biosynthesis of gamma-butyrolactone autoregulator in *Streptomyces virginiae*. *Arch Microbiol*. 2008, 189, 367-374. 10.1007/s00203-007-0327-5.

Lee YJ, Kitani S, and Nihira T. Null mutation analysis of an afsA-family gene, barX, that is involved in biosynthesis of the gamma-butyrolactone autoregulator in *Streptomyces virginiae*. *Microbiology (Reading)*. 2010, 156, 206-210. 10.1099/mic.0.032003-0.

Lewis K. The Science of Antibiotic Discovery. *Cell*. 2020, 181, 29-45. 10.1016/j.cell.2020.02.056.

Long KS, Poehlsgaard J, Kehrenberg C, Schwarz S, and Vester B. The Cfr rRNA Methyltransferase Confers Resistance to Phenicols, Lincosamides, Oxazolidinones, Pleuromutilins, and Streptogramin A Antibiotics. *Antimicrobial Agents and Chemotherapy*. 2006, 50, 2500-2505. 10.1128/aac.00131-06.

Mahlert C, Sieber SA, Grunewald J, and Marahiel MA. Chemoenzymatic approach to enantiopure streptogramin B variants: characterization of stereoselective pristinamycin I cyclase from *Streptomyces pristinaespiralis*. *J Am Chem Soc*. 2005, 127, 9571-9580. 10.1021/ja051254t.

Majhi S, and Das D. Chemical derivatization of natural products: Semisynthesis and pharmacological aspects- A decade update. *Tetrahedron*. 2021, 78, 131801. https://doi.org/10.1016/j.tet.2020.131801.

Mast Y, Weber T, Golz M, Ort-Winklbauer R, Gondran A, Wohlleben W, and Schinko E. Characterization of the 'pristinamycin supercluster' of *Streptomyces pristinaespiralis*. *Microb Biotechnol*. 2011a, 4, 192-206. 10.1111/j.1751-7915.2010.00213.x.

Mast YJ, Wohlleben W, and Schinko E. Identification and functional characterization of phenylglycine biosynthetic genes involved in pristinamycin biosynthesis in *Streptomyces pristinaespiralis*. *J Biotechnol*. 2011b, 155, 63-67. 10.1016/j.jbiotec.2010.12.001.

Mast Y, and Wohlleben W. Streptogramins - two are better than one! *Int J Med Microbiol*. 2014, 304, 44-50. 10.1016/j.ijmm.2013.08.008.

Mast Y, Guezguez J, Handel F, and Schinko E. A Complex Signaling Cascade Governs Pristinamycin Biosynthesis in *Streptomyces pristinaespiralis*. *Appl Environ Microbiol*. 2015, 81, 6621-6636. 10.1128/AEM.00728-15.

Meier-Kolthoff JP, and Göker M. TYGS is an automated high-throughput platform for state-of-the-art genome-based taxonomy. *Nature communications*. 2019, 10, 2182.

Meng J, Feng R, Zheng G, Ge M, Mast Y, Wohlleben W, Gao J, Jiang W, and Lu Y. Improvement of pristinamycin I (PI) production in *Streptomyces pristinaespiralis* by metabolic engineering approaches. *Synthetic and Systems Biotechnology*. 2017, 2, 130-136.

Mohr KI. History of Antibiotics Research. *Curr Top Microbiol Immunol*. 2016, 398, 237-272. 10.1007/82_2016_499.

Moore RM, Harrison AO, McAllister SM, Polson SW, and Wommack KE. Iroki: automatic customization and visualization of phylogenetic trees. *PeerJ*. 2020, 8, e8584.

Mukhtar TA, Koteva KP, Hughes DW, and Wright GD. Vgb from *Staphylococcus aureus* inactivates streptogramin B antibiotics by an elimination mechanism not hydrolysis. *Biochemistry*. 2001, 40, 8877-8886. 10.1021/bi0106787.

Mukhtar TA, Koteva KP, and Wright GD. Chimeric streptogramin-tyrocidine antibiotics that overcome streptogramin resistance. *Chem Biol*. 2005, 12, 229-235. 10.1016/j.chembiol.2004.12.009.

Murray CJ. Global burden of bacterial antimicrobial resistance in 2019: a systematic analysis. *Lancet*. 2022, 399, 629-655. 10.1016/S0140-6736(21)02724-0.

Negash KH, Norris JKS, and Hodgkinson JT. Siderophore-Antibiotic Conjugate Design: New Drugs for Bad Bugs? *Molecules*. 2019, 24. 10.3390/molecules24183314.

Neumann CS, Fujimori DG, and Walsh CT. Halogenation strategies in natural product biosynthesis. *Chemistry & biology*. 2008, 15, 99-109.

Nicole JJ, Tariq AM, and Gerard DW. Streptogramin Antibiotics: Mode of Action and Resistance. *Current Drug Targets*. 2002, 3, 335-344. http://dx.doi.org/10.2174/1389450023347678.

O'Neill J. Tackling Drug-Resistant Infections Globally: Final Report and Recommendations. Review on Antimicrobial Resistance. *Wellcome Trust and HM Government*. 2016

Oren A, and Garrity GM. Valid publication of the names of forty-two phyla of prokaryotes. *Int J Syst Evol Microbiol*. 2021, 71. 10.1099/ijsem.0.005056.

Osipenkov N, Kulik A, and Mast Y. Characterization of the phenylglycine aminotransferase PglE from *Streptomyces pristinaespiralis*. *J Biotechnol*. 2018, 278, 34-38. 10.1016/j.jbiotec.2018.05.007.

Parfait R, Giambattista MD, and Cocito C. Competition between erythromycin and virginiamycin for *in vitro* binding to the large ribosomal subunit. *Biochimica et Biophysica Acta (BBA) - Nucleic Acids and Protein Synthesis*. 1981, 654, 236-241. https://doi.org/10.1016/0005-2787(81)90177-5.

Park SR, Tripathi A, Wu J, Schultz PJ, Yim I, McQuade TJ, Yu F, Arevang CJ, Mensah AY, Tamayo-Castillo G, et al. Discovery of cahuitamycins as biofilm inhibitors derived from a convergent biosynthetic pathway. *Nat Commun*. 2016, 7, 10710. 10.1038/ncomms10710.

Pelzer S, Sussmuth R, Heckmann D, Recktenwald J, Huber P, Jung G, and Wohlleben W. Identification and analysis of the balhimycin biosynthetic gene cluster and its use for manipulating glycopeptide biosynthesis in *Amycolatopsis mediterranei* DSM5908. *Antimicrobial agents and chemotherapy*. 1999, 43, 1565-1573.

Poehlsgaard J, and Douthwaite S. The bacterial ribosome as a target for antibiotics. *Nat Rev Microbiol*. 2005, 3, 870-881. 10.1038/nrmicro1265.

Prescott JF. The resistance tsunami, antimicrobial stewardship, and the golden age of microbiology. *Vet Microbiol*. 2014, 171, 273-278. 10.1016/j.vetmic.2014.02.035.

Prusov EV. Total synthesis of antibiotics: recent achievements, limitations, and perspectives. *Appl Microbiol Biotechnol*. 2013, 97, 2773-2795. 10.1007/s00253-013-4757-5.

Pulsawat N, Kitani S, and Nihira T. Characterization of biosynthetic gene cluster for the production of virginiamycin M, a streptogramin type A antibiotic, in *Streptomyces virginiae*. *Gene*. 2007, 393, 31-42. 10.1016/j.gene.2006.12.035.

Reissier S, and Cattoir V. Streptogramins for the treatment of infections caused by Gram-positive pathogens. *Expert Rev Anti Infect Ther*. 2021, 19, 587-599. 10.1080/14787210.2021.1834851.

Rinehart KL. Mutasynthesis of new antibiotics. *Pure and Applied Chemistry*. 1977, 49, 1361-1384. doi:10.1351/pac197749091361.

Scheffler RJ, Colmer S, Tynan H, Demain AL, and Gullo VP. Antimicrobials, drug discovery, and genome mining. *Appl Microbiol Biotechnol*. 2013, 97, 969-978. 10.1007/s00253-012-4609-8.

Seoane A, and Lobo JMG. Identification of a Streptogramin A Acetyltransferase Gene in the Chromosome of *Yersinia enterocolitica*. *Antimicrobial Agents and Chemotherapy*. 2000, 44, 905-909. doi:10.1128/aac.44.4.905-909.2000.

Sharkey LK, Edwards TA, and O'Neill AJ. ABC-F Proteins Mediate Antibiotic Resistance through Ribosomal Protection. *mBio*. 2016, 7, e01975. 10.1128/mBio.01975-15.

Shikura N, Yamamura J, and Nihira T. barS1, a gene for biosynthesis of a γ-butyrolactone autoregulator, a microbial signaling molecule eliciting antibiotic production in Streptomyces species. *Journal of bacteriology*. 2002, 184, 5151-5157.

Sun H, Liu Z, Zhao H, and Ang EL. Recent advances in combinatorial biosynthesis for drug discovery. *Drug Des Devel Ther*. 2015, 9, 823-833. 10.2147/DDDT.S63023.

Svetlov MS, Syroegin EA, Aleksandrova EV, Atkinson GC, Gregory ST, Mankin AS, and Polikanov YS. Structure of Erm-modified 70S ribosome reveals the mechanism of macrolide resistance. *Nature Chemical Biology*. 2021, 17, 412-420. 10.1038/s41589-020-00715-0.

Toscano L, Fioriello G, Spagnoli R, Cappelletti L, and Zanuso G. New fluorinated erythromycins obtained by mutasynthesis. *The Journal of Antibiotics*. 1983, 36, 1439-1450.

Tu D, Blaha G, Moore PB, and Steitz TA. Structures of MLS_B Antibiotics Bound to Mutated Large Ribosomal Subunits Provide a Structural Explanation for Resistance. *Cell*. 2005, 121, 257-270. 10.1016/j.cell.2005.02.005.

Ulanova D, Novotna J, Smutna Y, Kamenik Z, Gazak R, Sulc M, Sedmera P, Kadlcik S, Plhackova K, and Janata J. Mutasynthesis of lincomycin derivatives with activity against drug-resistant staphylococci. *Antimicrob Agents Chemother*. 2010, 54, 927-930. 10.1128/AAC.00918-09.

Vannuffel P, and Cocito C. Mechanism of action of streptogramins and macrolides. *Drugs*. 1996, 51 Suppl 1, 20-30. 10.2165/00003495-199600511-00006.

Voorhees RM, and Ramakrishnan V. Structural basis of the translational elongation cycle. *Annu Rev Biochem*. 2013, 82, 203-236. 10.1146/annurev-biochem-113009-092313.

Waksman SA. Microbial Antagonisms and Antibiotic Substances. *Soil Science*. 1945, 59, 482.

Walker AS, and Clardy J. A Machine Learning Bioinformatics Method to Predict Biological Activity from Biosynthetic Gene Clusters. *J Chem Inf Model*. 2021, 61, 2560-2571. 10.1021/acs.jcim.0c01304.

Wang Z, Koirala B, Hernandez Y, Zimmerman M, and Brady SF. Bioinformatic prospecting and synthesis of a bifunctional lipopeptide antibiotic that evades resistance. *Science*. 2022, 376, 991-996.

Watve MG, Tickoo R, Jog MM, and Bhole BD. How many antibiotics are produced by the genus *Streptomyces*? *Arch Microbiol*. 2001, 176, 386-390. 10.1007/s002030100345.

Weissman KJ. Mutasynthesis - uniting chemistry and genetics for drug discovery. *Trends Biotechnol*. 2007, 25, 139-142. 10.1016/j.tibtech.2007.02.004.

Weist S, and Sussmuth RD. Mutational biosynthesis--a tool for the generation of structural diversity in the biosynthesis of antibiotics. *Appl Microbiol Biotechnol*. 2005, 68, 141-150. 10.1007/s00253-005-1891-8.

Wex KW, Saur JS, Handel F, Ortlieb N, Mokeev V, Kulik A, Niedermeyer TH, Mast Y, Grond S, and Berscheid A. Bioreporters for direct mode of action-informed screening of antibiotic producer strains. *Cell Chemical Biology*. 2021, 28, 1242-1252. e1244.

Wilson DN. Ribosome-targeting antibiotics and mechanisms of bacterial resistance. *Nat Rev Microbiol*. 2014, 12, 35-48. 10.1038/nrmicro3155.

Winand L, Sester A, and Nett M. Bioengineering of Anti-Inflammatory Natural Products. *ChemMedChem*. 2021, 16, 767-776. https://doi.org/10.1002/cmdc.202000771.

Wohlleben W, Mast Y, Muth G, Rottgen M, Stegmann E, and Weber T. Synthetic biology of secondary metabolite biosynthesis in actinomycetes: Engineering precursor supply as a way to optimize antibiotic production. *FEBS Lett*. 2012, 586, 2171-2176. 10.1016/j.febslet.2012.04.025.

Wright F, and Bibb MJ. Codon usage in the G+C-rich *Streptomyces* genome. *Gene*. 1992, 113, 55-65. 10.1016/0378-1119(92)90669-g.

Xie Y, Wang B, Liu J, Zhou J, Ma J, Huang H, and Ju J. Identification of the biosynthetic gene cluster and regulatory cascade for the synergistic antibacterial antibiotics griseoviridin and viridogrisein in *Streptomyces griseoviridis*. *Chembiochem*. 2012, 13, 2745-2757. 10.1002/cbic.201200584.

Yun X, Zhang Q, Lv M, Deng H, Deng Z, and Yu Y. In vitro reconstitution of the biosynthetic pathway of 3-hydroxypicolinic acid. *Org Biomol Chem*. 2019, 17, 454-460. 10.1039/c8ob02972e.

8. List of Publications

8.1. Research articles

Hennrich O, Weinmann L, Kulik A, Harms K, Klahn P, Youn JW, Surup F, Mast Y. Biotransformation-coupled mutasynthesis for the generation of novel pristinamycin derivatives by engineering the phenylglycine residue. *RSC Chem Biol.* 2023, 4::1050-1063. doi: 10.1039/d3cb00143a.

Aryal N, Chen J, K. Bhattarai, **Hennrich O**, Handayani I, Kramer M, Straetener J, Wommer T, Berscheid A, Peter S, Reiling N, Brötz-Oesterhelt H, Geibel C, Lämmerhofer M, Mast Y, Gross H. High Plasticity of the Amicetin Biosynthetic Pathway in *Streptomyces* sp. SHP 22-7 Led to the Discovery of Streptcytosine P and Cytosaminomycins F and G and Facilitated the Production of 12F-Plicacetin. *J Nat Prod.* 2022, 85::530-539. doi:10.1021/acs.jnatprod.1c01051.

Hennrich O, Handel F, Ort-Winklbauer R, Mast Y. Genome Sequences of Two Putative Streptogramin Producers, *Streptomyces* sp. Strains TÜ 2975 and TÜ 3180, from the Tübingen Strain Collection. *Microbiol Resour Announc*. *Microbiol Resour Announc.* 2020, 9::e01582-19. doi:10.1128/MRA.01582-19.

Moosmann D, Mokeev V, Kulik A, Osipenkov N, Kocadinc S, Ort-Winklbauer R, Handel F, **Hennrich O**, Youn YW, Sprenger G, Mast Y. Genetic engineering approaches for the fermentative production of phenylglycines. *Appl Microbiol Biotechnol.* 2020*,* 104::3433-3444. doi:10.1007/s00253-020-10447-9.

Nouioui I, Zimmermann A, **Hennrich O**, Xia S, Rössler O, Makitrynskyy R, Gomez-Escribano JP, Pötter G, Jando M, Döppner M, Wolf J, Neumann-Schaal M, Hughes C, Mast Y. Challenging old microbiological treasures for natural compound biosynthesis capacity. *Front Bioeng Biotechnol.* 2024, 12::1255151. doi:10.3389/fbioe.2024.1255151.

8.2. Relevant articles

Feeney MA, Newitt JT, Addington E, Algora-Gallardo L, Allan C, Balis L, Birke AS, Castaño-Espriu L, Charkoudian LK, Devine R, Gayrard D, Hamilton J, **Hennrich O**, Hoskisson PA, Keith-Baker M, Klein JG, Kruasuwan W, Mark DR, Mast Y, McHugh RE, McLean TC, Mohit E, Munnoch JT, Murray J, Noble K, Otani H, Parra J, Pereira CF, Perry L, Pintor-Escobar L, Pritchard L, Prudence SMM, Russell AH, Schniete JK, Seipke RF, Sélem-Mojica N, Undabarrena A, Vind K, van Wezel GP, Wilkinson B, Worsley SF, Duncan KR, Fernández-Martínez LT, Hutchings MI. ActinoBase: tools and protocols for researchers working on *Streptomyces* and other filamentous actinobacteria. *Microb Genom*. 2022, 8::mgen000824. doi:10.1099/mgen.0.000824.

9. Publications

9.1. Publication 1

RSC Chemical Biology

ROYAL SOCIETY OF CHEMISTRY

PAPER

View Article Online
View Journal | View Issue

Cite this: *RSC Chem. Biol.*, 2023, 4, 1050

Biotransformation-coupled mutasynthesis for the generation of novel pristinamycin derivatives by engineering the phenylglycine residue†

Oliver Hennrich,[a] Leoni Weinmann,[b] Andreas Kulik,[c] Karen Harms,[d] Philipp Klahn,[ef] Jung-Won Youn,[b] Frank Surup[d] and Yvonne Mast[*agh]

Streptogramins are the last line of defense antimicrobials with pristinamycin as a representative substance used as therapeutics against highly resistant pathogenic bacteria. However, the emergence of (multi)drug-resistant pathogens renders these valuable antibiotics useless; making it necessary to derivatize compounds for new compound characteristics, which is often difficult by chemical *de novo* synthesis due to the complex nature of the molecules. An alternative to substance derivatization is mutasynthesis. Herein, we report about a mutasynthesis approach, targeting the phenylglycine (Phg) residue for substance derivatization, a pivotal component of streptogramin antibiotics. Mutasynthesis with halogenated Phg(-like) derivatives altogether led to the production of two new derivatized natural compounds, as there are 6-chloropristinamycin I and 6-fluoropristinamycin I based on LC-MS/MS analysis. 6-Chloropristinamycin I and 6-fluoropristinamycin I were isolated by preparative HPLC, structurally confirmed using NMR spectroscopy and tested for antimicrobial bioactivity. In a whole-cell biotransformation approach using an engineered *E. coli* BL21(DE3) pET28-*hmo*/pACYC-*bcd-gdh* strain, Phg derivatives were generated fermentatively. Supplementation with the *E. coli* biotransformation fermentation broth containing 4-fluorophenylglycine to the pristinamycin mutasynthesis strain resulted in the production of 6-fluoropristinamycin I, demonstrating an advanced level of mutasynthesis.

Received 6th August 2023,
Accepted 6th October 2023

DOI: 10.1039/d3cb00143a

rsc.li/rsc-chembio

1. Introduction

Antibiotics are undoubtedly the most important and impactful medical advancement of all time and a cornerstone of modern medicine.[1,2] However, the rapid emergence of (multi)drug-resistant pathogens endangers their efficacy and poses a serious threat to global human health.[3] According to a recent estimate, more than 1.2 million people died worldwide in 2019 due to drug-resistant bacterial infections.[4] Accompanying this development, the pipeline for new antibacterial agents was feared to run empty in recent years with only slightly encouraging rising numbers of drug candidates from 2017 onwards.[5,6] Especially, new compound classes are rarely found. The most recent new compound classes that have been introduced to the market are cyclic lipopeptides (daptomycin by Cubist Pharmaceuticals in 2003) and oxazolidinones (linezolid by Pfizer in 2000).[7] Thus, discovering and developing new antimicrobials and strategies to combat resistance is a key challenge in the years ahead.

The most important sources for many powerful antibiotics are actinomycetes and fungi, which are the origin of up to two-thirds of all antibiotics in clinical use today.[8] These involve all different classes of antibiotics, such as aminoglycosides, macrolides, tetracyclines, glycopeptide antibiotics, β-lactams, rifamycins, or streptogramins.[8] While the biosynthetic potential of actinomycetes for unknown antibiotics is still considered high,[9,10] there are also other approaches that aim to get access to novel bioactive substances, as for instance the structural

[a] *Department Bioresources for Bioeconomy and Health Research, Leibniz Institute DSMZ-German Collection of Microorganisms and Cell Cultures, Inhoffenstraße 7B, 38124 Braunschweig, Germany. E-mail: yvonne.mast@dsmz.de*
[b] *Institute of Microbiology, University Stuttgart, Allmandring 31, D-70569 Stuttgart, Germany*
[c] *Department Microbial Bioactive Compounds, Interfaculty Institute of Microbiology and Infection Medicine, Faculty of Science, University of Tübingen, Auf der Morgenstelle 28, D-72076 Tübingen, Germany*
[d] *Microbial Drugs Department, Helmholtz-Centre for Infection Research, 38124 Braunschweig, Germany*
[e] *Division of Organic and Medicinal Chemistry, Department of Chemistry and Molecular Biology, University of Gothenburg, Kemigården 4, 412 96 Göteborg, Sweden*
[f] *Centre of Antimicrobial Resistance Research in Gothenburg (CARe), Gothenburg, Sweden*
[g] *Technische Universität Braunschweig, Institut für Mikrobiologie, Rebenring 56, 38106 Braunschweig, Germany*
[h] *German Center for Infection Research (DZIF), Partner Site Tübingen, Tübingen, Germany*

† Electronic supplementary information (ESI) available. See DOI: https://doi.org/10.1039/d3cb00143a

modification of already existing potent bioactive drugs.[11] A good example of modification of a chemical scaffold is the macrolide antibiotic erythromycin, where the natural compound served as a starting point for chemical modification at the C12 position, resulting in a series of novel ketolides.[12] All modified compounds showed high activity against Gram-positive bacteria, such as *Staphylococcus aureus*, *Streptococcus pneumoniae*, and *Streptococcus pyogenes*.[12] The challenge in modifying such a kind of antibiotics lies in their complex chemical structures, which originate from a multistep biosynthesis. Many compounds are difficult to generate by chemical or semi-synthesis, which limits the ability to optimize compounds by chemical derivatization.[13,14] For example, the chemical synthesis of the aglycone of the glycopeptide antibiotic vancomycin involves 19 chemical steps and is associated with several problems, notably the lack of kinetic atroposelectivity in the construction of the tricyclic scaffold, low overall yields, and the difficult synthesis of unnatural amino acids.[15,16]

Genetic engineering methods are suitable alternatives for the targeted derivatization of complex natural products.[17] These methods are based on the biotechnological manipulation of genes involved in antibiotic biosynthesis, which in bacterial antibiotic producers are usually organized in biosynthetic gene clusters (BGCs).[18] Mutasynthesis is a method of metabolic engineering that combines aspects of chemical synthesis with genetic engineering techniques (= mutational biosynthesis). The principle of mutasynthesis involves the genetic disruption of one or more gene(s) responsible for the biosynthesis of a key precursor, with subsequent supply of synthetic analogues of the missing precursor, designated as mutasynthons. The incorporation of a mutasynthon into the biosynthetic assembly line of the secondary metabolite then leads to the formation of novel compound derivatives (Fig. 1).[19] In this way, mutasynthesis combines genetic manipulation with the principle of precursor-directed biosynthesis[20] to exploit substrate promiscuity in the biosynthetic assembly lines of natural product producers.[13] This can be used to modify complex natural products that are inaccessible or difficult to access by means of chemical synthesis.[13,14,21] The advantage of mutasynthesis over precursor-directed biosynthesis is that by using a precursor block mutant, there is no competition between the natural precursor and the unnatural mutasynthon building block, resulting in the biosynthesis of the desired mutasynthesis product only. A prerequisite for this powerful technology is the knowledge of the biosynthetic pathway, especially that the respective precursor genes are known, the genetic tractability of the antibiotic producer strain, as well as that the mutasynthon is readily taken up by the cell and accepted by the biosynthetic machinery.[19,22–24] Mutasynthesis has been successfully applied for the derivatization of various compound classes, such as polyketides,[25–27] nonribosomal peptides[28] glycopeptide antibiotics,[14] aminoglycosides,[29] alkaloids,[30] aminocoumarins,[31] or lincomycins.[32] For example, regarding drug optimization, mutasynthesis has successfully been applied to generate derivatives of lincomycin, which showed increased activities against low-level lincosamide resistant staphylococci compared to the original compound.[32] Another example includes a series of novel physostigmine alkaloids generated by mutasynthesis,

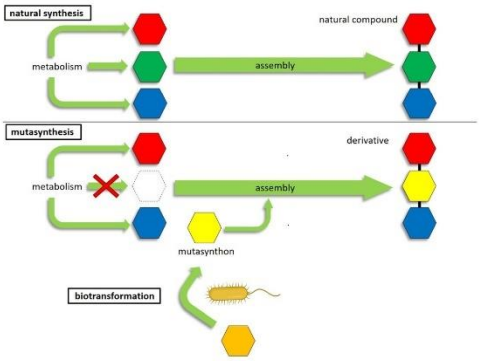

Fig. 1 Schematic presentation of the mutasynthesis principle. Colored hexagons represent the different antibiotic building blocks, which are assembled by the biosynthetic machinery. For mutasynthesis, a block mutant is required where the synthesis of a building block is abolished. Feeding with an unnatural analog (mutasynthon (yellow hexagon)) results in the synthesis of an altered product. The provision of the mutasynthon as a result of the conversion of the precursor (orange hexagon) by the biotransformation step (bacteria symbol) is indicated below.

where one of the modified compounds exhibited an improved selectivity and toxicity profile.[30]

Streptogramin antibiotics are a substance class that with pristinamycins (Synercid®, Pyostacin®) have found their way into clinical applications. Pristinamycins are used as an antibiotic of last resort to treat multidrug-resistant bacterial infections.[33] These antibiotics show good activities against numerous Gram-positive pathogens, including methicillin- and vancomycin-resistant *Staphylococcus aureus* (MRSA, VRSA) and vancomycin-resistant *Enterococcus faecium* strains (VREF). Despite the longstanding use of pristinamycin for more than 50 years, especially in French-speaking countries, the frequency of resistance remained low but has increased in recent years,[33] which makes it necessary to optimize the substance in terms of broad-spectrum activity and resistance breaking characteristics, which can be achieved by derivatization of the compound by mutasynthesis. However, so far mutasynthesis has been prevented by the lack of information about precursor biosynthesis and its encoding genes. In particular, the genes coding for the biosynthesis of the non-proteinogenic amino acid L-phenylglycine (L-Phg), which is a constituent of the peptide antibiotic pristinamycin I (**1**), were not known until recently.

L-Phg is essential for the bioactivity of streptogramin antibiotics, such as pristinamycin I (**1**) or its semi-synthetic derivative Synercid®.[34,35] Pristinamycin is a natural compound mixture produced by *Streptomyces pristinaespiralis* and consists of a mixture of two types of chemically unrelated substances – the macrocyclic polyketide/nonribosomal peptide hybrid compound pristinamycin II (= streptogramin group A (S_A)) and the cyclic hexadepsipeptide pristinamycin I (**1**) (= streptogramin group B (S_B)), the latter containing Phg as a structural component (Fig. 2).[36] Pristinamycin I and II are co-produced by

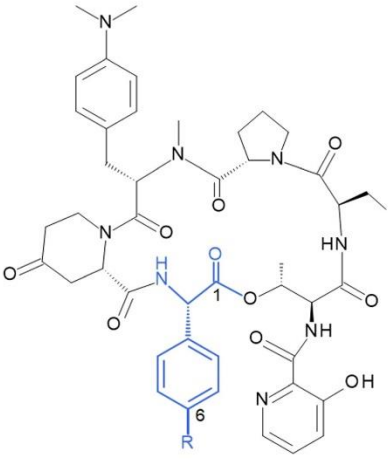

Pristinamycin I (1): R = H
6-chloropristinamycin I (3): R = Cl
6-fluoropristinamycin I (4): R = F

Fig. 2 Chemical structure of **1**, **3**, and **4** with Phg residue indicated in blue. Numbering indicates the order of incorporation into the peptide backbone.

S. pristinaespiralis in a synergistically active ratio of 30 : 70.[36] Both compounds inhibit the bacterial protein biosynthesis by binding to the 23S rRNA of the 50S subunit of bacterial ribosomes, whereby pristinamycin II prevents the binding of the aminoacyl-tRNA, while pristinamycin I (**1**) causes the dissociation of the peptidyl-tRNA from the ribosome.[35] Each component alone exhibits moderate bacteriostatic activity, whereas in combination they act synergistically, resulting in a potent bactericidal activity.[35] The synergistic mixture is used for clinical application, *e.g.* as Synercid®, which is a combination of semi-synthetic derivatives of pristinamycin I (quinupristin (**2**), Fig. 3) and pristinamycin II (dalfopristin).[35] Resistances against streptogramin antibiotics include, *e.g.* the active efflux of the antibiotics or the enzymatic inactivation of either of the two components.[36] The most prevalent resistance mechanism against S_B antibiotics is the N^6 (di)methylation of a specific adenine nucleotide residue (A2058, *Escherichia coli* numbering) of the ribosomal 23S rRNA.[37,38] This modification is mediated by Erm methyltransferases, encoded by plasmid-borne *erm* genes, which leads to a drastic reduction of affinity for members of the macrolide-lincosamide-streptogramin B (MLS_B) group of antibiotics.[39] In *S. pristinaespiralis*, the S_B antibiotic **1** is synthesized by the nonribosomal peptide synthetases (NRPSs) SnbA, SnbC, and SnbDE, whereby the latter one incorporates L-Phg as the final amino acid into the growing pristinamycin I peptide chain.[36,40] L-Phg biosynthesis occurs through a series of enzymatic reactions, catalyzed by the enzymes phenylpyruvate dehydrogenase (PglB/PglC), Phg dehydrogenase (PglA), thioesterase (PglD), and aminotransferase (PglE), which convert phenylpyruvate to L-Phg.[18,41,42] The genetic information for Phg biosynthesis is encoded on the *S. pristinaespiralis pglA-E* operon.[41] So far, this is the first reported Phg biosynthetic pathway and has been identified in the frame of characterizing the pristinamycin biosynthetic gene cluster.[40,41,43] Crystallographic analysis of a ribosome-bound streptogramin antibiotic revealed the formation of a hydrogen bond between the L-Phg carbonyl oxygen with nucleotide C2586 of the 23S rRNA (*E. coli* numbering) as part of the interactions involved in the binding of **1** to the ribosome.[35] Additionally, the aromatic ring of Phg is involved in establishing hydrophobic interactions with the ribosome[34] hinting at the functional importance of the amino acid for bioactivity.

The pristinamycin biosynthetic route is well-described and the producer strain *S. pristinaespiralis* is genetically tractable,[40] making it strain a suitable chassis strain for a streptogramin mutasynthesis approach. In the current study, we report on a mutasynthesis approach for the derivatization of pristinamycin I (**1**) by targeting the Phg-like residue for modification to generate novel antibiotic derivatives.

2. Results and discussion

2.1 Docking of pristinamycin into the ribosomal binding pocket reveals options for pristinamycin I derivatization

In order to estimate the potential for compound derivatisation, computational docking studies were carried out with known pristinamycin compounds and bacterial ribosomes as drug targets. Quinupristin (**2**), another clinically applied pristinamycin I derivative bearing an additional (*R*)-2-(quinuclidin-3-ylthio)ethyl substituent at the 4-oxo-L-pipecolic acid moiety (Fig. 3A), has been co-crystallized with the ribosome of different species including *E. coli* and the two extremophiles *Deinococcus radiodurans* and *Haloarcura marismortui*.[34,35,44] The structure analysis of these co-crystals reveals that quinupristin (**2**) binds the 23S rRNA of the bacterial large ribosomal subunit 50S at the entrance of the ribosomal tunnel through a network of hydrophobic interactions predominantly mediated and hydrogen bonds between the N6 nitrogen of the A2062 nucleotide (*E. coli nomenclature in green*) and the N4 nitrogen of the C2565 nucleotide (*E. coli nomenclature in green*) as outlined in Fig. 3A[34,35,44] with no direct contact to the ribosome protein backbone. Pristinamycin I (**1**) is believed to bind in a similar manner to the same binding pocket at 23S rRNA of the bacterial ribosomal 50S subunit. However, as no co-crystal structure of **1** with the bacterial ribosome is available, we have performed a virtual docking of pristinamycin I (**1**) into the binding pocket of quinupristin (**2**) at the ribosome based on the three available co-crystal structure with the ribosome of *E. coli* (PDB: 4U26), *D. radiodurans* (PDB: 1MS1), and *H. marismortui* (PBD: 1YJW)[34,35,44] using the software SeeSAR (SeeSAR version 13.0.1; BioSolveIT GmbH, Sankt Augustin, Germany, 2023, www.biosolveit.de/SeeSAR). The general overlap of pristinamycin (**1**) with quinupristin (**2**) in cases *E. coli* (Fig. 3B, see PDB file 3B_*E. coli* in the ESI†) and *H. marismortui* (Fig. 3C, see PDB file 3C_*H. marismorturi* in the ESI†) is very high, with only very little deviations

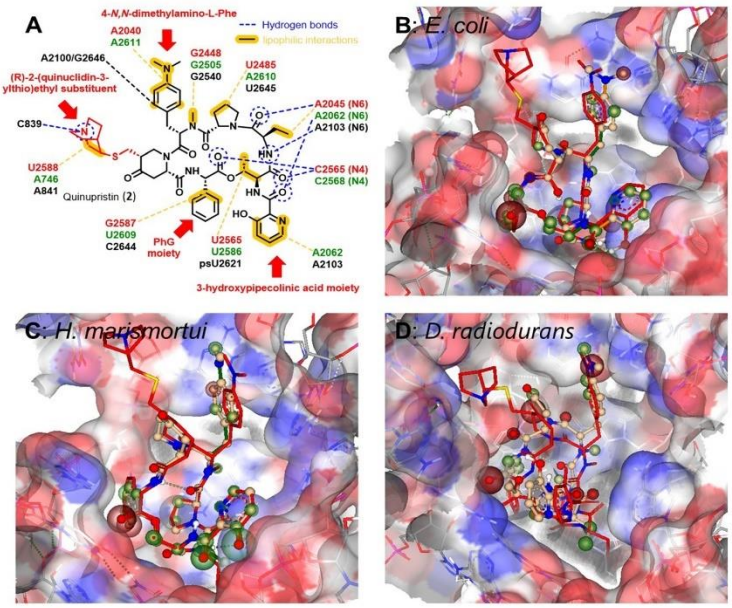

Fig. 3 (A) Structure of quinupristin (**2**) and illustration of the network of hydrogen bonds and lipophilic interactions with bacterial 23S rRNA bases in the 50S subunit of the bacterial ribosomes (green: *E. coli*, PBD: 4U26,[44] red: *Deinococcus radiodurans*, PBD: 1SM1,[35] Black: *Haloarcura marismortui*, PBD: 1YJW.[34] Illustration of docked pristinamycin (**1**) into the binding pocket at the 23S rRNA of *E. coli* (B), *H. marismortui* (C) and *D. radiodurans* (D) in comparison to quinupristin (**2**, depicted in red) prepared with SeeSAR software version 13.0.1 (**https://www.biosolveit.de/SeeSAR**). Colored spheres around atoms indicate positive (green) or negative (red) contributions to the overall binding affinity based on ligand–target interactions as well as desolvatization energies.

especially in the position of the 4-*N*,*N*-dimethylamino-L-Phe side chain and the 3-hydroxypipecolinic acid moiety. In the case of *D. radiodurans* (Fig. 3D, see PDB file 3D_*D. radiodurans* in ESI†) already **2** is bound in a slightly different orientation compared to *E. coli* and *H. marismortui*, in particular, the 3-hydroxypipecolinic acid moiety is oriented to the opposite direction. The docked structure of **1** is then shifted by approximately 2.1 Å into the binding pocket of the 23S rRNA compared to **2**. Presumably, this is a consequence of lacking the (*R*)-2-(quinuclidin-3-ylthio)ethyl substituent of **2** allowing **1** to enter deeper into the pocket. The Phg moiety of **1** points in all cases towards the inside of the 23S rRNA binding pocket. However, unoccupied space between the 23S rRNA nucleotides and the Phg moiety in all docking approaches encouraged us to virtually explore further possible Phg derivatives, which could be accessed through mutasynthesis *via* an *in silico* screening of 4-, 3- and 2-substituted Phg derivatives based on the docking of **1** into the binding pocket of *E. coli*. In general, smaller substituents in the 3- and 4-position seemed to be tolerated for binding to the target. Substitution in the 2-position of the Phg moiety mostly led to derivatives presumably not binding to the target structure anymore.

2.2 Construction of a biosynthetic mutant of *S. pristinaespiralis* for mutasynthesis

To allow for the mutasynthesis of Phg-containing pristinamycin I derivatives, an appropriate biosynthetic mutant deficient in Phg precursor supply had to be generated. In *S. pristinaespiralis*, *pglA* is the first gene of the L-Phg biosynthesis encoding operon *pglA-E* and has been shown to be essential for pristinamycin I production.[41] Inactivation of *pglA* in *S. pristinaespiralis* (M*pglA*) resulted in a loss of pristinamycin I production, whereas feeding *MpglA* with L-Phg restored pristinamycin I production, thus functionally complementing the *pglA* inactivation.[41] The production of the S_A antibiotic pristinamycin II is not affected in the *MpglA* mutant.[41] To obtain an *S. pristinaespiralis* mutasynthesis strain that produces pristinamycin I derivatives exclusively, we aimed to abolish the biosynthesis of the pristinamycin II compound as well. This should allow for PI derivative production in an antibiotic-free background so that the mutasynthesis samples can be directly tested for bioactivity. For this purpose, the gene *snaE1*, encoding a hybrid PKS/NRPS enzyme essential for pristinamycin II biosynthesis[45] was inactivated by insertion of a thiostrepton resistance cassette (*thio*^{R}) using the mutational plasmid pK18-*snaE1tsr*, which resulted in the double mutant *S. pristinaespiralis* Δ*pglA*Δ*snaE1* (Table S1, ESI†). The Δ*pglA*Δ*snaE1* mutant and the *S. pristinaespiralis* wild-type strain (control) were cultivated in pristinamycin production medium HT7T, respectively. After 72 h of cultivation, the culture extracts were analyzed for pristinamycin production by HPLC. The HPLC spectrum of the *S. pristinaespiralis* wild-type (WT) extract showed specific peaks at retention times (RT) 8.2 min and 10.35 min

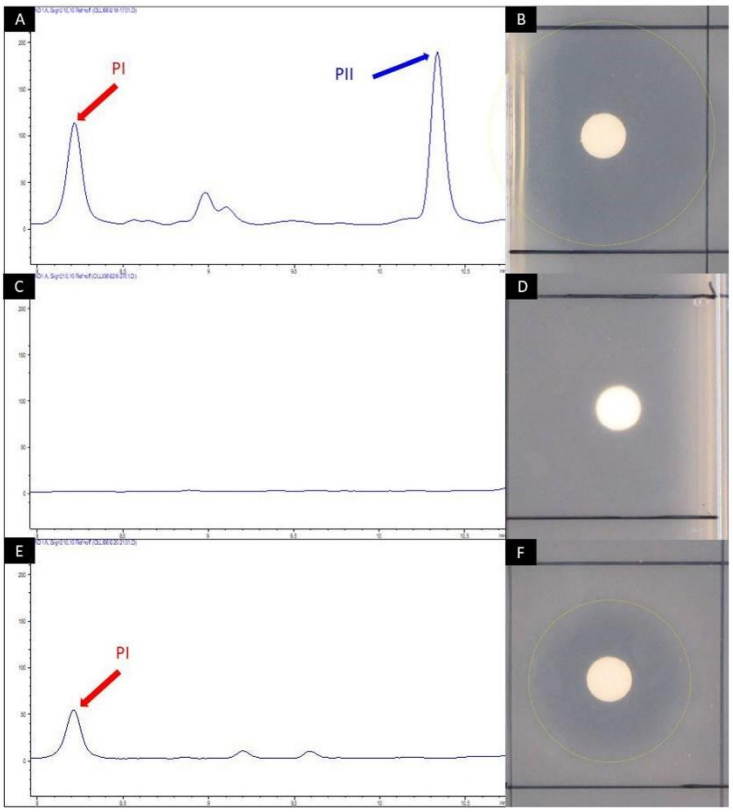

Fig. 4 HPLC chromatogram of crude extract samples from *S. pristinaespiralis* wild-type (A), *S. pristinaespiralis ΔpglAΔsnaE1* (C) and *ΔpglAΔsnaE1* supplemented with 100 μM L-Phg (E). The chromatogram shows peaks measured at 210 nm. Pristinamycin I (PI) and II (PII)-specific peaks were detected at retention times of 8.2 and 10.35 min and are indicated by red and blue arrows, respectively. Disc diffusion assays with the respective extract samples against *B. subtilis* (B), (D) and (F). Inhibition zones are marked with yellow circles.

(Fig. 4A) with characteristic pristinamycin I and II UV-Vis spectra, respectively (data not shown). In addition, the WT extracts exhibited bioactivity against *B. subtilis* (Fig. 4B). In contrast, such a HPLC peak pattern was not detected for the *S. pristinaespiralis ΔpglAΔsnaE1* extract samples (Fig. 4C) and extracts did not exert antibiotic activity against *B. subtilis* (Fig. 4D). These results confirmed that the *S. pristinaespiralis ΔpglAΔsnaE1* mutant was no longer capable of synthesizing pristinamycin I nor pristinamycin II. Extract samples obtained from *S. pristinaespiralis ΔpglAΔsnaE1* cultures, supplemented with L-Phg revealed a single peak at RT 8.2 min in HPLC analysis (Fig. 4E) and exerted moderate bioactivity against *B. subtilis* (Fig. 4F), which showed that pristinamycin I production was restored exclusively. These results proved the functional correctness of the *S. pristinaespiralis ΔpglAΔsnaE1* mutant and enabled its use as a mutasynthesis strain for Phg-directed derivatisation of pristinamycin I.

2.3 Generation of novel pristinamycin I derivatives by mutasynthesis

To conduct the mutasynthesis of pristinamycin I, a series of commercially available Phg derivatives was used as mutasynthons for feeding experiments with *S. pristinaespiralis ΔpglAΔsnaE1* (Table 1). These included a variety of halogenated and non-halogenated Phgs substituted at different positions of the aromatic residue, as well as enantiomers. The mutasynthons were added to the growing cultures of *S. pristinaespiralis ΔpglAΔsnaE1*, and ethyl acetate crude extract from *S. pristinaespiralis* cultures was analyzed for the production of pristinamycin I derivatives by HPLC and HPLC/MS. For *S. pristinaespiralis ΔpglAΔsnaE1*, feeding with six mutasynthons, namely D-Phg, 2,5-dihydro-D-Phg, 4-fluoro-L-Phg, 2-fluoro-DL-Phg, 4-chloro-DL-Phg, and hydroxy-DL-Phg led to the production of the respective pristinamycin I derivatives, which were identified by HPLC-MS analysis based on their expected calculated masses (Table 1). Thereof, extract samples

Table 1 List of tested mutasynthons with indication if pristinamycin I derivatives with expected masses have been detected by LC/MS analysis and antibacterial activity observed in bioassays (n.t. = not tested). + = derivative/bioactivity observed; – = not observed

Mutasynthon	Calculated mass of PI derivative	New PI-derivative/ mass detected	Bioactivity against *B. subtilis*
D-Phg	866.4	+	+
2,5-Dihydro-D-Phg	868.4	+	n.t.
4-Fluoro-L-Phg	884.4	+	+
2-Fluoro-DL-Phg	884.4	+	n.t.
4-Chloro-DL-Phg	900.4	+	+
2-Chloro-DL-Phg	900.4	—	n.t.
4-Bromo-DL-Phg	944.3	—	n.t.
4-Amino-DL-Phg	881.4	—	n.t.
4-Hydroxy-DL-Phg	882.4	+	n.t.
2,2-Di-Phg	942.4	—	n.t.
3-(Trifluoromethyl)-DL-Phg	934.4	—	n.t.
4-(Trifluoromethyl)-L-Phg	934.4	—	n.t.
4-Hydroxy-DL-2-fluoro-Phg	882.4	—	n.t.

of *S. pristinaespiralis ΔpglAΔsnaE1* cultures supplemented with D-Phg, 4-fluoro-L-Phg, and 4-chloro-DL-Phg showed activity in bioassays against the test organism *B. subtilis* (Table 1). Because of the comparatively stable and good antibiotic production behavior of the *ΔpglAΔsnaE1* mutant when supplemented with 4-fluoro-L-Phg, and 4-chloro-DL-Phg, further efforts were focused on the isolation of the two halogenated pristinamycin I derivatives, which were referred to as 6-fluoropristinamycin I (**3**) and 6-chloropristinamycin I (**4**), respectively. Notably, feeding of D-Phg also led to the production of a pristinamycin I derivative as identified by HPLC-MS analysis, although the enantiomeric L-Phg is the natural precursor of pristinamycin I biosynthesis. Here, it remains unclear whether the adenylation domain of SnbE is able to accept D-Phg as a substrate or whether D-Phg was converted to L-Phg prior to incorporation. Since Phgs were solubilized by using sodium hydroxide prior to addition to the culture, chemical racemisation to D/L-Phg mixtures is quite possible. Though, polarimetric analysis of L- and D-Phg under alkaline conditions did not indicate racemisation (data not shown), which however does not exclude racemization in the organism. In a previous study, it has been described that the thioesterase domain of SnbDE can only accept L-Phg but not D-Phg,[46] which makes incorporation of D-Phg in PI unlikely. Natural pristinamycin I (produced from *S. pristinaespiralis ΔpglAΔsnaE1* supplemented with L-Phg) was used as a control and was referred to as C-PI. Production of **3** and **4** (for structure see Fig. 2) was confirmed using HPLC-MS/MS analysis by comparing the fragmentation pattern of **1** with that of the respective halogenated derivatives (Fig. S1, ESI†). Three prominent, reoccurring mass signals (*m*/*z* = 578.3, 663.3, and 839.4) were detected and assigned to fractions of the parental ion pristinamycin I (Fig. S1a, ESI†). These fragments, which were determined to include the L-Phg residue in pristinamycin I, were shifted in masses corresponding to the addition of the respective halogen atom introduced (+34 for the chlorine main isotope, +18 for fluorine; shift is the mass of the atom −1 to account for the mass of the replaced hydrogen (Fig. S1b and c, respectively, ESI†)), suggesting the incorporation of the respective halogenated mutasynthons at the expected position in pristinamycin I. In order to produce sufficient amounts of substance for the structural elucidation of **3** and **4** by NMR analysis, mutasynthesis was carried out on a large scale. In total, 12 l and 6 l cultures were extracted for **3** and **4** isolation, respectively. HPLC fractions were analyzed by HRESIMS analysis to confirm the presence of **3** and **4** (Fig. S2 and S3, ESI†), respectively, whereby HRESIMS data of **1** served as a reference (Fig. S4, ESI†). HPLC fractions containing 0.6 mg of **3** and 1.54 mg of **4**, respectively, were subjected to NMR analysis (NMR data for **1**, **3**, and **4** are available in Table 2 and in ESI,† Fig. S5–S21). As expected, the NMR data of **3** were highly similar to those of **1** (Table 2). However, the presence of two broad doublets (δ_H 7.24 and 7.37) in the ^{1}H NMR spectrum as part of the characteristic AA′BB′ system indicated the incorporation of the 4-chloro-Phg unit. In the ^{13}C NMR spectrum of **4**, the splitting of the signals C-4/C-8, C-5/C-7 and C-6 with coupling constants $J_{C,F}$ = 8.6 Hz, 21.5 Hz and 245 Hz, respectively, indicated the coupling to the fluorine atom. Furthermore, the single peak at $\delta_F = -113.4$ ppm gave direct proof of fluorine incorporation (Table 2 and Fig. S22, ESI†). The production rates of the PI derivatives were difficult to determine due to the inconsistent production behavior of the *ΔpglAΔsnaE1* mutant. PI derivative concentrations were only measured for the pooled samples of C-PI, **3**, and **4**, which were produced in amounts of 1.52 μg mL^{-1}, 1.55 μg mL^{-1}, and 1.51 μg mL^{-1}, respectively. Thus, the data indicate an incorporation of the unnatural derivatives at almost the same efficiency as the natural L-Phg precursor. Furthermore, the production of C-PI reached roughly half the amount produced by the wild-type strain (Fig. 4), which yielded an average of about 5 μg mL^{-1} of **1**. Altogether, the lower PI derivative production yields are more likely due to the inconsistent production performance of the *ΔpglAΔsnaE1* mutant strain, rather than that the acceptance of the halogenated derivatives is limiting.

2.4 Pristinamycin I mutasynthesis products are antimicrobially active

To test, whether the generated pristinamycin I derivatives are antimicrobially active, bioassays were carried out with crude extracts mutasynthesis samples containing **3** and **4**. The antibiotic activity of crude extract samples was tested and confirmed against *B. subtilis* (data not shown). Bioactive samples were additionally tested against a panel of clinically relevant microorganisms from the WHO priority list of pathogens, including different Gram-positive and Gram-negative bacteria, as well as fungi. Namely, these were *Staphylococcus aureus* DSM 18827, CIP 111304, and CIP 108540, *Enterococcus faecium* DSM 20477, *Pseudomonas aeruginosa* DSM 1117, *Escherichia coli* DSM 1103, *Proteus vulgaris* DSM 2140, *Candida albicans* DSM 1386, and *Trichophyton rubrum* DSM 16111 (Table S1, ESI†). Of the three tested *S. aureus* strains, two strains (CIP 111304 and CIP 108540) were specifically selected due to their genetically encoded resistance to S_A and S_B antibiotics. CIP 111304 harbors the genes *vat(A)* and *vgb(A)*, each conferring resistance against S_A and S_B antibiotics, respectively, whereas CIP 108540 contained the S_A resistance genes *vga(A)*, *vga(B)*, and *vat(B)*, as well as the S_B resistance genes *erm(A)* and *erm(B)*.[47] DSM18827 was

Table 2 NMR (^{1}H 700 MHz, ^{13}C 175 MHz) for pristinamycin I (DMSO-d_6) (**1**), 6-chloropristinamycin I (CH_3OH-d_4) (**3**) and 6-fluoropristinamycin I (DMSO-d6) (**4**)

		Pristinamycin I (1)		6-Fluoropristinamycin I (4)		6-Chloropristinamycin I (3)	
Unit	Position	^{13}C, mult.	^{1}H, mult.	^{13}C, mult.	^{1}H, mult.	^{13}C, mult.[d]	^{1}H, mult.
Phg	1	168.5, C		168.6, C		169.6, C	
	2	56.8, CH	5.63, d (8.9)	55.3, CH	5.63, m	57.0, CH	5.63, s
	2-NH		8.48, d (8.9)		8.52, br s		
	3	136.2, C		132.7, C		135.9, C	
	4/8	127.7, CH	6.56, m	130.0, CH[a]	7.24, m	130.6, CH	7.24, br d (8.4)
	5/7	128.7, CH	7.35, m	115.6, CH[b]	7.20, m	129.9, CH	7.37, br d (8.4)
	6	128.3, C	7.34, m	161.8, C[c]		135.2, C	
Opp	9	168.4, C		168.8, C		170.1, C	
	10	56.1, CH	5.21, br d (5.4)	58.6, CH	5.45, m	58.0, CH	5.29, br s
	11	40.7, CH_2	2.04, m	40.7, CH_2	2.08, m	41.9, CH_2	2.25, m
			0.52, dd (15.0, 5.7)		0.57, dd (15.5, 4.0)		0.61, m
	12	203.1, C		203.7, C		206.6, C	
	13	38.5, CH_2	2.23, ddd (16.3, 11.9, 7.4)	38.6, CH_2	2.21, m	39.6, CH_2	2.33, m
			2.14, br d (16.3)		2.12, br d (16.3)		2.24, m
	14	36.0, CH_2	4.54, br dd (13.6, 7.4)	36.1, CH_2	4.53, m	37.7, CH_2	4.70, m
			2.63, ddd (13.6, 11.9, 4.5)		2.63, m		2.76, m
Mdp	15	170.5, C		170.7, C		173.5, C	
	16	53.7, CH	4.99, dd (11.6, 4.5)	53.7, CH	5.03, br s	56.0, CH	5.17, m
	17	35.1, CH_2	3.28, t (12.1)	35.1, CH_2	3.23, m	35.1, CH_2	3.26, m
			2.83, m		2.84, m		3.05, dd (12.5, 4.3)
	18	123.0, C		123.1, C		124.5, C	
	19/23	130.2, CH	6.99, br d (8.6)	130.2, CH	6.99, br d (8.4)	131.5, CH	7.07, br d (8.4)
	20/22	112.9, CH	6.78, br d (8.6)	112.9, CH	6.74, br d (8.4)	114.3, CH	6.75, br d (8.4)
	21	150.4, C		150.3, C		152.0, C	
	24/25	40.3, CH_3	2.83, s	40.4, CH_3	2.83, s	40.7, CH_3	2.90, s
	26	30.8, CH_3	3.18, s	30.8, CH_3	3.17, br s	31.3, CH_3	3.25, br s
Pro	27	173.2, C		172.9, C		173.8, C	
	28	56.8, CH	4.64, t (7.4)	56.9, CH	4.64, t (7.4)	58.8, CH	4.63, t (7.4)
	29	27.3, CH_2	2.04, m	27.4, CH_2	2.08, m	28.6, CH_2	2.17, m
			0.80, m		0.88, m		1.10, m
	30	24.4, CH_2	1.52, m	24.4, CH_2	1.56, m	25.5, CH_2	1.43, m
			1.23, m		1.20, m		
	31	47.3, CH_2	3.68, m	47.3, CH_2	3.65, m	49.1, CH_2	3.68, m
			3.31, m		3.28, m		
Abu	32	168.8, C		168.9, C		171.4, C	
	33	50.8, CH	4.77, dt (9.3, 7.7)	50.8, CH	4.73, q (7.5)	52.8, CH	4.81, m
	33-NH		8.28, d (9.3)		n.o.		
	34	23.5, CH_2	1.68, dtq (13.2, 7.7, 7.3)	23.7, CH_2	1.67, dtq (13.2, 7.5, 7.3)	25.3, CH_2	1.74, m
			1.53, m		1.52, m		1.63, m
	35	10.1, CH_3	0.79, t (7.3)	10.0, CH_3	0.79, t (7.3)	10.1, CH_3	0.92, t (7.4)
Thr	36	166.8, C		n.o.		169.4, C	
	37	54.4, CH	4.91, dd (10.5, 1.1)	54.7, CH	4.9, d (10.3)	56.8, CH	4.99, br s
	37-NH		8.07, d (10.5)		8.52, br s		
	38	71.6, CH	5.66, qd (6.5, 1.1)	71.7, CH	5.63, m	73.2, CH	5.80, qd (6.4, 1.7)
	39	15.9, CH_3	1.11, d (6.5)	16.0, CH_3	1.10, d (6.5)	16.4, CH_3	1.28, d (6.4)
Hpc	40	169.0, C		n.o.		171.0, C	
	41	131.6, C		n.o.		132.1, C	
	42	139.3, CH	7.80, m	n.o.		141.2, CH	7.98, br s
	43	129.5, CH	7.78, m	128.2, CH	7.30, m	130.3, CH	7.63, dd (8.1, 4.4)
	44	126.5, CH	7.58, dd (8.0, 1.7)	126.5, CH	7.23, m	127.5, CH	7.48, d (8.4)
	45	157.5, C		n.o.		n.o.	
	45-OH		11.97, s		11.97, br s		

n.o. not observed. [a] Doublet with $J_{C,F}$ = 8.6 Hz. [b] Doublet with $J_{C,F}$ = 21.5 Hz. [c] Doublet with $J_{C,F}$ = 245 Hz. [d] Signals assigned from HSQC and HMBC correlations.

selected as a multi-resistant test strain[48] (Table S1, ESI†). Of the different test strains, *Enterococcus faecium* was inhibited by the crude extract samples containing **3** and **4**, respectively, to a similar extent as observed with pure pristinamycin I substance and Synercid®, which were used as positive controls (Fig. S22A, ESI†). Bioassays with **1**, **3** and **4** were also carried out in combination with pure pristinamycin II compound (10 µg per compound and filter disc). Here, *E. faecium* and the *S. aureus*

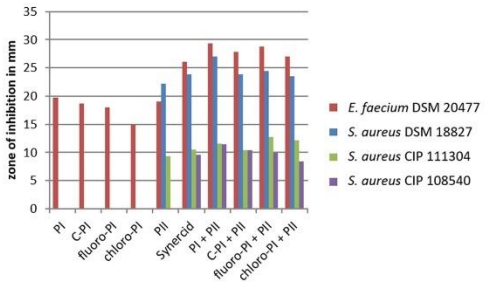

Fig. 5 Diameter of inhibition zones caused by pristinamycin I derivatives. Crude extract samples of C-PI, 6-fluoropristinamycin I (6-fluoro-PI), 6-chloropristinamycin I (6-chloro-PI) were used as well as pure pristinamycin I (PI) and II (PII). All S_8 samples were applied with and without the addition of pristinamycin II. Synercid® filter discs were used as a positive control.

test strains were inhibited by the respective pristinamycin I derivative plus pristinamycin II combination to a similar extent as with the respective positive control samples, which were pure pristinamycin I + II mixture and Synercid®, respectively (Fig. 5 and Fig. S22A–D, ESI†). Altogether, this showed that **3** and **4** have antimicrobial activities similar to that of the natural compound **1**. Furthermore, MIC assays and cytotoxicity tests were performed with pure **4** as this compound was available in sufficient amounts (approx. 1 mg of the pure compound) to allow for additional bioactivity tests. MIC analysis was performed using a panel of standard test organisms, including yeast, fungi, Gram-negative bacteria, as well as *B. subtilis*, *S. aureus*, and *Mycobacterium smegmatis* as Gram-positive test bacteria. Here, the derivative **4** inhibited the growth of *S. aureus* at a concentration of 33.2 μg mL^{-1} and that of *B. subtilis* at a concentration of 4.2 μg mL^{-1}, which were 16.7 μg mL^{-1} and 2.1 μg mL^{-1} for the pristinamycin I control, respectively (Table S2, ESI†). Since the MIC values of **4** and **1** resided in a similar range, the generated derivative **4** is obviously similarly bioactive as the natural compound **1**. Cytotoxicity assays were carried out with **4** and **1** against two standard human cell lines (KB3.1 and L929), respectively. As with the pristinamycin I (**1**) control, no effect on proliferation was observed for **4** (Table S3, ESI†). Thus, altogether the **4** derivative shows an equal bioactivity pattern as the natural pristinamycin I (**1**). So far, this represents the only example of successful mutasynthesis of streptogramin antibiotics.

In a recent study from Walker and Clardy, 2021[49] on a machine learning bioinformatics approach to predict bioactivities from BGCs, it has been found that BGCs containing Phg encoding genes are explicitly associated with antibacterial activities. Unlike proteinogenic amino acids, Phg does not have a β-carbon, so it has fewer rotatable bonds than proteinogenic aromatic amino acids like *e.g.* phenylalanine. Therefore, Phg-containing peptides should be more rigid, reducing the entropic cost for binding to a target.[50] Thus overall, we predict to be Phgs a good target residue for derivatization to improve compound properties.

2.5 Target related studies with pristinamycin I derivatives

To investigate the inhibitory effect of the pristinamycin I derivatives on protein biosynthesis as an antibiotic target, *in vitro* transcription/translation assays were performed using semi-purified pristinamycin I derivatives **3** and **4** and respective control samples (pristinamycin I (**1**) and II). Assays were carried out and evaluated as reported before.[51] Based on previous studies, *iv*TT fluorescence values of 0–20% indicate strong inhibition of the assay, 0–40% are considered to represent specific inhibition, whereas values above 40% do not indicate inhibition of the *iv*TT assay. In *iv*TT assays with pristinamycin derivatives, it was found that pristinamycin II resulted in strong inhibition of the *iv*TT assay, whereas neither pristinamycin I (**1**) nor the halogenated pristinamycin I derivatives **3** and **4** led to an inhibition (Fig. S23, ESI†). This might be explained by the insufficiency of the *iv*TT assay to sense streptogramin B-mediated protein synthesis inhibition as it has been reported previously that translational inhibition was also not detected in cell-free assays for streptogramin B antibiotics, such as virginiamycin S, quinupristin (**2**) or pristinamycin I (**1**).[52–54]

2.6 Extended mutasynthesis with *E. coli*-derived mutasynthons

To generally extent the possibility of accessing further, potentially not commercially available Phg derivatives, we established an *E. coli* BL21(DE3) whole cell biotransformation route from halogenated phenylalanines as precursors to produce Phg derivatives (Fig. S3, ESI†). We have demonstrated in a previous study that *E. coli* BL21(DE3) is a suitable microorganism to transform L-phenylalanine derivatives to the corresponding mandelic acid by using a heterologously expressed hydroxymandelate synthase gene *hmaS* from *A. mediterranei*.[55] To expand the production platform to Phg, we further expressed the genes for mandelate oxidase (*hmo*) from *S. coelicolor* and leucine dehydrogenase (*bcd*) from *B. thuringensis* in a second *E. coli* BL21(DE3) strain. To overcome a NADH cofactor limitation, the glucose dehydrogenase (*gdh*) was additionally expressed in *E. coli* BL21(DE3). To test the substrate spectrum of the Hmo-LeuDH-GDH cascade, a variety of halogenated mandelic acid derivatives were tested. Fluorinated Phgs were detected in the supernatant with a high enantiomeric excess of more than 95%, while chlorinated Phgs were detected with a lower enantiomeric excess of 50% for 2-chloro-L-Phg (Table S4, ESI†).

Mutasynthesis is usually carried out with chemically pure mutasynthons as building blocks that are supplied to the respective biosynthesis mutant. In order to establish a completely fermentative biosynthetic route from the production of the mutasynthon to the final mutasynthesis end product, we developed a mixed mutasynthesis set-up, involving samples from the *E. coli* biotransformation approach that were fed to *S. pristinaespiralis ΔpglAΔsnaE1* as pristinamycin I mutasynthesis strain. This should allow for a direct incorporation of non-commercially available mutasynthons and in principle also provide a more sustainable production route for drug derivatization. To test for the feasibility of such an approach, 100 mL of

S. pristinaespiralis ΔpglAΔsnaE1 main cultures were supplemented with 1 mL of sterile filtered culture supernatants of *E. coli* BL21(DE3) pET28-*hmo*/pACYC-*bcd-gdh*, which contained approx. 1 mg mL^{-1} of 4-fluoro-Phg as representative Phg mutasynthon for pristinamycin I derivatization. LC-MS analysis of crude extracts from *ΔpglAΔsnaE1* fed with 4-fluoro-Phg biotransformation supernatant samples led to mass signals characteristic of 6-fluoro-PI (Fig. S24, ESI†). Thus, 4-fluoro-Phg from *E. coli* supernatant samples was successfully incorporated into pristinamycin I, which proved the feasibility of the adapted mutasynthesis procedure. Thereby, the pristinamycin derivative production rates were comparable to those when supplemented with commercially available mutasynthons (Fig. S24A–F, ESI†). This shows that the biotransformation-based mutasynthesis approach is comparably efficient to conventional mutasynthesis. The extended version of the mutasynthesis approach including biotransformation-derived mutasynthon samples was termed "biotransformation-coupled mutasynthesis".

3. Conclusions

The streptogramin family of antibiotics represents a rare and underexplored family of antibiotics with pristinamycin I (**1**) as a representative substance in clinical application as an antibiotic of last resort against multi-drug resistant bacterial infections. Substance derivatization is difficult to implement chemically due to the structural complex nature structure of the streptogramin molecule(s). So far, the mutasynthesis of streptogramin antibiotics has been prevented by the lack of knowledge on precursor biosynthesis and the encoded genes. In this study, we present the first successful mutasynthesis approach for the derivatization of the streptogramin antibiotic pristinamycin I (**1**) based on a modification of the Phg residue. Two halogenated pristinamycin I derivatives, 6-chloropristinamycin I (**3**) and 6-fluoropristinamycin I (**4**), were generated by mutasynthesis, their chemical structures were confirmed by NMR and the bioactivity of both substances was demonstrated with antibacterial bioassays. The pristinamycin I mutasynthesis approach was extended by a biotransformation process using a genetically modified *E. coli* strain as a Phg mutasynthon producer, which provided Phg derivatives that were directly fed to the mutasynthesis strain. This mutasynthesis 2.0 process represents a novel extension of the original mutasynthesis method and the feasibility of the process has been demonstrated by the successful production of 46-fluoropristinamycin I (**4**).

4. Material and methods

4.1 Bacterial strains and plasmids

The bacterial strains and plasmids used in this study are listed in Table S1 (ESI†). For routine cloning work, *Escherichia coli* Novablue (Novagen) (Sigma-Aldrich, Germany) was used. *S. pristinaespiralis* PR11 (Sanofi-Aventis) was used for pristinamycin production analysis and *S. pristinaespiralis* M*pglA*[41] served as the host strain for the generation of the *S. pristinaespiralis* mutasynthesis strain. The biological samples used for the experiments were obtained from the Leibniz Institut DSMZ – Deutsche Sammlung von Mikroorganismen und Zellkulturen GmbH, Braunschweig, Germany.

4.2 Media and cultivation conditions

Strain cultivation procedures for *S. pristinaespiralis* were carried out as described before.[56] For cultivation and harvesting of genomic DNA, *S. pristinaespiralis* strains were grown in 100 mL of S-medium[57] in 500 mL Erlenmeyer flasks (with steel springs) on an orbital shaker (180 rpm) at 28 °C. Kanamycin (50 μg mL^{-1}), apramycin (50 μg mL^{-1}), and thiostrepton (50 μg mL^{-1}) were used for selection when appropriate. For pristinamycin production analysis, *S. pristinaespiralis* strains were grown in 100 mL of the HT7T medium.[58]

4.3 Preparation and manipulation of DNA

Total DNA isolation from *S. pristinaespiralis* was performed as described by Kieser *et al.*, 2000[57] and with the DNA Nucleospin Microbial DNA kit (Bioanalysis, Macherey-Nagel, Germany), respectively. Plasmid isolation was performed using the peqGold Plasmid MiniPrep kit (VWR, Life Science, USA), Pure Yield Plasmid MidiPrep System kit (Promega, USA), or according to Sambrook *et al.*, 1989.[59] PCR products were purified from 1% agarose gel using the Wizard® SV Gel and PCR Clean-Up System kit (Promega, USA). Enzymes, including restriction endonucleases, ligase, and Q5 DNA polymerase were used according to the manufacturer's recommendations (New England Biolabs, USA; Thermo Fischer Scientific, USA). The primers used for PCR were obtained from MWG Biotech AG (MWG; Ebersberg, Germany) and are listed in Table S1 (ESI†). The primers used for PCR were obtained from MWG Biotech AG (MWG; Ebersberg, Germany) and are listed in Table S1 (ESI†).

4.4 Cloning procedure for obtaining mutasynthesis strain *S. pristinaespiralis ΔpglAΔsnaE1*

The mutasynthesis strain *S. pristinaespiralis ΔpglAΔsnaE1* was generated using the following procedure: A 2.4 kb fragment (*snaE1′*), covering an internal part of the *snaE1* gene, was amplified with PCR using genomic DNA from strain *S. pristinaespiralis* PR11 as template and primer pair MsnaE1fw/rv (Table S1, ESI†). The *snaE1′* amplificate was subcloned into the *Eco*RV-restricted *E. coli* vector pDRIVE, resulting in the construct pDRIVE/snaE1′. The *snaE1′* fragment was isolated from pDRIVE/snaE1′ as an *Eco*RI fragment and then ligated into the *Eco*RI-restricted *E. coli* vector pK18, resulting in the construct pK18/snaE1′. A 1.1 kb thiostrepton resistance cassette (*tsr*^{R}) was isolated as a *Sna*BI/*Ale*I fragment from pDRIVE/thio and cloned into the *Stu*I restriction site of *snaE1′*, resulting in the mutational construct pK18/snaE1tsr (Fig. S25, ESI†). The plasmid was transferred to the *pglA* deletion mutant *S. pristinaespiralis* M*pglA*[41] by protoplast transformation, followed by selection for apramycin/thiostrepton-resistant and kanamycin-sensitive transformants, which resulted in the double mutant *S. pristinaespiralis ΔpglAΔsnaE1*. The correctness of the mutant was verified by PCR using genomic DNA from *ΔpglAΔsnaE1*. For verification of the *snaE1* gene inactivation, primer pairs

were used, which annealed to the *tsr*^{R} cassette (thio1/2) and to internal parts of the *snaE1* gene (K*snaE1*fw/rv), respectively. A 0.4 kb fragment was amplified with the primer pair thio1/2, a 2.1 kb fragment with primer pair K*snaE1*fw/rv, a 0.8 kb fragment with the primer pair K*snaE1*fw/thio2, and a 1.7 kb fragment with the primer pair thio1/K*snaE1*rv, confirming the correctness of the *S. pristinaespiralis ΔpglAΔsnaE1* mutant (Fig. S26, ESI†).

4.5 Mutasynthesis with Phg derivatives

For mutasynthesis experiments with *S. pristinaespiralis*, strains were grown in 100 mL of HT7T medium as a preculture. After 72 hours, 10 mL of preculture was used to inoculate 100 mL of fresh HT7T medium as the main culture. For feeding experiments, the main cultures were supplemented with different mutasynthons (Table 1) (solubilized with 70 μL of 1 N NaOH and neutralized with 50 μL of 1 N HCl per mg compound) to reach a final concentration of 10 μg mL^{-1}. The cells were grown for 168 hours at 28 °C under shaking at 180 rpm. To perform mutasynthesis with *E. coli* biotransformation samples, main cultures were prepared as described above and supplemented with 1 mL of *E. coli* BL21(DE3) pET28-*hmo*/pACYC-*bcd-gdh* culture supernatant containing approx. 1 mg mL^{-1} of the respective mutasynthon.

4.6 Compound extraction and purification

For initial compound detection and bioassay testing with *S. pristinaespiralis* samples, 5 mL of culture was extracted with 5 mL of ethyl acetate (1 : 1) for 1 h at room temperature (RT) in an overhead shaker. After centrifugation at 5000 rpm for 20 min, ethyl acetate phases were concentrated *in vacuo* completely and then dissolved in 500 μL of methanol. Crude extracts were used for bioassays, high-performance liquid chromatography (HPLC) and high-performance liquid chromatography-mass spectrometry (HPLC-MS, HPLC-MS/MS) analysis. Batch cultures of *S. pristinaespiralis ΔpglAΔsnaE1* fed with chlorinated or fluorinated mutasynthons were grown, extracted, and treated for compound purification following Protocol S1 and S2, respectively. In total, 12 l and 6 l of culture were extracted for **3** and **4** isolation, respectively. Pure fractions were used to elucidate the structure of halogenated derivatives using NMR.

4.7 HPLC and HPLC-ESI-MS(/MS) analyses of pristinamycin variants

HPLC analyses of pristinamycin derivatives were performed using an HP1090M system with ChemStation 3D software rev. A.08.03 (Agilent Technologies, Waldbronn, Germany) on a Waters Symmetry C18 (3.0 × 150 mm, 5 μm) with a flow rate of 850 μL min^{-1}. Chromatography was done by linear step gradient elution from 80% solvent A (water with 0.1% phosphoric acid) and 20% solvent B (acetonitrile to 50% solvent B over 12 min, 50% solvent B to 100% solvent B over 3 min followed by a 3 min hold of 100% solvent B). The injection volume was 5 μL. Multiple wavelength monitoring was performed at 210, 230, 260, 280, 310, 360, 435 and 500 nm. UV-Vis spectra were measured from 200 to 600 nm. The evaluation of the chromatograms (210 nm only) was done by means of an in-house HPLC-UV-Vis database. HPLC-MS and HPLC-MS/MS analyses of pristinamycin derivatives were performed using an Agilent 1200 series chromatography system (binary pump, high performance autosampler, DAD-detector) coupled with an LC/MSD Ultra Trap System XCT 6330 (Agilent Technologies, Waldbronn, Germany). The sample (2.5 μL) was injected on a Nucleosil 100 C18 column (100 × 2 mm, 3 μm) fitted with a precolumn (10 × 2 mm, 3 μm) at a flow rate of 400 μL min^{-1} and a linear gradient from 90% solvent A (0.1% formic acid in water) to 100% solvent B (0.06% formic acid in acetonitrile) over 15 minutes at 40 °C. UV-Vis-detection was done at 220, 260, 280, 360 and 435 nm. Electrospray ionization was performed in positive and negative ultra-scan modes (alternating) with a capillary voltage of 3.5 kV and a drying gas temperature of 350 °C. Detection of *m*/*z* values was conducted with Agilent DataAnalysis for 6300 Series IonTrap LC/MS Version 3.4 (Bruker Daltonik). Upon HPLC-MS analysis, pristinamycin I derivatives were identified by comparison of their UV-Vis spectra, retention times and molecular masses with an authentic pristinamycin I (PI) standard (Sanofi-Aventis) and predicted masses for **1** = *m*/*z* 867.4034 $[M + H]^+$, and derivatives **3** = *m*/*z* 901.3646 $[M + H]^+$, and **4** = *m*/*z* 885.3941 $[M + H]^+$.

Pristinamycin I (**1**): white powder; $[\alpha]_D^{20\,°C}$ −50 (*c* 0.6 g/100 mL, MeOH); UV (MeOH) λ_{max} (log ε) 202 (4.8), 260 (4.2), 304 (3.9); ESI-MS: *m*/*z* 865.32 $[M-H]^-$ and 867.56 $[M + H]^+$; HR-ESI-MS: *m*/*z* 867.4034 $[M + H]^+$ (calculated for sum formula $C_{45}H_{55}N_8O_{10}$, 867.4036).

6-Chloro-PI (**3**): white to slightly brown powder; UV (MeOH) λ_{max} (log ε) 201 (4.9), 255 (4.3), 302 (4.0); ^{1}H NMR data (700 MHz, CH_3OH-d_4): see Table 2; ^{13}C NMR data (175 MHz, CH_3OH-d_4): see Table 2; ESI-MS: *m*/*z* 899.47 $[M-H]^-$ and 901.44 $[M + H]^+$; HR-ESI-MS: *m*/*z* 901.3645 $[M + H]^+$ (calculated for $C_{45}H_{54}N_8O_{10}Cl$, 901.3646).

6-Fluoro-PI (**4**): white powder; $[\alpha]_D^{20\,°C}$ −45 (*c* 0.1 g mL^{-1}, MeOH); UV (MeOH) λ_{max} (log ε) 203 (4.8), 260 (4.2), 303 (3.9); ESI-MS: *m*/*z* 883.55 $[M-H]^-$ and 885.54 $[M + H]^+$; ^{1}H NMR data (700 MHz, DMSO-d_6): see Table 2; ^{13}C NMR data (175 MHz, DMSO-d_6): see Table 2; ^{19}F NMR (470 MHz, DMSO-d_6): δ_F 113.38 ppm; HR-ESI-MS: *m*/*z* 885.3945 $[M + H]^+$ and 907.3762 $[M + Na]^+$ (calculated $C_{45}H_{54}N_8O_{10}F$, 885.3941 and $C_{45}H_{53}N_8O_{10}FNa$, 907.3748).

Atom numbering refers to Oku *et al.* 2004.[60]

4.8 Structure elucidation

NMR spectra were recorded using an Avance III 700 spectrometer with a 5 mm TCI cryoprobe (^{1}H 700 MHz, ^{13}C 175 MHz) and an Avance III 500 spectrometer (^{1}H 500 MHz, ^{13}C 125 MHz) (both Bruker BioSpin, Rheinstetten, Germany). Chemical shifts δ were referenced to DMSO-d_6 (δ_H = 2.50 ppm; ^{13}C, δ_C = 39.51 ppm), $CHCl_3$-d (δ_H = 7.27 ppm; ^{13}C, δ_C = 77.0 ppm) and trifluoroacetic acid (δ_F = −74.95 ppm in DMSO).

ESI mass spectra were recorded with an UltiMate 3000 Series uHPLC (Thermo Fisher Scientific, Waltman, MA/USA) by utilizing a C18 Acquity UPLC BEH column (50 × 2.1 mm, 1.7 μm; Waters, Milford, USA) connected to an amaZon speed ESI-Iontrap-MS (Bruker Daltonics, Bremen, Germany). The HPLC parameters were

set as follows: solvent A: H_2O + 0.1% formic acid, solvent B: acetonitrile (MeCN) + 0.1% formic acid, gradient: 5% B for 0.5 min, increasing to 100% B over 19.5 min, keeping 100% B for a further 10 min, flow rate 0.6 mL min^{-1}, and DAD detection 190–600 nm.

HRESIMS was performed using a maXis ESI-TOF (electrospray ionization-time of flight) mass spectrometer (Bruker GmbH, Bremen, Germany) coupled to an Agilent 1260 series HPLC-UV system equipped with a C18 Acquity UPLC BEH 2.1 × 50 mm, 1.7 µm (Waters) column; DAD-UV detection at 200–600 nm; solvent A (H_2O) and solvent B (MeCN) supplemented with 0.1% FA as a modifier; flowrate of 0.6 mL min^{-1}, 40 °C oven temperature, gradient elution system with stationary phase of 0.5 min at 5% B, followed by an increase from 5% to 100% B in 19.5 min and holding at 100% B for 5 min.

4.9 Computational docking studies of pristinamycins with the ribosome

For computational docking studies with pristinamycins, SeeSAR version 13.0.1 was used; BioSolveIT GmbH, Sankt Augustin, Germany, 2023, **https://www.biosolveit.de/SeeSAR**. PDB files of the co-crystal structures of quinupristin (**2**) with the ribosome of *E. coli* (PDB: 4U26), *D. radiodurans* (PDB: 1MS1), and *H. marismortui* (PBD: 1YJW)[34,35,44] were downloaded from **https://www.rcsb.org/**. Fragment growing and truncation approaches were performed based on the structure of quinupristin (**2**) and poses of pristinamycin I (**1**) as well as new derivatives with modifications of the Phg moiety were generated and re-docked into the binding pockets of quinupristin (**2**).

4.10 Disk diffusion bioassays

General antibiotic activity of pristinamycin variants was analyzed by disc diffusion assays using *Bacillus subtilis* ATCC 6633 as the test organism and was carried out as reported before.[61] Additionally, a panel of pathogenic organisms including, Gram-positive and Gram-negative bacteria, as well as eukaryotic organisms was used (Table S1, ESI†). 30 µL of *S. pristinaespiralis* culture extracts were pipetted on a filter disc, which was placed on a *Bacillus subtilis* test plate. Synercid® filter discs (15 µg; Oxoid) were used as a positive control and 30 µL of methanol as a negative control. The plates were incubated overnight at 37 °C. The bioactivity of the samples was determined qualitatively by measuring the diameter of the inhibition zone. For more quantitative activity tests of halogenated pristinamycin I derivatives **3** and **4** using streptogramin susceptible pathogenic test organisms (*Enterococcus faecium* DSM 20477 and *Staphylococcus aureus* (DSM 18827, CIP 111304, CIP 108540)), the amount of used extract was calculated to contain approximately 10 µg of the respective derivative and was added to filter discs with or without 10 µg of pristinamycin II, respectively.

4.11 Minimal inhibition concentration (MIC) tests

Compound **4** was tested in MIC assays in serial dilutions to determine the minimum inhibitory concentration against standard test organisms, which included fungi, Gram-positive and Gram-negative test bacteria (Table S2, ESI†). Appropriate antibiotics were used as positive controls. Assays were performed following the protocol described by Becker *et al.*[62]

4.12 Cytotoxicity tests

Compound **4** was tested in cytotoxicity assays against two different mammalian cell lines, including human endocervical adenocarcinoma KB 3.1 and mouse fibroblasts L929 cell lines, with epothilone B as a positive control (Table S3, ESI†). Assays were performed following the protocol described by Becker *et al.*[62]

4.13 *In vitro* transcription and translation (*iv*TT) assay with pristinamycin I derivatives

Semi-purified HPLC fractions of **1**, **3**, and **4** were tested in *iv*TT assays. Assays were carried out as reported before[51] and were conducted in triplicates. Each assay had an end concentration of approximately 0.5 µg mL^{-1} of **1**, **3**, **4**, or PI standard (Sanofi-Aventis) with or without the addition of 0.5 µg mL^{-1} pristinamycin II standard (Sanofi-Aventis), respectively. Fluorescence of generated eGFP was measured using a Varioskan LUX plate reader (Thermo Scientific) to quantify the effect of tested samples on transcription/translation.

4.14 Construction of a whole cell biotransformation route for Phg mutasynthon production

In order to biotechnologically produce Phg mutasynthons, a synthetic enzymatic cascade was applied (Fig. S27, ESI†). A whole cell biotransformation route with resting cells was established by heterologous expression of the genes encoding hydroxymandelate synthase (*hms*) from *Amycolatopsis mediterranei*, mandelate oxidase (*hmo*) from *S. coelicolor*, leucine dehydrogenase (*bcd*) from *Bacillus thuringensis*, and glucose dehydrogenase (*gdh*) from *B. megaterium* in *E. coli* BL21(DE3). The construction of the plasmids used is described in Protocol S3. For the formation of cells used for whole cell biotransformation, production of Hms was done as described before.[55] Coproduction of the Hmo, Bcd and Gdh was performed in 2 L shaking flasks containing 400 mL of LB medium (kanamycin (50 µg mL^{-1}) and chloramphenicol (30 µg mL^{-1}). The media were inoculated with an overnight culture to an OD_{600} of 0.02 and incubated at 37 °C and 180 rpm to an OD_{600} of 0.8. Expression was induced with 0.1 mM IPTG and further incubated at 30 °C and 100 rpm for 4 h. Cells were harvested by centrifugation (10 min, RT, 4000 × *g*) and washed twice with 200 mM Tris–HCl buffer (pH 7.5). The optical density at 600 nm was monitored photometrically using a Cary 50 Bio spectrophotometer (Varian, Mulgrave, Australia). The biotransformation was performed in two steps in 250 mL shaking flasks with a reaction volume of 20 mL. The transformation of the phenylalanine derivative to the corresponding mandelic acid was performed as described before.[55] The supernatant was isolated after 24 h of incubation by centrifugation (10 min, RT, 4000 × *g*) and was used directly as a substrate for the transformation to the Phg synthesis with *E. coli* BL21(DE3) pET28-*hmo*/pACYC-*bcd-gdh*. 20 mM glucose and 50 mM ammonium acetate were added after 1 h and 16 h to the HMO-LeuDH-GDH reaction to ensure the cofactor supply. After 24 h of biotransformation, the supernatant was isolated by centrifugation (10 min, RT, 4000 × *g*), sterile

filtrated (Filtropur S (0.45 μm), Sarstedt) and stored at −20 °C until use. The respective enantiomeric excess (ee) of the produced Phgs was determined using HPLC analysis with comparison to standards of available racemic and enantiomeric pure Phgs (Fig. S28, ESI†). The separation of Phg enantiomers was achieved by using a Chirex 3126 (D)-penicillamine column (150 × 4.6 mm, Phenomenex, Aschaffenburg, Germany) with 2 mM copper(II) sulfate and 15% methanol as mobile phase at 30 °C. The isocratic flow was set to 1 mL min^{-1} and 4 μL of sample was injected.

Author contributions

OH carried out a mutasynthesis experiment with *S. pristinaespiralis*. LW and J-WY performed biotransformation experiments for Phg-derivative supply. KH, FS, and AK performed chemical analysis (HPLC, MS/MS, NMR). KH and FS carried out MHC and cytotoxicity tests. PK carried out SeeSAR modeling analysis. J-WY designed and supervised biotransformation studies. YM designed and supervised mutasynthesis studies and coordinated the study.

Conflicts of interest

The authors declare that the research was conducted in the absence of any commercial or financial relationships that could be construed as a potential conflict of interest.

Acknowledgements

We thank Sabine Gronow and the DZIF Pathogen Repository team for supplying us with pathogenic strains from the DSMZ culture collection. Pure pristinamycin I and II compounds were kindly provided by Sanofi-Aventis Pharma. We acknowledge technical assistance from Meike Döppner with *iv*TT assays, Wera Collisi for conducting the MIC and cytotoxicity assays, Esther Surges with NMR and Aileen Gollasch with HRMS measurements. This work was supported by the Baden-Württemberg-Stiftung (BWST_WSF-035). We also acknowledge funding received from the German Center for Infection Research (DZIF) (TTU 09.819) and from the Leibniz Association through the Collaborative Excellence funding program (K445/2022).

References

1 F. Haney and E. W. Hancock, Addressing Antibiotic Failure—Beyond Genetically Encoded Antimicrobial Resistance, *Front. Drug Discov.*, 2022, **2**, 892975.
2 T. Maxson and D. A. Mitchell, Targeted Treatment for Bacterial Infections: Prospects for Pathogen-Specific Antibiotics Coupled with Rapid Diagnostics, *Tetrahedron*, 2016, **72**, 3609–3624.
3 J. F. Prescott, The resistance tsunami, antimicrobial stewardship, and the golden age of microbiology, *Vet. Microbiol.*, 2014, **171**, 273–278.
4 C. J. L. Murray, *et al.*, Global burden of bacterial antimicrobial resistance in 2019: a systematic analysis, *Lancet*, 2022, **399**, 629–655.
5 M. S. Butler, V. Gigante, H. Sati, S. Paulin, L. Al-Sulaiman, J. H. Rex, P. Fernandes, C. A. Arias, M. Paul, G. E. Thwaites, L. Czaplewski, R. A. Alm, C. Lienhardt, M. Spigelman, L. L. Silver, N. Ohmagari, R. Kozlov, S. Harbarth and P. Beyer, Analysis of the Clinical Pipeline of Treatments for Drug-Resistant Bacterial Infections: Despite Progress, More Action Is Needed, *Antimicrob. Agents Chemother.*, 2022, **66**, e0199121.
6 F. Kloß and S. Gerbach, Obstacles and perspectives of new antimicrobial concepts within research and development, *Bundesgesundheitsblatt Gesundheitsforschung Gesundheitsschutz*, 2018, **61**, 595–605.
7 A. R. Coates, G. Halls and Y. Hu, Novel classes of antibiotics or more of the same?, *Br. J. Pharmacol.*, 2011, **163**, 184–194.
8 E. A. Barka, P. Vatsa, L. Sanchez, N. Gaveau-Vaillant, C. Jacquard, J. P. Meier-Kolthoff, H. P. Klenk, C. Clément, Y. Ouhdouch and G. P. van Wezel, Taxonomy, Physiology, and Natural Products of Actinobacteria, *Microbiol. Mol. Biol. Rev.*, 2016, **80**, 1–43.
9 A. Gavriilidou, S. A. Kautsar, N. Zaburannyi, D. Krug, R. Müller, M. H. Medema and N. Ziemert, Compendium of specialized metabolite biosynthetic diversity encoded in bacterial genomes, *Nat. Microbiol.*, 2022, **7**, 726–735.
10 R. H. Baltz, Renaissance in antibacterial discovery from actinomycetes, *Curr. Opin. Pharmacol.*, 2008, **8**, 557–563.
11 M. Miethke, M. Pieroni, T. Weber, M. Brönstrup, P. Hammann., L. Halby, P. B. Arimondo, P. Glaser, B. Aigle, H. B. Bode, R. Moreira, Y. Li, A. Luzhetskyy, M. H. Medema, J. L. Pernodet, M. Stadler, J. R. Tormo, O. Genilloud, A. W. Truman, K. J. Weissman, E. Takano, S. Sabatini, E. Stegmann, H. Brötz-Oesterhelt, W. Wohlleben, M. Seemann, M. Empting, A. K. H. Hirsch, B. Loretz, C. M. Lehr, A. Titz, J. Herrmann, T. Jaeger, S. Alt, T. Hesterkamp, M. Winterhalter, A. Schiefer, K. Pfarr, A. Hoerauf, H. Graz, M. Graz, M. Lindvall, S. Ramurthy, A. Karlén, M. van Dongen, H. Petkovic, A. Keller, F. Peyrane, S. Donadio, L. Fraisse, L. J. V. Piddock, I. H. Gilbert, H. E. Moser and R. Müller, Towards the sustainable discovery and development of new antibiotics, *Nat. Rev. Chem.*, 2021, **5**, 726–749.
12 D. Pavlović, S. Mutak, D. Andreotti, S. Biondi, F. Cardullo, A. Paio, E. Piga, D. Donati and S. Lociuro, Synthesis and Structure-Activity Relationships of α-Amino-γ-lactone Ketolides: A Novel Class of Macrolide Antibiotics, *ACS Med. Chem. Lett.*, 2014, **5**, 1133–1137.
13 H. Sun, Z. Liu, H. Zhao and E. L. Ang, Recent advances in combinatorial biosynthesis for drug discovery, *Drug Des., Dev. Ther.*, 2015, **9**, 823–833.
14 S. Weist, C. Kittel, D. Bischoff, B. Bister, V. Pfeifer, G. J. Nicholson, W. Wohlleben and R. Süssmuth, Mutasynthesis of glycopeptide antibiotics: variations of vancomycin's AB-ring amino acid 3, 5-dihydroxyphenylglycine, *J. Am. Chem. Soc.*, 2004, **126**, 5942–5943.
15 K. C. Nicolaou, H. J. Mitchell, N. F. Jain, N. Winssinger, R. Hughes and T. Bando, Total synthesis of vancomycin, *Angew. Chem., Int. Ed.*, 2004, **38**, 240–244.

16 M. J. Moore, S. Qu, C. Tan, Y. Cai, Y. Mogi, D. Jamin Keith and D. L. Boger, Next-generation total synthesis of vancomycin, *J. Am. Chem. Soc.*, 2020, **142**, 16039–16050.
17 S. Pelzer and A. Dziarnowski, Sulfation: a new biocombinatorial tool, *Chem. Biol.*, 2006, **13**, 113–114.
18 W. Wohlleben, Y. Mast, G. Muth, M. Röttgen, E. Stegmann and T. Weber, Synthetic biology of secondary metabolite biosynthesis in actinomycetes: Engineering precursor supply as a way to optimize antibiotic production, *FEBS Lett.*, 2012, **586**, 2171–2176.
19 K. L. Rinehart, Mutasynthesis of new antibiotics, *Pure Appl. Chem.*, 1977, **49**, 1361–1384.
20 J. Kennedy, Mutasynthesis, chemobiosynthesis, and back to semi-synthesis: combining synthetic chemistry and biosynthetic engineering for diversifying natural products, *Nat. Prod. Rep.*, 2008, **25**, 25–34.
21 H. B. Bode and R. Müller, The Impact of Bacterial Genomics on Natural Product Research, *Angew. Chem., Int. Ed.*, 2005, **44**, 6828–6846.
22 A. Kirschning and F. Hahn, Merging chemical synthesis and biosynthesis: a new chapter in the total synthesis of natural products and natural product libraries, *Angew. Chem.*, 2012, **51**, 4012–4022.
23 L. Gou, Q. Wu, S. Lin, X. Li, J. Liang, X. Zhou, D. An, Z. Deng and Z. Wang, Mutasynthesis of pyrrole spiroketal compound using calcimycin 3-hydroxy anthranilic acid biosynthetic mutant, *Appl. Microbiol. Biotechnol.*, 2013, **97**, 8183–8191.
24 M. Kaniusaite, T. Kittila, R. J. Goode, R. B. Schittenhelm and M. J. Cryle, Redesign of substrate selection in glycopeptide antibiotic biosynthesis enables effective formation of alternate peptide backbones, *ACS Chem. Biol.*, 2020, **15**, 2444–2455.
25 K. J. Weissman, Mutasynthesis – uniting chemistry and genetics for drug discovery, *Trends Biotechnol.*, 2007, **25**, 139–142.
26 S. Eichner, T. Knobloch, H. G. Floss, J. Fohrer, K. Harmrolfs, J. Hermane, A. Schulz, F. Sasse, P. Spiteller, F. Taft and A. Kirschning, The Interplay between Mutasynthesis and Semisynthesis: Generation and Evaluation of an Ansamitocin Library, *Angew. Chem., Int. Ed.*, 2012, **51**, 752–757.
27 L. Toscano, G. Fioriello, R. Spagnoli, L. Cappelletti and G. Zanuso, New fluorinated erythromycins obtained by mutasynthesis, *J. Antibiot.*, 1983, **36**, 1439–1450.
28 Z. Hojati, C. Milne, B. Harvey, L. Gordon, M. Borg, F. Flett, B. Wilkinson, P. J. Sidebottom, B. A. M. Rudd, M. A. Hayes, C. P. Smith and J. Micklefield, Structure, Biosynthetic Origin, and Engineered Biosynthesis of Calcium-Dependent Antibiotics from *Streptomyces coelicolor*, *Chem. Biol.*, 2002, **9**, 1175–1187.
29 J. Delzer, H. P. Fiedler, H. Müller, H. Zähner, R. Rathmann, K. Ernst and W. A. König, New nikkomycins by mutasynthesis and directed fermentation, *J. Antibiot.*, 1984, **37**, 80–82.
30 L. Winand, P. Schneider, S. Kruth, N. J. Greven, W. Hiller, M. Kaiser, J. Pietruszka and M. Nett, Mutasynthesis of Physostigmines in *Myxococcus xanthus*, *Org. Lett.*, 2021, **23**, 6563–6567.
31 U. Galm, Marco A. Dessoy, J. Schmidt, L. A. Wessjohann and L. Heide, In Vitro and In Vivo Production of New Aminocoumarins by a Combined Biochemical, Genetic, and Synthetic Approach, *Chem. Biol.*, 2004, **11**, 173–183.
32 D. Ulanova, J. Novotná, Y. Smutná, Z. Kameník, R. Gazák, M. Sulc, P. Sedmera, S. Kadlcík, K. Plháčková and J. Janata, Mutasynthesis of lincomycin derivatives with activity against drug-resistant staphylococci, *Antimicrob. Agents Chemother.*, 2010, **54**, 927–930.
33 S. Reissier and V. Cattoir, Streptogramins for the treatment of infections caused by Gram-positive pathogens, *Expert Rev. Anti-Infect. Ther.*, 2021, **19**, 587–599.
34 D. Tu, G. Blaha, P. B. Moore and T. A. Steitz, Structures of MLSBK Antibiotics Bound to Mutated Large Ribosomal Subunits Provide a Structural Explanation for Resistance, *Cell*, 2005, **121**, 257–270.
35 J. M. Harms, F. Schlünzen, P. Fucini, H. Bartels and A. Yonath, Alterations at the peptidyl transferase centre of the ribosome induced by the synergistic action of the streptogramins dalfopristin and quinupristin, *BMC Biol.*, 2004, **2**, 4.
36 Y. Mast and W. Wohlleben, Streptogramins – Two are better than one!, *Int. J. Med. Microbiol.*, 2014, **304**, 44–50.
37 N. J. Johnston, T. A. Mukhtar and G. D. Wright, Streptogramin Antibiotics: Mode of Action and Resistance, *Curr. Drug Targets*, 2002, **3**, 335–344.
38 M. S. Svetlov, E. A. Syroegin, E. V. Aleksandrova, G. C. Atkinson, S. T. Gregory, A. S. Mankin and Y. S. Polikanov, Structure of Erm-modified 70S ribosome reveals the mechanism of macrolide resistance, *Nat. Chem. Biol.*, 2021, **17**, 412–420.
39 S. Schwarz, J. Shen, K. Kadlec, Y. Wang, G. B. Michael, A. T. Feßler and B. Vester, Lincosamides, streptogramins, phenicols, and pleuromutilins: mode of action and mechanisms of resistance, *Cold Spring Harbor Perspect. Med.*, 2016, **6**, a027037.
40 Y. Mast, T. Weber, M. Gölz, R. Ort-Winklbauer, A. Gondran, W. Wohlleben and E. Schinko, Characterization of the 'pristinamycin supercluster' of *Streptomyces pristinaespiralis*, *Microb. Biotechnol.*, 2011, **4**, 192–206.
41 Y. Mast, W. Wohlleben and E. Schinko, Identification and functional characterization of phenylglycine biosynthetic genes involved in pristinamycin biosynthesis in *Streptomyces pristinaespiralis*, *J. Biotechnol.*, 2011, **155**, 63–67.
42 D. Moosmann, V. Mokeev, A. Kulik, N. Osipenkov, S. Kocadinc, R. Ort-Winklbauer, F. Handel, O. Hennrich, J. W. Youn, G. A. Sprenger and Y. Mast, Genetic engineering approaches for the fermentative production of phenylglycines, *Appl. Microbiol. Biotechnol.*, 2020, **104**, 3433–3444.
43 N. Osipenkov, A. Kulik and Y. Mast, Characterization of the phenylglycine aminotransferase PglE from *Streptomyces pristinaespiralis*, *J. Biotechnol.*, 2018, **278**, 34–38.
44 J. Noeske, J. Huang, N. B. Olivier, R. A. Giacobbe, M. Zambrowski and J. H. Cate, Synergy of streptogramin antibiotics occurs independently of their effects on translation, *Antimicrob. Agents Chemother.*, 2014, **58**, 5269–5279.

45 J. Meng, R. Feng, G. Zheng, M. Ge, Y. Mast, W. Wohlleben, J. Gao, W. Jiang and Y. Lu, Improvement of pristinamycin I (PI) production in *Streptomyces pristinaespiralis* by metabolic engineering approaches, *Synth. Syst. Biotechnol.*, 2017, **2**, 130–136.

46 C. Mahlert, S. A. Sieber, J. Grünewald and M. A. Marahiel, Chemoenzymatic approach to enantiopure streptogramin B variants: characterization of stereoselective pristinamycin I cyclase from *Streptomyces pristinaespiralis*, *J. Am. Chem. Soc.*, 2005, **127**, 9571–9580.

47 S. K. Gupta, P. Sharma, J. B. Barrett, L. M. Hiott, T. A. Woodley, J. G. Frye and C. R. Jackson, Draft genome sequence of a human-associated streptogramin-resistant *Staphylococcus aureus*, *J. Glob. Antimicrob. Resist.*, 2019, **16**, 72–73.

48 B. M. Grüner, S. R. Han, H. G. Meyer, U. Wulf, S. Bhakdi and E. K. Siegel, Characterization of a catalase-negative methicillin-resistant *Staphylococcus aureus* strain, *J. Clin. Microbiol.*, 2007, **45**, 2684–2685.

49 A. S. Walker and J. Clardy, A Machine Learning Bioinformatics Method to Predict Biological Activity from Biosynthetic Gene Clusters, *J. Chem. Inf. Model.*, 2021, **61**, 2560–2571.

50 R. S. Al Toma, C. Brieke, M. J. Cryle and R. D. Süssmuth, Structural aspects of phenylglycines, their biosynthesis and occurrence in peptide natural products, *Nat. Prod. Rep.*, 2015, **32**, 1207–1235.

51 F. Handel, A. Kulik, K. W. Wex, A. Berscheid, J. S. Saur, A. Winkler, D. Wibberg, J. Kalinowski, H. Brötz-Oesterhelt and Y. Mast, Ψ-Footprinting approach for the identification of protein synthesis inhibitor producers, *NAR Genom. Bioinform.*, 2022, **4**, lqac055.

52 G. Chinali, E. Nyssen, M. Di Giambattista and C. Cocito, Inhibition of polypeptide synthesis in cell-free systems by virginiamycin S and erythromycin. Evidence for a common mode of action of type B synergimycins and 14-membered macrolides, *Biochim. Biophys. Acta, Gene Struct. Expression*, 1988, **949**, 71–78.

53 T. A. Mukhtar, K. P. Koteva and G. D. Wright, Chimeric Streptogramin-Tyrocidine Antibiotics that Overcome Streptogramin Resistance, *Chem. Biol.*, 2005, **12**, 229–235.

54 C. Cocito and F. Vanlinden, Inhibitory action of virginiamycin components on cell-free systems for polypeptide formation from *Bacillus subtilis*, *Arch. Mikrobiol.*, 1983, **135**, 8–11.

55 J.-W. Youn, C. Albermann and G. A. Sprenger, *In vivo* cascade catalysis of aromatic amino acids to the respective mandelic acids using recombinant *E. coli* cells expressing hydroxymandelate synthase (HMS) from *Amycolatopsis mediterranei*, *Mol. Catal.*, 2020, **483**, 110713.

56 Y. Mast, J. Guezguez, F. Handel and E. Schinko, A Complex Signaling Cascade Governs Pristinamycin Biosynthesis in *Streptomyces pristinaespiralis*, *Appl. Environ. Microbiol.*, 2015, **81**, 6621–6636.

57 T. Kieser, M. J. Bibb, M. J. Buttner, K. F. Chater and D. A. Hopwood, *Practical Streptomyces genetics*, John Innes Foundation, Norwich, 2000.

58 M. Folcher, H. Gaillard, L. T. Nguyen, K. T. Nguyen, P. Lacroix, N. Bamas-Jacques, M. Rinkel and C. J. Thompson, Pleiotropic functions of a *Streptomyces pristinaespiralis* autoregulator receptor in development, antibiotic biosynthesis, and expression of a superoxide dismutase, *J. Biol. Chem.*, 2001, **276**, 44297–44306.

59 J. Sambrook, E. F. Fritsch and T. Maniatis, *Molecular cloning: a laboratory manual*, Cold Spring Harbor Laboratory Press, New York, 2nd edn, 1989.

60 N. Oku, S. Takemura, H. Onaka and Y. Igarashi, NMR characterization of streptogramin B and L-156,587, a non-synergistic pair of the streptogramin family antibiotic complexes produced inductively by a combined culture of *Streptomyces albogriseolus* and *Tsukamurella pulmonis*, *Magn. Reson. Chem.*, 2022, **60**, 261–270.

61 I. Handayani, H. Saad, S. Ratnakomala, P. Lisdiyanti, W. Kusharyoto, J. Krause, A. Kulik, W. Wohlleben, S. Aziz, H. Gross, A. Gavriilidou, N. Ziemert and Y. Mast, Mining Indonesian microbial biodiversity for novel natural compounds by a combined genome mining and molecular networking approach, *Mar. Drugs*, 2021, **19**, 316.

62 K. Becker, S. Pfütze, E. Kuhnert, R. J. Cox, M. Stadler and F. Surup, Hybridorubrins A–D: Azaphilone heterodimers from stromata of *Hypoxylon fragiforme* and insights into the biosynthetic machinery for azaphilone diversification, *Chem. – Eur. J.*, 2020, **27**, 1438–1450.

9.1.1. Publication 1: Supplementary information

Electronic Supplementary Material (ESI) for RSC Chemical Biology.

Biotransformation-coupled mutasynthesis for the generation of novel pristinamycin derivatives by engineering the phenylglycine residue

Oliver Hennrich, [a] Leoni Weinmann, [b] Andreas Kulik, [c] Karen Harms, [d] Philipp Klahn, [e,f] Jung-Won Youn, [b] Frank Surup, [d] and Yvonne Mast *[a,g,h]

[a] Department Bioresources for Bioeconomy and Health Research, Leibniz Institute DSMZ - German Collection of Microorganisms and Cell Cultures, Inhoffenstraße 7B, 38124 Braunschweig, Germany

[b] Institute of Microbiology, University Stuttgart, Allmandring 31, D-70569 Stuttgart, Germany

[c] Department Microbial Bioactive Compounds, Interfaculty Institute of Microbiology and Infection Medicine, Faculty of Science, University of Tübingen, Auf der Morgenstelle 28, D-72076 Tübingen, Germany

[d] Microbial Drugs Department, Helmholtz-Centre for Infection Research, 38124 Braunschweig, Germany

[e] Division of Organic and Medicinal Chemistry, Department of Chemistry and Molecular Biology, University of Gothenburg, Kemigården 4, 412 96 Göteborg, Sweden

[f] Centre of Antimicrobial Resistance Research in Gothenburg (CARe)

[g] Technische Universität Braunschweig, Institut für Mikrobiologie, Rebenring 56, 38106 Braunschweig, Germany

[h] German Center for Infection Research (DZIF), Partner Site Tübingen, Tübingen, Germany

*Correspondence:
Prof. Dr. Yvonne Mast
yvonne.mast@dsmz.de

Running title: Mutasynthesis with phenylglycines

Key words: actinomycetes, antibiotic, genetic engineering, mutasynthesis, phenylglycine

Table of Contents

Protocol S1: Fermentation and purification of 6-chloropristinamycin I (**3**)

For batch cultivations, 100 mL of HT7T medium was inoculated with 1 mL of mycelium of *S. pristinaespiralis ΔpglAΔsnaE1* and cultivated for 72 h in 500 mL Erlenmeyer flasks (with baffles) on an orbital shaker (110 rpm) at 28°C as a preculture. 100 mL of preculture was used to inoculate 1 L of HT7T medium (supplemented with 100 µM 4-chloro-DL-Phg solubilized as mentioned above) in a 5-L Erlenmeyer flask (with baffles) on an orbital shaker (110 rpm) at 28°C for 48-72h. The whole culture was extracted with two times 1 L ethyl acetate and the organic phase was concentrated in a rotary evaporator. For initial purifications, the extract was first dissolved in 20 mL of methanol/water (ratio: 85/15) and mixed twice with 20 mL of heptane. After separation, the heptane phase was discarded. The mixture was adjusted to a 70/30 methanol/water ratio and mixed twice with 20 mL of dichloromethane. The dichloromethane phase was mixed with 20 mL of water. After discarding the water phase, the extract was evaporated in a rotary evaporator and weighed. In total, 12 L of culture were extracted. For isolation of **3**, 180 mg of the crude extract solved in MeOH were separated using a PLC 2250 preparative HPLC system (Gilson, Middleton, WI, USA) with a Gemini® 10u C18 110Å column (250 × 50 mm, 10 µm; Phenomenex, Torrance, CA, USA) as the stationary phase and in the following conditions: solvent A: H_2O + 0.1% formic acid, solvent B: MeCN + 0.1% formic acid; flow: for 1 min 20 mL/min, afterwards 45 mL/min, fractionation: 15 mL, gradient: increase from 5% B to 100% B in 41 min followed by a final isocratic step of 100% B for 10 min. This yielded one pure fraction of **3** (F3: 0.6 mg, retention time (tR) = 34.02–35.15 min).

Protocol S2: Fermentation and purification of 6-fluoropristinamycin I (**4**)

For batch cultivations, 100 mL of HT7T medium was inoculated with 1 mL of mycelium of *S. pristinaespiralis ΔpglAΔsnaE1* and cultivated for 72h in 500-mL Erlenmeyer flasks (with baffles) on an orbital shaker (110 rpm) at 28°C as a preculture. 100 mL of preculture was used to inoculate 1 L of HT7T medium (supplemented with 100 µM 4-fluoro-L-Phg solubilized as mentioned above) in a 5-L Erlenmeyer flask (with baffles) on an orbital shaker (110 rpm) at 28°C for 48-72 h. The whole culture was extracted with two times 1 L ethyl acetate and the organic phase was concentrated in a rotary evaporator. For initial purifications, the extract was first dissolved in 20 mL of 85/15 methanol/water and mixed twice with 20 mL of heptane. After separation, the heptane phase was discarded. The extract was adjusted to 70/30 methanol/water and mixed twice with 20 mL of dichloromethane. The dichloromethane phase was mixed with 20 mL of water. After discarding the water phase, the extract was evaporated in a rotary evaporator and weighed. In total, 6 L of culture were extracted. 320 mg crude extract were subjected to flash chromatography (Grace Reveleris®, Columbia, MD, USA) (silica cartridge 12 g [FlashPure, Büchi Switzerland, USA], solvent A: DCM, solvent B: DCM/MeOH 95%/5%, solvent C: DCM:MeOH 9/1, solvent D: MeOH), gradient: 100% A for 10 min, increasing to 50% B in 2 min, followed by an isocratic step of 50% B for 2 min, increasing to 100% B in 2 min followed by an isocratic step at 100% B for 2 min, followed by a change from 100% B to 50 % A and 50% C with an increase to 80% C in 2 min, followed by a further increase to 100% C in 2 min, followed by a change to 100% D in 10 min and an isocratic step of 100% D for 10 min. One fraction containing **4** was collected with an amount of 73 mg at the retention time 19.6 min. The yielded fraction from the flash-chromatography was separated using a PLC 2250 preparative HPLC system (Gilson, Middleton, WI, USA) with a Gemini® 10u C18 110Å column (250 × 50 mm, 10 µm; Phenomenex, Torrance, CA, USA) as the stationary phase and

in the following conditions: solvent A: H_2O + 0.1% formic acid, solvent B: MeCN + 0.1% formic acid; flow: 45 mL/min, fractionation: 10 mL, gradient: increase from 5% B to 40% B in 10 min followed by an increase to 42% B in 30 min and a isocratic step in 42% B for 3 min, followed by an increase to 100% B in 8 min and an isocratic step in 100% B for 10 min. This yielded to two pure fractions of **4** (F2: 1.54 mg, tR = 43.36–44.21 min; F2.1 (1.88 mg, tR = 42.23–43.36 min).

Protocol S3: Construction of plasmids pET28a-*hmo* and pACYC-*bcd-gdh* biotransformation approach for the synthesis of L-Phg derivatives

Cloning of pET28a-*hmo*
The synthetic codon optimized *hmo* gene (GeneArt, Regensburg, Germany) from *Streptomyces coelicolor* was cloned into pET28a(+). For this purpose, *hmo* as well as the pET28a plasmid were double-digested with *Nde*I and *Bam*HI. The digested *hmo* gene fragment was ligated into the pET28a plasmid with T4 DNA ligase (NEB). The ligation product was transferred to competent *E. coli* DH5α for plasmid multiplication. The isolated plasmid pET28a-*hmo* was verified by sequencing (Eurofins Genomics, Germany).

Cloning of pACYC-*bcd-gdh*
The gene *bcd* from *Bacillus thuringiensis* was amplified from chromosomal DNA using primers bcd-fw/-rv with KOD Hot Start Polymerase (Novagen). The PCR fragment and pET28a were digested with *Nco*I and *BamH*I and ligated with T4 DNA ligase (NEB). The ligation product was transferred to competent *E. coli* DH5α. The isolated plasmid pET28-*bcd* was verified by sequencing (Eurofins Genomics, Germany). The *Hin*dIII restriction sites in the plasmid were deleted by insertion of point mutations with the primer pairs pET28a-Hind-fw/-rv and bcd-Hind-fw/rv.
The glucose dehydrogenase gene (*gdh*) from *Bacillus megaterium* was amplified from chromosomal DNA using primers gdh-fw/-rv with KOD Hot Start Polymerase (Novagen). The PCR fragment and pET28a were digested with *Nde*I and *Bam*HI and ligated with T4 DNA ligase. The constructed plasmid pET28-*gdh* was verified by sequencing (Eurofins Genomics, Germany). The *Hin*dIII restriction site in the plasmid was deleted by insertion of a point mutation with the primer pET28-Hind-fw/rv. The *bcd* gene was amplified with OP-fw/-rv by using pET28-*bcd* as template with the KOD Hot Start Polymerase (Novagen). The *bcd* fragment was digested with *Kpn*I and *Spe*I. The *gdh* gene was amplified with OP-fw/-rv from the template pET28-*gdh* with the KOD Hot Start Polymerase (Novagen). The *gdh* fragment was digested with *Nhe*I and *Hin*dIII. The *Nhe*I restriction site in pACYC was deleted by insertion of a point mutation with the primer pACYC-Nhe-fw/rv. Afterwards, the pACYC plasmid was amplified with pACYC-fw/-rv with KOD Hot Start Polymerase (Novagen) and afterwards digested with *Kpn*I and *Hin*dIII. All three digested fragments were ligated with T4 DNA ligase to obtain pACYC-*bcd-gdh,* which was transferred to *E. coli* DH5α. The isolated plasmid was verified by sequencing (Eurofins Genomics, Germany).

Table S1: Bacterial strains, plasmids and oligonucleotides used in this study.

5

Strains/ plasmids/ oligonucleotides	Genotype/phenotype/sequence	Source/ reference
S. pristinaespiralis		
PR11	Pristinamycin producing strain/wild-type, natural isolate of *S. pristinaespiralis* ATCC 25486	Sanofi-Aventis
M*pglA*	gene interruption of *pglA*, *apra*^{R}, PI non-producing	Mast *et al.*, 2011
Δ*pglA*Δ*snaE1*	gene interruption of *pglA*, *apra*^{R}, PI non-producing gene interruption of *snaE1*, *tsr*^{R}, PII non-producing	This study
E. coli		
Novablue	*endA1 hsdR17* (r_{K12}^- m_{K12}^+) *supE44 thi-1 recA1 gyrA96 relA1 lac* F'[*proA*$^+$*B*$^+$ *lacI*^{q}*ZΔM15*::Tn*10*] (Tet^R)	Novagen, SigmaAldrich
DH5α	*fhuA2 lac(del)U169 phoA glnV44 Φ80' lacZ(del)M15 gyrA96 recA1 relA1 endA1 thi-1 hsdR17*	Novagen, Merck Millipore
Bioassay test strains		
Bacillus subtilis ATCC 6633	Bioassay test strain	Pelzer *et al.*, 1999
Pseudomonas aeruginosa DSM 1117	Bioassay test strain	DSMZ strain collection
Proteus vulgaris DSM 2140	Bioassay test strain	DSMZ strain collection
Enterococcus faecium DSM 20477	Bioassay test strain	DSMZ strain collection
Staphylococcus aureus DSM 18827	Bioassay test strain	DSMZ strain collection
Staphylococcus aureus CIP 111304	Bioassay test strain; *vat(A), vgb(A)*	Collection de L´Institut Pasteur
Staphylococcus aureus CIP 108540	Bioassay test strain; *vgb(A), vgb(B), vat(B), erm(A), erm(B)*	Collection de L´Institut Pasteur
Candida albicans DSM 1386	Bioassay test strain	DSMZ strain collection
Trichophyton rubrum DSM 16111	Bioassay test strain	DSMZ strain collection
Plasmids		
pDRIVE	*lacZ'*-complementation system, *amp*^{R}, *kan*^{R}	Qiagen
pDRIVE/thio	*lacZ'*-complementation system, *amp*^{R}, *kan*^{R}, *tsr*^{R}	Moosmann et al., 2020
pK18	pUC derivative, *aph*II, *lacZ'*-complementation system	Pridmore, 1987
pK18/snaE1tsr	pK18 derivative, *aph*II, *tsr*^{R}, *lacZ'α*, *snaE1ab*	This study
pET28a	pET28a, *kan*^{R}	Novagen
pET28a-*hms*	pET28a derivate with *hms* from *A. mediterranei*, *kan*^{R}	Youn *et al.*, 2019
pET28a-*hmo*	pET28a derivate with *hmo* from *S. coelicolor*, *kan*^{R}	This study
pET28a-*bcd*	pET28a derivate with *bcd* from *B. thuringiensis*, *kan*^{R}	This study
pET28a-*gdh*	pET28a derivate with *gdh* from *B. megaterium*, *kan*^{R}	This study
pACYC	pACYC, *cm*^{R}	Chang & Cohen 1978
pACYC-*leuDH-gdh*	pACYC derivate, *cm*^{R}	This study
Oligonucleotides	**5'→3'**	
MsnaE1fw	AGCCGATGCTGTGCACGATG	This study
MsnaE1rv	CCACGTCGTCCTGGAAGAAG	This study
thio1	CGTTGGTGATTGCCGGTCAG	This study

thio2	GGCGATGCCGAATGTCTTGG	This study
KsnaE1fw	TGTCCCACTCGGGTACCAGG	This study
KsnaE1rv	TTCGAGCGGCAGTCCTACTGG	This study
bcd-fw	ATACCATGGGCACATTAGAAATCTTCGAATACTTAGAAAAATATG	This study
bcd-rv	TTCGGATCCTTAGCGACGGCTAATAATATCGTG	This study
pET28-Hind-fw	GAGCTCCGTCGACATGCTTGCGGCCGC	This study
pET28-Hind-rv	GCGGCCGCAAGCATGTCGACGGAGCTC	This study
bcd-Hind-fw	TGAAGAGCGCATTGCTAGCTTGAAAAATTC	This study
bcd-Hind-rv	GAATTTTTCAAGCTAGCAATGCGCTCTTCA	This study
gdh-fw	TTTCATATGATGTATAAAGATTTAGAAGGAAAAGTAGTTGTCATAACAGG	This study
gdh-rv	TTTGGATCCTTATCCGCGT-CCTGCTTGGAATG	This study
OP-fw	GCAGGTACCGCGGCCGCGCTAGCGATATAGGCGCCAGCAACCGCAC	This study
OP-rv	AGCAAGCTTCTAGCCGGCCGCTACTAGTCAGCAAAAAACCCCTCAAGACCCGTTT	This study
pACYC-Nhe-fw	CAGTATACACTCCGCCAGCGCTGATGTCCGG	This study
pACYC-Nhe-rv	CCGGACATCAGCGCTGGCGGAGTGTATACTG	This study
pACYC-fw	GTCAAGCTTAAGCTGTCAAACATGAGAATTACAAC	This study
pACYC-rv	ATGGGTACCATTTCAGAATATTTGCCAGAACCGT	This study

Table S2: MIC assay of pristinamycin IA (**1**) and its 6-fluoro derivative (**4**) against standard test organisms. Inhibited organisms are highlighted in bold; n.i. = not identified.

		1	**4**	
test organism	**DSM-Nr.**	**MIC µg/mL**	**MIC µg/mL**	**positive control**
Schizosaccharomyces pombe	70572	n.i.	n.i.	Nystatin
Pichia anomala	6766	n.i.	n.i.	Nystatin
Mucor hiemalis	2656	n.i.	n.i.	Nystatin
Candida albicans	1665	n.i.	n.i.	Nystatin
Rhodotorula glutinis	10134	n.i.	n.i.	Nystatin
Acinetobacter baumannii	30008	n.i.	n.i.	Ciprofloxacin
Escherichia coli	1116	n.i.	n.i.	Oxytetracyclin
Bacillus subtilis	**10**	**2,1**	**4,2**	Oxytetracyclin
Mycobacterium smegmatis	ATCC 700084	n.i.	n.i.	Kanamycin
Staphylococcus aureus	**346**	**16,7**	**33,3**	Oxytetracyclin
Pseudomonas aeruginosa	PA14	n.i.	n.i.	Gentamycin

7

Chromobacter violaceum	30191	n.i.	n.i.	Oxytetracyclin

Table S3: Cytotoxicity assay of 6-fluoropristinamycin I (**4**) against human cell lines (* = no changed cells, no cytotoxic activity; ** = no changed cells, low inhibition in proliferation)

Compound	KB3.1 cell line	Tox-Nr.	L929 cell line	Tox-Nr.
4	**	**3548**	*	**3549**

Table S4: Determination of enantiomeric excesses (ee) of L-Phg synthons from the whole cell biotransformation approach with *E. coli* BL21(DE3) pET28-*hmo/* pACYC-*bcd-gdh* with different mandelic acids. *The ee of 4-chloro-L-Phg produced by HMO-LeuDH-GDH could not be determined.

Product	Enantiomeric excess of L-phenylglycine derivatives [%]
L-phenylglycine	>99
2-fluoro-L-phenylglycine	>95
3-fluoro-L-phenylglycine	>99
4-fluoro-L-phenylglycine	>99
2-chloro-L-phenylglycine	50
3-chloro-L-phenylglycine	67
4-chloro-L-phenylglycine	-*

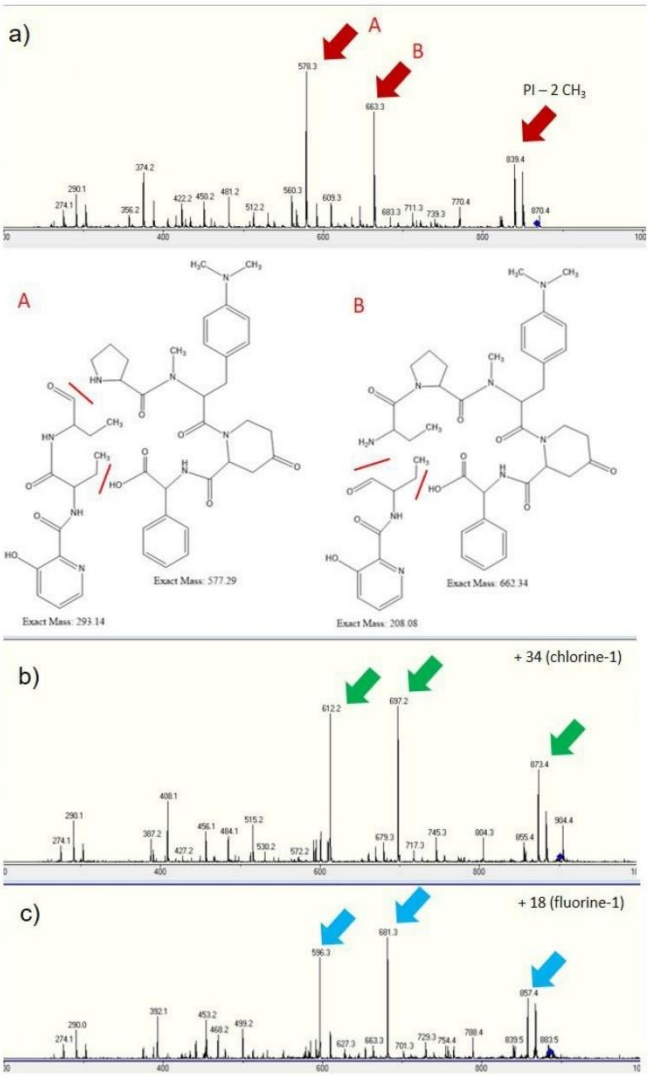

Figure S1: MS/MS fragmentation pattern of pristinamycin I (**1**) (a), 6-chloropristinamycin I (**3**) (b) and 6-fluoropristinamycin I (**4**) (c). Extracts of *S. pristinaespiralis* PR11 (1; m/z of precursor ion: 867.4) and *S. pristinaespiralis ΔpglAΔsnaE1* supplemented with 4-chloro-DL-Phg (2; *m/z* of precursor ion: 901.4) and 4-fluoro-L-Phg (3; *m/z* of precursor ion: 885.4). Distinct fragments of 1 are marked by arrows and likely fragmentation results are shown (A, B). Corresponding fragments that show the expected mass shift for the respective halogenation are marked by arrows in green (chlorination) or blue (fluorination). Measurements were conducted in positive mode.

9

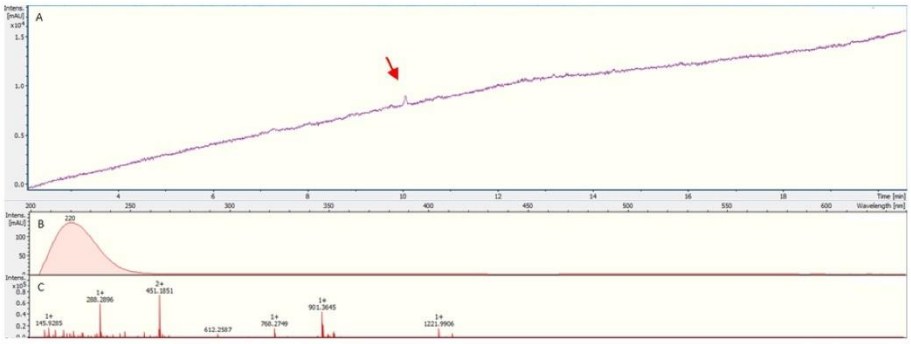

Figure S2: HRESIMS of 6-chloropristinamycin I (**3**). A is the chromatogram at 210 nm (peak indicated by red arrow). B and C are the UV spectrum and the mass spectrum of **3**.

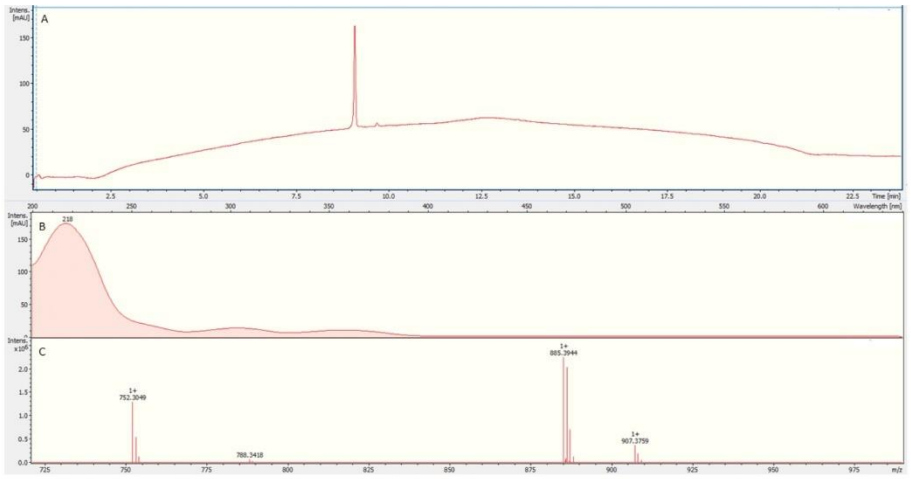

Figure S3: HRESIMS of 6-fluoropristinamycin I (**4**). A is the chromatogram at 210 nm. B and C are the UV spectrum and the mass spectrum of **4**.

10

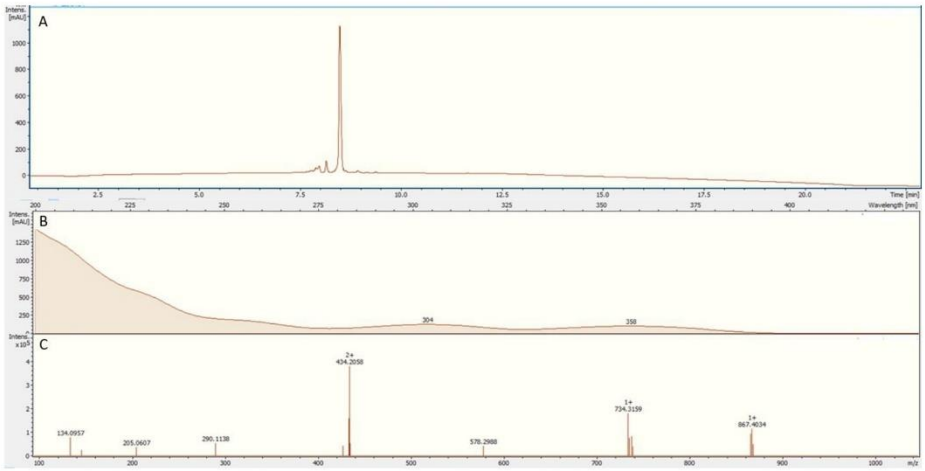

Figure S4: HRESIMS of pristinamycin I (**1**). A is the chromatogram 210 nm. B and C are the UV spectrum and the mass spectrum of **1**.

11

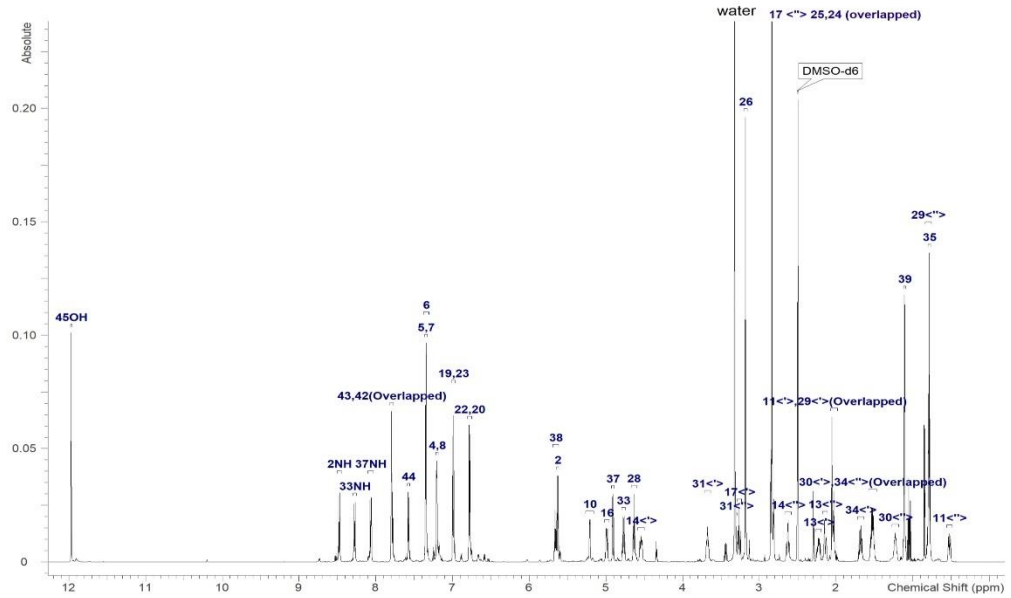

Figure S5: ^{1}H NMR spectrum (700 MHz) pristinamycin I (**1**) in DMSO-d_6.

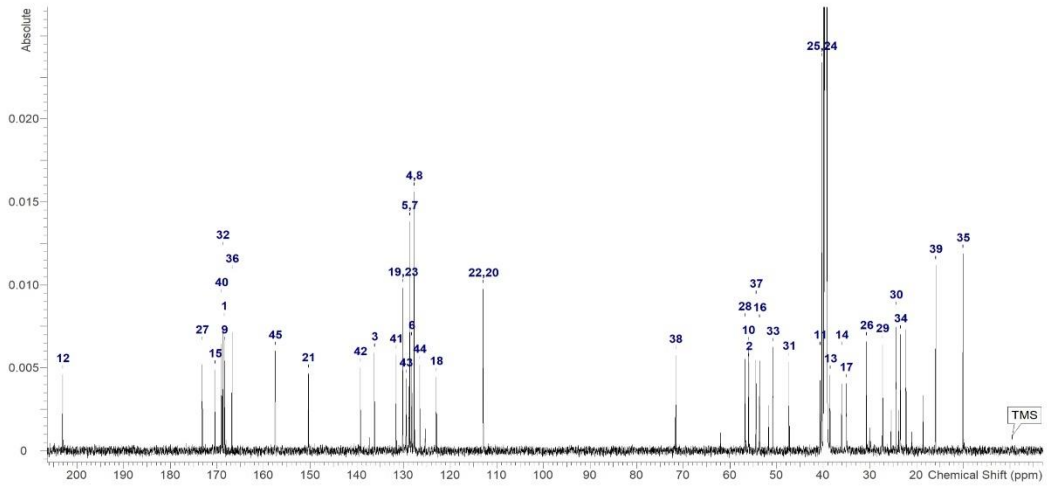

Figure S6: ^{13}C NMR spectrum (700 MHz) pristinamycin I (**1**) in DMSO-d_6.

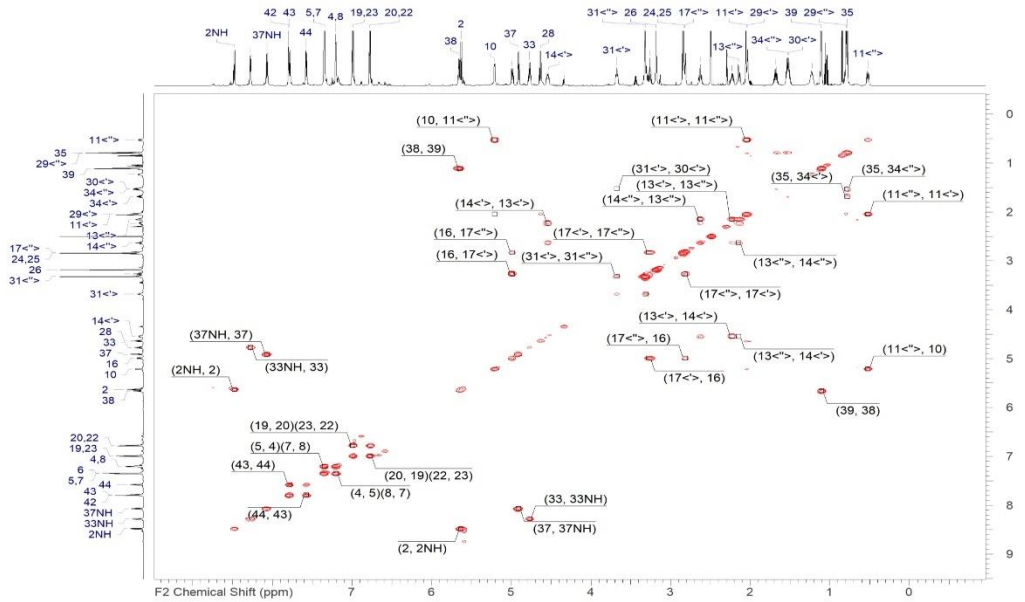

Figure S7: COSY NMR spectrum (700 MHz) pristinamycin I (**1**) in DMSO-d_6.

14

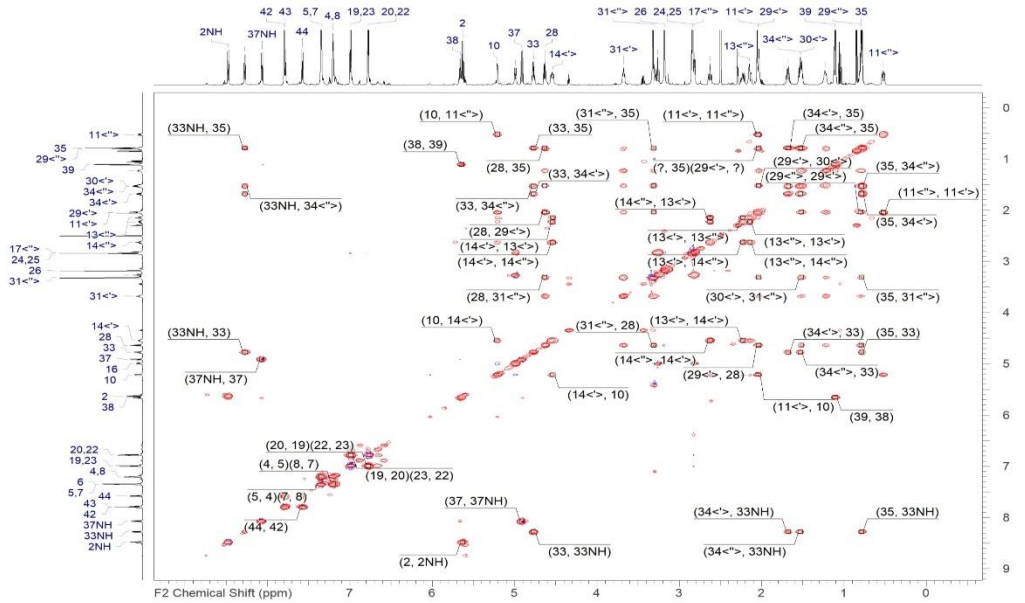

Figure S8: TOCSY NMR spectrum (700 MHz) pristinamycin I (**1**) in DMSO-d_6.

15

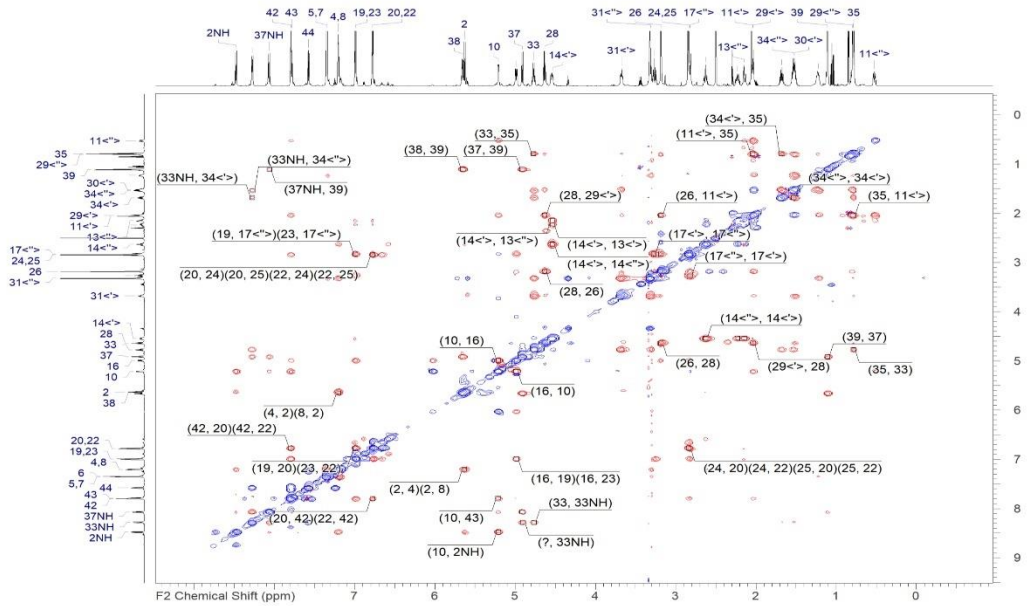

Figure S9: ROESY NMR spectrum (700 MHz) pristinamycin I (**1**) in DMSO-d_6.

16

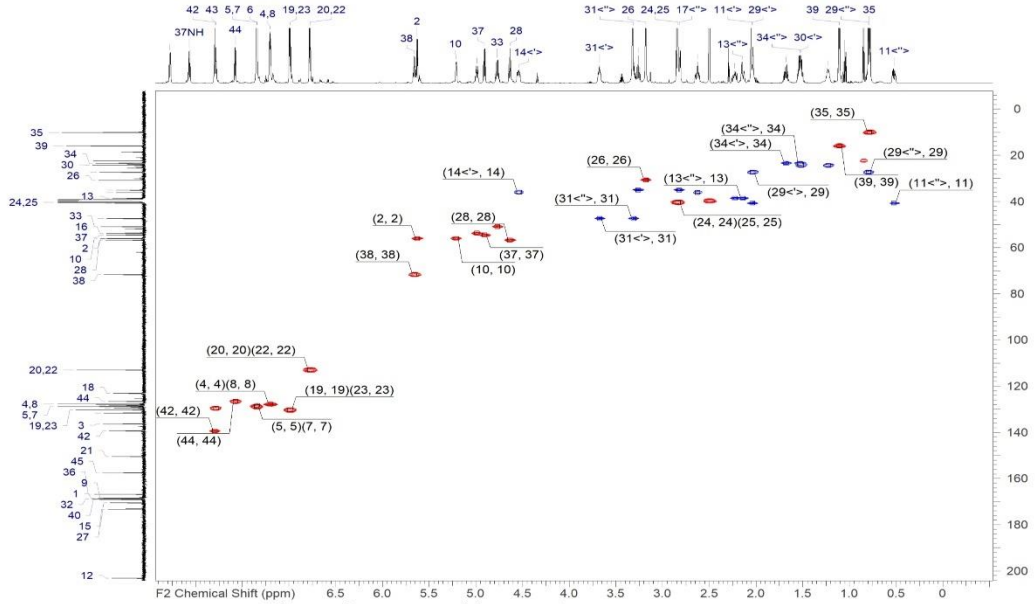

Figure S10: HSQC-DEPT NMR spectrum (700 MHz) pristinamycin I (**1**) in DMSO-d_6.

17

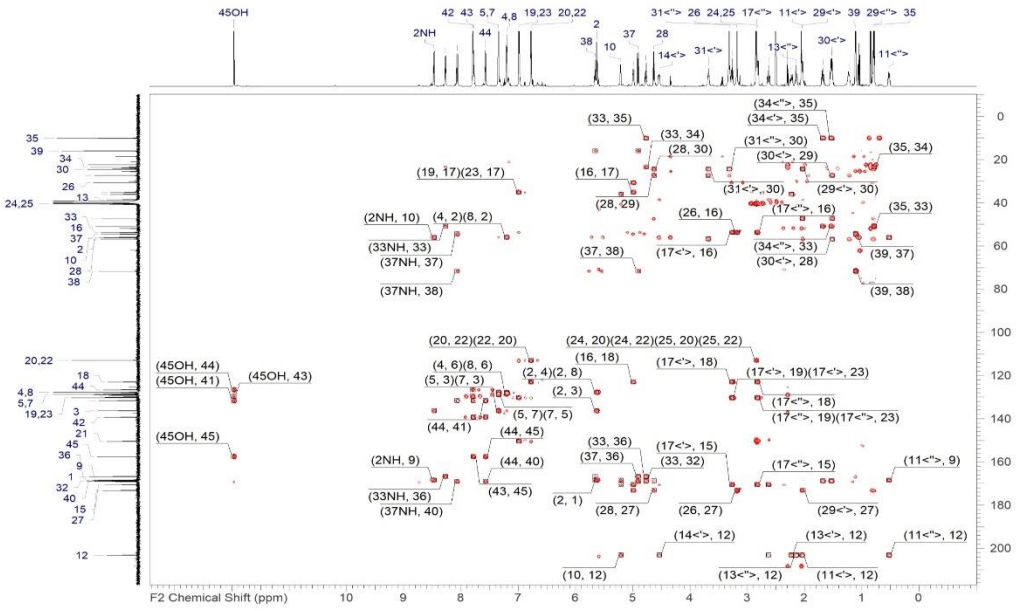

Figure S11: HMBC NMR spectrum (700 MHz) pristinamycin I (**1**) in DMSO-d_6.

18

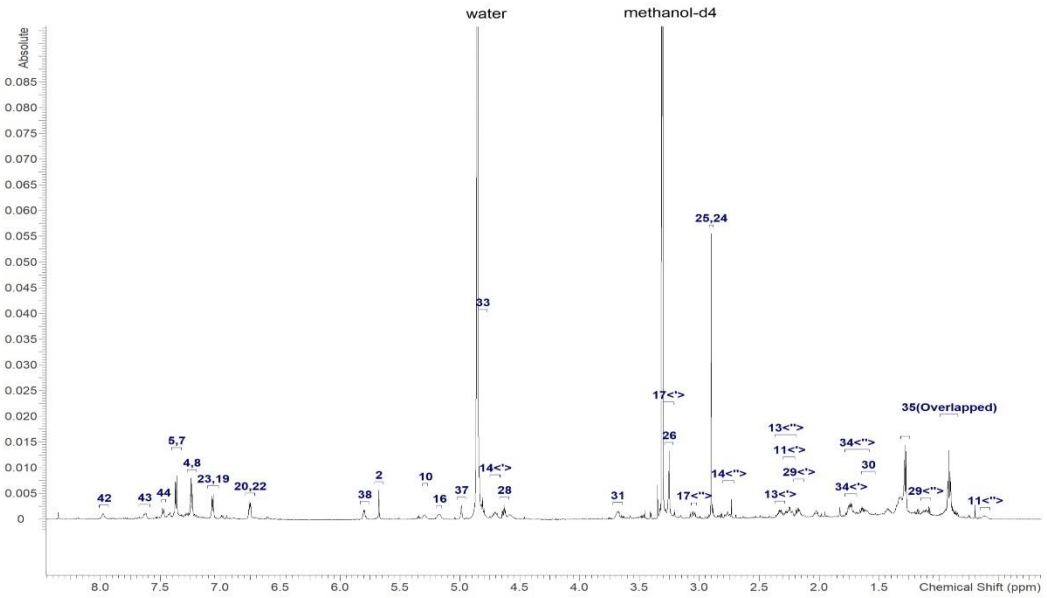

Figure S12: ^{1}H NMR spectrum (700 MHz) 6-chloropristinamycin I (**3**) in MeOD.

19

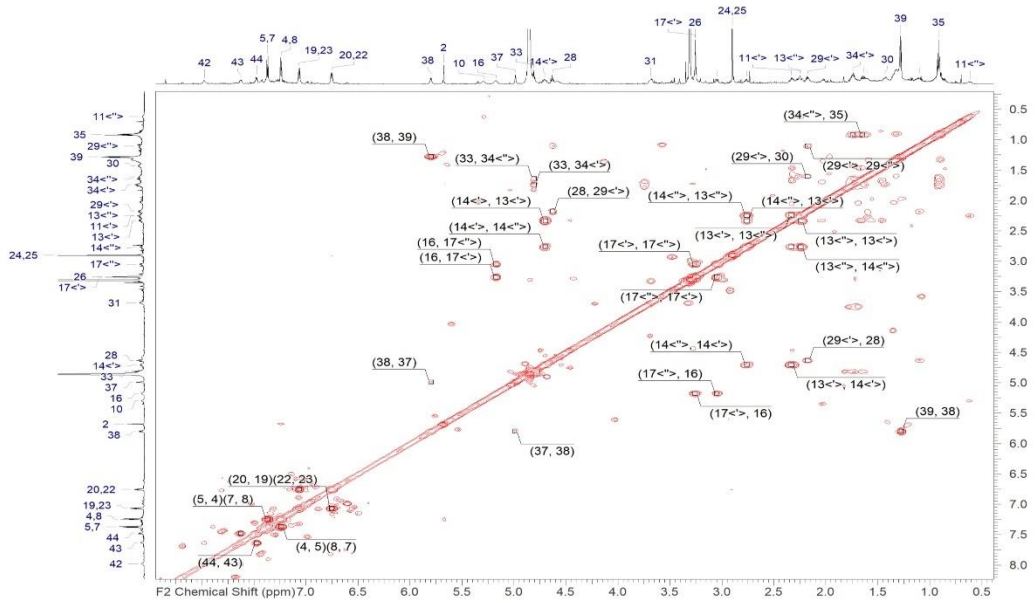

Figure S13: COSY NMR spectrum (700 MHz) 6-chloropristinamycin I (**3**) in MeOD.

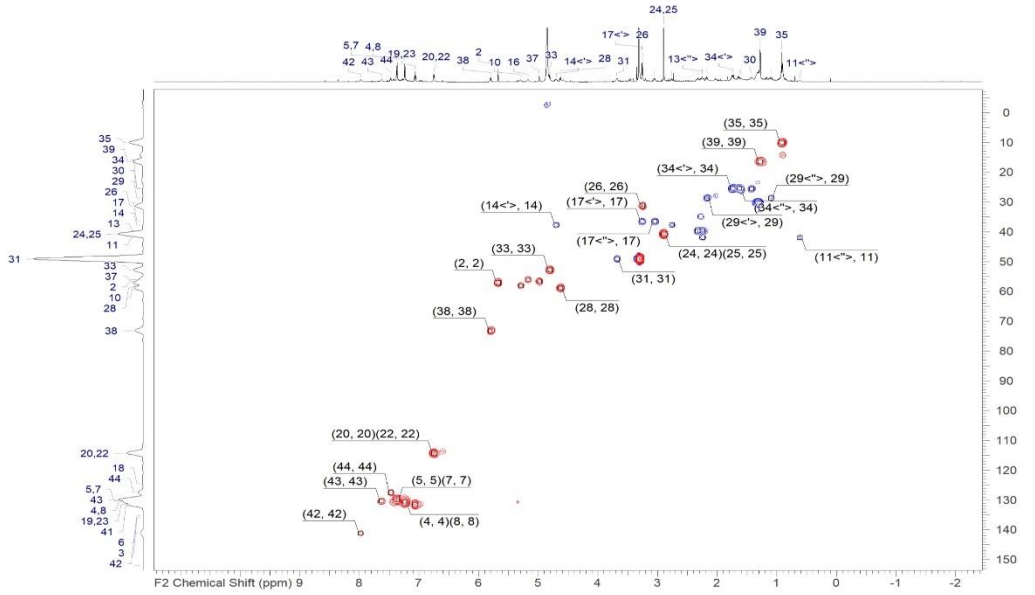

Figure S14: HSQC-DEPT NMR spectrum (700 MHz) 6-chloropristinamycin I (**3**) in MeOD.

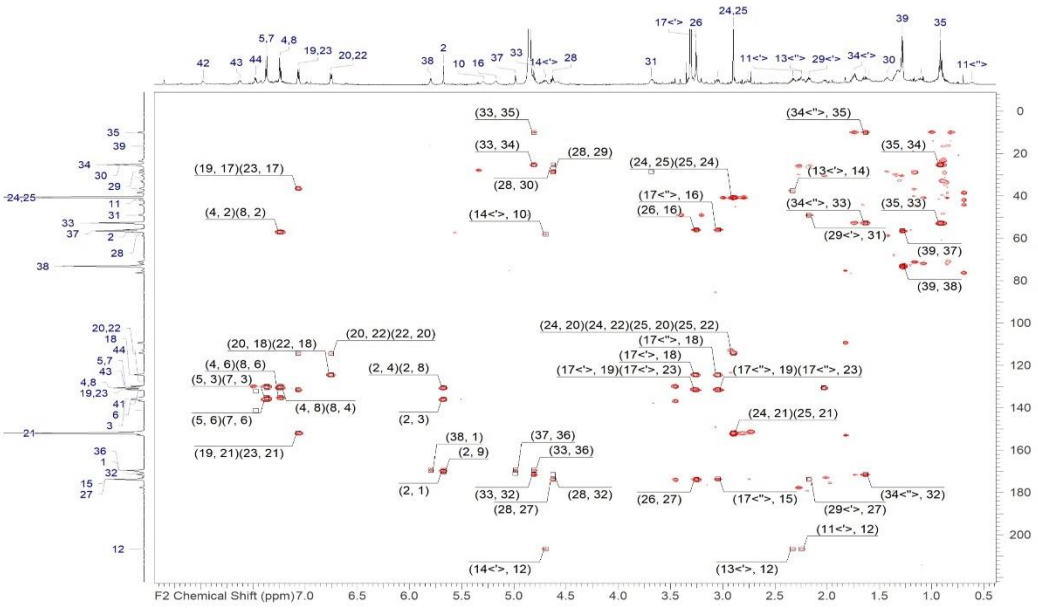

Figure S15: HMBC NMR spectrum (700 MHz) 6-chloropristinamycin I (**3**) in MeOD.

22

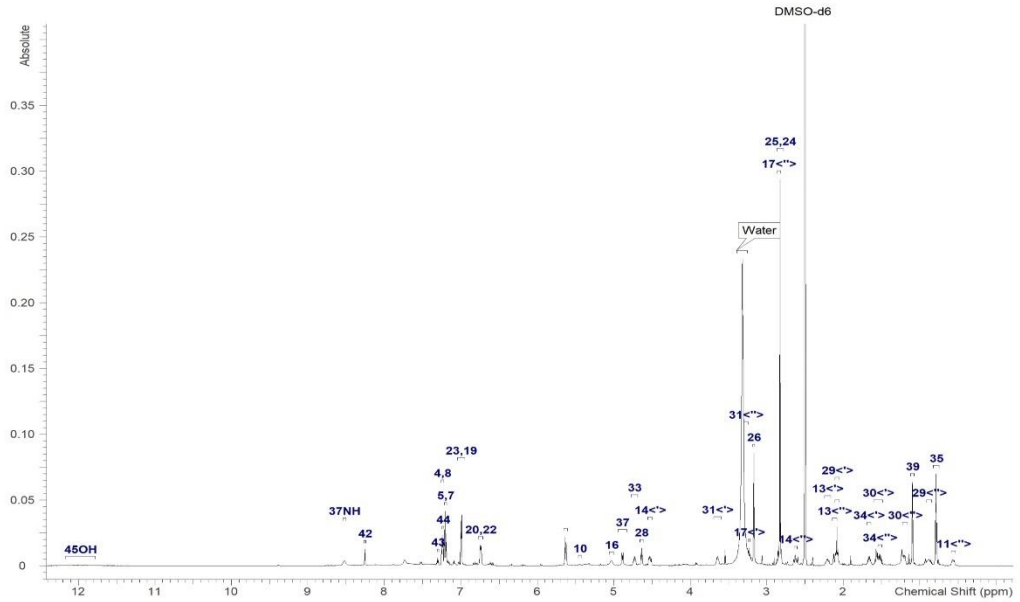

Figure S16 ^{1}H NMR spectrum (700 MHz) 6-fluoropristinamycin I (**4**) in DMSO-d_6.

23

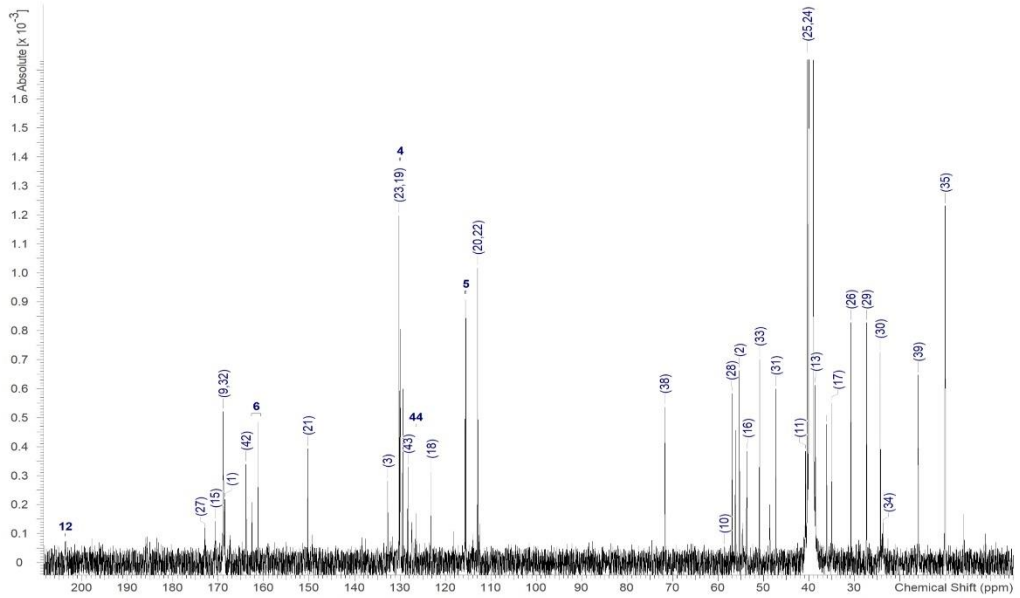

Figure S17: ^{13}C NMR spectrum (700 MHz) 6-fluoropristinamycin I (**4**) in DMSO-d_6.

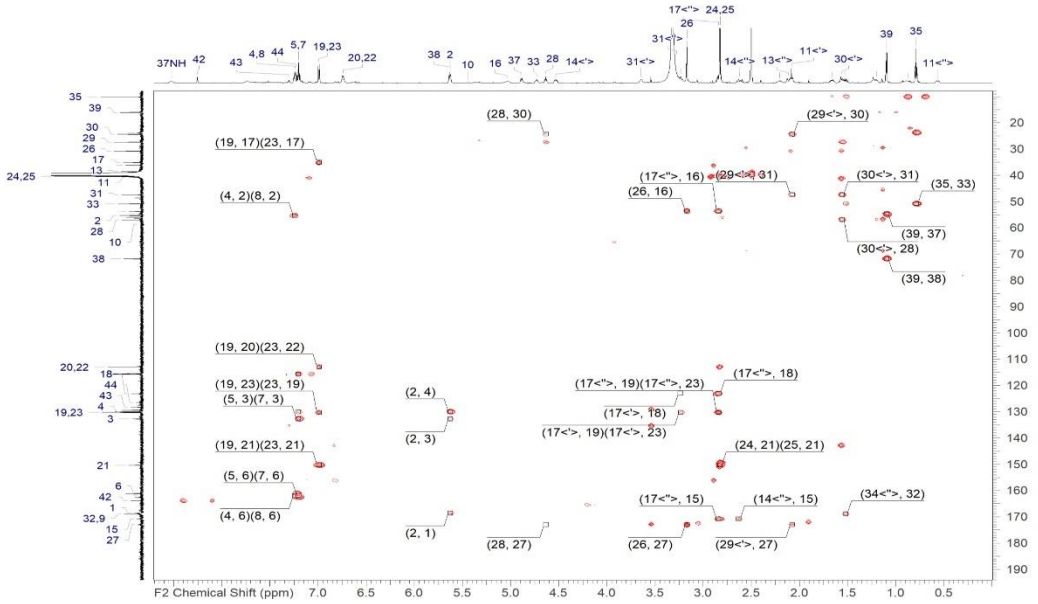

Figure S18: HMBC spectrum (700 MHz) 6-fluoropristinamycin I (**4**) in DMSO-d_6.

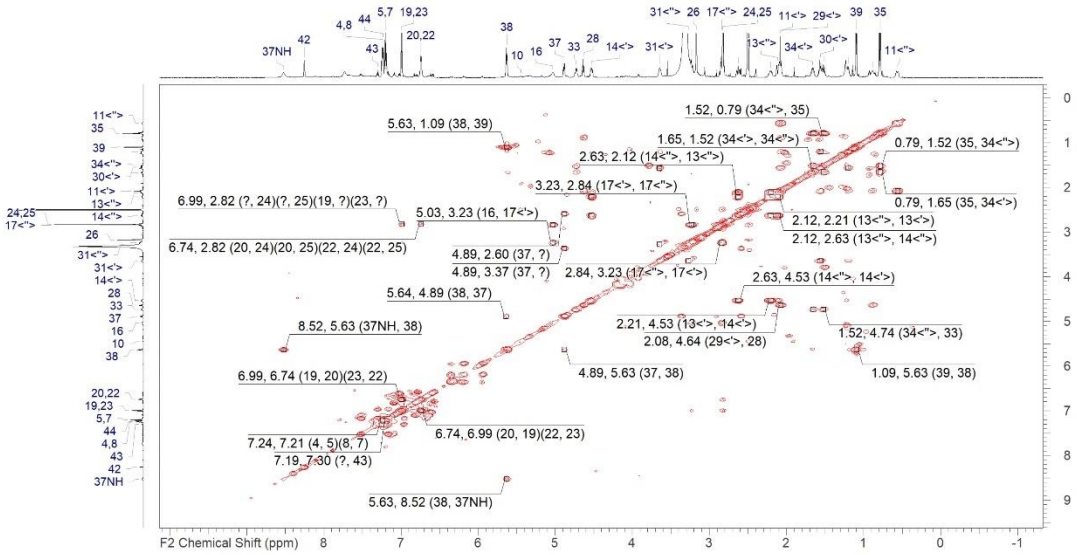

Figure S19: COSY spectrum (700 MHz) 6-fluoropristinamycin I (**4**) in DMSO-d_6.

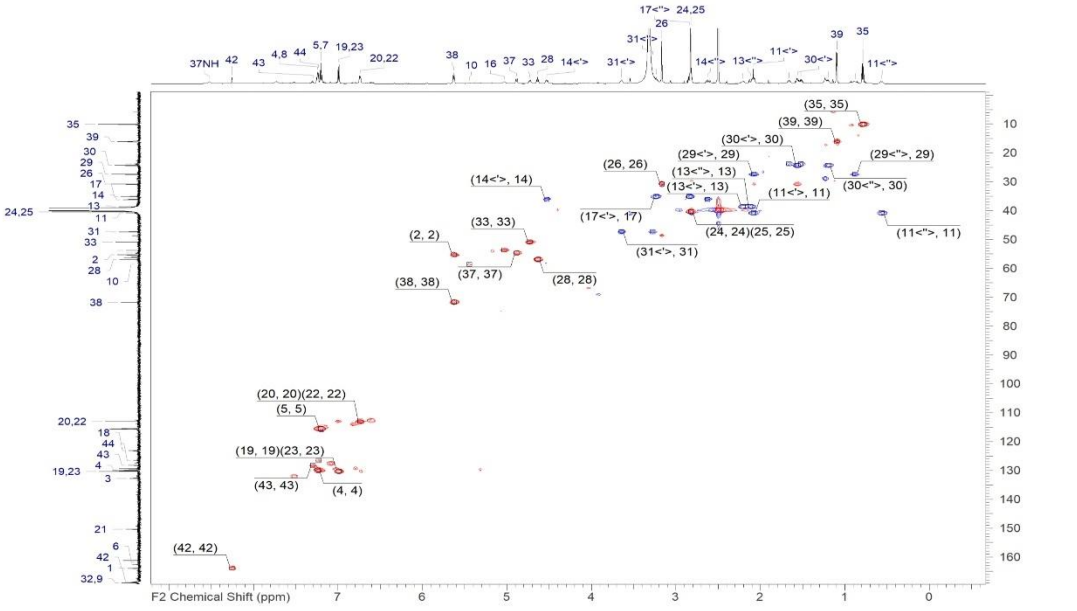

Figure S20: HSQC-DEPT NMR spectrum (700 MHz) 6-fluoropristinamycin I (**4**) in DMSO-d_6.

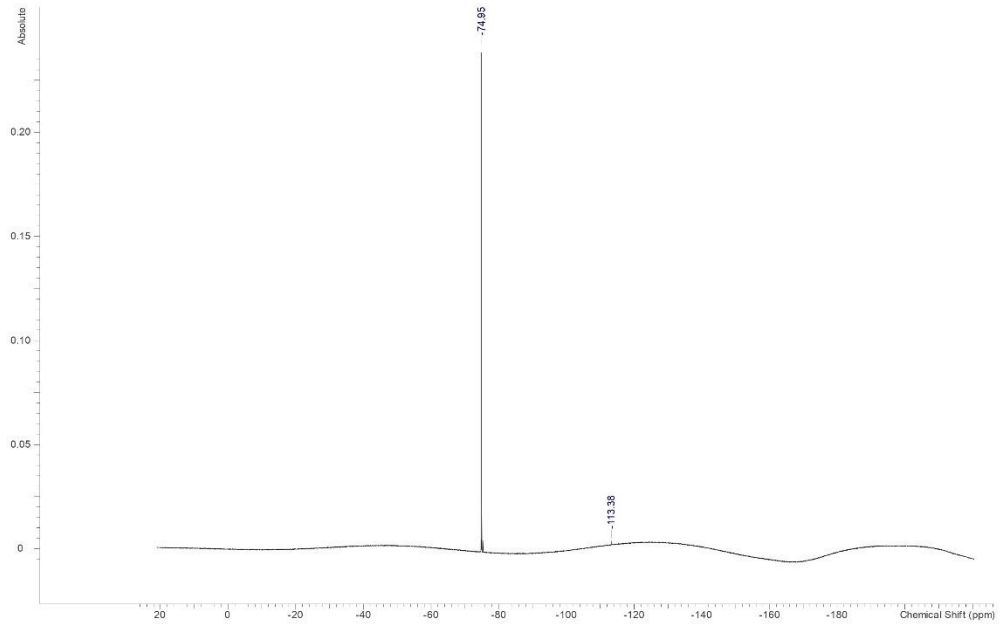

Figure S21: ^{19}F NMR spectrum (470 MHz) 6-fluoropristinamycin I (**4**) in DMSO-d_6.

28

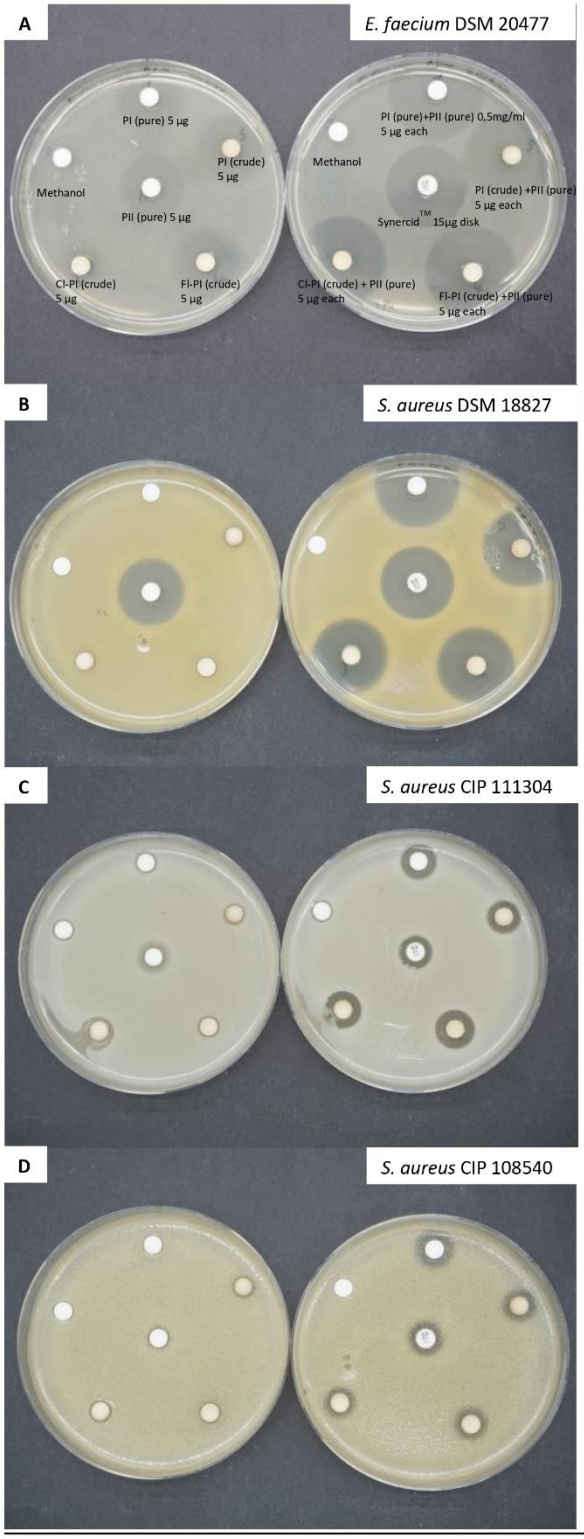
A
E. faecium DSM 20477
PI (pure) 5 µg
PI (crude) 5 µg
Methanol
PII (pure) 5 µg
Cl-PI (crude) 5 µg
Fl-PI (crude) 5 µg
PI (pure)+PII (pure) 0,5mg/ml 5 µg each
Methanol
PI (crude) +PII (pure) 5 µg each
Synercid™ 15µg disk
Cl-PI (crude) + PII (pure) 5 µg each
Fl-PI (crude) +PII (pure) 5 µg each
B
S. aureus DSM 18827
C
S. aureus CIP 111304
D
S. aureus CIP 108540

29

Figure S22: Results of the agar diffusion test of PI derivatives alone and in combination with PII against streptogramin susceptible clinical isolates. The pattern of sample application follows that of the *E. faecium* DSM 20477 example.

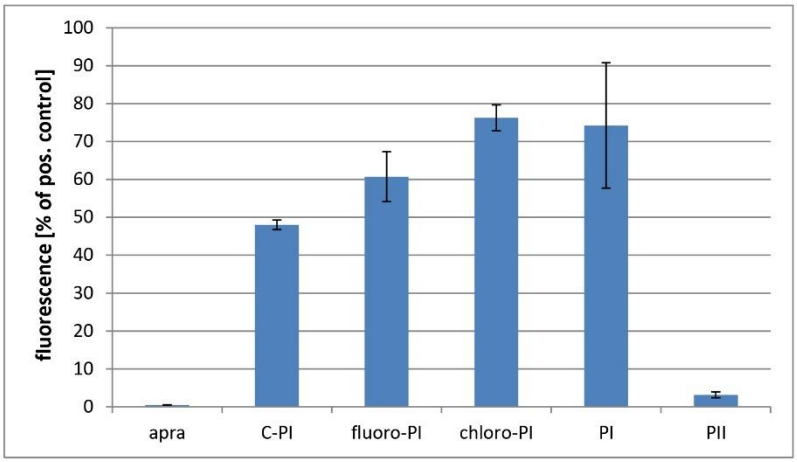

Figure S23: Results of the *in vitro* transcription translation assay used to investigate the effect of semi purified PI derivatives as well as pure pristinamycin I (PI) and II (PII) on bacterial protein biosynthesis. Apramycin (apra) served as a positive control (C-PI = PI isolated from *S. pristinaespiralis ΔpglAΔsnaE1* supplemented with L-Phg).

30

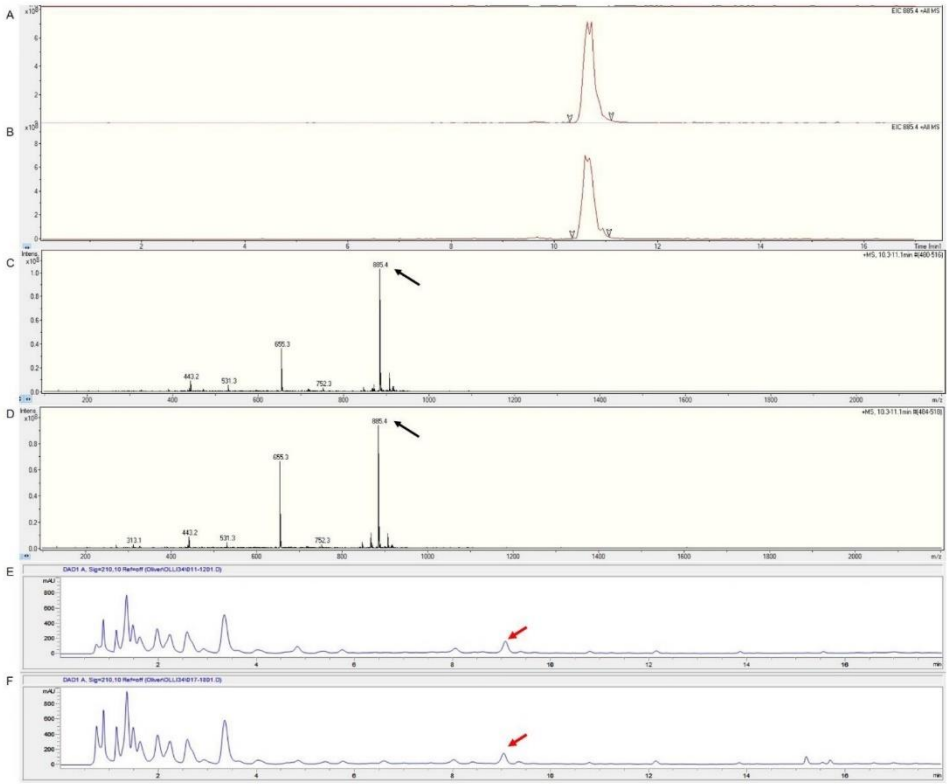

Figure S24: HPLC/MS analysis of *S. pristinaespiralis ΔpglAΔsnaE1* extracts from cultures supplemented with pure 4-fluoro-Phg (A, C, E) and 4-fluoro-Phg containing *E. coli* BL21(DE3) pET28-*hmo*/pACYC-*bcd-gdh* supernatant (B, D, F), respectively. A and B are the extracted ion chromatograms (EIC) for the mass corresponding to 6-fluoropristinamycin I (**4**) (*m/z* 885.4 $[M+H]^+$) in positive mode. C and D are the corresponding mass spectra. E and F are separate UV chromatograms at 210 nm (at the same scale). The mass signals for **4** are marked with black arrows and the respective UV signals are marked with red arrows.

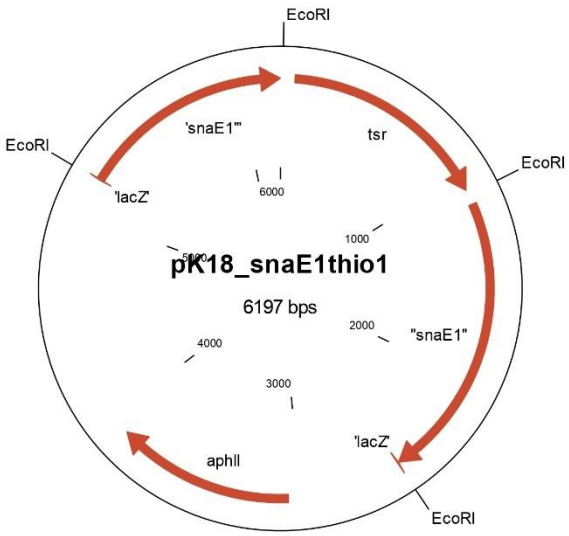

Figure S25: Cloning chart of mutagenesis plasmid pK18/snaE1tsr.

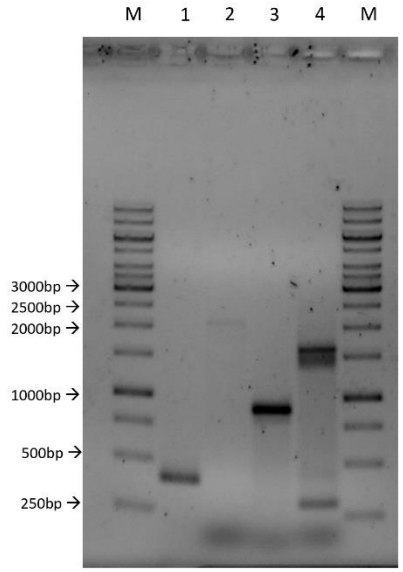

Figure S26: Verification of the *snaE1* mutation by PCR. Amplificates are shown for PCR with primer pairs thio1/2 (lane 1; ≈0.4 kb), KnsaE1fw/rv (lane 2; ≈2.1 kb), KnsaE1fw/thio2 (lane 3; ≈0.8 kb), and KnsaE1rv/thio1 (lane 4; ≈1.7 kb) separated in a 1% agarose gel. Marker (M): 1 kb length marker, Thermo Fisher Scientific.

32

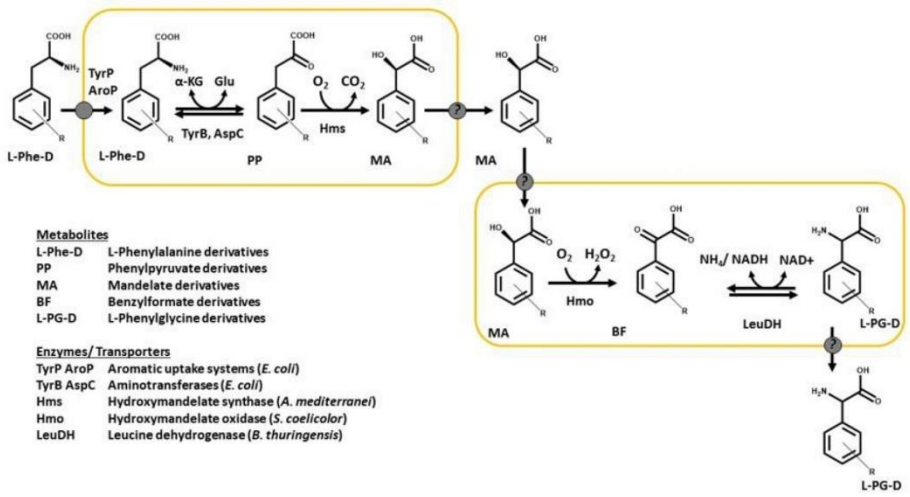

Figure S27: Schematic representation of the biotransformation approach for the synthesis of L-Phg derivatives including respective enzymes and metabolites involved in each step.

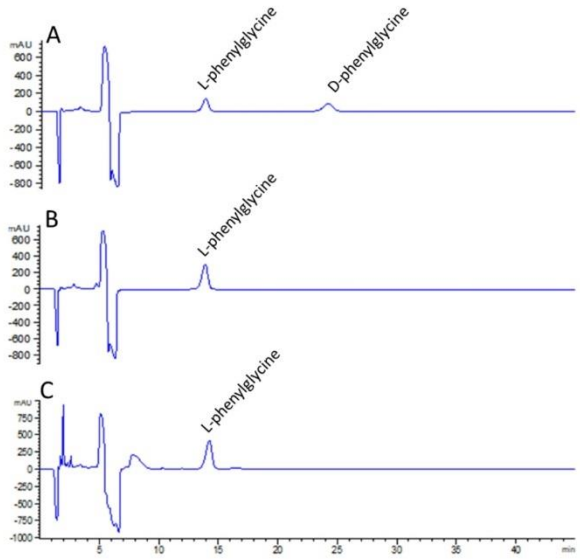

Figure S28: Representative chiral HPLC chromatogram of the separation of Phg enantiomers at 210 nm. Chromatogram A and B illustrate the separation of commercially available standards for DL-Phg and L-Phg. C is showing a typical chromatogram of the whole cell biotransformation approach with *E. coli* BL21(DE3) pET28-*hmo/* pACYC-*bcd-gdh* with L-mandelic acid.

References

1. Y. Mast, W. Wohlleben, E. Schinko, Identification and functional characterization of phenylglycine biosynthetic genes involved in pristinamycin biosynthesis in *Streptomyces pristinaespiralis. J. Biotechnol.*, 2011, **155**, 63-67.
2. D. Moosmann, V. Mokeev, A. Kulik, N. Osipenkov, S. Kocadinc, R. Ort-Winklbauer, F. Handel, O. Hennrich, JW. Youn, GA. Sprenger, Y. Mast, Genetic engineering approaches for the fermentative production of phenylglycines. *Appl Microbiol Biotechnol*, 2020, **104**, 3433–3444.
3. RD. Pridmore, New and versatile cloning vectors with kanamycin-resistance marker. *Gene*, 1987, **56**, 309-312.
4. J-W. Youn, C. Albermann, G. A. Sprenger, *In vivo* cascade catalysis of aromatic amino acids to the respective mandelic acids using recombinant *E. coli* cells expressing hydroxymandelate synthase (HMS) from *Amycolatopsis mediterranei*. *Molecular Catalysis*, 2020, **483**, 110713.
5. A.C. Chang, S.N Cohen, Construction and characterization of amplifiable multicopy DNA cloning vehicles derived from the P15A cryptic miniplasmid. *J Bacteriol.,* 1978, **134**, 1141-1156.

Reproduced from

Hennrich O, Weinmann L, Kulik A, Harms K, Klahn P, Youn JW, Surup F, Mast Y. Biotransformation-coupled mutasynthesis for the generation of novel pristinamycin derivatives by engineering the phenylglycine residue. *RSC Chem Biol.* 2023, 4::1050-1063. doi: 10.1039/d3cb00143a.

with permission from the Royal Society of Chemistry.

9.2. Publication 2

JOURNAL OF NATURAL PRODUCTS

pubs.acs.org/jnp Article

High Plasticity of the Amicetin Biosynthetic Pathway in *Streptomyces* sp. SHP 22-7 Led to the Discovery of Streptcytosine P and Cytosaminomycins F and G and Facilitated the Production of 12F-Plicacetin

Niraj Aryal, Junhong Chen, Keshab Bhattarai, Oliver Hennrich, Ira Handayani, Markus Kramer, Jan Straetener, Tatjana Wommer, Anne Berscheid, Silke Peter, Norbert Reiling, Heike Brötz-Oesterhelt, Christian Geibel, Michael Lämmerhofer, Yvonne Mast, and Harald Gross*

Cite This: *J. Nat. Prod.* 2022, 85, 530−539 Read Online

ACCESS | Metrics & More | Article Recommendations | Supporting Information

ABSTRACT: A chemical reinvestigation of the Indonesian strain *Streptomyces* sp. SHP 22-7 led to the isolation of three new pyrimidine nucleosides, along with six known analogues and zincphyrin. The structures of the new compounds (**6**, **7**, **10**) were elucidated by employing spectroscopic techniques (NMR, MS, CD, and IR) as well as enantioselective analyses of methyl branched side chain configurations. Application of the precursor-directed feeding approach led to the production and partial isolation of nine further pyrimidine analogues. The new compounds **6**, **7**, and **11** and three of the known compounds (**2**−**4**) were found to possess antimycobacterial and cytotoxic properties.

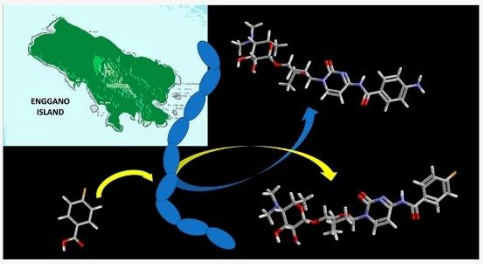

Within the framework of a previous campaign in which Indonesian microbial biodiversity was scrutinized for bioactive natural products, the mangrove-derived strain *Streptomyces* sp. SHP 22-7 was prioritized due to its antibacterial activity toward Gram-positive bacteria. The bioactivity could readily be assigned to the production of amicetin (Figure S1).[1]

Amicetin, originally isolated in the early 1950s from *Streptomyces vinaceusdrappus* and *S. fasciculatis*,[2a,b] represents the founding member of a large family of pyrimidine nucleoside antibiotics. Structurally, these compounds share a disaccharide pyrimidine nucleoside motif, termed cytosamine, in which the sugar amosamine (4,6-dideoxy-4-dimethylamine-D-glucose) is linked to amicetose, which is in turn bonded to a cytosine nucleus (Figure 1). The amino group of the amosamine moiety is commonly dimethylated. Deviating from this standard motif, the amosamine moiety can be solely monomethylated[2c] or completely absent, and position 3′ of amicetose can be in rare cases additionally hydroxylated. However, the highest degree of molecular diversity within this compound class is given by the acylation of the amino group (NH_2-7) of cytosine with a huge variety of aminobenzoic or aliphatic carboxylic acids.[2d] Several members of the amicetin family exhibit antiviral and antibiotic activity.[3a] The latter effect is mediated by inhibition of protein synthesis through binding to the ribosomal P-site, ultimately inhibiting prokaryotic translation.[3] Furthermore, also the corresponding biosynthetic gene cluster (BGC) was identified and proven by heterologous expression.[4]

In follow-up studies with the strain SHP 22-7, the amicetin BGC and its specific regulation were further investigated.[5,6] Both during the molecular MS networking approach[1] and during the regulator-overexpression studies[6] it became apparent that SHP 22-7 produces a plethora of potentially new pyrimidine nucleoside analogues.

Thus, we herein report the isolation and the structure elucidation of three structurally new pyrimidine nucleosides (**6**, **7**, and **10**) and their evaluation in bioassays. In addition, we exploited the flexibility of the biosynthetic pathway and complemented the study with a precursor-directed feeding approach, leading to several new amicetin derivatives including halogenated versions.

Special Issue: Special Issue in Honor of William H. Gerwick

Received: November 6, 2021
Published: March 9, 2022

https://doi.org/10.1021/acs.jnatprod.1c01051
J. Nat. Prod. 2022, 85, 530−539

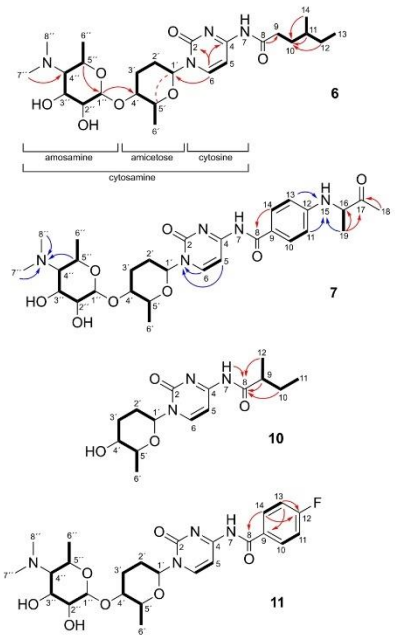

Figure 1. Key NMR correlations of compounds **6**, **7**, **10**, and **11**. Bold lines indicate ^{1}H−^{1}H-COSY or ^{1}H−^{13}C-HSQC-TOCSY correlations, while red arrows and dashed lines show key ^{1}H−^{13}C-HMBC and ^{1}H−^{1}H-NOESY cross correlations, respectively. Blue arrows represent key ^{1}H−^{15}N HMBC correlations.

■ RESULTS AND DISCUSSION

Target Compound Identification by HR-LC-MS/MS-Based Dereplication. The new derivatives were produced in a heterogeneous complex mixture and in small quantities. Therefore, in order to identify the new amicetin congeners, an MS-guided fractionation approach was applied. During the MS/MS fragmentation process, amicetins split off the monosaccharide amosamine and the disaccharide amicetose/amosamine, producing the characteristic fragments m/z 174.11 and 288.18, respectively (Figure S1). Consequently, employing HR-LC-MS/MS, we focused on fractions exhibiting the above-mentioned fragmentation pattern.

Isolation and Structural Analysis of Natural Nucleoside Antibiotics. In order to obtain sufficient amounts for structure elucidation and biological testing, repeated batches were cultivated, and the whole broth was extracted with EtOAc. Chromatographic separation of the crude extract using Sephadex LH20, C_{18} reversed phase vacuum liquid chromatography (VLC), SPE, and HPLC led to the identification and isolation of 10 compounds. One thereof was recognized as zincphyrin III (**1**),[7] while the remaining compounds **2**−**10** were identified as cytosine-type nucleoside derivatives. The known compounds thereof were verified by comparison of their spectral data with those previously reported,[2,8] while the structures of the new pyrimidine nucleosides **6**, **7**, and **10** were elucidated by extensive NMR spectroscopic and mass spectrometric experiments.

The HR-ESI-MS spectra of **6** gave molecular ions consistent with the formula $C_{25}H_{42}N_4O_7$ and required seven degrees of unsaturation. Initial evaluation of the ^{1}H and ^{13}C NMR spectra already supported the hypothesis that **6** was a cytosine derivative, similar to compounds **2**−**5**. Briefly, the ^{1}H NMR spectrum of **6** exhibited two aromatic protons at δ_H 7.48 and 8.11 (Table 1), which were connected to carbons at δ_C 98.4 and 146.3 (Table 2), respectively, and are typical of the CH-5 and CH-6 resonances of a cytosine unit.[2] Further ^{1}H−^{13}C-HMBC cross correlations substantiated this assumption. In addition, the ^{1}H NMR spectrum of **6** displayed typical resonances for the two sugar units amicetose and amosamine as in plicacetin (**2**) (Tables 1, 2, and S2). The two major spin systems of the disaccharidic moiety were delineated from the combined analysis of the ^{1}H−^{1}H-COSY and ^{1}H−^{13}C-HSQC-TOCSY spectrum of **6**. For each sugar moiety, a continuous spin system from H-1′ through H_3-6′ and from H-1″ through H_3-6″ could be observed (Figure 1). The HMBC correlation H-1″/C-5′′ and the ^{1}H−^{1}H-NOESY-based through-space interaction of H-1′ with H-5′, respectively, proved both sugar moieties to be cyclic. Furthermore, the HMBC spectrum of **6** demonstrated coupling between two magnetically equivalent lower field methyl groups at δ_H 2.46 (CH_3-7″ and CH_3-8″) and carbon C-4′′, which proved that a $N(CH_3)_2$ moiety is attached to the hexose residue, thereby completing the structure of amosamine.

The connectivity of the established compound fragments resulted from long-range couplings in the HMBC spectrum of the anomeric proton H-1″ of amosamine with C-4′ of amicetose, whereas the anomeric carbon C-1′ of the latter sugar showed a heteronuclear correlation with H-6 of the cytosine unit. Subtraction of the C, N, and O atoms accounted for by the cytosamine residue ($C_{18}N_4O_6$) from the molecular formula of **6** showed that the remaining partial structure of the molecule had to contain one oxygen and seven carbon atoms. The DEPT135 and ^{1}H−^{13}C-HSQC NMR data showed that two CH_3, three CH_2, one CH, and one amide carbonyl were involved. From the ^{1}H−^{1}H-COSY and ^{1}H−^{13}C-HSQC-TOCSY spectrum, the complete spin system of the side chain formed by C-9 through C-14 could be readily delineated (Figures 1 and S28−S30). The methylene proton resonances of atom 9 were in turn correlated in the HMBC spectrum to the amide carbonyl carbon C-8. Taken together, the above evidence suggested the presence of 4-methyl hexanoic acid. The remaining amidic linkage between the fatty acid and the cytosamine residue followed by deduction, but was also corroborated by MS/MS and by IR (1673 cm^{-1}) data. Thus, the skeletal structure of **6** was assigned and recognized as a cytosaminomycin analogue. Being the sixth member of this compound subfamily,[2d,8c] the metabolite was named cytosaminomycin F.

With the planar structure of **6** determined, the configuration of the sugar moieties and the chiral center at C-11 required resolution. Since cytosaminomycin F (**6**) was obtained together with its analogues from strain SHP 22-7, it was assumed that these building blocks will be biosynthesized by the same pathway and therefore possess the same absolute configuration. This hypothesis was supported by NOESY data, which showed that **6** shared the same relative configuration with **2**. In addition, the experimental ECD curve showed a negative Cotton effect at 222 nm (ε −5.00) and three positive effects at 204 (ε +4.15), 262 (ε +4.05), and 299 (ε +2.83) nm, which were comparable in wavelength and ε-values with CD

https://doi.org/10.1021/acs.jnatprod.1c01051
J. Nat. Prod. 2022, 85, 530−539

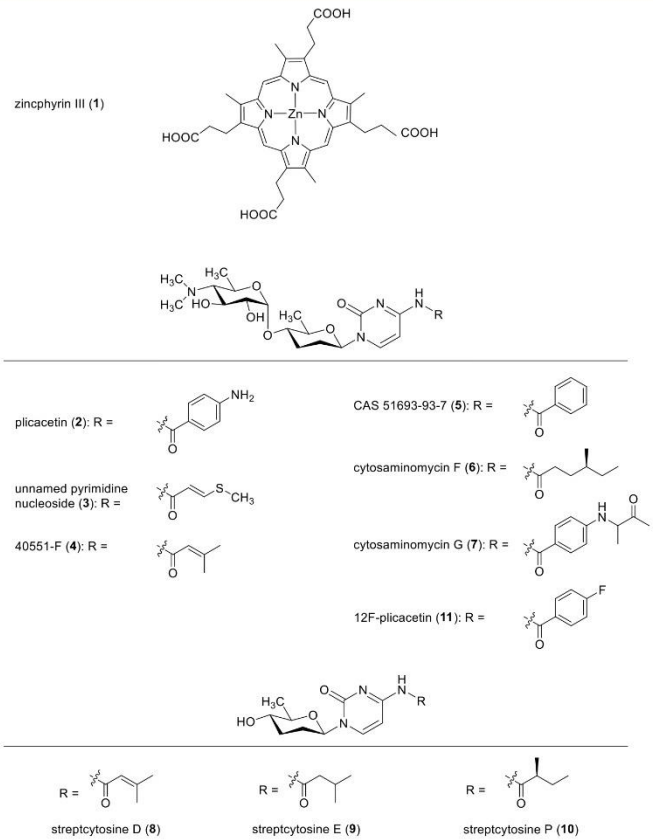

spectra of established analogues, particularly with cytosaminomycin E.[8c] Thus, in combination with the NOESY data, these data demonstrated that the absolute configuration of the disaccharide was 1′*R*, 4′*S*, 5′*R*, 1″*R*, 2″*R*, 3″*S*, 4″*R*, 5″*R*. In order to determine the absolute configuration at C-11, a small sample of **6** was hydrolyzed with 6 N HCl to its fragments and derivatized with 1-naphthylamine. These were analyzed by chiral HPLC and compared with the retention times of authentic standards. Employing this workflow, the 4-methyl hexanoic acid unit of **6** was shown to possess an *S*-configuration, thus completing the 3D structure of cytosaminomycin F (**6**).

The molecular formula of **7** was determined to be $C_{29}H_{41}N_5O_8$ by HR-ESI-MS. Comparison of the ^{1}H and ^{13}C NMR spectral data with those of **6** (Tables 1 and 2) revealed that compound **7** contains also the cytosamine substructure. However, two aromatic resonances (δ_H/δ_C 6.64, d, 8.7 Hz/114.4 and 7.82, d, 8.7 Hz/131.5) were indicative for the presence of a *para*-amino benzoic acid at NH-7. The remaining unassigned fragment consisting of $C_4H_7O_1$ was identified as butan-2-one using the following information. The ^{1}H−^{13}C-HSQC-TOCSY and ^{1}H−^{1}H-COSY spectrum provided evidence that H-16 was directly bonded to H_3-19 (Figure 1). ^{1}H−^{13}C-HMBC correlations from H_3-19 and H_3-18 to the keto-carbonyl C-17 (δ_C 212.3) allowed the acetyl group to be located at C-16. The attachment of the butanone moiety at C-16, via an aza-ether linkage to NH-15, was corroborated by ^{1}H−^{15}N-HMBC correlations from H-11, H-13, and H_3-19 to N-15. The NOESY data, which showed cross correlations of H-1′/H-5′, H-4′/H-1″, H-2″/H-4″, and H-3″/H-5″, proved that the relative configuration of the sugar units of **7** was the same as that of **2**. A stereoanalysis of C-16 was not undertaken since chiral standards were not commercially available. For **7**, the trivial name cytosaminomycin G is proposed.

Compound **10** had a molecular formula of $C_{15}H_{23}N_3O_4$, as deduced from its HR-ESI-MS spectrum, indicating six ring double bond equivalents. In the ^{1}H and ^{13}C NMR spectra, resonances for amosamine were absent; however COSY and HMBC NMR data established firmly the presence of the amicetosylcytosine unit. The remaining substructure (C_5H_9O) required the assignment of two CH_3, one CH_2, one CH, and one C═O group. From the COSY spectrum, the spin system $-CH_3-CH-CH_2-CH_3-$ could be deduced, which ranges from atom 9 to 12 (Figure 1). HMBC correlations between carbonyl atom C-8 and H-9/H_2-10/H_3-12 showed that C-8 was directly bonded to CH-9, establishing thereby the partial structure 2-methylbutanoic acid. The latter substructure could be linked to the cytosine unit via NH-7 by cross-peaks between

https://doi.org/10.1021/acs.jnatprod.1c01051
J. Nat. Prod. 2022, 85, 530−539

Table 1. ^{1}H NMR Data for Compounds **6**, **7**, **10**, and **11** (δ in ppm, J in Hz)

moiety	no.	**6**[a,c]	**7**[a,d]	**10**[b,d]	**11**[a,c]
cytosine	5	7.48, d (7.5)	7.58, d (7.4)	7.26, d (7.5)	7.59, d (7.6)
	6	8.11, d (7.5)	8.12, d (7.4)	8.07, d (7.5)	8.18, d (7.6)
	7		10.79, brs[b]	10.85, s	
side chain	9	2.45, dd		2.55, m	
	10	1.47, m	7.82, d (8.7)	1.37, m	8.05, dd (5.3, 8.7)[e]
		1.71, m		1.55, m	
	11	1.39, m	6.64, d (8.7)	0.82, t (7.4)	7.28,dd (8.7, 8.7)[e]
	12	1.20, m		1.04, d (6.6)	
	13	0.90, t (7.5)	6.64, d (8.7)		7.28, dd (8.7, 8.7)[e]
	14	0.92, d (6.8)	7.82, d (8.7)		8.05, dd (5.3, 8.7)[e]
	15		6.84, d (7.3)[b]		
	16		4.17, m		
	18		2.17, s		
	19		1.42, d (7,0)		
amicetose	1′	5.76, m	5.77, dd (10.8, 2.3)	5.62, dd (10.8, 2.2)	5.79, m
	2′	1.64, m	1.65, m	1.66, m	n.o.[f]
		2.37, m	2.15, m	1.88, m	2.18, m
	3′	1.64, m	1.68, m	1.52, m	1.66, m
		2.15, m	2.38, m	2.00, m	2.39, m
	4′	3.40, m	3.41, m	3.11, m	3.43, m
	5′	3.74, dq (9.1, 6.1)	3.75, m	3.38, dq (9.1, 6.1)	3.75, m
	6′	1.36, d (6.1)	1.36, d (6.4)	1.20, d (6.1)	1.37, d (6.1)
amosamine	1″	4.91, m	4.92, d (3.7)		4.91, d (3.8)
	2″	3.42, dd (9.5, 3.8)	3.41, m		3.43, m
	3″	3.87, m	3.87, t (9.6)		3.88, m
	4″	2.13, m	2.13, t (10.1)		2.16, m
	5″	3.82, m	3.83, m		3.83, m
	6″	1.24, d (6.2)	1.24, d (6.4)		1.25, m
	7″	2.46, s	2.47, s		2.48, s
	8″	2.46, s	2.47, s		2.48, s

[a]Recorded in d_4-MeOH. [b]Recorded in d_6-DMSO. [c]400 MHz. [d]700 MHz. [e]Besides regular homonuclear ^{1}H−^{1}H-coupling, the protons of the fluorine-substituted aromatic ring being located in *ortho* and *meta* position to the fluorine, further exhibit heteronuclear ^{1}H−^{19}F-coupling. [f]n.o.: not observed.

NH-7 and C-8 in the corresponding ^{1}H−^{13}C HMBC spectrum. Compound **10** was thus similar to streptcytosine C[8a] and differed solely by the fact that its side chain is saturated instead of bearing a double bond. Being the 16th member of the streptcytosine compound family,[8a,c] **10** was consequently named streptcytosine P. The relative stereochemistry of the sugar portion was based on the close similarity of ^{1}H and ^{13}C NMR shifts between **8**, **9**, and **10** (Tables 1, S7, and S8) and confirmed by NOESY correlations. Furthermore, the ECD spectrum of **10** was similar to that of **6** (Figures S35 and S69), thereby establishing the absolute configuration for the sugar portion. For the elucidation of the absolute configuration of the chiral center at C-9, chiral HPLC upon derivatization of the hydrolysis products was applied in a similar fashion to that conducted with **6** and showed atom 9 of **10** to be *S*-configured.

Precursor-Directed Feeding Study. The diversity of pyrimidine nucleosides is generated by the variation of either the sugar units (mono vs disaccharide, extra-hydroxylation, demethylation) or the side chain, that gets attached to NH-7 by an amide bond by highly promiscuous acyltransferases. Considering the metabolite spectrum obtained (compounds **2**−**10**), the latter mechanism appears to be dominant in strain SHP 22-7. Based on the discovery of the amicetin biosynthetic gene cluster and deletion experiments,[4] the acyltransferases AmiF and transacylase AmiR were identified as responsible for the amidic fusion of *p*-aminobenzoic acid to NH-7 and the amidic attachment of terminal side chains, respectively. With the exception of the deoxy-sugar biosynthesis cassette *amiABCDE*, the complete *ami* gene cluster is also present in the strain SHP 22-7 (Figure S82). Both transferase encoding genes, *amiF* and *amiR*, are present therein and show a very high level of identity (>99%) to their orthologues in *S. vinaceusdrappus* NRRL 2363 (Table S11). The obtained compounds are in line with the biosynthetic knowledge, accumulated so far, except for compound **7**. Here, it is striking that the linkage between the *p*-aminobenzoic acid and its terminal side is provided by an amine instead of the commonly observed amide bond. To the best of our knowledge, such a terminal amine linkage was not observed before in the amicetin compound family. However, *p*-amino benzoic acid condensates, within of the frame of the bacterial folate pathway, physiologically with dihydropteroate-diphosphate and the help of the enzyme dihydropteroate synthase (DHPS) via an amine bridge.[9] Likewise, it can be envisioned that a 1-methyl-2-keto-propanone-1-pyrophosphate precursor, in interaction with a DHPS-like enzyme, leads to the targeted side chain moiety given in **7**. It is noteworthy to mention that the *ami* gene cluster of SHP 22-7 contains no obvious additional candidate gene nearby, encoding such a protein, but the corresponding gene can be still located elsewhere in the genome.

We hypothesized that we could exploit the extensive substrate flexibility of AmiF and AmiR to generate optimized

https://doi.org/10.1021/acs.jnatprod.1c01051
J. Nat. Prod. 2022, 85, 530−539

Table 2. ^{13}C NMR and ^{15}N NMR Data for Compounds 6, 7, 10, and 11 (δ in ppm)

moiety	no.	6[b,c]	7[b,c]	10[b,d]	11[a,c]
cytosine	1		168.4, tN[d,e]		
	2	157.5, qC	157.4, qC	154.0, qC	157.3, qC
	3		n.o.[d,e,i]		
	4	164.3, qC	164.8, qC	162.5, qC	164.8, qC
	5	98.4, CH	98.7, CH	95.8, CH	98.8, CH
	6	146.3, CH	145.8, CH	145.4, CH	146.4, CH
	7		n.o.[d,e]	147.6, NH[f]	
side chain	8	176.2, qC	168.6, qC	177.3, qC	168.1, qC
	9	36.0, CH_2	12.1, qC	41.8, CH	131.1, qC, d, $^4J_{C,F}$ = 3.0 Hz
	10	32.6, CH_2	131.5, CH	26.5, CH_2	132.1, CH, d, $^3J_{C,F}$ = 9.4 Hz
	11	35.4, CH	114.4, CH	11.4, CH_3	116.8, CH, d,[2] $J_{C,F}$ = 22.4 Hz
	12	30.3, CH_2	155.0, qC	16.8, CH_3	165.7, qC, d, $^1J_{C,F}$ = 250.9 Hz[g]
	13	11.6, CH_3	114.4, CH		116.8, CH, d, $J_{C,F}$ = 22.4 Hz
	14	19.3, CH_3	131.5, CH		132.1, CH, d, $J_{C,F}$ = 9.4 Hz
	15		85.4, NH[d,e]		
	16		59.2, CH		
	17		212.3, qC		
	18		25.4, CH_3		
	19		17.3, CH_3		
amicetose	1′	84.7, CH	84.6, CH	82.1, CH	84.7, CH
	2′	30.8, CH_2	31.0, CH_2	29.8, CH_2	31.1, CH_2
	3′	27.7, CH_2	27.7, CH_2	31.4, CH_2	27.7, CH_2
	4′	75.0, CH	75.0, CH	69.6, CH	75.0, CH
	5′	78.5, CH	78.5, CH	78.5, CH	78.5, CH
	6′	19.1, CH_3	19.1, CH_3	18.2, CH_3	19.2, CH_3
amosamine	1″	96.2, CH	96.1, CH		96.2, CH
	2″	74.7, CH	74.6, CH		74.6, CH
	3″	70.2, CH	70.2, CH		70.2, CH
	4″	71.9, CH	71.8, CH		71.9, CH
	5″	67.4, CH	67.4, CH		67.3, CH
	6″	19.7, CH_3	19.6, CH_3		19.6, CH_3
	7″	42.4, CH_3	42.3, CH_3		42.3, CH_3
	8″	42.4, CH_3	42.3, CH_3		42.3, CH_3
	N		18.4, tN[d,e,h]		

[a]100 MHz. [b]175 MHz. [c]Recorded in d_4-MeOH. [d]Recorded in d_6-DMSO. [e]41 MHz. [f]71 MHz. [g]Shift value was not observed in the ^{13}C NMR experiment but extractable from the corresponding $^1H-^{13}C$-HMBC NMR experiment. The indicated $^1J_{C,F}$ coupling constant value was read out from a data set, recorded in d_6-DMSO, in which C-12 was detectable. [h]Tertiary amine. [i]n.o.: not observed.

or clickable[10] new-to-nature analogues by feeding either fatty acids or benzoic acid analogues within the framework of a precursor-directed feeding approach.[11] In order to determine an optimal feeding time point, a growth curve was established and the production rate was monitored. These time course studies indicated that nucleoside production coincided with the start of the exponential log phase; that is, it begins approximately 40 h after inoculation, reaches its maximum at about 90 h, and is then followed by an ongoing but fluctuating production (Figure S83). Thus, the precursors were added before production starts, typically 32 h after inoculation, while the harvest time point was scheduled for 96 h after inoculation. Forty-three commercially available precursors were fed to small-scale cultures, extracted, and analyzed by HR-LC-MS and MS^2. As depicted in Figures 2 and S84−S93, 10 out of 43 tested precursors were incorporated into the pyrimidine nucleoside backbone and led to the corresponding plicacetin congeners. The successful examples consisted foremost of halogenated benzoic acid derivatives, while none of the linear fatty acids were accepted. Notably, precursor **1a** enhanced the production of analogue **5** approximately 10-fold, while the other accepted precursors led to the production of the expected new-to-nature pyrimidine nucleosides. However, the majority of the new derivatives were only produced in minute amounts. One derivative, 12-fluoro-plicacetin (**11**), could be obtained in amounts sufficient for NMR analysis and bioassay testing upon large-scale cultivation and feeding of precursor **4c**.

The molecular formula $C_{25}H_{33}FN_4O_7$ of **11** was ascertained by HR-ESI-MS. Furthermore, the structure of **11** was verified by NMR. Its ^{13}C NMR spectrum was nearly superimposable with the one obtained for plicacetin (**2**), except for the resonances belonging to the aromatic moiety (Figure S72). Beside a downfield shift of C-12 from 155.0 to 165.7 ppm, a typical $J_{C,F}$ coupling constant pattern over 1−4 bonds[12] was observed (Table 2), hinting at the successful incorporation of a fluorobenzene moiety in **11**. The detection of a characteristic resonance at δ_F at −107.7 in the ^{19}F NMR spectrum[12] of **11**, together with $^1H-^1H$-COSY correlations between H-10/H-14 and H-11/H-13 in combination with HMBC cross-peaks between qC-8/H-14, H-14/qC-12, H-13/qC-12, and H-13/qC-9, provided final evidence for the presence of a *para*-substituted fluorobenzene residue (Figure 1).

Biological Activity. Pyrimidine nucleosides have been reported to be strongly active against various Gram-positive

https://doi.org/10.1021/acs.jnatprod.1c01051
J. Nat. Prod. 2022, 85, 530−539

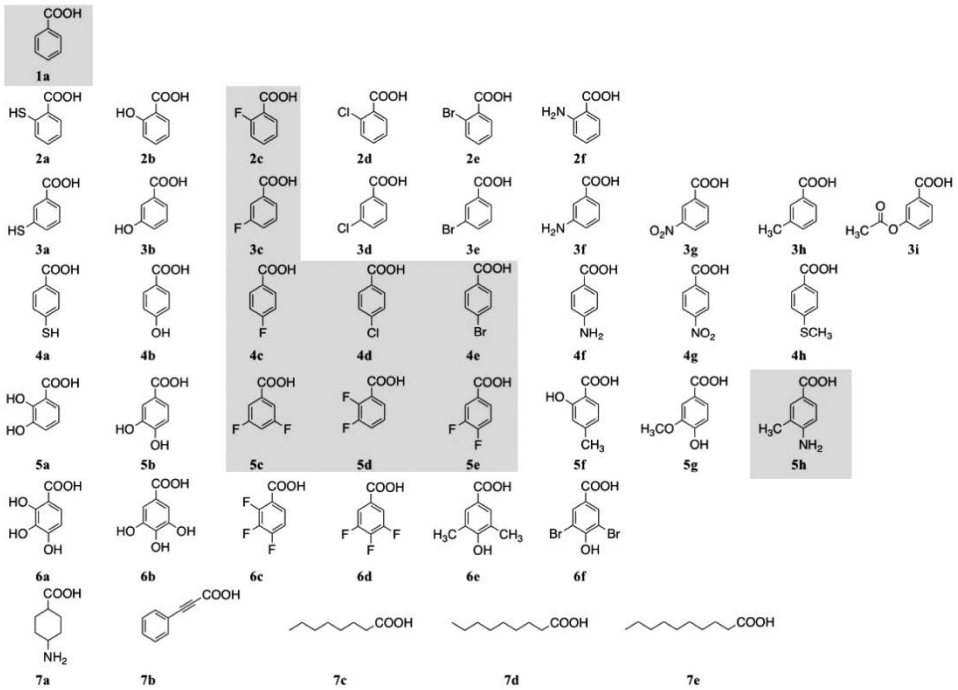

Figure 2. Overview of the precursors, supplemented to cultures of SHP 22-7. Gray-shaded structures represent precursors that were incorporated into the pyrimidine nucleoside backbone, leading to the corresponding plicacetin derivatives.

Table 3. Biological Activities of the Isolated Pyrimidine Nucleosides

	compound								
organism	2	3	4	6	7	8	9	10	11
Antibacterial Assays, MIC [μg/mL]									
C. albicans Tü01	>32	>32	>32	>32	>32	>32	>32	>32	>32
C. glabrata Tü04	>32	>32	>32	>32	>32	>32	>32	>32	>32
Antibacterial Assays, MIC [μg/mL]									
E. faecium BM4147−1	>32	>32	>32	>32	>32	>32	>32	>32	>32
S. aureus ATCC 29213	>32	16	>32	>32	>32	>32	>32	>32	>32
K. pneumoniae ATCC 12657	>32	>32	>32	>32	>32	>32	>32	>32	>32
A. baumannii 09987	>32	>32	>32	>32	>32	>32	>32	>32	>32
P. aeruginosa ATCC 27853	>32	>32	>32	>32	>32	>32	>32	>32	>32
E. aerogenes ATCC 13048	>32	>32	>32	>32	>32	>32	>32	>32	>32
E. coli ATCC 25922	>32	>32	>32	>32	>32	>32	>32	>32	>32
B. subtilis 168	32	8	32	>32	>32	>32	>32	>32	>32
S. aureus NCTC 8325	>32	16	>32	>32	>32	>32	>32	>32	>32
M. smegmatis mc^2 155	2	4	4	16	2	>32	>32	>32	8
Antitubercular Assays, MIC_{95} [μM]									
M. tuberculosis	16	8	32	n.d.[a]	32	n.d.	n.d.	n.d.	64
In Vitro Translation Assay, IC_{50} [μg/mL]									
	12.0	1.0	1.6	9.5	13.0	n.d.	n.d.	n.d.	n.d.
Cytotoxicity Assays, IC_{50} [μg/mL]									
HeLa cell line	16−32	1−2	2−4	>64	16−32	>64	>64	>64	>64

[a]n.d.: not determined.

bacteria and mycobacteria since the 1960s.[2,3,8] Since they demonstrated instabilities and cytotoxicity, they were not developed further as a drug. Nevertheless, they are considered as a tractable lead structure that can be optimized for

https://doi.org/10.1021/acs.jnatprod.1c01051
J. Nat. Prod. 2022, 85, 530−539

selectivity, stability, and potency and serve foremost as antitubercular agents. Consequently, all compounds that could be obtained in sufficient amounts were subjected to a cytotoxicity and antimicrobial screening. In antifungal assays no activity could be observed. Overall, the tested compounds were at best weakly active against a panel of human pathogenic bacteria (Table 3). However, the known compounds plicacetin (**2**), the unnamed pyrimidine nucleoside (**3**),[8d] and 40551-F (**4**)[8c] as well as the new compounds **6**, **7**, and **11** were found to be active toward mycobacteria. In the case of the known pyrimidine nucleosides and to a lesser extent compound **7**, this activity was accompanied by cytotoxicity (Table 3). Complementary to the *in vivo* assays, the compounds were further tested, employing an *in vitro* translation assay (IVTA). Unexpectedly, the binding to the ribosomal target did not correlate necessarily with the whole cell activity. This can be demonstrated by compound **4**, which exhibited comparably strong inhibition in the IVTA, but displayed weak or moderate activity against *M. tuberculosis* and *M. smegmatis*, respectively. In contrast, **7** showed only a weak effect in the IVTA and weak activity against *M. tuberculosis* but a potent activity against *M. smegmatis*. Thus, it appears that inhibition of translation is possibly not the only mode of action by which pyrimidine nucleosides mediate their activity against mycobacteria.

■ EXPERIMENTAL SECTION

General Experimental Procedures. Optical rotation values were measured on a Jasco P-2000 polarimeter, using a 3.5 mm × 10 mm cylindrical quartz cell. UV spectra were taken on a PerkinElmer Lambda 25 UV/vis spectrometer. ECD spectra were conducted using a Jasco J-720 spectropolarimeter. Infrared spectra were obtained employing a Jasco FT/IR 4200 spectrometer, interfaced with a MIRacle ATR device (ZnSe crystal). 1D and 2D NMR spectra were acquired on either a 400 MHz Bruker AVANCE III HD (400, 100, 40.56, and 376.5 MHz for ^{1}H, ^{13}C, ^{15}N, and ^{19}F isotopes, respectively), a 600 MHz Bruker Avance III HDX (600 and 150 MHz for ^{1}H and ^{13}C), or a 700 MHz Avance III HDX (700, 175, and 70.97 MHz for ^{1}H, ^{13}C, and ^{15}N isotopes) NMR spectrometer, equipped with a 5 mm broadband SMART, Prodigy BBO-cryo, or Prodigy TCI cryo probe head, respectively. All spectra were recorded in either d_4-MeOH (δ_H/δ_C 3.31/49.0) or d_6-DMSO (δ_H/δ_C 2.50/39.5), respectively, and referenced to the residual solvent signals or the internal offset for ^{15}N assigned by the instrument manufacturer. ^{19}F NMR chemical shifts were calculated relative to CF_3COOH (δ_F −76.55). High-resolution mass spectra were acquired on an HR-ESI-TOF-MS Bruker maXis 4G mass spectrometer. HPLC was performed with a Waters system, consisting of a Waters 1525 pump with a built-in degasser, a Waters 996 photodiode array detector, and a Rheodyne 7725i injector, operated by the software Millenium32. For LC-MS analysis, an 1100 Series Agilent HPLC system was fitted with a G1322A degasser, a G1312A binary pump, a G1329A autosampler, and a G1315A diode array detector. The Agilent HPLC components were connected with an ABSCIEX 3200 QTRAP LC/MS/MS mass spectrometer. All solvents were purchased as HPLC or LC-MS grade, respectively. Steam sterilization of medium components and waste was performed at 121 °C for 15 min at 2.1 bar using a Systec VX-150 autoclave, equipped with air exhaust filtration.

Bacterial Strains. Strain SHP 22-7 was collected and isolated by one of the authors (I.H.) from a mangrove soil sample obtained from Enggano Island, Indonesia, and subsequently genome sequenced.[1,5] For the bioassay experiments, all ATCC strains were provided by the American Type Culture Collection, while *A. baumannii* 09987 was obtained from the University of Bonn, Germany, and *Bacillus subtilis* 168 was provided by Prof. Hamoen, University of Amsterdam, The Netherlands, respectively.

Cultivation of SHP 22-7. For production of the nucleoside antibiotics, strain SHP 22-7 was grown in 200 mL of NL 410 preculture medium, consisting of glucose (10 g L^{-1}), glycerol (10 g L^{-1}), oatmeal (5 g L^{-1}), soy flour (10 g L^{-1}), yeast extract (5 g L^{-1}), Bacto casamino acids (5 g L^{-1}), $CaCO_3$ (1 g L^{-1}), and distilled water (pH was adjusted to 7.0 with NaOH) in 1 L Erlenmeyer flasks (with steel springs) on an orbital shaker (180 rpm) at 28 °C. After 3 days of cultivation, 200 mL of preculture was transferred to 2 L of main culture medium NL 300, consisting of mannitol (20 g L^{-1}), cotton seed (20 g L^{-1}), and distilled water (pH adjusted to pH 7.5 with NaOH). Cultures were grown for 4 days at 28 °C in 5 L Erlenmeyer flasks (with steel springs) on an orbital shaker (180 rpm). In total, a volume of 26 L of SHP 22-7 culture has been used for the isolation of compounds **1**−**10**.

Extraction and Isolation. Portions of 2 L of the culture broth were extracted with the same volume of ethyl acetate for 3 h at RT. Samples were centrifuged at 4.000 rpm for 15 min. The upper organic phase was dried *in vacuo*. The crude extract was subjected to open column chromatography employing Sephadex LH20 as stationary phase and MeOH as mobile phase, yielding five subfractions. LC-MS profiling of these fractions indicated the presence of compound **1** (1.9 mg) in the first fraction and that the third fraction contained compounds with the targeted fragmentation pattern. The separation of this fraction was performed by RP-HPLC using a linear gradient of 50:50 to 100:0 MeOH−H_2O (0.1% TFA) over a period of 30 min, followed by isocratic elution at 100% MeOH for an additional 10 min (Phenomenex C_{18} Luna, 10 × 250 mm, 5 μm; 2 mL/min flow rate; UV monitoring at 215 nm). It is noteworthy to mention that initially the aqueous phase contained 0.1% trifluoracetic acid. However, this solvent system led to rapid degradation of the nucleosides. Therefore, either purified H_2O or a 1 M phosphate buffer was used as aqueous solvent. RP-HPLC separation of the three obtained subfractions (Phenomenex Omega-polar, 250 × 10.0 mm, 5 μm; isocratic elution with MeOH−H_2O (65:35), 2 mL/min) yielded compounds **2** (44.0 mg), **3** (4.1 mg), **4** (4.9 mg), **5** (2.5 mg), **6** (9.2 mg), **7** (13.9 mg), **8** (5.9 mg), **9** (8.4 mg), **10** (11.3 mg), and upon feeding **11** (3.7 mg). In case of contamination with lipids, the same conditions were applied, using a Phenomenex C_5 column (250 × 4.6 mm).

Zincphyrin III (1): reddish-pink powder (Figure S2); ^{1}H NMR and ^{13}C NMR data, see Table S1; HRESIMS *m/z* 715.1754 $[M - H]^-$ (calcd for $C_{36}H_{36}N_4O_8{}^{64}Zn$, 715.1746; Δ +1.1 ppm) (Figure S3).

Plicacetin (2): amorphous, white opaque powder; $[\alpha]_D^{23}$ +92.3 (*c* 0.95, MeOH); UV (MeOH) λ_{max} (log ε) 255 (4.36), 326 (4.67) nm; FT-IR (ATR) ν_{max} 3352, 3228, 2928, 1648, 1603, 1482, 1253, 1180, 1026 cm^{-1}; ^{1}H NMR and ^{13}C NMR data, see Table S2; HRESIMS *m/z* 518.2602 $[M + H]^+$ (calcd for $C_{25}H_{36}N_5O_1$, 518.2615; Δ −2.5 ppm).

Unnamed pyrimidine nucleoside (3): amorphous, white opaque powder; $[\alpha]_D^{23}$ +95.1 (*c* 0.41, MeOH); UV (MeOH) λ_{max} (log ε) 255 (4.16), 313 (4.59) nm; FT-IR (ATR) ν_{max} 3362, 2924, 1653, 1569, 1490, 1137, 1087, 1023 cm^{-1}; ^{1}H NMR and ^{13}C NMR data, Table S3; HRESIMS *m/z* 499.2215 $[M + H]^+$ (calcd for $C_{22}H_{35}N_4O_7S$, 499.2226; Δ −2.2 ppm).

40551-F (4): amorphous, white opaque powder; $[\alpha]_D^{23}$ +100.6 (*c* 2.46, MeOH); UV (MeOH) λ_{max} (log ε) 263 (4.34), 303 (4.06) nm; FT-IR (ATR) ν_{max} 3419, 2924, 1674, 1443, 1189, 1132 cm^{-1}; ^{1}H NMR and ^{13}C NMR data, see Table S4; HRESIMS *m/z* 481.2657 $[M + H]^+$ (calcd for $C_{23}H_{37}N_4O_7$, 481.2662; Δ −1.0 ppm).

CAS 51693-93-7 (5): amorphous, white opaque powder; ^{1}H NMR and ^{13}C NMR data, see Table S5; HRESIMS *m/z* 503.2497 $[M + H]^+$ (calcd for $C_{25}H_{35}N_4O_7$, 503.2506; Δ −1.8 ppm).

Cytosaminomycin F (6): amorphous, white opaque powder; $[\alpha]_D^{22}$ +75.3 (*c* 0.76, MeOH); UV (MeOH) λ_{max} (log ε) 204 (4.49), 248 (4.33), 298 (3.95) nm; ECD (MeOH) λ_{max} (Δε) 204 (+4.15), 222 (−5.00), 262 (+4.05), 299sh (+2.83) nm; FT-IR (ATR) ν_{max} 3383, 2925, 1673, 1201, 1133, 1026 cm^{-1}; ^{1}H NMR and ^{13}C NMR data, see Tables 1 and 2; HRESIMS *m/z* 511.3119 $[M + H]^+$ (calcd for $C_{25}H_{43}N_4O_7$, 511.3132; Δ +1.8 ppm).

Cytosaminomycin G (7): amorphous, white opaque powder; $[\alpha]_D^{23}$ +92.3 (*c* 0.59, MeOH); UV (MeOH) λ_{max} (log ε) 255 (4.31), 332 (4.59) nm; ; FT-IR (ATR) ν_{max} 3317, 2967, 2926, 2868, 1653, 1603, 1482, 1253, 1181, 1034 cm^{-1}; ^{1}H NMR and ^{13}C NMR data, see

https://doi.org/10.1021/acs.jnatprod.1c01051
J. Nat. Prod. 2022, 85, 530−539

Tables 1, 2, and S6; HRESIMS m/z 588.3035 $[M + H]^+$ (calcd for $C_{29}H_{42}N_5O_8$, 588.3033; Δ +0.3 ppm).

*Streptcytosine D (**8**):* amorphous, white opaque powder; $[\alpha]_D^{23}$ +33.3 (c 0.30, MeOH); UV (MeOH) λ_{max} (log ε) 264 (4.27), 300 (3.92) nm; FT-IR (ATR) ν_{max} 2928, 2868, 1674, 1636, 1489, 1202, 1132, 1054 cm^{-1}; ^1H NMR and ^{13}C NMR data, see Table S7; HRESIMS m/z 308.1610 $[M + H]^+$ (calcd for $C_{15}H_{22}N_3O_4$, 308.1610; Δ 0.0 ppm).

*Streptcytosine E (**9**):* amorphous, white opaque powder; $[\alpha]_D^{23}$ +50.0 (c 0.24, MeOH); UV (MeOH) λ_{max} (log ε) 214 (4.45), 248 (4.32), 300 (3.94) nm; ^1H NMR and ^{13}C NMR data, see Table S8; HRESIMS m/z 310.1766 $[M + H]^+$ (calcd for $C_{15}H_{24}N_3O_4$, 310.1767; Δ −0.3 ppm).

*Streptcytosine P (**10**):* amorphous, white opaque powder; UV (MeOH) λ_{max} (log ε) 211 (4.52), 248 (4.33), 292 (4.09) nm; ECD (MeOH) λ_{max} ($\Delta\varepsilon$) 206 (+8.86), 223 (−12.49), 263 (+8.75), 298 (+7.47) nm; FT-IR (ATR) ν_{max} 2924, 2871, 1672, 1491, 1183, 1134, 1056 cm^{-1}; ^1H NMR and ^{13}C NMR data, see Tables 1 and 2; HRESIMS m/z 310.1766 $[M + H]^+$ (calcd for $C_{15}H_{24}N_3O_4$, 310.1767; Δ −0.3 ppm).

*12F-Plicacetin (**11**):* amorphous, white opaque powder; $[\alpha]_D^{23}$ +47.4 (c 0.97, MeOH); UV(MeOH) λ_{max} (log ε) 259 (4.15), 305 (3.85) nm; FT-IR (ATR) ν_{max} 3361, 2921, 2850, 1682, 1655, 1489, 1202, 1136, 1023 cm^{-1}; ^1H NMR and ^{13}C NMR data, see Tables 1 and 2; HRESIMS m/z 521.2413 $[M + H]^+$ (calcd for $C_{25}H_{33}FN_4O_7$, 521.2412; Δ +0.2 ppm).

Enantioselective HPLC-MS Analysis of the Branched Fatty Acid Side Chains of Compounds 6 and 10. For the determination of the absolute configuration of the side chains of **6** and **10**, both compounds were subjected to the same sample preparation procedure. The compounds were dissolved in 6 N HCl and heated to 110 °C overnight. With this hydrolysis step, the chiral carboxylic acids 2-methyl butyric acid of **10** and 4-methyl hexanoic acid of **6**, respectively, were cleaved from the nucleoside backbone. After hydrolysis, a liquid−liquid extraction step of the branched short-chained fatty acids was performed with hexane. The organic layer was collected and dried, and the residue was directly employed for derivatization. As derivatization agent, 1-naphthylamine was used in combination with 1-ethyl-3-(3-dimethylaminopropyl)carbodiimide (EDC), dissolved in 2-propanol. Derivatization was allowed to proceed while shaking at 25 °C for 12 h. After drying of the product, it was reconstituted in the respective mobile phase.

The analytical standards, *rac*-2-methyl butyric acid, (*S*)-2-methyl butyric acid, and *rac*-4-methyl hexanoic acid, were supplied by Sigma-Aldrich (Merck, Munich, Germany), (*R*)-2-methyl butyric acid was from Activate Scientific (Prien am Chiemsee, Germany), and (*S*)-4-methyl hexanoic acid and (*R*)-4-methyl hexanoic acid were supplied by Chemspace (Riga, Latvia).

HPLC-UV analysis was performed on an Agilent 1260 LC-system from Agilent Technologies (Waldbronn, Germany) equipped with a quaternary pump, a degasser, an autosampler, and a UV-DAD detector.

HPLC-MS analysis was performed on an Agilent 1290 LC-system with an API 4000 QQQ MS system from AB Sciex (Toronto, Ontario, Canada) and an HTC PAL autosampler from CTC Analytics (Zwingen, Switzerland). For data acquisition an MS^2 product ion scan was performed for both compounds with the following settings: declustering potential: 100.0 V, entrance potential: −10.0 V, collision energy: −30.0 V, collision cell exit potential: 36.0 V, collision gas: 4 psi, curtain gas: 30 psi, ion source gas 1: 30 psi, ion source gas 2: 20 psi, ionspray voltage: 5500.0 V, temp: 450 °C. Measurements were performed in multiple reaction monitoring mode, using the following transitions: m/z 228.138 → 144.080 (2-methyl butyric acid); m/z 256.160 → 144.080 (4-methyl hexanoic acid).

Both chiral columns (Chiralpak IB-U and IH-U, 100 × 3 mm, 1.6 μm fully porous particles) were obtained from Daicel (Tokyo, Japan). HPLC-UV measurements for 2-methyl butyric acid on Chiralpak IB-U were performed in normal phase, using hexane−isopropanol (95/5; v/v) as mobile phase. Flow rate was set to 1 mL/min, and column temperature was held constant at 25 °C. Detection wavelength was 215 nm. MS measurements for this compound were conducted on the same column but in reversed phase gradient elution mode with water + 0.1% acetic acid (A) and acetonitrile + 0.1% acetic acid (B) in isocratic mode (55/45). Column temperature was set to 10 °C, and flow rate was 0.2 mL/min. HPLC-UV measurements for 4-methyl hexanoic acid on Chiralpak IH-U were performed in reversed phase gradient elution mode with water + 0.1% acetic acid (A) and acetonitrile + 0.1% acetic acid (B). The gradient was as follows: 0 min 20% B, 30 min 90% B, 30.01 min 20% B, 36 min 20% B. Flow rate was set to 0.2 mL/min, and column temperature was held constant at 25 °C. Detection wavelength was 215 nm. MS measurements for this compound were conducted with the following gradient: 0 min 20% B, 37.50 min 90% B, 37.51 min 20% B, 45 min 20% B. Flow rate was set to 0.2 mL/min, and column temperature was held constant at 10 °C.

The IH-U column showed an elution order of *R* before *S* for 4-methyl-*N*-1-naphthylhexanamide and hence proved that the hydrolysis product of **6** is *S*-configured (Figures S79 and S80). On the IB-U column an elution order of *S* before *R* was determined for 2-methyl-*N*-1-naphthylbutanamide. Injection of the sample and co-injections with enantiomeric standards established an *S*-configuration for the hydrolysis product of **10** (Figure S81).

Antifungal Assay. The minimal inhibitory concentration (MIC) of pure compounds against different *Candida* clinical isolates was determined by broth microdilution using the direct colony suspension method with an inoculum of (0.5−2.5) × 10^5 CFU/mL, according to the recommendations of the European Committee on Antimicrobial Susceptibility Testing (EUCAST).[13] Caspofungin was used as reference antifungal agent. MIC testing was performed in sterile 96-well microdilution plates using MOPS-buffered RPMI 1640 medium supplemented with glucose to a final concentration of 2%, pH 7.0. MICs were read after incubation of the microplates at 37 °C for 48 h.

Antibacterial Assay. The MIC was determined in cation-adjusted Mueller-Hinton medium that contains casein, beef extract, and starch by using a 2-fold serial dilution method according to the standards and guidelines of the Clinical and Laboratory Standards Institute.[14] In brief, a 2-fold serial dilution of the test compound was prepared in microtiter plates and seeded using a final test concentration of bacteria of 5 × 10^5 CFU/mL. After the overnight incubation at 37 °C, the MIC was determined as the lowest compound concentration preventing visible bacterial growth. The strain panel included representative species of nosocomial pathogens, known as "ESKAPE" bacteria. Specifically, the following strains were used: *Enterococcus faecium* BM 4147-1, *Staphylococcus aureus* ATCC 29213, *Klebsiella pneumoniae* ATCC 12657, *Acinetobacter baumannii* 09987, *Pseudomonas aeruginosa* ATCC 27853, and *Enterobacter aerogenes* ATCC 13048. *Bacillus subtilis* 168, *Escherichia coli* ATCC 25922, and *Mycobacterium smegmatis* mc^2 155 ATCC 700084 were used as further reference strains.

Antibacterial Assay against *Mycobacterium tuberculosis*. *M. tuberculosis* (Mtb) strain H37Rv (ATCC 25618) carrying an mCherry-expressing plasmid (pCherry10)[15] was cultured in 7H9 complete medium (BD Difco; Becton Dickinson) supplemented with oleic acid−albumin dextrose−catalase (OADC, 10%; BD), 0.2% glycerol, and 0.05% Tween80. At mid log phase (OD_{600} = 0.4) cultures were harvested and frozen in aliquots at −80 °C as previously described.[16] Frozen aliquots of mCherry-Mtb H37Rv were thawed and centrifuged (3700g, 10 min). Supernatants were discarded, and bacteria were thoroughly resuspended in 7H9 medium (10% OADC) in the absence of glycerol and Tween80 by use of a syringe and a 26-gauge syringe needle. Compounds were tested in triplicates (2 × 10^5 bacteria, volume 100 μL) for their antitubercular activity in 2-fold serial dilutions starting from 64 μM using 96-well flat clear-bottom black polystyrene microplates (Corning CellBIND, New York, USA) as recently described.[17] Bacterial growth was measured as relative light units (RLU) from the fluorescence intensity obtained at an excitation wavelength of 575 nm and an emission wavelength of 635 nm (Synergy 2, BioTek Instruments, VT, USA) after 7 days of culture at 37 °C. Obtained values were normalized to RLU values of the solvent control (DMSO-treated bacteria set to 100%), and a MIC_{95} value of each compound was determined. MIC_{95} was defined as the minimum

https://doi.org/10.1021/acs.jnatprod.1c01051
J. Nat. Prod. 2022, 85, 530−539

concentration of the compound required to achieve a reduction in fluorescence by 95%. Obtained MIC values were validated by a visual resazurin microtiter assay[18] by adding 30 μL of 0.02% resazurin (Cayman) solution to each well followed by another 20 h of culture without agitation (data not shown).

***In Vitro* Translation Assay.** An *in vitro* translation assay was performed to assess the potency of the compounds on bacterial translation in a cell-free system. The assay is based on S30 extracts prepared from logarithmically growing *E. coli* MRE600,[19] an RNase I deficient strain, according to a procedure described by Zubay.[20] For the assay, the pET14b-luc plasmid was constructed by integrating the gene encoding firefly (*Photinus pyralis*) luciferase into the pET14b (Novagen) vector. In the pET14b-luc plasmid, the luciferase is transcribed from a phage T7 promoter, allowing the selective detection of bacterial translation inhibitors by measuring luminescence. Inhibitors of bacterial transcription do not affect the assay because transcription is performed by the phage T7 RNA polymerase. Apart from the S30 extract and the pET14b-luc plasmid, the reaction mixture contained the following supplements: T7 RNA polymerase (182 U/mL, Thermo Scientific), 2.5 mM ATP, 0.5 mM GTP, 0.5 mM UTP, 0.5 mM CTP, 20 amino acids (0.04 mM each), an ATP regenerating system (creatine phosphokinase/phosphocreatine), 3.2% (w/v) polyethylene glycol 600, 8 mM putrescine, and 2 mM DTT in an appropriate buffer system (40 mM triethylamine pH 7.5, 140 mM potassium acetate, 8 mM magnesium acetate, 20 mM ammonium acetate, 1.4 mM spermidine). *In vitro* translation reactions were performed for 2 h at 25 °C. After addition of the substrate luciferin, chemiluminescence was recorded in a multiplate reader (SPARK, TECAN). The IC_{50} was determined as the concentration that led to 50% reduction of luminescence compared to an untreated control.

Cytotoxicity Assay. The cytotoxicity test against the HeLa human cervical carcinoma cell line was performed in RPMI cell culture medium supplemented with 10% fetal bovine serum using the 7-hydroxy-3*H*-phenoxazin-3-one-10-oxide (resazurin) assay. A 2-fold serial dilution of the test compounds was prepared in duplicates in a microtiter plate and seeded with trypsinized HeLa cells to a final cell concentration of 1×10^4 cells per well. After 24 h of incubation at 37 °C, with 5% CO_2 and 95% relative humidity, resazurin was added at a final concentration of 200 μM, and cells were again incubated overnight. Cell viability was assessed by determining the reduction of resazurin to the fluorescent resorufin. Fluorescence was measured in a TECAN M200 reader at an excitation wavelength of 560 nm and an emission wavelength of 600 nm in relation to an untreated control.

■ ASSOCIATED CONTENT

Supporting Information

The Supporting Information is available free of charge at https://pubs.acs.org/doi/10.1021/acs.jnatprod.1c01051.

Spectroscopic data (HRESIMS, IR, UV, 1D and 2D NMR spectra), enantioselective analyses, bioinformatics analyses, and biological assay details (PDF)

■ AUTHOR INFORMATION

Corresponding Author

Harald Gross − *Pharmaceutical Institute, Department of Pharmaceutical Biology, University of Tübingen, 72076 Tübingen, Germany; German Center for Infection Research (DZIF), partner site Tübingen, 72076 Tübingen, Germany;* orcid.org/0000-0002-0731-821X; Phone: +49-7071-2976970; Email: harald.gross@uni-tuebingen.de; Fax: +49-7071-295250

Authors

Niraj Aryal − *Pharmaceutical Institute, Department of Pharmaceutical Biology, University of Tübingen, 72076 Tübingen, Germany*

Junhong Chen − *Pharmaceutical Institute, Department of Pharmaceutical Biology, University of Tübingen, 72076 Tübingen, Germany*

Keshab Bhattarai − *Pharmaceutical Institute, Department of Pharmaceutical Biology, University of Tübingen, 72076 Tübingen, Germany*

Oliver Hennrich − *Department of Microbial Bioactive Compounds, Interfaculty Institute of Microbiology and Infection Medicine, Tübingen (IMIT), Cluster of Excellence 'Controlling Microbes to Fight Infections', University of Tübingen, 72076 Tübingen, Germany*

Ira Handayani − *Research Center for Biotechnology, National Research and Innovation Agency of Indonesia (RC Biotechnology BRIN), 16911 Bogor, West Java, Indonesia*

Markus Kramer − *Institute of Organic Chemistry, University of Tübingen, 72076 Tübingen, Germany*

Jan Straetener − *Department of Microbial Bioactive Compounds, Interfaculty Institute of Microbiology and Infection Medicine, Tübingen (IMIT), Cluster of Excellence 'Controlling Microbes to Fight Infections', University of Tübingen, 72076 Tübingen, Germany*

Tatjana Wommer − *Department of Microbial Bioactive Compounds, Interfaculty Institute of Microbiology and Infection Medicine, Tübingen (IMIT), Cluster of Excellence 'Controlling Microbes to Fight Infections', University of Tübingen, 72076 Tübingen, Germany*

Anne Berscheid − *Department of Microbial Bioactive Compounds, Interfaculty Institute of Microbiology and Infection Medicine, Tübingen (IMIT), Cluster of Excellence 'Controlling Microbes to Fight Infections', University of Tübingen, 72076 Tübingen, Germany;* orcid.org/0000-0003-1585-8715

Silke Peter − *Institute of Medical Microbiology and Hygiene, University of Tübingen, 72076 Tübingen, Germany; German Center for Infection Research (DZIF), partner site Tübingen, 72076 Tübingen, Germany*

Norbert Reiling − *Microbial Interface Biology, Research Center Borstel, Leibniz Lung Center, 23845 Borstel, Germany; German Center for Infection Research (DZIF), partner site Hamburg-Lübeck-Borstel-Riems, 20095 Hamburg, Germany;* orcid.org/0000-0001-6673-4291

Heike Brötz-Oesterhelt − *Department of Microbial Bioactive Compounds, Interfaculty Institute of Microbiology and Infection Medicine, Tübingen (IMIT), Cluster of Excellence 'Controlling Microbes to Fight Infections', University of Tübingen, 72076 Tübingen, Germany; German Center for Infection Research (DZIF), partner site Tübingen, 72076 Tübingen, Germany;* orcid.org/0000-0001-9364-1832

Christian Geibel − *Pharmaceutical Institute, Department of Pharmaceutical Analysis and Bioanalysis, University of Tübingen, 72076 Tübingen, Germany*

Michael Lämmerhofer − *Pharmaceutical Institute, Department of Pharmaceutical Analysis and Bioanalysis, University of Tübingen, 72076 Tübingen, Germany;* orcid.org/0000-0002-1318-0974

Yvonne Mast − *German Center for Infection Research (DZIF), partner site Tübingen, 72076 Tübingen, Germany; Department of Bioresources for Bioeconomy and Health Research, Leibniz Institute DSMZ-German Collection of Microorganisms and Cell Cultures, 38124 Braunschweig, Germany*

Complete contact information is available at:

https://doi.org/10.1021/acs.jnatprod.1c01051
J. Nat. Prod. 2022, 85, 530−539

https://pubs.acs.org/10.1021/acs.jnatprod.1c01051

Notes

The authors declare no competing financial interest.

■ ACKNOWLEDGMENTS

We like to thank Dr. D. Wistuba and her team (Mass Spectrometry Department, Institute for Organic Chemistry, University of Tübingen, Germany) for HR-MS measurements. Thanks are also due to L. Niwinski (Research Center Borstel, Leibniz Lung Center Borstel, Germany), to A. Heyne (Pharmaceutical Institute, University of Tübingen, Germany), and to Leo Endres (Institute for Microbiology and Infection Medicine, University of Tübingen) for performing the antitubercular assays, for supporting the compound isolation process, and for validating the T7 translation assay, respectively. We gratefully acknowledge the funding received from the BMBF German−Indonesian cooperation project NAbaUnAk (16GW0124K) and the Baden-Württemberg-Stiftung (BWST_WSF-035). I.H. is grateful for the RISET-Pro scholarship program from the Indonesian Ministry for Research and Technology (World Bank Loan No. 8245-ID). N.A. is thankful for his Ph.D. scholarship (grant PKZ 91609054), generously provided by the German Academic Exchange Service (DAAD). H.B.-O. and S.P. acknowledge funding by the German Center for Infection Research (DZIF, TTU 09.818), and A.B. and T.W. support by the BMBF (Gram-NEG design). The authors H.G. and H.B.-O. gratefully acknowledge financial support from the German Research Foundation (DFG), TRR261, project ID 398967434.

■ DEDICATION

Dedicated to Dr. William H. Gerwick, University of California at San Diego, for his pioneering work on bioactive natural products.

■ REFERENCES

(1) Handayani, I.; Saad, H.; Ratnakomala, S.; Lisdiyanti, P.; Kusharyoto, W.; Krause, J.; Kulik, A.; Wohlleben, W.; Aziz, S.; Gross, H.; Gavriilidou, A.; Ziemert, N.; Mast, Y. *Mar. Drugs* **2021**, *19*, 316.

(2) (a) Flynn, E. H.; Hinman, J. W.; Caron, E. L.; Woolf, D. O., Jr. *J. Am. Chem. Soc. USA* **1953**, *75*, 5867−6871. (b) Stevens, C. L.; Nagarajan, K.; Haskell, T. H. *J. Org. Chem.* **1962**, *2*, 2991−3005. (c) Evans, J. R.; Weare, G. *J. Antibiot.* **1977**, *30*, 604−606. (d) Shiomi, K.; Haneda, K.; Tomoda, H.; Iwai, Y.; Omura, S. *J. Antibiot.* **1994**, *47*, 782−786.

(3) (a) Carrasco, L.; Vázquez, D. *Med. Res. Rev.* **1984**, *4*, 471−512. (b) Shammas, C.; Donarski, J. A.; Ramesh, V. *Magn. Reson. Chem.* **2007**, *45*, 133−141. (c) Serrano, C. M.; Reddy, H. R. K.; Eiler, D.; Koch, M.; Tresco, B. I. C.; Barrows, L. R.; VanderLinden, R. T.; Testa, C. A.; Sebahar, P. R.; Looper, R. E. *Angew. Chem., Int. Ed.* **2020**, *59*, 11330−11333. (d) Nelli, M. R.; Heitmeier, K. N.; Looper, R. E. *Acc. Chem. Res.* **2021**, *54*, 2798−2811.

(4) Zhang, G.; Zhang, H.; Li, S.; Xiao, J.; Zhang, G.; Zhu, Y.; Niu, S.; Ju, J.; Zhang, C. *Appl. Environ. Microbiol.* **2012**, *87*, 2393−2401.

(5) Handayani, I.; Ratnakomala, S.; Lisdiyanti, P.; Fahrurrozi, F.; Kusharyoto, W.; Alanjary, M.; Ort-Winklbauer, R.; Kulik, A.; Wohlleben, W.; Mast, Y. *Microbiol. Resour. Announc.* **2018**, *7*, e01317−18.

(6) Krause, J.; Handayani, I.; Blin, K.; Kulik, A.; Mast, Y. *Front. Microbiol.* **2020**, *11*, 225.

(7) (a) Toriya, M.; Yaginuma, S.; Murofushi, S.; Ogawa, K.; Muto, N.; Hayashi, M.; Matsumoto, K. *J. Antibiot.* **1993**, *46*, 196−200. (b) Anttila, J.; Heinonen, P.; Nenonen, T.; Pino, A.; Iwai, H.; Kauppi, E.; Soliymani, R.; Baumann, M.; Saksi, J.; Suni, N.; Haltia, T. *Biochim. Biophys. Acta Bioenergetics* **2011**, *1807*, 311−318. (c) Nguyen, H. T.; Pham, V. T. T.; Nguyen, C. T.; Pokhrel, A. R.; Kim, T.-S.; Kim, D.; Na, K.; Yamaguchi, T.; Sohng, J. K. *Appl. Microbiol. Biotechnol.* **2020**, *104*, 713−724.

(8) (a) Bu, Y.-Y.; Yamazaki, H.; Ukai, K.; Namikoshi, M. *Mar. Drugs* **2014**, *12*, 6102−6112. (b) Aksoy, S. C.; Uzel, A.; Bedir, E. *J. Antibiot.* **2016**, *69*, 51−56. (c) Xu, C.-D.; Zhang, H.-J.; Ma, Z.-J. *J. Nat. Prod.* **2019**, *82*, 2509−2516. (d) Kate, A. S.; George, S. D.; Sonawane, S.; Periyasamy, G. Patent, WO 2013/144894, 2013. . (e) Tomoda, H.; Koyama, N.; Kanamoto, A.; Hashimoto, J.; Kozone, I. Patent, WO 2019/044941, 2019.

(9) Yun, M.-K.; Wu, Y.; Li, Z.; Zhao, Y.; Waddell, M. B.; Ferreira, A. M.; Lee, R. E.; Bashford, D.; White, S. W. *Science* **2012**, *335*, 1110−1114.

(10) (a) Guo, H.; Schmidt, A.; Stephan, P.; Raguz, L.; Braga, D.; Kaiser, M.; Dahse, H.-M.; Weigel, C.; Lackner, G.; Beemelmanns, C. *ChemBioChem.* **2018**, *19*, 2307−2311. (b) Moschny, J.; Lorenzen, W.; Hilfer, A.; Eckenstaler, R.; Jahns, S.; Enke, H.; Enke, D.; Schneider, P.; Benndorf, R. A.; Niedermeyer, T. H. J. *J. Nat. Prod.* **2020**, *83* (83), 1960−1970.

(11) (a) Thiericke, R.; Rohr, J. *Nat. Prod. Rep.* **1993**, *10*, 265−289. (b) Kirschning, A.; Taft, F.; Knobloch, T. *Org. Biomol. Chem.* **2007**, *5*, 3245−3259.

(12) (a) Weigert, F. J.; Roberts, J. D. *J. Am. Chem. Soc. USA* **1971**, *93*, 2361−2369. (b) Pretsch, E.; Bühlmann, P.; Badertscher, M. *Spektroskopische Daten zur Strukturaufklärung organischer Verbindungen*; Springer Spektrum Press: Berlin, 2019. (c) Berger, S.; Braun, S.; Kalinowski, H.-O. *NMR-Spektroskopie von Nichtmetallen, Band 4, ^{19}F-NMR-Spektroskopie*; Georg Thieme Press: Stuttgart, 1994.

(13) Arendrup, M. C.; Meletiadis, J.; Mouton, J. W.; Lagrou, K.; Hamal, P.; Guinea, J.; Subcommittee on Antifungal Susceptibility Testing (AFST) of the ESCMID European Committee for Antimicrobial Susceptibility Testing (EUCAST). *Method for the determination of broth dilution minimum inhibitory concentrations of antifungal agents for yeasts*. EUCAST Definitive Document E.DEF 7.3.2; April 2020. Accessed under https://www.eucast.org/astoffungi/methodsinantifungalsusceptibilitytesting/susceptibility_testing_of_yeasts/.

(14) Patel, J. B.; Cockerill, F. R.; Bradford, P. A.; Eliopoulos, G. M.; Hindler, J. A.; Jenkins, S. G.; Lewis, J. S.; Limbago, B.; Miller, L. A.; Nicolau, D. P.; Powell, M.; Swenson, J. M.; Turnidge, J. D.; Weinstein, M. P.; Zimmer, B. L. *Methods for Dilution Antimicrobial Susceptibility Tests for Bacteria that Grow Aerobically. Approved Standard*, Vol. 35, 10th ed.; Clinical and Laboratory Standards Institute, USA, 2015.

(15) Zelmer, A.; Carroll, P.; Andreu, N.; Hagens, K.; Mahlo, J.; Redinger, N.; Robertson, B. D.; Wiles, S.; Ward, T. H.; Parish, T.; Ripoll, J.; Bancroft, G. J.; Schaible, U. *J. Antimicrob. Chemother.* **2012**, *67*, 1948−1960.

(16) Reiling, N.; Homolka, S.; Walter, K.; Brandenburg, J.; Niwinski, L.; Ernst, M.; Herzmann, C.; Lange, C.; Diel, R.; Ehlers, S.; Niemann, S. *mBio* **2013**, *4*, e00250−13.

(17) Jumde, R. P.; Guardigni, M.; Gierse, R. M.; Alhayek, A.; Zhu, D.; Hamid, Z.; Johannsen, S.; Elgaher, W. A. M.; Neusens, P. J.; Nehls, C.; Haupenthal, J.; Reiling, N.; Hirsch, K. H. H. *Chem. Sci.* **2021**, *12*, 7775−7785.

(18) Franzblau, S. G.; DeGroote, M. A.; Cho, S. H.; Andries, K.; Nuermberger, E.; Orme, I. M.; Mdluli, K.; Angulo-Barturen, I.; Dick, T.; Dartois, V.; Lenaerts, A. J. *Tuberculosis* **2012**, *92*, 453−488.

(19) Wade, H. E.; Robinson, H. K. *Biochem. J.* **1966**, *101*, 467−79.

(20) Zubay, G. *Annu. Rev. Genetics* **1973**, *7*, 267−287.

Reprinted (adapted) with permission from

Aryal N, Chen J, K. Bhattarai, Hennrich O, Handayani I, Kramer M, Straetener J, Wommer T, Berscheid A, Peter S, Reiling N, Brötz-Oesterhelt H, Geibel C, Lämmerhofer M, Mast Y, Gross H. High Plasticity of the Amicetin Biosynthetic Pathway in *Streptomyces* sp. SHP 22-7 Led to the Discovery of Streptcytosine P and Cytosaminomycins F and G and Facilitated the Production of 12F-Plicacetin. *J Nat Prod.* 2022, 85::530-539. doi:10.1021/acs.jnatprod.1c01051.

9.3. Publication 3

AMERICAN SOCIETY FOR MICROBIOLOGY | Microbiology Resource Announcements

GENOME SEQUENCES

Genome Sequences of Two Putative Streptogramin Producers, *Streptomyces* sp. Strains TÜ 2975 and TÜ 3180, from the Tübingen Strain Collection

Oliver Hennrich,[a] Franziska Handel,[a,b] Regina Ort-Winklbauer,[a] Yvonne Mast[a,b,c,d]

[a]Department of Microbiology/Biotechnology, Interfaculty Institute of Microbiology and Infection Medicine, Faculty of Science, Eberhard Karls University of Tübingen, Tübingen, Germany

[b]German Center for Infection Research (DZIF), Partner Site Tübingen, Tübingen, Germany

[c]Department of Bioresources for Bioeconomy and Health Research, Leibniz Institute DSMZ–German Culture Collection for Microorganisms and Cell Cultures, Braunschweig, Germany

[d]Institute for Microbiology, Technical University of Braunschweig, Braunschweig, Germany

ABSTRACT *Streptomyces* sp. TÜ 2975 and TÜ 3180 are two strains from the Tübingen *Actinomycetes* strain collection. Here, we present the draft genome sequences of TÜ 2975 and TÜ 3180, with sizes of 7.62 Mb and 8.63 Mb, respectively.

Streptogramin antibiotics such as pristinamycin and griseoviridin/viridogrisein are valuable drugs used in human medicine and agriculture which act as protein synthesis inhibitors by binding to the 50S subunit of the bacterial ribosome (1). In the context of screening strains from the Tübingen *Actinomycetes* strain collection (https://uni-tuebingen.de/fakultaeten/mathematisch-naturwissenschaftliche-fakultaet/fachbereiche/interfakultaere-einrichtungen/imit/technologien/natresource/) for antibiotics that target bacterial protein synthesis, *Streptomyces* sp. strain TÜ 2975 and *Streptomyces* sp. strain TÜ 3180 were identified. Here, we present the annotated genome sequences of both strains and report on their genetic potential to produce streptogramin antibiotics.

For DNA isolation, TÜ 2975 and TÜ 3180 cells were cultivated for 2 days in 50 ml of R5 medium (2) at 30°C. For cell lysis, lysozyme (10 mg/ml; Serva) and achromopeptidase (5 mg/ml; Sigma) were added as reported previously (3). Genomic DNA was extracted and purified using the Genomic-tip 100/G kit from Qiagen (catalog number 10243). The genomic DNA isolation procedure was carried out following the standard protocol provided by the manufacturer. For genome sequencing, a single SMRTbell library was prepared according to the Pacific Biosciences sample preparation protocol (https://www.pacb.com/wp-content/uploads/2015/09/User-Bulletin-Guidelines-for-Preparing-20-kb-SMRTbell-Templates.pdf), and sequencing was performed with the PacBio RS II platform. The genomes were assembled with Hierarchical Genome Assembly Process (HGAP) v3.0 (4). HGAP data processing consisted of PreAssembler v1 for filtering, PreAssembler v2 and AssembleUnitig v1 for assembly (4), BLASR v1 (5) for mapping, and Quiver v1 (4) for consensus polishing using only unambiguously mapped reads. HGAP3 settings were kept at their defaults, except for the genome size estimate parameter, which was set to 8.0 Mbp. For TÜ 2975, 136,147 filtered reads with an N_{50} value of 10,822 bp were assembled into one contig, yielding a 7,623,788-bp draft sequence with a coverage depth of 87× and an average G+C content of 71.04%. The average read length was 7,111 bp. Genome annotation was performed with the NCBI Prokaryotic Genome Annotation Pipeline (PGAP) software tool v4.6 (6), yielding 6,950 coding sequences (CDSs), 80 tRNAs, and 18 rRNAs. For TÜ 3180, 146,177 filtered reads with an N_{50} value of 13,352 bp were assembled into two contigs, yielding an

Citation Hennrich O, Handel F, Ort-Winklbauer R, Mast Y. 2020. Genome sequences of two putative streptogramin producers, *Streptomyces* sp. strains TÜ 2975 and TÜ 3180, from the Tübingen strain collection. Microbiol Resour Announc 9:e01582-19. https://doi.org/10.1128/MRA.01582-19.

Editor Vincent Bruno, University of Maryland School of Medicine

Address correspondence to Yvonne Mast, yvonne.mast@dsmz.de.

Received 13 January 2020
Accepted 27 April 2020
Published 21 May 2020

8,634,962-bp draft sequence with a coverage depth of 95× and an average G+C content of 72.97%. The average read length was 9,812 bp. Genome annotation was performed with PGAP v4.6 (6), yielding 7,470 CDSs, 97 tRNAs, and 18 rRNAs.

Using 16S marker genes, EzTaxon v2.1 (7) identified TÜ 2975 as most similar to *Streptomyces xantholiticus* NBRC13354^T, with 99.86% similarity (8, 9). TÜ 3180 showed 99.38% similarity to *Streptomyces carpiensis* NBRC14214^T (10). The Type (Strain) Genome Server (TYGS) v1.0 (11) was applied to conduct phylogenomic analyses based on full-length genome sequences. It was found that TÜ 2975 is related to the type strain *Streptomyces lunaelactis* DSM 42149 (12), and TÜ 3180 is similar to the type strain *Streptomyces ghanaensis* ATCC 14672 (13, 14), with digital DNA-DNA hybridization (dDDH) values (formula d_4) of 26% and 44%, respectively. For all software analyses, default settings were used.

In order to identify biosynthetic gene clusters (BGCs), the TÜ 2975 and TÜ 3180 genome sequences were analyzed with antiSMASH v4.0 (15). For TÜ 2975, antiSMASH predicted 20 BGCs, and 1 cluster shows >60% similarity to a known gene cluster encoding pristinamycin (16). For TÜ 3180, antiSMASH predicted 27 BGCs, and 1 cluster shows >70% similarity to a known cluster encoding griseoviridin/viridogrisein (17). Thus, TÜ 2975 and TÜ 3180 host the genetic potential to synthesize the streptogramin antibiotics pristinamycin and griseoviridin/viridogrisein, respectively.

Data availability. This whole-genome shotgun project has been deposited at GenBank under the accession numbers CP047140 (TÜ 2975) and WOXS00000000 (TÜ 3180). The raw sequencing data are available under SRA accession numbers SRX7351729 (TÜ 2975) and SRX7351340 (TÜ 3180).

ACKNOWLEDGMENTS

We gratefully acknowledge funding received from the German Center for Infection Research (DZIF), project TTU 09.819, and the Baden-Württemberg Stiftung (BWST_WSF-035).

REFERENCES

1. Mast Y, Wohlleben W. 2014. Streptogramins—two are better than one! Int J Med Microbiol 304:44–50. https://doi.org/10.1016/j.ijmm.2013.08.008.
2. Kieser T, Bibb MJ, Buttner MJ, Chater KF, Hopwood DA. 1985. Practical *Streptomyces* genetics. John Innes Foundation, Norwich, England.
3. Jiao J-Y, Carro L, Liu L, Gao X-Y, Zhang X-T, Hozzein WN, Lapidus A, Huntemann M, Reddy TBK, Varghese N, Hadjithomas M, Ivanova NN, Göker M, Pillay M, Eisen JA, Woyke T, Klenk H-P, Kyrpides NC, Li W-J. 2017. Complete genome sequence of *Jiangella gansuensis* strain YIM 002^T (DSM 44835^T), the type species of the genus *Jiangella* and source of new antibiotic compounds. Stand Genomic Sci 12:21. https://doi.org/10.1186/s40793-017-0226-6.
4. Chin C-S, Alexander DH, Marks P, Klammer AA, Drake J, Heiner C, Clum A, Copeland A, Huddleston J, Eichler EE, Turner SW, Korlach J. 2013. Nonhybrid, finished microbial genome assemblies from long-read SMRT sequencing data. Nat Methods 10:563–569. https://doi.org/10.1038/nmeth.2474.
5. Chaisson MJ, Tesler G. 2012. Mapping single molecule sequencing reads using basic local alignment with successive refinement (BLASR): application and theory. BMC Bioinformatics 13:238. https://doi.org/10.1186/1471-2105-13-238.
6. Tatusova T, DiCuccio M, Badretdin A, Chetvernin V, Nawrocki EP, Zaslavsky L, Lomsadze A, Pruitt KD, Borodovsky M, Ostell J. 2016. NCBI Prokaryotic Genome Annotation Pipeline. Nucleic Acids Res 44:6614–6624. https://doi.org/10.1093/nar/gkw569.
7. Yoon S-H, Ha S-M, Kwon S, Lim J, Kim Y, Seo H, Chun J. 2017. Introducing EzBioCloud: a taxonomically united database of 16S rRNA gene sequences and whole-genome assemblies. Int J Syst Evol Microbiol 67:1613–1617. https://doi.org/10.1099/ijsem.0.001755.
8. Konev IE, Tsyganov VA. 1962. A new species in the yellow actinomycetes group, Actinomyces xantholiticus n. sp. Mikrobiologiia 31:1023–1028. (In Russian.)
9. Pridham TG. 1970. New names and new combinations in the order Actinomycetales Buchanan 1917. U.S. Department of Agriculture, Washington, DC.
10. Goodfellow M, Williams ST, Alderson G. 1986. Transfer of *Chainia* species to the genus *Streptomyces* with emended description of species. Syst Appl Microbiol 8:55–60. https://doi.org/10.1016/S0723-2020(86)80148-5.
11. Leibniz Institute DSMZ. Type (strain) genome server. https://tygs.dsmz.de/.
12. Maciejewska M, Pessi IS, Arguelles-Arias A, Noirfalise P, Luis G, Ongena M, Barton H, Carnol M, Rigali S. 2015. *Streptomyces lunaelactis* sp. nov., a novel ferroverdin A-producing *Streptomyces* species isolated from a moonmilk speleothem. Antonie Van Leeuwenhoek 107:519–531. https://doi.org/10.1007/s10482-014-0348-4.
13. Linder F, Wallhausser KH, Huber G. July 1972. Moenomycin and process for producing same. U.S. patent 3,674,866A.
14. Skerman VBD, McGowan V, Sneath PHA. 1980. Approved lists of bacterial names. Int J Syst Evol Microbiol 30:225–420. https://doi.org/10.1099/00207713-30-1-225.
15. Blin K, Wolf T, Chevrette MG, Lu X, Schwalen CJ, Kautsar SA, Suarez Duran HG, de Los Santos ELC, Kim HU, Nave M, Dickschat JS, Mitchell DA, Shelest E, Breitling R, Takano E, Lee SY, Weber T, Medema MH. 2017. antiSMASH 4.0—improvements in chemistry prediction and gene cluster boundary identification. Nucleic Acids Res 45:W36–W41. https://doi.org/10.1093/nar/gkx319.
16. Mast Y, Weber T, Gölz M, Ort-Winklbauer R, Gondran A, Wohlleben W, Schinko E. 2011. Characterization of the "pristinamycin supercluster" of *Streptomyces pristinaespiralis*. Microb Biotechnol 4:192–206. https://doi.org/10.1111/j.1751-7915.2010.00213.x.
17. Xie Y, Wang B, Liu J, Zhou J, Ma J, Huang H, Ju J. 2012. Identification of the biosynthetic gene cluster and regulatory cascade for the synergistic antibacterial antibiotics griseoviridin and viridogrisein in *Streptomyces griseoviridis*. Chembiochem 13:2745–2757. https://doi.org/10.1002/cbic.201200584.

The Article

Hennrich O, Handel F, Ort-Winklbauer R, Mast Y. Genome Sequences of Two Putative Streptogramin Producers, Streptomyces sp. Strains TÜ 2975 and TÜ 3180, from the Tübingen Strain Collection. Microbiol Resour Announc. Microbiol Resour Announc. 2020, 9::e01582-19. doi:10.1128/MRA.01582-19.

9.4. Publication 4

Applied Microbiology and Biotechnology (2020) 104:3433–3444
https://doi.org/10.1007/s00253-020-10447-9

APPLIED GENETICS AND MOLECULAR BIOTECHNOLOGY

Genetic engineering approaches for the fermentative production of phenylglycines

David Moosmann[1] · Vladislav Mokeev[1] · Andreas Kulik[1] · Natalie Osipenkov[1] · Susann Kocadinc[1] · Regina Ort-Winklbauer[1] · Franziska Handel[1] · Oliver Hennrich[1] · Jung-Won Youn[2] · Georg A. Sprenger[2] · Yvonne Mast[1,3,4,5]

Received: 16 November 2019 / Revised: 29 January 2020 / Accepted: 6 February 2020 / Published online: 20 February 2020

Abstract
L-phenylglycine (L-Phg) is a rare non-proteinogenic amino acid, which only occurs in some natural compounds, such as the streptogramin antibiotics pristinamycin I and virginiamycin S or the bicyclic peptide antibiotic dityromycin. Industrially, more interesting than L-Phg is the enantiomeric D-Phg as it plays an important role in the fine chemical industry, where it is used as a precursor for the production of semisynthetic β-lactam antibiotics. Based on the natural L-Phg operon from *Streptomyces pristinaespiralis* and the stereo-inverting aminotransferase gene *hpgAT* from *Pseudomonas putida*, an artificial D-Phg operon was constructed. The natural L-Phg operon, as well as the artificial D-Phg operon, was heterologously expressed in different actinomycetal host strains, which led to the successful production of Phg. By rational genetic engineering of the optimal producer strains *S. pristinaespiralis* and *Streptomyces lividans*, Phg production could be improved significantly. Here, we report on the development of a synthetic biology-derived D-Phg pathway and the optimization of fermentative Phg production in actinomycetes by genetic engineering approaches. Our data illustrate a promising alternative for the production of Phgs.

Keywords Synthetic biology · Genetic engineering · Non-proteinogenic amino acids · D-amino acids · Phenylglycine · Actinomycetes

Introduction

To date, more than 900 naturally occurring amino acids have been identified (Lu and Freeland 2006) of which the 20 proteinogenic L-amino acids only constitute 2%. The majority of the residual 98% of non-proteinogenic amino acids serve as building blocks for bioactive natural compounds (Walsh et al. 2013). Non-proteinogenic amino acids are becoming ever more important as tools for modern drug discovery and development. On the one hand, freestanding non-proteinogenic amino acids act as antimetabolites of common amino acids and are effective inhibitors for various metabolic targets. Besides that, non-proteinogenic amino acids serve as building blocks for numerous bioactive compounds and drugs. Especially D-amino acids are of particular importance for the production of pharmaceuticals and fine chemicals. They are utilized in drugs, drug intermediates, food additives, artificial sweeteners, deodorants, insecticides, or commodity chemicals (Barredo 2005; Global Industry Analysts Inc. 2016). Annually, several tons of D-amino acids are produced.

Electronic supplementary material The online version of this article (https://doi.org/10.1007/s00253-020-10447-9) contains supplementary material, which is available to authorized users.

✉ Yvonne Mast
yvonne.mast@dsmz.de

[1] Microbiology/Biotechnology, Interfaculty Institute of Microbiology and Infection Medicine, Faculty of Science, University of Tübingen, Auf der Morgenstelle 28, D-72076 Tübingen, Germany

[2] Institute of Microbiology, University Stuttgart, Allmandring 31, D-70569 Stuttgart, Germany

[3] German Center for Infection Research (DZIF), Partner Site Tübingen, Tübingen, Germany

[4] Department "Bioresources for Bioeconomy and Health Research", Leibniz Institute DSMZ-German Culture Collection for Microorganisms and Cell Cultures, 38124 Braunschweig, Germany

[5] Institute for Microbiology, Technical University of Braunschweig, 38106 Braunschweig, Germany

Due to an aging world population, there is a strong demand for dietary and pharmaceutical supplements, which in turn will increase the need for D-amino acids in the coming years (Global Industry Analysts Inc. 2016). One of the industrially relevant D-amino acids is D-phenylglycine (D-Phg), which is used as precursor for the production of various β-lactam antibiotics. D-Phg is a constituent of a number of semisynthetic penicillins (ampicillin, apalcillin (Boehringer Ingelheim), mezlocillin (Bayer), pivampicillin, LEO Pharma), etc.) and cephalosporins (cefalexin, cefradine, cefaclor, cefaloglycine, etc.) (Stevenazzi et al. 2014; Shiau et al. 2005; Schmid et al. 2001; Müller et al. 2013). Currently, D-Phg is produced in a scale > 5000 tons per year worldwide (Vedha-Peters et al. 2006). Until now, the amino acid is synthesized by classical or enzymatic resolution of a racemic mixture (Wegman et al. 2001). This production process is based on petrochemical feedstocks. The disadvantage of such a conventional method is that it includes many individual processing steps, which make the entire production process commercially less attractive. Besides that, chemical syntheses often need numerous chemicals and solvents, are energetically unfavorable, and/or produce a lot of waste substances. It would therefore be highly desirable to avail a more environmentally friendly fermentative route for the production of the unnatural amino acid D-Phg in future. With a fermentative production process, the substance of interest is produced by microorganisms obtained from renewable raw materials, such as glucose, whereby the end-products are characterized by a high chemo-, regio-, and stereo-selectivity. In terms of Phg, fermentative production was hampered by the fact that the amino acid is not accessible by any natural biosynthetic pathway from microbes or other organisms. In a previous approach, an artificial D-Phg production pathway has been designed in *E. coli* that applies three different enzymes from three different organisms (HmaS-hydroxymandelate synthase from *Amycolatopsis orientalis*, Hmo-hydroxymandelate oxidase from *Streptomyces coelicolor* and HpgAT–D-(4-hydroxy)phenylglycine aminotransferase from *Pseudomonas putida*), which led to the successful production of D-Phg (Müller et al. 2006). Only recently, the first natural Phg biosynthetic pathway has been reported for the antibiotic producer *Streptomyces pristinaespiralis* (Mast et al. 2011a; Osipenkov et al. 2018), which can now serve as the basis for the development of a fermentative D-Phg production route.

S. pristinaespiralis is the producer of the streptogramin antibiotic pristinamycin, which consists of the two chemically non-related substances pristinamycin I (PI) and pristinamycin II (PII). PI is synthesized by the nonribosomal peptide synthetases (NRPSs) SnbA, SnbC, and SnbDE, whereby the latter one incorporates L-Phg as the final amino acid into the growing PI peptide chain (Mast et al. 2011b; Mast and Wohlleben 2014). Within the pristinamycin biosynthetic gene region, the genes *pglA*, *pglB*, *pglC*, *pglD*, and *pglE* are organized in an operon-like structure (*lpg*) and together encode for L-Phg biosynthesis (Mast et al. 2011a, 2015, Osipenkov 2016). These genes are located downstream of the NRPS genes *snbC* and *snbDE* and are under control of the pathway-specific transcriptional activator PapR2 (Mast et al. 2015) (Fig. 1a).

L-Phg in *S. pristinaespiralis* is suggested to originate from the shikimate pathway. As a first metabolic step, phenylpyruvate is converted to phenylacetyl-CoA by the action of a pyruvate dehydrogenase–like complex PglB/C. Phenylacetyl-CoA is oxidized to benzoylformyl-CoA via the Phg dioxygenase PglA. The CoA residue from benzoylformyl-CoA is cleaved off by the thioesterase PglD, resulting in the formation of phenylglyoxylate. In a final reaction step, phenylglyoxylate is converted to L-Phg by the aminotransferase PglE (Mast et al. 2011b). As PglE uses L-phenylalanine as amino group donor for the transamination reaction, phenylpyruvate is formed as the α-keto acid product, which can re-enter Phg biosynthesis as a precursor (Osipenkov et al. 2018) (see Fig. 2).

L-Phg is a rare amino acid, which only occurs in a few natural products, such as the related streptogramin antibiotic virginiamycin S from *Streptomyces virginiae* (Ningsih et al. 2011) or the bicyclic peptide antibiotics dityromycin, produced by *Streptomyces* sp. strain AM-2504; GE82832 of *Streptosporangium cinnabarinum* strain GE82832, or MBJ-0086 and MBJ-0087, isolated from *Sphaerisporangium* sp. 3226 (Al Toma et al. 2015). There is also an industrial demand for L-Phg since it is used as a component of the synthetic cyclic hexadepsipeptide pasireotide (Signifor®, Novartis), which is a somatostatin analogue used for the treatment of Cushing's disease. L-Phg is also used for the synthesis of the antitumor compound taxol (Croteau et al. 2006; Denis et al. 1991; Wang et al. 1994) and the synthesis of DAPT (N-[N-(3,5-difluorophenacetyl)-L-alanyl]-S-*phenylglycine* t-butyl ester), which acts as an inhibitor of the human γ-*secretase, a target used for the treatment of Alzheimer's disease and different types of cancer* (Kan et al. 2004). Besides its application for diverse pharmaceuticals, L-Phg, as well as the enantiomeric D-Phg, can be used for the synthesis of the artificial non-nutritive sweetener aspartame (Ebeling 1998; Janusz 1986; Schutt 1981).

In this study, we describe the development of a synthetic biology-derived D-Phg pathway. Furthermore, we report on genetic engineering approaches in order to optimize Phg production in actinomycetal expression strains.

Material and methods

Bacterial strains, plasmids, and cultivation conditions

Bacterial strains, plasmids, cosmids, and primers used in this study are listed in Table S1. An overview of genes used for this study is given in Table 1. For routine cloning strategies, *Escherichia coli* XL1-Blue was used. *E. coli* strains were grown

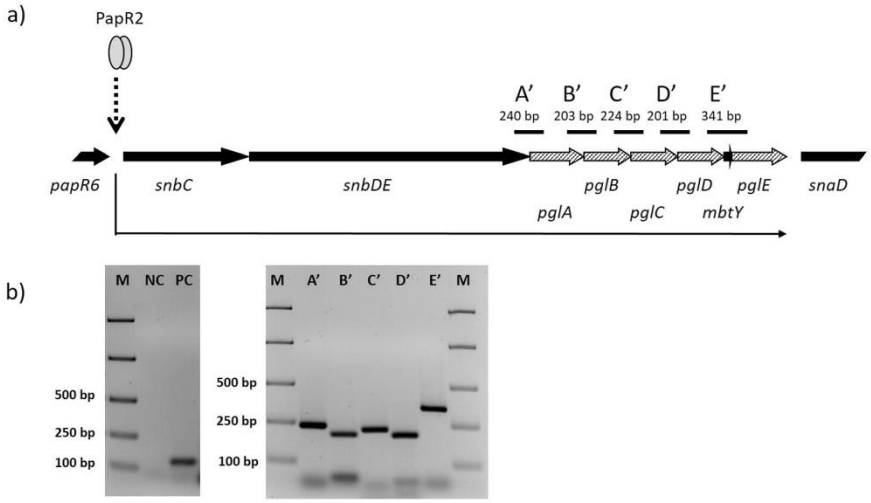

Fig. 1 Schematic presentation of the *lpg* operon. L-Phg biosynthesis genes are shown as dashed arrows and adjacent genes as black arrows. Predicted RT-PCR amplificates (A′–E′) are shown as black lines. Transcriptional activation by PapR2 (gray ellipses) is indicated as broken arrow. Thin black arrow depicts co-transcription of genes (**a**). Transcriptional analysis of the *lpg* operon in *S. pristinaespiralis*. Total RNA was harvested after 24 h. Left figure shows RT-PCR results with *hrdB*-specific primers and total RNA (negative control, NC) and cDNA (positive control, PC) as template, respectively. Right figure shows RT-PCR results from amplification of *pgl* gene overlapping regions (amplificate A′, B′, C′, D′, and E′, respectively). A total of 5 µl of the 1 kb ladder from Fermentas was used as an internal standard (M) (**b**)

in Luria-Bertani (LB) medium at 37 °C (Sambrook et al. 1989) supplemented with kanamycin or apramycin (50 or 100 µg/ml, respectively) when appropriate. For cultivation and harvesting of genomic DNA, *Streptomyces* strains were grown in 100 ml of S-medium (Kieser et al. 2000) in 500-ml Erlenmeyer flasks (with steel springs) on an orbital shaker (180 rpm) at 28 °C. For pristinamycin production analyses, cells were grown and treated as reported previously (Mast et al. 2011a).

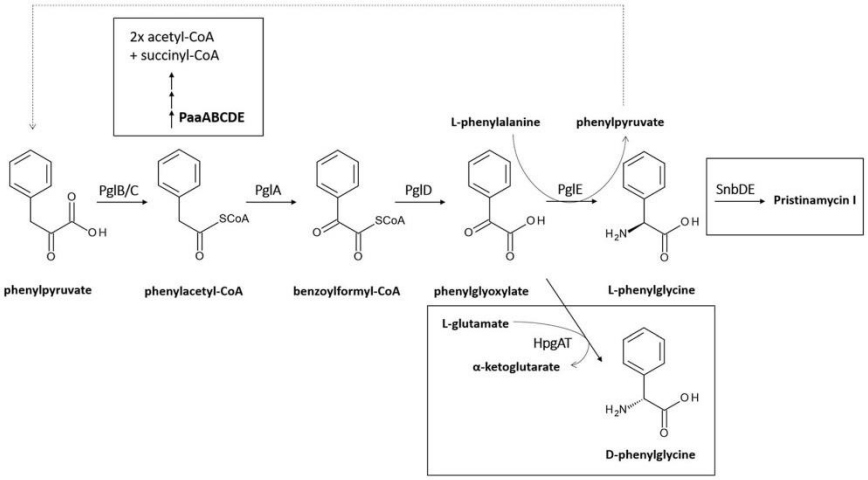

Fig. 2 Schematic presentation of the natural L-Phg biosynthetic pathway from *S. pristinaespiralis*. Biochemical reactions targeted by genetic engineering, such as the HpgAT catalyzed reaction resulting in D-Phg production, PaaABCDE-catalyzed Phenylacetyl-CoA degradation, and SnbDE-catalyzed incorporation of L-Phg into PI, are highlighted in black boxes

Table 1 List of genes mentioned in this study with encoded functions

Gene	Origin	Function
pglA	*S. pristinaespiralis*	Phenylglycine dehydrogenase
pglB	*S. pristinaespiralis*	Pyruvate dehydrogenase α-subunit
pglC	*S. pristinaespiralis*	Pyruvate dehydrogenase β-subunit
pglD	*S. pristinaespiralis*	Thioesterase
pglE	*S. pristinaespiralis*	L-phenylglycine aminotransferase
hpgAT	*P. putida*	D-phenylglycine aminotransferase
snbDE	*S. pristinaespiralis*	Pristinamycin I–specific nonribosomal peptide synthetase
papR5	*S. pristinaespiralis*	TetR-like repressor of pristinamycin biosynthesis
paaABCDE (*paa* operon)	*S. pristinaespiralis*, *S. lividans*	phenylacetyl-CoA epoxidase multicomponent enzyme system

Transcriptional analysis by RT-PCR experiments

S. pristinaespiralis Pr11 wild type was grown in pristinamycin inoculum and production medium as reported previously (Mast et al. 2011a). Samples were harvested after 24 h. RNA isolation and RT-PCR procedure were carried out as described before (Mast et al. 2015). For RT-PCR reactions, primers RTpglfw/rv were used that anneal to overlapping regions of the *pgl* gene sequences. As an internal control, RT-PCR was performed with primers targeting the major sigma factor transcript *hrdB*. To exclude DNA contamination, negative controls were carried out by using total RNA as a template for each RT-PCR reaction.

Construction of Phg expression plasmids

lpg expression construct

For cloning of the native *lpg* operon from *S. pristinaespiralis*, the pYJM1 cosmid DNA, harboring the *pglA-E* genes, was used as a template in a PCR approach with the primers lpgfw/rv and KAPAHiFi™ polymerase (Peqlab). The lpgfw/rv primer pair was designed in a way that a *Nde*I (5′ end) and *Hin*dIII (3′ end) restriction sequence is added to the *lpg* amplificate. The ~ 6-kb *lpg* fragment was subcloned into the linear PCR cloning vector pJET1.2/blunt (Fermentas), which resulted in the construct pJET/lpg. *lpg* was isolated from pJET/lpg as a *Nde*I/*Hin*dIII fragment and was cloned into the *Nde*I/*Hin*dIII-restriction site of the expression vector pRM4 under control of the constitutive erythromycin resistance gene promoter, P_{ermE}, resulting in the *lpg* expression construct pYM/lpg (Fig. S1).

dpg expression construct

On the basis of the natural *lpg* operon from *S. pristinaespiralis,* an artificial *dpg* operon was constructed. For this purpose, the *Nde*I/*Hin*dIII *lpg* fragment from pJET/lpg (see above) was subcloned into the *Nde*I/*Hin*dIII-restricted *E. coli* vector pK18 (Pridmore 1987), resulting in construct pK18/lpg. For cloning of the *dpg* operon, a recombinant PCR approach was conducted in order to fuse the *pglD* gene from *S. pristinaespiralis* to the *hpgAT* gene of *P. putida*. To amplify the *pglD* fragment, the pYJM1 cosmid DNA was used as a template together with primers pglDfus1/2 for PCR amplification, resulting in fragment *pglD′* with a size of ~ 800 bp. The *hpgAT* gene (accession number AX467211) from *P. putida* was synthesized de novo (Mr. Gene GmbH, Regensburg) and used as a template for PCR amplification with primers hpgATfus1/2, which resulted in the ~ 1.4-kb fragment *hpgAT′*. Primers pglDfus2 and hpgATfus1 had 20-bp complementary 5′-3′ sequences, which allowed annealing of the fragments in a recombinant PCR approach. *pglD′* and *hpgAT′* were used as templates for recombinant PCR with primers pglDfus1/hpgATfus2, resulting in the fusion product *pglD-hpgAT′* (~ 2.2 kb). *pglD-hpgAT′* was subcloned in the PCR cloning plasmid pDrive (Qiagen), which resulted in the construct pDrive/*pglD-hpgAT′*. The correctness of the gene sequence was verified by the primer walking method (GATC Biotech, Konstanz). The plasmid pK18/lpg was cleaved with *SfiI/HindIII* and the ~ 6.3-kb pK18/*pglA-pglC* fragment was ligated to the *pglD-hpgAT′* fragment, which was excised with the same restriction enzymes from pDrive/*pglD-hpgAT′*, resulting in the construct pK18/dpg. The artificial *dpg* operon was isolated from pK18/dpg as a *Nde*I/*Hin*dIII fragment and was subcloned into the *Nde*I/*Hin*dIII-restricted pRM4 plasmid, resulting in the *dpg* expression construct pYM/dpg (Fig. S1).

Expression constructs with thiostrepton resistance cassettes

In order to select for Phg operon containing transformants of apramycin-resistant mutants (*MpglE* (Mast et al. 2011a) and *papR5::apra (*Mast et al. 2015)), expression constructs were designed, which harbor a thiostrepton resistance cassette ($thio^R$). For this purpose, the $thio^R$ cassette was isolated as a *Xba*I-restricted fragment from pDrive-thio and was cloned into the *Xba*I restriction site of pRM4, pYM/lpg, and pYM/

dpg, resulting in the expression constructs pYMT, pYMT/lpg, and pYMT/dpg, respectively (Fig. S1).

Transformation of strains and culture conditions

The targeting plasmids pYM/*lpg* and pYM/*dpg* were each transferred to *S. pristinaespiralis* Pr11, *S. lividans* T7, *S. albus*, *A. balhimycina*, and *R. jostii* RHA1 by protoplast transformation (Kieser et al. 2000), resulting in the expression strains *SPlpg-OE*, *SPdpg-OE*, *SLlpg-OE*, *SLdpg-OE*, *SAlpg-OE*, *SAdpg-OE*, *ABlpg-OE*, *ABdpg-OE*, *RJlpg-OE*, and *RJdpg-OE*, respectively. Strains with the empty pRM4 vector served as control (*SP-C*, *SL-C*, *SA-C*, *AB-C*, and *RJ-C*, respectively). All strains were inoculated from R5 agar into three independent replicates of 100 ml of preculture medium (R5 or pristinamycin production medium HT7T). R5 contained (per liter) the following: sucrose 103 g; yeast extract, 5 g; glucose, 10 g; TES ([N-tris(hydroxymethyl)methyl-2-aminoethanesulfonic acid], 5.75 g; K_2SO_4, 0.25 g; $MgCl_2$, 10.12 g; casamino acids, 0.1 g; L-proline, 3 g; KH_2PO_4, 0.05 g; $CaCl_2x2H_2O$, 2.94 g, 2 ml of trace elements stock solution; pH 7.4 and HT7T contained (per liter): white dextrin, 10 g; NZ amine-A, 2 g; LabLemco beef powder, 1 g; yeast extract, 1 g; 1 ml of trace elements stock solution; pH 7.4 (Kieser et al. 2000; Folcher et al. 2001). Strains were cultivated in 500-ml Erlenmeyer flasks (with steel springs) on an orbital shaker (180 rpm) at 30 °C. After 72 h, 7 ml of preculture were inoculated into 100 ml of production medium (R5 or HT7T, respectively) and the main culture was grown for 24, 30, 48, 72, or 96 h, respectively. Ten milliliters of sample was harvested and centrifuged at 5000 rpm for 10 min. One milliliter of culture filtrate was used for HPLC-MS/MS analysis.

Construction of mutants and mutant-derived expression strains

Construction and verification of the mutants *MsnbDE::thio*, *SPpaa::thio*, and *SLpaa::thio*, as well as construction of all mutant-derived expression strains, is described in Supplementary File.

HPLC-MS/MS analysis of phenylglycine

HPLC-MS/MS analysis has been performed as described previously (Osipenkov et al. 2018). Tandem MS (MS/MS) was carried out in the positive mode for phenylglycine (Phg) (precursor ion m/z 152) with the corresponding target mass. Phg amount was measured in counts corresponding to the peak height. Phg concentration was calculated by reference to a standard curve using suitable concentrations of pure Phg (Fluka). Data are presented as the averages of the results from three independent biological replicates.

Results

Phg biosynthetic genes are co-transcribed as a multi-gene operon

As described above, the L-Phg biosynthetic genes (*pglA-E*) are organized in an operon-like structure (*lpg*) within the pristinamycin biosynthetic gene region (Fig. 1a) (Mast et al. 2011b). *lpg* is localized between the genes *snbDE* and *snaD*, which encode PI- and PII-specific peptide synthetases, respectively (Mast et al. 2011a). The gene *mbtY* is embedded in the *lpg* region and encodes a MbtH-like protein, which is suggested to interact with SnbDE but is not directly involved in Phg biosynthesis (Mast et al. 2011b). In order to determine if the *pgl* genes are co-transcribed and to ensure a successful transcription of the *lpg* operon in the heterologous expression studies later on, RT-PCR experiments have been conducted with RNA isolated from the *S. pristinaespiralis* wild type and primers that anneal to overlapping regions of the *pgl* genes (Fig. 1a). With these experiments, amplicons were obtained, which are specific for the overlapping regions between *snbDE* and *pglA* (A′), *pglA* and *pglB* (B′), *pglB* and *pglC* (C′), *pglC* and *pglD* (D′), and *pglD* and *pglE* (E′), respectively, revealing that all *pgl* genes are transcribed as one polycistronic mRNA and form an operon together with the Phg-specific NRPS gene *snbDE* (Fig. 1b). Since *snbDE* is located directly downstream of *snbC* with overlapping stop and start codons, respectively, and *snbC* has been shown to be regulated by PapR2, it can be estimated that *snbC*, *snbDE*, and the *pgl* genes together form a multi-gene operon, which is under regulatory control of the pristinamycin pathway-specific activator PapR2 (Fig. 1a).

Expression of L- and D-Phg operons in suitable host strains

To obtain constructs for the fermentative production of L-Phg, the native ~ 6-kb *lpg* operon from *S. pristinaespiralis* was cloned into the integrative vector pRM4 under control of the constitutive *ermE** promoter, resulting in the expression construct pYM/lpg (Fig. S1). For production of the D-Phg enantiomer, an artificial D-Phg operon (*dpg*) was generated on the basis of the native *lpg* operon from *S. pristinaespiralis:* In a synthetic biology approach, the gene *pglE,* encoding the L-Phg aminotransferase in *S. pristinaespiralis,* was exchanged by the gene *hpgAT* from *P. putida*, which codes for a stereospecific D-Phg aminotransferase. This D-Phg aminotransferase is the only currently known L to D stereo-inverting aminotransferase (Walton et al. 2018). A recombinant PCR yielded the artificial *dpg* operon, which was cloned into pRM4, resulting in the expression construct pYM/dpg (Fig. S1). Both plasmids, pYM/lpg and pYM/dpg, were each transferred into different actinomycetes (*S. pristinaespiralis* Pr11, *Streptomyces lividans* T7, *Streptomyces albus* J1074, *Amycolatopsis balhimycina*, and *Rhodococcus jostii* RHA1) as

homologous or heterologous host strains, respectively (–OE strains; Supplementary File). Strains with the empty pRM4 vector served as control (–C strains; Supplementary File). *S. pristinaespiralis* was used as expression strain because it is the natural producer of L-Phg, which is a building block for the biosynthesis of the streptogramin antibiotic PI. *A. balhimycina* was tested since it produces the structurally related non-proteinogenic amino acids hydroxy- and dihydroxyphenylglycine, which are components of the glycopeptide antibiotic balhimycin (Pfeifer et al. 2001). *S. lividans* and *S. albus* are established heterologous expression strains (Nah et al. 2017) and *R. jostii* has a well-studied, intensive aromatic compound metabolism (Yam et al. 2011). All strains were grown in R5 medium in triplicate. After 30-h, supernatant samples were harvested and Phg amount (given in μg/L) was determined by HPLC-MS/MS analysis. Here, it should be noted that the applied method does not allow to distinguish between different Phg enantiomers. In order to determine enantiomerism of the produced Phg compounds, chiral HPLC analyses have been performed with various expression samples. However, Phg concentrations were too low to be detected (data not shown). HPLC-MS/MS analysis revealed that Phg amount was largest in samples from *S. lividans* (SL) and *S. pristinaespiralis* (SP) expression strains (> 1 μg/L), whereas only minor Phg amounts were measured for samples of *S. albus* (SA), *A. balhimycina* (AB), and *R. jostii* (RJ) expression strains (< 0.75 μg/L) (Fig. 3). No, or only trace amounts of Phg were detected in the respective pRM4 control samples (–C strains, data not shown). Interestingly, all D-Phg expression samples contained higher amounts of Phg than the respective L-Phg expression samples (Fig. 3). Altogether, from all tested strains, *S. lividans* and *S. pristinaespiralis* turned out to be the optimal hosts for fermentative Phg production.

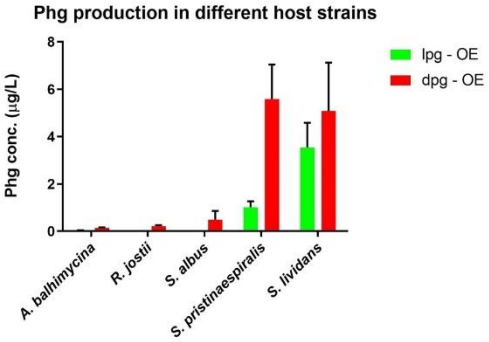

Fig. 3 Phg production of the different expression strains *A. balhimycina* (*ABlpg-OE*, *ABdpg-OE*), *R. jostii* (*RJlpg-OE*, *RJdpg-OE*), *S. albus* (*SAlpg-OE*, *SAdpg-OE*), *S. pristinaespiralis* (*SPlpg-OE*, *SPdpg-OE*), and *S. lividans* (*SLlpg-OE*, *SLdpg-OE*) grown in R5 medium. Phg production was measured at 30 h. Phg concentration is given in micrograms per liter. Data were obtained from three independent biological replicates

Optimal production media for Phg production

In order to define the best Phg production conditions, the optimal producer strains *S. pristinaespiralis* (*SPlpg-OE*, *SPdpg-OE*) and *S. lividans* (*SLlpg-OE*, *SLdpg-OE*) were grown in two different culture media—the complex medium R5 and the pristinamycin production medium HT7T. Samples were taken at different time points (24, 48, 72, and 96 h) and Phg amount was determined by HPLC-MS/MS. Phg was detected in all *S. pristinaespiralis* (*SPlpg-OE*, *SPdpg-OE*) and *S. lividans* (*SLlpg-OE*, *SLdpg-OE*) expression samples, whereas only trace amounts of Phg were measured in the respective pRM4 control samples (Fig. 4a–d). Overall, Phg production was generally higher (even if statistically significant only for L-Phg expression samples as shown in Fig. S2) and more consistent in HT7T medium than in R5 (Fig. 4b, d vs a, c). Interestingly, Phg concentrations decreased in nearly all media and all expression hosts after reaching the maximal level, which suggests a degradation or metabolization of the expression product. An exception was found for *S. lividans* expression strains in HT7T medium, where Phg production steadily increased to cultivation time point 96 h (Fig. 4b). Thus, Phg metabolization in *S. lividans* seems to be medium dependent. For *S. pristinaespiralis* samples, Phg decrease in the pristinamycin production medium HT7T might also be explained by a subsequent incorporation of Phg into PI. Furthermore, it was observed that Phg concentrations in general were higher in D-Phg expression strains than in L-Phg expression strains, which was consistent with the data obtained from the Phg expression studies in different host strains (Fig. 4a–d vs Fig. 3). D-amino acids are known for their poor metabolic usability (Elmadfa and Leitzmann 2015). Hence, the higher Phg amount in the D-Phg expression strains might be explained by a rather poor metabolization of the unnatural D-Phg enantiomer. Due to the observation that overall Phg production was more stable and consistent in HT7T and with regard to subsequent genetic engineering approaches targeting pristinamycin-specific genes in *S. pristinaespiralis* host strains (see below), the pristinamycin production medium HT7T was used as Phg production medium for further analyses.

Deletion of a gene of the phenylacetyl-CoA degradation pathway significantly improves Phg production in *S. pristinaespiralis* but not in *S. lividans*

In order to increase Phg production in the optimal producer strains *S. lividans* and *S. pristinaespiralis*, we aimed to genetically manipulate key steps within primary metabolism involved in precursor supply to direct the metabolic flux towards Phg production. As a target of manipulation, we chose the phenylacetyl-CoA degradation pathway since phenylacetyl-CoA is a suggested precursor for the biosynthesis of Phg (Mast et al. 2011a; Osipenkov et al. 2018) (Fig. 2). In a previous study from Zhao et al. (2015), it has been reported that the

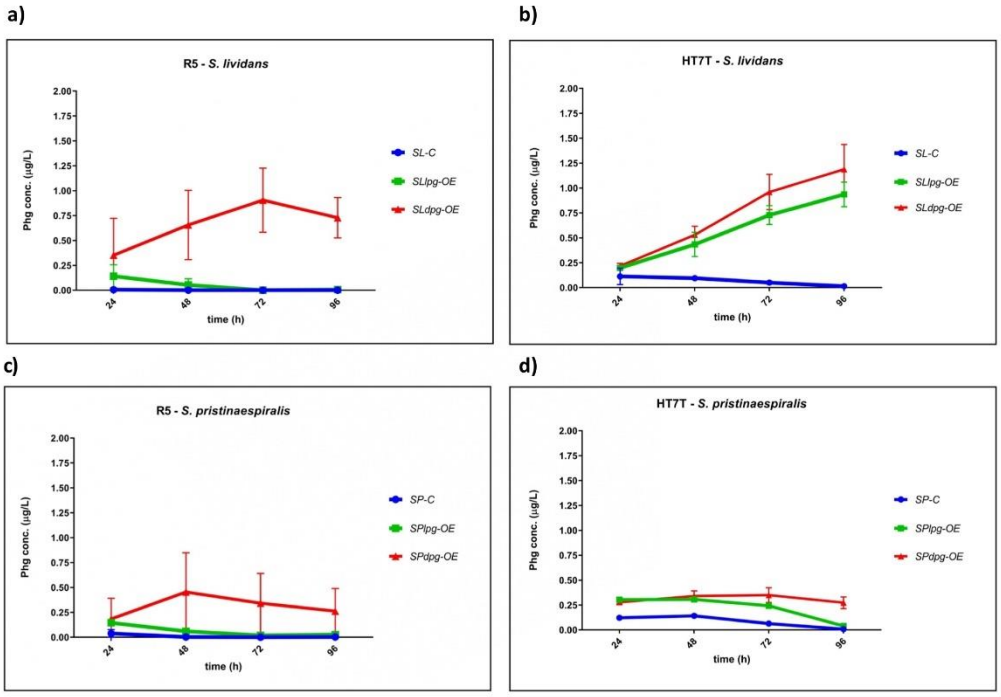

Fig. 4 Phg production of *S. lividans* Phg expression strains *SLlpg-OE* and *SLdpg-OE*, (control: *SL-C*) in R5 (**a**) and HT7T (**b**). Phg production of *S. pristinaespiralis* Phg expression strains *SPlpg-OE* and *SPdpg-OE*, (control: *SP-C*) in R5 (**c**) and HT7T (**d**). Phg production was measured at 24, 48, 72, and 96 h. Phg concentration is given in micrograms per liter. Data were obtained from three independent biological replicates

paaABCDE (*paa*) operon from *S. pristinaespiralis* encodes a putative phenylacetyl-CoA epoxidase multicomponent enzyme system, which is responsible for the degradation of phenylacetyl-CoA (Zhao et al. 2015). It was suggested that derepression of the *paa* operon in *S. pristinaespiralis* leads to a higher flux of phenylacetyl-CoA towards the phenylacetic acid catabolic pathway and thus to less precursor supply for L-Phg biosynthesis (Zhao et al. 2015). By contrast, it can be assumed that an inactivation of the *paa* genes in *S. pristinaespiralis* drives the phenylacetyl-CoA flux towards Phg biosynthesis. Thus, we aimed to inactivate the *paa* operon in *S. pristinaespiralis*—but also *S. lividans*, since a homologous *paa* operon is present in the *S. lividans* genome (Supplementary File)—and overexpress the Phg operons in the engineered mutant strains in order to increase production yields. For this purpose, the gene region *paaA-E* in *S. pristinaespiralis* and *S. lividans*, respectively, was inactivated by replacing it against a thiostrepton resistance cassette (*thio*^{R}) (Supplementary File, Fig. S3). This resulted in the mutants *SPpaa::thio* and *SLpaa::thio*, respectively, in which the Phg expression constructs pYM/lpg and pYM/dpg, as well as the empty vector as a control, were each transferred to. The *paa* control strains, *SPpaa::thio-C* and *SLpaa::thio-C* and the host strains *SPpaa::thio lpg-OE*, *SPpaa::thio dpg-OE*, *SLpaa::thio lpg-OE*, and *SLpaa::thio dpg-OE* were grown in HT7T medium and supernatant samples at different time points were used for Phg production analysis. HPLC-MS/MS measurements of the samples from the engineered host strains revealed that Phg production in the *S. lividans paa* expression samples was almost the same as in the wild-type-derived expression samples (Fig. 5a vs Fig. 4b): maximal Phg production at 96 h was measured for *SLpaa::thio lpg-OE* at 1.00 µg/L compared with 0.94 µg/L for *SLlpg-OE* and 0.95 µg/L for *SLpaa::thio dpg-OE* compared with 1.2 µg/L for *SLdpg-OE*. In contrast, Phg production was strongly improved for *S. pristinaespiralis paa*-derived expression samples (Fig. 5b vs Fig. 4d): Already after 24 h, Phg amount in *SPpaa::thio lpg-OE* (1.57 µg/L) was 5-fold higher than in *SPlpg-OE* (0.31 µg/L) and remained high until 96 h. Here, the production decline at 72 h might be an artifact since standard deviations for the *SPpaa::thio lpg*-OE samples in general were quite high. Phg production was also significantly improved for *SPpaa::thio dpg-OE* strains, where

the maximal Phg production at 96 h (1.30 μg/L) was 3.7-fold higher than in non-engineered *SPdpg-OE* strains (0.35 μg/L). Overall, the significant improvement of Phg production in *S. pristinaespiralis paa* host strains most likely results from the directed flux of the phenylacetyl-CoA precursor towards the Phg biosynthetic pathway. The fact that Phg production was improved for *SPpaa::thio lpg*-OE compared with *SPpaa::thio dpg*-OE might be explained by the different enzyme kinetics of the two aminotransferases. D-amino acid transaminases, such as HpgAT (encoded in the *dpg* operon), are commonly known to have a very low transamination activity towards D-Phg (Soda and Esaki 1994). Thus, PglE may convert the accruing phenylglyoxylate precursor more efficiently to L-Phg than HpgAT can convert it to D-Phg.

Deletion of Phg aminotransferase gene *pglE* slightly improves Phg production in *S. pristinaespiralis*

In a recent study, we showed that the L-Phg aminotransferase PglE is responsible for the conversion of phenylglyoxylate to L-Phg in *S. pristinaespiralis* (Osipenkov et al. 2018) (Fig. 2). Deletion of *pglE* leads to an accumulation of phenylglyoxylate (Osipenkov et al. 2018). Due to this increased basal precursor availability, we were interested how the Phg operon expression in the *S. pristinaespiralis pglE* mutant (*MpglE*) would influence production performance. Besides that, inactivation of the native *pglE* gene could deliver a genetic background for the production of enantiopure Phgs in *S. pristinaespiralis*. Thus, the *MpglE* mutant was used as parental strain for the expression of the Phg operons. Strain denomination is similar as reported above and samples were treated as outlined before. HPLC-MS/MS analysis revealed that Phg production in *MpglE* host strains (*MpglE lpg-OE* and *MpglE dpg-OE*) was overall slightly higher than in *S. pristinaespiralis* wild-type-derived strains (Fig. 6 vs Fig. 4d): An improvement was observed for the *MpglE lpg-OE* samples, where a maximal production of 0.56 μg/L Phg at 48 h was measured, which is an increase of 1.8-fold compared with the maximal value of 0.31 μg/L Phg at 24 h in the *SPlpg-OE* sample. For *MpglE dpg-OE* expression samples, no tremendous Phg production improvement was observed (Fig. 6). Therefore, one could speculate that the slightly increased Phg rates in *MpglE lpg-OE* may result from a somehow favorable basal phenylglyoxylate precursor supply.

Deletion of the PI-NRPS gene *snbDE* significantly improves Phg production in *S. pristinaespiralis*

As suggested above, the decrease of Phg in *SPlpg-OE* samples may be due to an incorporation of L-Phg into PI (Fig. 4d). Thus, a strategy to increase Phg production in *S. pristinaespiralis* is to block PI biosynthesis. In order to do that, we inactivated the gene *snbDE* in *S. pristinaespiralis* (Supplementary File), which encodes the PI-specific NRPS module SnbDE that uses L-Phg as a building block for PI biosynthesis (Mast et al. 2011b). The respective mutant *MsnbDE::thio* was used as expression host for the Phg operon expression. The derived host strains *MsnbDE::thio lpg-OE* and *MsnbDE::thio dpg-OE*, as well as the control *MsnbDE::thio-C*, were grown in HT7T and samples were analyzed for Phg production by HPLC-MS/MS. HPLC-MS/MS analysis revealed a maximal Phg production in samples *MsnbDE::thio lpg-OE* (0.87 μg/L) and *MsnbDE::thio dpg-OE* (1.27 μg/L) at 96 h, which was an increase of ~ 3-fold compared with maximal production values in wild-type-derived samples *SPlpg-OE* and *SPdpg-OE* (0.30 μg/L and 0.35 μg/L), respectively (Fig. 7 vs Fig. 4d). Furthermore, it was found that Phg concentration in the *MsnbDE::thio*-derived strains increased continuously, whereas a decrease was observed in the wild-type-derived samples at later time points. Actually, the Phg production profile of the *MsnbDE::thio*-derived strains more resembled the production profile of the

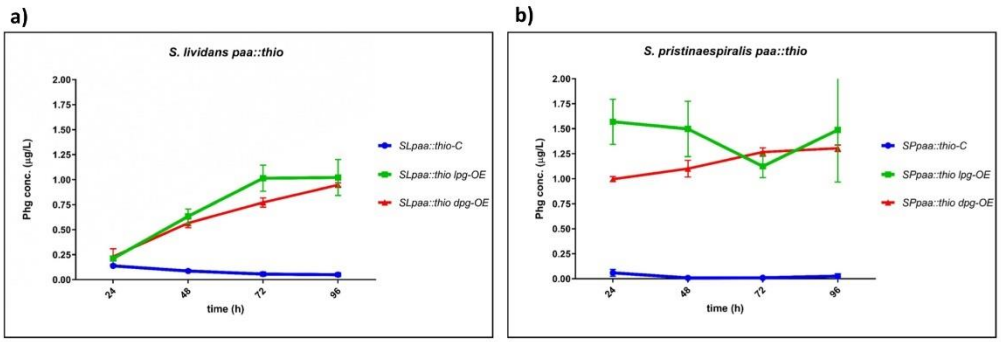

Fig. 5 Phg production of *S. lividans paa* host strains *SLpaa::thio lpg-OE* and *SLpaa::thio dpg-OE*, (control: *SLpaa::thio-C*) (**a**) and *S. pristinaespiralis paa* host strains *SPpaa::thio lpg-OE* and *SPpaa::thio dpg-OE*, (control: *SPpaa::thio-C*) (**b**) grown in HT7T. Phg production was measured at 24, 48, 72, and 96 h. Phg concentration is given in micrograms per liter. Data were obtained from three independent biological replicates

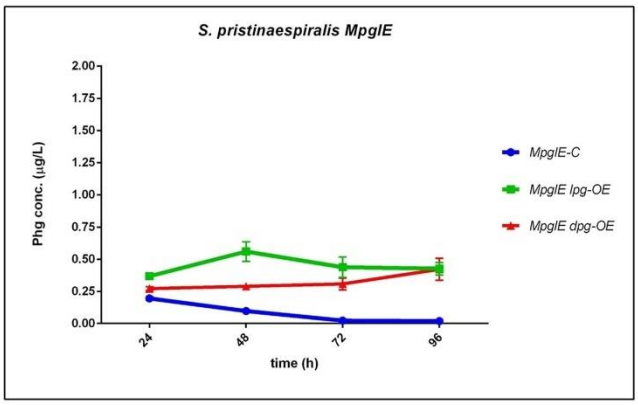

Fig. 6 Phg production of *S. pristinaespiralis MpglE* host strains *MpglE lpg-OE* and *MpglE dpg-OE*, (control: *MpglE-C*) grown in HT7T. Phg production was measured at 24, 48, 72, and 96 h. Phg concentration is given in micrograms per liter. Data were obtained from three independent biological replicates

S. lividans host strains (Fig. 7 vs Fig. 4b). Thus, it can be assumed that Phg production in the *MsnbDE::thio*-derived strains is steadily increasing because Phg is not utilized for PI biosynthesis and thus accumulates, which may also happen in *S. lividans* because this strain does not produce pristinamycin.

Deletion of the pristinamycin TetR–like regulatory gene *papR5* significantly improves Phg production in *S. pristinaespiralis*

As we had incident that Phg production performance in *S. pristinaespiralis* depends on the pristinamycin biosynthesis capability (see above for *MpglE, MsnbDE* samples), we aimed to further enhance Phg production by using a pristinamycin superproducer as expression host. In a previous study, we showed that the *S. pristinaespiralis* repressor mutant *papR5::apra* produces up to ~ 300% more pristinamycin than the wild-type strain (Mast et al. 2015). Due to this high pristinamycin production capability, we used *papR5::apra* as a host for Phg operon expression. The derived host strains *papR5::apra lpg-OE* and *papR5::apra dpg-OE*, as well as the control strain *papR5::apra-C*, were grown in HT7T and samples were analyzed by HPLC-MS/MS for Phg production. HPLC-MS/MS data revealed that Phg production was significantly increased in *papR5::apra*-derived host strains compared with the wild-type-derived ones: *papR5::apra lpg-OE* and *papR5::apra dpg-OE* produced approximately 3.3-fold and 2-fold, respectively, more Phg than the wild-type-derived expression strains (*papR5::apra lpg-OE*: 1 µg/L; *papR5::apra dpg-OE*: 0.72 µg/L Phg) (Fig. 8 vs Fig. 4d). Phg production was increased especially in the *papR5::apra lpg-OE* host strain, which was also observed for the other Phg precursor–engineered host strains (*SLpaa::thio*, *SPpaa::thio*, and *MpglE*). Thus, Phg-related precursor engineering seems to affect more L-Phg than D-Phg biosynthesis. This might be explained by the less favorable enzymatic properties of HpgAT, as

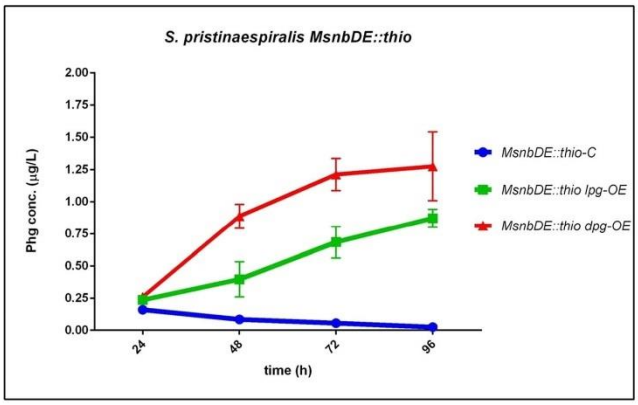

Fig. 7 Phg production of *S. pristinaespiralis snbDE* host strains *MsnbDE::thio lpg-OE* and *MsnbDE::thio dpg-OE*, (control: *MsnbDE::thio-C*) grown in HT7T. Phg production was measured at 24, 48, 72, and 96 h. Phg concentration is given in micrograms per liter. Data were obtained from three independent biological replicates

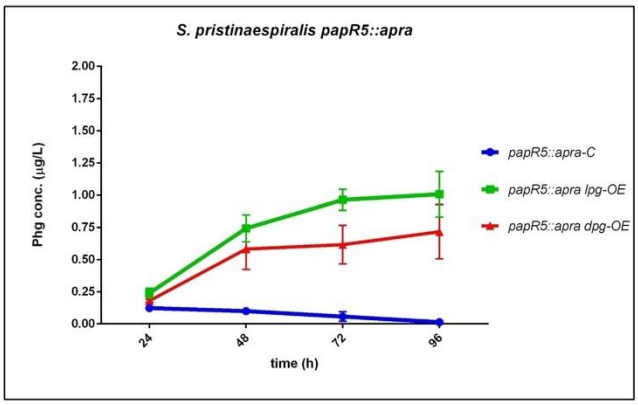

Fig. 8 Phg production in the *S. pristinaespiralis papR5* host strains *papR5::apra lpg-OE* and *papR5::apra dpg-OE*, (control: *papR5::apra-C*) grown in HT7T. Phg production was measured at 24, 48, 72, and 96 h. Phg concentration is given in micrograms per liter. Data were obtained from three independent biological replicates

mentioned before. The reason why Phg concentration is stable or even increasing in these expression hosts might be because PI production is oversaturated with Phg precursor and thus Phg would accumulate. Overall, the improvement of Phg production in the *papR5::apra*-derived host strains most likely results from the elevated levels of precursor supply in the course of an increased pristinamycin biosynthesis.

Discussion

Non-proteinogenic amino acids, such as Phg, are important building blocks and precursors for the synthesis of industrial relevant pharmaceuticals and other fine chemicals. We could show that genetic engineering of suitable target genes in appropriate expression strains allows improvement of Phg production. As expression hosts, we tested different actinomycetal species. This is the first time that Phg production has been accomplished in actinomycetes. Even if Phg production was quite efficient in *S. lividans* expression strains, *S. pristinaespiralis* is preferred as producer host since it offers a broader range of target genes, suitable for genetic engineering to increase production yields. The strongest Phg production improvement was observed for *S. pristinaespiralis* expression strains with an inactivated phenylacetyl-CoA degradation pathway (*SPpaa::thio* strains). Here, production levels were quite high from the beginning on, which might be the result of so far unknown feedback/feedforward control of Phg biosynthesis in *S. pristinaespiralis*. Maximal production of *SPpaa::thio* was measured at ~ 1.6 μg/L Phg, which corresponds to a 4.6-fold increase compared with the production levels of wild-type-derived strains. However, also mutations of specific PI biosynthesis genes (*pglE, snbDE*) and a pristinamycin transcriptional regulator gene (*papR5*) led to an increase of Phg production. Especially for these producer strains it would be interesting to also determine PI production levels in order analyze how they correlate with Phg production profiles. Furthermore, it should be investigated if D-Phg can be used as a building block for PI biosynthesis, which is not known so far. This could be assumed since Phg production was increased in both PI-NRPS deletion host strains, *MsnbDE::thio lpg-OE* and *MsnbDE::thio dpg-OE*, suggesting that both Phg enantiomers are used as PI building blocks.

A logic strategy to further increase Phg production is to perform a combinatory genetic engineering approach and inactivate all the above-mentioned genes in *S. pristinaespiralis*. An additional target gene for further production improvement is *papR2*, which encodes a SARP-type transcriptional regulator that is suggested to activate the L-Phg operon in *S. pristinaespiralis* (Mast et al. 2015). Thus, additional overexpression of *papR2* in an engineered *S. pristinaespiralis* Phg superhost could further increase production yields. Due to these multifarious manipulation opportunities, *S. pristinaespiralis* indeed represents a good chassis strain for fermentative Phg production. However, even if production improvement worked out quite well for *S. pristinaespiralis*, the overall product concentrations are still low. Maximal production was ~ 1.6 μg/L Phg, which is still far away from mg production levels previously reported for *E. coli* fermentation (Müller et al. 2006).

In *E. coli*, Phg production was accomplished by expressing an artificial Phg operon, consisting of at least three genes (*hmaS*, *hmo*, *hpgAT*, or *pgat*) from different organisms (*Streptomyces coelicolor*, *Amycolatopsis orientalis*, and *Pseudomonas putida*) in a suitable pathway-engineered *E. coli* strain (Müller et al. 2006; Liu et al. 2014). Thereby, Phg production was optimized to 51.6 mg/g dry cell weight L-Phg (Liu et al. 2014, 2015) and 102 mg/g dry cell weight D-Phg (Müller et al. 2006). In another approach, L-Phg production was accomplished in *E. coli* by co-expression of a leucine dehydrogenase from *Bacillus cereus* (*Bc*LeuDH) and a NAD^+-dependent mutant formate dehydrogenase from *Candida boidinii* ($CbFDH_{A10C}$), which yielded 28.4 mg/g dry cell weight L-Phg (Liu et al. 2018). However, these values

are not comparable with those of our study since production volumes are given in mg/g biomass in the *E. coli* studies but were measured in micrograms per liter of Phg from culture supernatant samples in the present study. Indeed, it was not possible to correlate biomass values (dry cell weight) with Phg production outputs in *Streptomyces* samples due to their irregular growth in liquid cultures, which leads to strong deviations in biomass values. In any way, absolute Phg concentrations for *Streptomyces* samples are hard to determine exactly by HPLC-MS/MS quantification. What we rather would like to depict is that Phg production and optimization can clearly be followed by comparison with control strains. Notably, this is the first time that fermentative Phg production has been reported for actinomycetes. Furthermore, it is important to mention that, unlike the studies in *E. coli*, the precursor supply of phenylpyruvate was not modified in our strains. This is a pivotal target for further studies as usually the aromatic amino acid biosynthesis pathway in bacteria is strictly regulated and limits the precursor supply (Huccetogullari et al. 2019; Lee and Wendisch 2017; Rodriguez et al. 2014; Sprenger 2007). It was shown for *Streptomyces venezuelae* that an improved flux through the shikimate pathway by overexpressing the genes of shikimate kinase (*aroK*) and dehydroquinate synthase (*aroB*) increased the production of the aromatic antibiotic chloramphenicol (Vitayakritsirikul et al. 2016). Overexpression of the gene chorismate synthase (*aroC*) in *Streptomyces tsukubaensis* improved the production of the immunosuppressant tacrolimus (Wang et al. 2017). Furthermore, overexpression of the 3-deoxy-D-arabino-heptulosonate 7-phosphate synthase gene (*dahp*) and the prephenate dehydrogenase gene (*pdh*) in *A. balhimycina* resulted in improved balhimycin production (Thykaer et al. 2010). Thus, it is very likely that Phg amount can be further increased by improving precursor supply from the shikimate pathway. In our study, we could ensure and show that the final reaction, the conversion of phenylpyruvate to Phg, can be improved by deleting the competing reaction for Phg biosynthesis.

S. pristinaespiralis-derived Phg operons indeed are interesting molecular entities for future applications. So far, the *pgl* genes from *S. pristinaespiralis* encode the only known natural Phg biosynthesis pathway. One could assume that this pathway is already evolutionary optimized and under appropriate conditions might be more powerful than an artificially assembled pathway harboring genes from different origins. However, this would require further investigations. Overall, the Phg operons represent promising biobricks for Phg-related production processes. A purely fermentative production route has mainly been prevented by the absence of a natural Phg pathway. In this study, we could describe the functionality of the natural L-Phg operon from *S. pristinaespiralis* and its derived D-Phg operon obtained by a synthetic biology approach. The new fermentative Phg production route serves as a basis to replace the environmentally unfriendly industrial Phg production process.

Authors' contributions DM, VM, NO, and SK performed experiments; ROW, FH, OH, and JWY contributed to experiments; GS contributed to data analysis, AK carried out HPLC-MS/MS analysis; YM designed, supervised, and coordinated the study. YM wrote the manuscript. OH contributed to manuscript editing. All authors read and approved the final manuscript.

Funding information Open Access funding provided by Projekt DEAL. This work was supported by the Institutional Strategy of the University of Tübingen (Deutsche Forschungsgemeinschaft, ZUK 63). We further received funding from the Baden-Württemberg Stiftung (BWST_WSF-035) and the German Center for Infection research (DZIF) (TTU 09.819).

Compliance with ethical standards

Conflict of interest The authors declare that they have no competing interests.

Ethical approval This article does not contain any studies with human participants or animals performed by any of the authors.

References

Al Toma RS, Brieke C, Cryle MJ, Süssmuth RD (2015) Structural aspects of phenylglycines, their biosynthesis and occurrence in peptide natural products. Nat Prod Rep 32:1207–1235

Barredo JL (2005) Methods in biotechnology: microbial enzymes and biotransformations. Humana Press, Totowa ISSN 1940-6061

Croteau R, Ketchum REB, Long RM, Kaspera R, Wildung MR (2006) Taxol biosynthesis and molecular genetics. Phytochem Rev 5:75–97

Denis JN, Correa A, Greene AE (1991) Direct, highly efficient synthesis from (S)-(+)-phenylglycine of the taxol and taxotere side chains. J Org Chem 56:6939–6942

Ebeling SC (1998) The synthesis of artificial sweeteners (phenylglycine-analogues of aspartame) in order to evaluate changes in the γ-glycophore component. Food Chem 61:107–112

Elmadfa I, Leitzmann C (2015) Ernährung des Menschen, 5th edn. Eugen Ulmer KG, Stuttgart

Folcher M, Gaillard H, Nguyen LT, Nguyen KT, Lacroix P, Bamas-Jacques N, Rinkel M, Thompson CJ (2001) Pleiotropic functions of a *Streptomyces pristinaespiralis* autoregulator receptor in development, antibiotic biosynthesis, and expression of a superoxide dismutase. J Biol Chem 276:44297–44306

Global Industry Analysts Inc (2016) A worldwide business strategy & market intelligence source. MCP-7644: D-Amino Acids - A Global Strategic Business Report. http://www.strategyr.com/PressMCP-7644.asp. Accessed June 13, 2019

Huccetogullari D, Lou ZW, Lee SY (2019) Metabolic engineering of microorganisms for production of aromatic compounds. Microb Cell Factories 18:41

Janusz JM (1986) Alpha-L-aspartyl-D-phenylglycine esters and amides useful as high intesity sweeteners. European patent EP0168112A2

Kan T, Tominari Y, Rikimaru K, Morohashi Y, Natsugari H, Tomita T, Iwatsubo T, Fukuyama T (2004) Parallel synthesis of DAPT derivatives and their gamma-secretase-inhibitory activity. Bioorg Med Chem Lett 14:1983–1985

Kieser T, Bibb MJ, Buttner MJ, Chater KF, Hopwood DA (2000) Practical *Streptomyces genetics*. John Innes Foundation, Norwich

Lee JH, Wendisch VF (2017) Biotechnological production of aromatic compounds of the extended shikimate pathway from renewable biomass. J Biotechnol 257:211–221

Liu SP, Liu RX, El-Rotail AAMM, Ding ZY, Gu ZH, Zhang L, Shi GY (2014) Heterologous pathway for the production of L-phenylglycine from glucose by *E. coli*. J Biotechnol 186:91–97

Liu SP, Zhang L, Mao J, Ding ZY, Shi GY (2015) Metabolic engineering of *Escherichia coli* for the production of phenylpyruvate derivatives. Metab Eng 32:55–65

Liu Q, Zhou J, Yang T, Zhang X, Xu M, Rao Z (2018) Efficient biosynthesis of L-phenylglycine by an engineered *Escherichia coli* with a tunable multi-enzyme-coordinate expression system. Appl Microbiol Biotechnol 102:2129–2141

Lu Y, Freeland S (2006) On the evolution of the standard amino-acid alphabet. Genome Biol 7:102

Mast Y, Wohlleben W (2014) Streptogramins - two are better than one! Int J Med Microbiol 304:44–50

Mast Y, Wohlleben W, Schinko E (2011a) Identification and functional characterization of phenylglycine biosynthetic genes involved in pristinamycin biosynthesis in *Streptomyces pristinaespiralis*. J Biotechnol 155:63–67

Mast Y, Weber T, Gölz M, Ort-Winklbauer R, Gondran A, Wohlleben W, Schinko E (2011b) Characterization of the "pristinamycin supercluster" of *Streptomyces pristinaespiralis*. Microb Biotechnol 4:192–206

Mast Y, Guezguez J, Handel F, Schinko E (2015) A complex signaling cascade governs pristinamycin biosynthesis in *Streptomyces pristinaespiralis*. Appl Environ Microbiol 81:6621–6636

Müller U, van Assema F, Gunsior M, Orf S, Kremer S, Schipper D, Wagemans A, Townsend CA, Sonke T, Bovenberg R, Wubbolts M (2006) Metabolic engineering of the *E. coli* L-phenylalanine pathway for the production of D-phenylglycine (D-Phg). Metab Eng 8:196–208

Müller UM, Boer R, Bovenberg R (2013) MbtH-like proteins in the production of semi-synthetic antibiotics. Patent WO2013113646A1

Nah H-J, Pyeon H-R, Kang S-H, Choi S-S, Kim E-S (2017) Cloning and heterologous expression of a large-sized natural product biosynthetic gene cluster in *Streptomyces* species. Front Microbiol 8:394

Ningsih F, Kitani S, Fukushima E, Nihira T (2011) VisG is essential for biosynthesis of virginiamycin S, a streptogramin type B antibiotic, as a provider of the nonproteinogenic amino acid phenylglycine. Microbiology 157:3213–3220

Osipenkov N (2016) Biosyntheseweg eines natürlichen Phenylglycins, Biochemische Analyse und Perspektiven einer nachhaltigen Produktion. Springer Fachmedien, Wiesbaden ISBN: 9783658118648

Osipenkov N, Kulik A, Mast Y (2018) Characterization of the phenylglycine aminotransferase PglE from *Streptomyces pristinaespiralis*. J Biotechnol 278:34–38

Pfeifer V, Nicholson GJ, Ries J, Recktenwald J, Schefer AB, Shawky RM, Schröder J, Wohlleben W, Pelzer S (2001) A polyketide synthase in glycopeptide biosynthesis. The biosynthesis of the non-proteinogenic amino acid (S)-3,5-dihydroxyphenylglycine. J Biol Chem 276:38370–38377

Pridmore RD (1987) New and versatile cloning vectors with kanamycin-resistance marker. Gene 56:309–312

Rodriguez A, Martnez J, Flores N, Escalante A, Gosset G, Bolivar F (2014) Engineering *Escherichia coli* to overproduce aromatic amino acids and derived compounds. Microb Cell Factories 13:126

Sambrook J, Fritsch EF, Maniatis T (1989) Molecular cloning: a laboratory manual, 2nd edn. Cold Spring Harbor laboratory press, New York

Schmid A, Dordick JS, Hauer B, Kiener A, Wubbolts M, Witholt B (2001) Industrial biocatalysis today and tomorrow. Nature 11:258–268

Schutt H (1981) Stereoselective resolution of phenylglycine derivatives and 4-hydroxyphenylglycine derivatives with enzyme resins. US patent US4260684A

Shiau CY, Pai SC, Lin WP, Ji DD, Liu YT (2005) Purification and characterization of inducible cephalexin synthesizing enzyme in *Gluconobacter oxydans*. Biosci Biotechnol Biochem 69:463–469

Soda K, Esaki N (1994) Pyridoxal enzymes acting on D-amino acids. Pure Appl Chem 66:709–714

Sprenger GA (2007) From scratch to value: engineering *Escherichia coli* wild type cells to the production of L-phenylalanine and other fine chemicals derived from chorismate. Appl Microbiol Biotechnol 75:739–749

Stevenazzi A, Marchini M, Sandrone G, Vergani B, Lattanzio M (2014) Amino acidic scaffolds bearing unnatural side chains: an old idea generates new and versatile tools for the life sciences. Bioorg Med Chem Lett 24:5349–5356

Thykaer J, Nielsen J, Wohlleben W, Weber T, Gutknecht M, Lantz AE, Stegmann E (2010) Increased glycopeptide production after overexpression of shikimate pathway genes being part of the balhimycin biosynthetic gene cluster. Metab Eng 12:455–461

Vedha-Peters K, Gunawardana M, Rozzell JD, Novick SJ (2006) Creation of a broad-range and highly stereoselective D-amino acid dehydrogenase for the one-step synthesis of D-amino acids. J Am Chem Soc 128:10923–10929

Vitayakritsirikul V, Jaemsaeng R, Lohmaneeratana K, Thanapipatsiri A, Daduang R, Chuawong P, Thamchaipenet A (2016) Improvement of chloramphenicol production in *Streptomyces venezuelae* ATCC 10712 by overexpression of the *aroB* and *aroK* genes catalysing steps in the shikimate pathway. Antonie Van Leeuwenhoek 109:379–388

Walsh CT, O'Brien RV, Khosla C (2013) Nonproteinogenic amino acid building blocks for nonribosomal peptide and hybrid polyketide scaffolds. Angew Chem Int Ed 52:7098–7124

Walton CJ, Thiebaut F, Brunzelle JS, Couture J, Chica RA (2018) Structural determinants of the stereo-inverting activity of *Pseudomonas stutzeri* D-phenylglycine aminotransferase. Biochemistry 57:5437–5446

Wang ZM, Kolb HC, Sharpless KB (1994) Large-scale and highly Enantioselective synthesis of the taxol C-13 side chain through asymmetric dihydroxylation. J Org Chem 59:5104–5105

Wang C, Liu J, Liu H, Liang S, Wen J (2017) Combining metabolomics and network analysis to improve tacrolimus production in *Streptomyces tsukubaensis* using different exogenous feedings. J Ind Microbiol Biotechnol 44:1527–1540

Wegman MA, Janssen MHA, van Rantwijk F, Sheldon RA (2001) Towards biocatalytic synthesis of beta-lactam antibiotics. Adv Synth Catal 343:559–576

Yam KC, Okamoto S, Roberts JN, Eltis LD (2011) Adventures in *Rhodococcus*- from steroids to explosives. Can J Microbiol 57: 155–168

Zhao Y, Feng R, Zheng G, Tian J, Ruan L, Ge M, Jiang W, Lu Y (2015) Involvement of the TetR-type regulator PaaR in the regulation of pristinamycin I biosynthesis through an effect on precursor supply in *Streptomyces pristinaespiralis*. J Bacteriol 197:2062–2071

The Article

Moosmann D, Mokeev V, Kulik A, Osipenkov N, Kocadinc S, Ort-Winklbauer R, Handel F, Hennrich O, Youn YW, Sprenger G, Mast Y. Genetic engineering approaches for the fermentative production of phenylglycines. Appl Microbiol Biotechnol. 2020, 104::3433-3444. doi:10.1007/s00253-020-10447-9.

10. Contributions

Publication 1: Biotransformation-coupled mutasynthesis for the generation of novel pristinamycin derivatives by engineering the phenylglycine residue

The project described in Publication 1 aimed at modifying the peptide antibiotic pristinamycin I (PI) and investigate the effects of those modifications on its bioactivity. For the employed mutasynthesis method, the production of L-phenylglycine (L-Phg), a precursor to pristinamcin I, was disrupted in the natural producer *Streptomyces pristinaespiralis* by genetic modification. Commercially available derivatives of L-Phg (mutasynthons) were then fed to the mutant to generate new PI congeners. The isolated new compounds were investigated by agar diffusion, MIC and cytotoxicity assays, as well as by NMR analysis. Additionally, an *Escherichia coli*-based biotransformation process was developed to generate further mutasynthons in a biological system. I was responsible for the execution of the mutasynthesis experiments concerning the generation of pristinamycin I derivatives. This included generation of mutants and feeding experiments with those mutants, isolation and HPLC analysis of halogenated derivatives, as well as performing agar diffusion and *iv*TT bioassays. I performed the purification of halogenated PI derivatives together with F. Surup and K. Harms. F. Surup and K. Harms also performed MIC and cytotoxicity assays as well as NMR analysis. A. Kulik conducted HPLC-MS/MS analysis of pristinamycin I derivatives. JW. Youn and L. Weinmann developed the Phg biotransformation system and carried out the generation of Phg derivatives. P. Klahn performed SeeSAR modelling analysis. The manuscript was written by me and Y. Mast with contributions from all co-authors. Y. Mast designed the mutasynthesis concept and coordinated the study.

Publication 2: High Plasticity of the Amicetin Biosynthetic Pathway in *Streptomyces* sp. SHP 22-7 Led to the Discovery of Streptcytosine P and Cytosaminomycins F and G and Facilitated the Production of 12F-Plicacetin

In Publication 2, *Streptomyces* sp. SHP 22-7 was shown to produce the nucleoside antibiotics amicetin and plicacetin, as well as several new nucleoside antibiotic derivatives. Additionally, new fluorinated amicetin analogs were generated by a precursor directed biosynthesis approach with SHP 22 7. New amicetin analogs were

isolated, their structure was elucidated by NMR and their bioactivity against multiple organisms was investigated. I performed large scale cultivations of SHP 22-7 and prepared crude extracts for isolation and analysis of natural amicetin derivatives. I wrote the respective Material and Methods part for the publication. I. Handayani identified the strains as amicetin producer and provided the strain on plate. Y. Mast supervised the amicetin cultivation part and was involved in writing the Material and Methods section. A. Berscheid performed *in vitro* translation assays. H. Brötz-Oesterhelt supervised mode-of-action analysis studies. N. Reiling performed anti-mycobacterial assays. J. Chen, K. Bhattarai, M. Kramer, J. Straetener, T. Wommer S. Peter, C. Geibel, and M. Lämmerhofer were in involved in chaemical analsis of the compound and bioassays/cytotoxicity assays, respectively. N. Aryal performed compound isolation and analysis. H. Gross conceptualized, supervised the study and wrote the publication.

Publication 3: Genome Sequences of Two Putative Streptogramin Producers, *Streptomyces* sp. Strains TÜ 2975 and TÜ 3180, from the Tübingen Strain Collection

Publication 3 discloses the genome sequences of the two *Streptomyces* sp. strains, TÜ 2975 and TÜ 3180, from the Tübingen Strain Collection which were previously shown to produce the streptogramin antibiotics pristinamycin and griseoviridin/viridogrisein, respectively. F. Handel identified TÜ 2975 and TÜ 3180 as streptogramin producers and provided the strains on solid medium. R. Ort-Winklbauer cultivated the strains and isolated genomic DNA. I deposited the genome sequence data of the two strains at the GenBank database. The manuscript was written by me and Y. Mast.

Publication 4: Genetic engineering approaches for the fermentative production of phenylglycines

Publication 4 describes a project for the biogenic production of the industrially significant non-proteinogenic amino acid D-phenylglycine (D-Phg) by *Streptomyces pristinaespiralis*. *S. pristinaespiralis* possesses the first natural synthesis pathway of L-phenylglycine (L-Phg) ever described and was therefore seen as a promising

starting platform for the fermentative production of D-Phg by genetic modification, including the introduction of the stereo-inverting aminotransferase gene *hpgAT* from *Pseudomonas putida*. I performed multiple control experiments concerning residual pristinamycin production levels of multiple *S. pristinaespiralis* mutant strains used in this study. I was involved in the editing process including generation of figures and organisation of literature references. D. Moosmann, V. Mokeev, N. Osipenkov, S. Kocadinc, and F. Handel generated the cloning constructs, carried out genetic manipulation of the expression strains, and performed Phg analysis. F. Handel and R. Ort-Winklbauer contributed to cloning experiments and strain cultivation. R. A. Kulik performed HPLC-MS/MS analysis. J-W. Youn performed Phg analysis for detection of enantiomers, which was supervised by G. Sprenger. Y. Mast wrote the manuscript, designed, supervised and coordinated the study.

Publication 5: Challenging old microbiological treasures for natural compound biosynthesis capacity

The project described in Publication 5 focused on underexplored *Streptomyces* strains from the DSMZ strain collection which were investigated for their phenotypic, chemotaxonomic and genetic features, as well as their biosynthetic potential concerning bioactive compounds. I performed cultivations of strain DSM 40484 and prepared crude extracts for the identification of the antibiotic cinerubin. Furthermore, I conducted agar diffusion assays and fractionation of extracts. I also contributed with writing parts of the respective Material and Methods section for the publication. I. Nouioui conceptualized and supervised the study. She carried out data analysis for species description and was involved in writing. A. Zimmermann performed bioassays and edited phylogenetic trees. She was involved in formatting of the publication. O. Rössler and R. Makitrynskyy carried out genetic manipulation of strains. R. Makitrynskyy was involved in compound analysis. S. Xia and C. Hughes performed compound analysis. J-P. Gomez-Escribano, submitted genomes to GenBank. M. Neumann-Schaal and J. Wolf performed phospholipid fatty acid profiling. G. Pötter, M. Jando, M. Döppner carried out lab work as technical assistants. J-P. Gomez-Escribano, R. Makitrynskyy, C. Hughes were involved in writing. Y. Mast did BGC analysis, supervised the study and wrote the publication together with I. Nouioui.

Publication 6: ActinoBase: tools and protocols for researchers working on Streptomyces and other filamentous actinobacteria

This article introduces researchers working in the field of streptomycetes to the tools, protocols and forums provided by the community powered platform ActinoBase. I was an organizer, presenter and chairman of the ActinoBase E seminars 2021. I was also involved in the editing process for this publication. MA. Feeney, JT. Newitt, KR. Duncan, LT. Fernández-Martínez and MI. Hutchings conceived the paper and wrote the manuscript. All additional authors read and edited the manuscript and contributed to Actin-oBase.org and/or were organizers and hosts of the ActinoBase seminar series.

11. Acknowledgements

I would like to thank:

Prof. Dr. Yvonne Mast for providing me with the opportunity to work in the fascinating field of secondary metabolites and the chance to earn my doctorate. You always listened to my concerns or problems and provided advice and guidance. I especially want to thank you for following up on me in the time when I was doubting if I would ever finish this dissertation. I could not have wished for a more patient, supportive and encouraging supervisor.

Prof. Dr. Wolfgang Wohlleben and Prof. Dr. Heike Brötz-Oesterhelt for taking the time to review my dissertation.

Those who still remember me at the Department of Microbiology/Biotechnology at the University of Tübingen and the Department of Bioresources for Bioeconomy and Health Research at the Leibniz Institute DSMZ in Braunschweig. You all provided a welcoming and supportive atmosphere and made my time during the respective stay with you truly special. Here, special thanks go to Dr. Günther Muth and Dr. Juan-Pablo Gomez Escribano for providing me with a plethora of knowledge and practical advice concerning genetic work on bacteria in general and streptomycetes in particular.

My parents, who not only supported me for my whole life and enabled me to pursue my goals but also listened with interest when their son started to ramble about bacteria, antibiotics and genetic manipulation.

My sister, for emotional support and motivation when I was feeling disheartened during this long journey, and Benedikt Rilling for initiating our (almost) weekly meetings that got us both to move and finish our respective dissertations.

Hannes Frohnmeyer, Jonathan Feicht, Katja Fromm, Melina and Tobias Frenzel who I started the path of studying biology with and who are still my dear and cherished friends to this day. Your support and the example you present are truly appreciated.

My colleagues at NOVIS for your help in staying (mostly) sane while navigating a challenging new job and finishing my dissertation at the same time.

All the other people, be they friends or family, who kept pushing me forward by being the most annoying human beings imaginable when the conversation moved to my dissertation. You know who you are!